Physicochemical
Problems
of Mineral Processing
42 (2008)

Instructions for preparation of manuscripts

It is recommended that the following guidelines be followed by the authors of the manuscripts:

- Original papers dealing with the principles of mineral processing and papers on technological aspects of mineral processing will be published in the journal which appears once a year
- The manuscript should be sent to the Editor for reviewing before February 15 each year
- The manuscript should be written in English. For publishing in other languages an approval of the editor is necessary
- Contributors whose first language is not the language of the manuscript are urged to have their manuscript competently edited prior to submission.
- The manuscript should not exceed 10 pages
- Two copies of the final manuscript along with an electronic version should be submitted for publication before April 15
- There is a 80 USD fee for printing the paper. No fee is required for the authors participating in the Annual Symposium on Physicochemical Problems on Mineral Processing
- Manuscripts and all correspondence regarding the symposium and journal should be sent to the editor.

Address of the Editorial Office
Wrocław University of Technology
Wybrzeże Wyspiańskiego 27, 50-370 Wrocław, Poland
Institute of Mining Engineering
Laboratory of Mineral Processing

Location of the Editiorial Office:
pl. Teatralny 2, Wrocław, Poland
phone: (071) 320 68 79, (071) 320 68 78
fax: (071) 344 81 23
zygmunt.sadowski@pwr.wroc.pl
andrzej.luszczkiewicz@pwr.wroc.pl
jan.drzymala@pwr.wroc.pl
http://www.ig.pwr.wroc.pl/minproc

Physicochemical Problems of Mineral Processing 42 (2008)

www.ig.pwr.wroc.pl/minproc

WROCŁAW 2008

The papers published in the Physicochemical Problems of Mineral Processing journal are abstrated in Chemical Abstracts, Thomson Reuters (Science Citation Index Expanded, Materials Science Citation Index, Journal Citation Reports), Coal Abstracts, Google Scholar and other sources

This publication was supported in different forms by:
Komitet Górnictwa PAN
(Sekcja Wykorzystania Surowców Naturalnych)
Akademia Górniczo-Hutnicza w Krakowie
Politechnika Śląska w Gliwicach
Politechnika Wrocławska

ISSN 1643-1049

OFICYNA WYDAWNICZA POLITECHNIKI WROCŁAWSKIEJ
WYBRZEŻE WYSPIAŃSKIEGO 27, 50-370 WROCŁAW, POLAND

CONTENTS

Physicochemical Problems of Mineral Processing, 42 (2008), 5-16
Fizykochemiczne Problemy Mineralurgii, 42 (2008), 5-16

A.A. Negm*, A.-Z. M. Abouzeid*

UTILIZATION OF SOLID WASTES FROM PHOSPHATE PROCESSING PLANTS

Received April 19, 2008; reviewed; accepted July 31, 2008

Most of the existing phosphate rocks are of low grade. For the production of marketable phosphate commodity, these low grade ores need upgrading before being utilized. Large quantities of solid-waste materials, with considerable amounts of P_2O_5 content are generated in phosphate processing plants. In addition of being environmental hazards and a source of pollution for air, water and soil, these waste materials add to the production cost for waste removal. The positive use of mineral processing plant tailings is becoming a common practice nowadays, to avoid pollution hazards and to improve the techno-economics of the mineral processing plants. In this paper, the solid-waste of Sebaeya phosphate washing plant, Upper Egypt, was successfully used to produce a high grade phosphate concentrate, to produce aggregates for road paving and for concrete mixes, in brick manufacturing, pottery making, and direct application for improving agriculture soils.

key words: phosphate, wastes, aggregates, road paving, concrete mixes, brick, pottery, agriculture soil

INTRODUCTION

Phosphate occurs in all igneous and sedimentary rocks in the form of phosphate minerals. However, most of the economic recovery of phosphate is of sedimentary origin. The world production of phosphate rock was 146 Tg in the year 2006. Most of the phosphate rock is produced by open-pit mining rather than underground mining.Most phosphate rocks as mined are of low-grade and need beneficiation. Beneficiation plants produce large quantities of waste materials relatively high in P_2O_5 content, which are considered as environmental hazard and a source of pollution of air, water and land. In addition, disposal of these materials represents a loss of valuable natural resource and adds additional cost to the production for waste removal. Dis-

* *Cairo University, Faculty of Engineering, Department of Mining. Giza 12613, Egypt*

posal of ore processing plant tailings is a major environmental problem, which is becoming more serious with increasing exploitation of low grade ores and deposits due to depletion of rich ones (Negm, 1997). The method used to dispose tailings have been developed due to the environmental pressures, changing milling practice and realization of profitable applications (Abouzeid, 2007). Early methods included discharge of tailings into rivers and streams which still practiced at some mines, and the dumping of coarse dewatered tailings on to land (Down, 1977). An alternative for the disposal of mineral processing tailings is the positive use of it, either in the raw state or after further processing (Down, 1977). Accordingly, utilization of waste mineral slimes discarded by ore milling plants is becoming a common practice to avoid pollution hazards and to improve the techno-economic feasibility of new mining projects. The concept of waste utilization is appealing because it offers two major advantages: 1- waste dispersal problem may be reduced or eliminated, 2- conservation of resources, by partly replacing natural material. There are three obvious positive uses for tailings. Firstly, they may be reprocessed to recover additional values, secondly, all or a portion of tailings may be used for backfill applications, and thirdly, the tailings may be used as one of the raw materials to manufacture higher values products (Michael, 1979)Processing of Sebaeya phosphate ore yields huge amounts of solid wastes and slime clayey fractions. It is estimated that approximately 1.5 megagrams (Mg) of coarse waste(-80mm) and about 1.0 Mg of slimes (–100 μm) are accumulated as stock piles or in tailing ponds. These wastes cause environmental and waste disposal problems. Therefore, this study is devoted to find some alternative uses for these wastes, to reduce their accumulated quantities as well as their enviromentals harms and change them into value-added products. These alternatives can be summarized as follows:

- obtaining a phosphate concentrate product
- manufacture of bricks suitable for non–load bearing walls
- pottery making
- aggregates for road bases and sub-bases
- aggregate for plain concrete
- direct application as natural fertilizer.

UTILIZATION OF PHOSPHATE WASTE

MINERAL PROCESSING OF PHOSPHATE WASTE

There is a large accumulation of waste material produced from the washing plant of Sebaeya phosphate company. The coarse waste dump produced by the crushing and screening section is estimated to be over 1.5 Tg assaying 18-24% P_2O_5. The fine

tailings in the tailing pond is estimated to be over 1.0 million ton assaying 12-19% P_2O_5. These accumulated quantities of waste constitute an environmental hazard and must be reduced and removed. It is advantageous to change these wastes into useful product through mineral processing techniques in order to get high-grade marketable concentrate.

BRICK MAKING

Clay is one of the most abundant mineral material on earth. For production of brick, clay must, however, posses some specific properties. Clay must have plasticity, which permits them to be shaped or molded when mixed with water, and it must have sufficient wet and air-dried tensile strength to maintain their shape after forming. Also when subjected to raising temperatures, the clay particles must be fused together.

Clay bricks are used for an extremely wide range of applications in an equally extensive range of buildings and engineering structures (El-Wageeh, 1995). Among the most common applications are partition walls, party walls, claddings and facings, foundations, paving and floorings.

Bricks are classified according to their variety, quality, and type as follows:

1) varieties: common bricks, facing brick sand engineering bricks
2) quality: internal quality, ordinary quality and special quality
3) types: solid, perforated, hollow, and special shapes and standard.

The physical and mechanical properties of different types of bricks are mentioned in many texts (Nash, 1966). The most important properties are water absorption 20-32 %, compressive strength 30-40 kg/cm^2, and dimension 25x12x6 cm.

POTTERY MAKING

Phosphate slimes, which is a waste material produced from the beneficiation of phosphate ore, can be used in pottery making because it contains very fine clay and clay-like minerals suspended in water (Robertson, 1986). These slimes can be also used with kaolin, feldspar and quartz for the production of satisfactory ceramic tiles.

AGGREGATES FOR ROAD BASES AND SUB-BASES

Road structure today generally consists of four layers shown in Fig. 1, which are collectively termed the pavement. The type of aggregates and thickness of each layer depends on the type of the road and the use to which it is being put. The behavior of all four layers is crucial to the stability and safety of the road.

Unbound granular material is generally used as an important component in road payments as base and sub-base. The foundations as well as the surfaces of the roads can be constructed from these materials. As a base course, they play a structurally im-

portant role, especially in medium and low volume roads. As a sub-base, they protect the soil acting as a working platform and insulating layer against frost action.

The substantial benefits of using these waste materials for road building purpose can be summarized in the reduction of costs, in addition to the solution of the environmental problems.

Crushed rock, mine and mill refuse, and tailings can be used locally in low volume roads, where a lower quality aggregate is more appropriate. The solid wastes generated from the beneficiation of phosphate ores can be used as cheap local waste materials, for road and rail roadbeds. This positive use of wastes can be applied in the areas surrounding the mining zones in roads with less traffic.

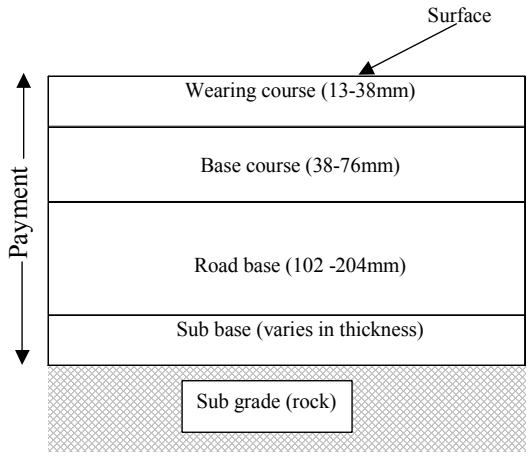

Fig.1. Structural layers in road construction.
Numbers refer to thickness of layers

SOLID WASTE AS CONCRETE AGGREGATES

The possibility of using solid wastes as aggregates in concrete received increasing attention in recent years as one of the promising solution to the escalating solid waste problems. The use of solid wastes for concrete has concentrated mostly on service as aggregates, since this provides the only real utilization of larger quantities of waste materials. The successful utilization of solid wastes in concrete will depend on anticipating potential problems and the ensuing properties of the concrete, and developing uses that comply with these restraints. The mining industry has traditionally made use of its own waste materials, either by reprocessing to recover additional minerals, or by using them for internal construction purposes. Portland cement concrete is made up of Portland cement, water and aggregates. Each of these must meet certain requirements in order that quality concrete is produced. Compressive strength is the simplest and easiest one of all the strength characteristics of concrete to be determined, and

concrete design usually based on this property. Normal strength concrete of grades between 180 to 300 kg/cm^2 is widely used in usual building. Aggregates generally occupy about 70 to 80 % of the volume of concrete and can therefore be expected to have an important influence on its properties.

Aggregates must conform to certain standards for optimum engineering use: clean, hard, strong, durable, practically free of absorbed chemicals, coatings of clay, and other fine materials in amounts that could affect hydration and bond of the cement paste. It is generally advantageous to use as large size of aggregates as possible, although experimental investigations have indicated that the improvement in the properties of concrete with an increase in the size of aggregate does not extend beyond about 40 mm. The normal sizes of coarse aggregate used in concrete mix in Egypt are 40, 20 and 10 mm. Generally, the maximum nominal size of 40 mm is 15x15x15cm (Internet, 2003). They are made in a specified manner, allowed to set, and then cured in the laboratory in a humid room until a specified age. Proper curing requires water and a favorable temperature. Usually the strength is determined 28-day after casting because this is the design strength or common specified strength. However, 7-day strength may also be obtained either as an indication of the expected 28-day strength or as a specified strength.

The purpose of this study is to evaluate the possibility of using solid waste of mill tailings (over screen reject of Sebaeya phosphate company) as a substitution of natural coarse aggregate in a Portland cement concrete mix to produce concrete with compressive strength able to satisfy the construction purposes of small buildings.

DIRECT USE OF WASTE ROCK PHOSPHATE IN AGRICULTURE

Phosphorus is an essential element for the life of animals and plants. Animals get their phosphorus from eating plants and other animals, while plants get their phosphorus from soil.

Phosphorus is also essential in livestock nutrition. Some 80% of the phosphorus in the animal body is in the skeleton. Phosphorus also occurs in many proteins and is necessary for the utilization of carbohydrate. Although phosphorus is a major plant nutrient, its deficiency reduces animal productivity. Serious deficiencies can result in bone disorders and infertility.

In many respects the phosphorus cycle is analogous to the nitrogen cycle. Next to nitrogen, phosphorus is the most abundant nutrient contained in microbial tissue, making up as much as 2% of the dry weight. Partly for this reason phosphorus is the second most abundant nutrient in soil organic matter.

MATERIAL PREPARATION AND CHARACTERIZATION

Head samples of consolidated slimes and solid wastes of Sebaeya phosphate were used. In this investigation, each sample was crushed by jaw crusher followed by roll

mill to minus 0.5mm. The particle size analyses of these prepared wastes are given in Table 1. For pottery making the phosphate slimes and shale were ground to minus 250 micrometers. Table 2 gives the chemical analysis of the used materials.

Table 1. Size analyses of slimes and coarse solid waste samples

Waste type	Slimes			Solid wastes		
Screen size, (μm)	Wt.%ret.	Cum.wt.% ret.	Cum.wt.% Passed	Wt.%ret	Cum.Wt.% ret.	Cum.wt.% passed
+500	00.00	00.00	100.0	00.00	00.00	100.0
-500+315	12.50	12.50	100.0	37.50	35.50	100.0
-315+250-	05.50	18.00	87.50	08.25	43.75	64.50
250+160	19.00	37.00	82.00	17.50	61.25	56.25
-160+125	12.25	49.25	63.00	05.50	66.75	38.75
-125+063	37.25	86.50	50.75	16.50	83.25	33.25
-063	13.50	100.0	13.50	16.75	100.0	16.75

Table 2. Chemical analyses of slimes, solid wastes, and El-Ballas shale

Component	Slimes	Solid wastes	El-Ballas shale	Component	Slimes	Solid wastes	El-Ballas shale
%	%	%	%	%	%	%	%
SiO_2	27.05	08.62	39.05	Na_2O	00.41	00.42	01.08
TiO_2	00.13	00.06	00.41	K_2O	00.17	<0.01	00.75
Al_2O_3	02.15	00.22	19.45	P_2O_5	16.90	24.45	00.40
Fe_2O_3	03.70	01.94	03.65	Cl	00.05	00.06	00.65
MnO	00.20	00.24	00.12	SO_3	00.51	02.80	00.32
MgO	01.10	00.28	01.18	L.O.I	09.33	07.94	19.06
CaO	36.45	48.95	12.85	-	-	-	-

EXPERIMENTAL RESULTS AND DISCUSSION

MINERAL PROCESSING OF PHOSPHATE WASTE

Phosphate waste rock contains certain value of P_2O_5. Due to the variation in composition of each particle according to its size, it was found that the most suitable way to release the phosphate particles from the associated gangue minerals by wet attrition scrubbing at high solid/liquid ratio. The classification of the products into different sizes is carried out by screening for coarse fractions and by hydraulic classification for fine and sub sieve fractions. Suitable sizes were used as feed to study the concentration of the proper feed by direct anionic froth flotation technique in a single stage. In these experiments the effect of the different flotation variables were studied. These variables were solid/liquid ratio, amount of collector, amount of frother, type of

frother, and amount of kerosene. Pure oleic acid was used as a collector while pine oil, Aerofroth 70 and Aerofroth 65 were used as frothers. A sample of rice bran oil supplied by El-Nasr Mining Company was also used as a collector to compare with the oleic acid.

a) Effect of solid /liquid ratio(s/l)

Table 3. Effect of solid/liquid ratio on the grade and recovery

s/l, %	Product	Wt., %	P_2O_5, %	Insol.,	L.O.I	Recovery, %
5	Conc. Tail	80.2 19.8	29.0 ---	10.0 67.0	11.0 8.0	93.0 ---
10	Conc. Tail	81.9 18.1	31.2 ---	10.0 63.0	10.0 8.0	99.0 ---

b) Effect of collector amount

Table 4. Effect of collector consumption on grade and recovery

Collector, (kg/Mg)	Product	Wt, %	P_2O_5	Insol. %	L.O.I	Recovery %
2.8	Concentrate tailings	83.3 16.7	31.5 ---	17.0 44.0	--- ---	99.5
1.4	Concentrate tailings	80.2 19.8	29.5 ---	10.0 67.0	11.0 8.0	94.6
0.70	Concentrate tailings	81.9 18.1	31.2 ---	10.0 63.0	10.0 8.0	99.0

The 0.7 kg/Mg dose of collector gave a reasonable concentrate grade and recovery.

c) Effect of feed size

Table 5. Effect of feed size on flotation products

Feed size (μm)	Product	Wt %	P_2O_5 %	Insol. %	L.O.I %	Recovery %
-500+40	Concentrate Tailing	61.5 38.5	32.2 ---	7.0 36.	7.5 8.5	79.2
-250+40	Concentrate Tailing	77.0 23.0	30.7 ---	7.0 60.0	9.0 ---	94.6
-120+40	Concentrate Tailing	81.9 18.1	31.2 ---	10.0 63.0	10.0 8.0	99.0
-120+20	Concentrate Tailing	66.0 34.0	25.2 ---	30.0 29.0	--- ---	66.5

From the above table it can be seen that the suitable size for flotation was -250+40 μm with a higher weight recovery and concentrate assay of more than 30 percent P_2O_5.

d) Effect of frother type

Table 6. Effect of frother type

Frother	Product	Wt, %	P_2O_5	Insol., %	L.O.I, %	Recovery, %
Pine oil	Conc. Tailings	81.9 18.1	31.2 ---	10.0 63.0	10.0 8.0	99.0
Aero froth 70	Conc. Tailings	75.5 24.5	30.7 ---	9.0 58.0	7.5 7.0	95.0
Aero froth 65	Conc. Tailings	80.5 19.5	33.8 ---	8.0 65.0	10.0 7.0	99.0

It is seen from the above table that Aerofroth 65 is superior to other types of frothers.

e) Effect of collector type

Table 7. Effect of collector type on flotation

Collector	Product	Wt, %	P_2O_5	Insol., %	L.O.I, %	Recovery, %
Oleic acid	Conc. Tailings	80.5 19.5	33.8 ---	8.0 65.0	10.0 7.0	99.5
Rice bran oil	Conc. Tailings	80.5 19.0	31.85 ---	9.5 60.5	10.0 6.5	99.1

Oleic acid as a collector gave better results. However due to the low price of rice bran oil (as a by-product), we recommend its use in flotation.

f) Effect of the amount of kerosene

Table 8. Effect of amount of kerosene

Kerosene, cm^3	Product	Wt, %	P_2O_5	Insol., %	L.O.I, %	Recovery, %
without	Conc . Tailing	10.0 90.0	34.5 ---	--- ---	9.0 7.0	13.8
0.25	Conc . Tailing	80.5 19.0	29.5 ---	10.0 57.0	11.0 7.0	95.0
0.50	Conc . Tailing	80.5 19.0	31.9 ---	9.5 60.5	10.0 60.5	99.0

It is necessary to use kerosene as a collecting aid in the flotation of phosphate waste in order to minimize the use of collector.

g) Effect of grinding method

Table 9. Effect of grinding

Type of grinding	product	Wt%	P_2O_5	Insol. %	L.O.I%	Recovery %
Attrition scrub-bing	Conc . Tailings	91.1 8.9	30.2	7.5 52.0	11.0 9.0	99.5
Disc crusher	Conc . Tailings	51.5 48.5	26.5	8.5 33.0	8.5 9.5	52.5

Attrition scrubbing gave better grade and recovery than disc grinding.

The result of the present study of production of high grade concentrate from waste material of the phosphate washing plant of Sebaeya, the following remarks can be concluded:

1. for a successful flotation process using oleic acid as a collector, it is necessary to remove slime particles less than 40 μm as it has a bad effect on grade and recovery of the flotation process
2. it was possible to obtain a high-grade concentrate of more than 30 percent P_2O_5 at a 10 percent solids in a single stage flotation process
3. the optimum dosage of collector was 0.7 kg/Mg at P_2O_5 31.2 % and a recovery of 95 %. Rice bran oil was also successfully used as a collector
4. optimum results of flotation were obtained for feed size range of -250+40 μm. This fraction was about 35% of the original sample because the coarse and slime fractions were relatively low in P_2O_5
5. different types of frothers were used and Aerofroth 65 gave the best result
6. it is necessary to use sodium silicate to depress silica and kerosene as a collecting aid
7. attrition scrubbing of the feed is better than grinding in a ball mill or disc crusher
8. magnetic separation step prior to flotation reduced the iron content of the concentrate
9. a proposed flow sheet is suggested to obtain a high grade concentrate from this waste material.

USE OF PHOSPHATE WASTE IN BRICKS, POTTERY, ROAD PAVING AND PLAIN CONCRETE

Positive uses of phosphate tailings consume huge amounts of waste materials, which reduce their environmental harms, conserve the natural resources, and add to mining profits.

1. Bricks with acceptable qualities (average comp. strength 152 kg/cm^3 and slake durability index of 99.18%) are produced from a mixture of 90%phosphate slimes and 10% shale.
2. Pottery making is another alternative use of Sebaeya phosphate slimes. The mixture composed of 90% slimes and 10% shale gave pots and jars of reasonable quality. The produced potteries gave water seepage rate of about 0.0075 mm^3/sec·cm^2 without any defected products during firing process and its slake durability index was 99.3%.
3. Solid wastes of the over screen reject can be used in construction of low volume roads where a low quality aggregates is more appropriate.
4. Slime fraction of -40 μm generated from desliming phosphate tailings can be used in either potteries or brick making. For potteries it has a high workability

as it retains high percentage water. Bricks made from the slime fraction and shale show good qualities.

5. Coarse solid wastes can be used in concrete mix without seriously hindering its mechanical properties.
6. Concrete of about 240 kg/cm^2 compressive strength is obtained, which is suitable for the construction of small buildings.
7. The present study matches society's needs for safe and economic disposal of mill tailing of phosphate ores.

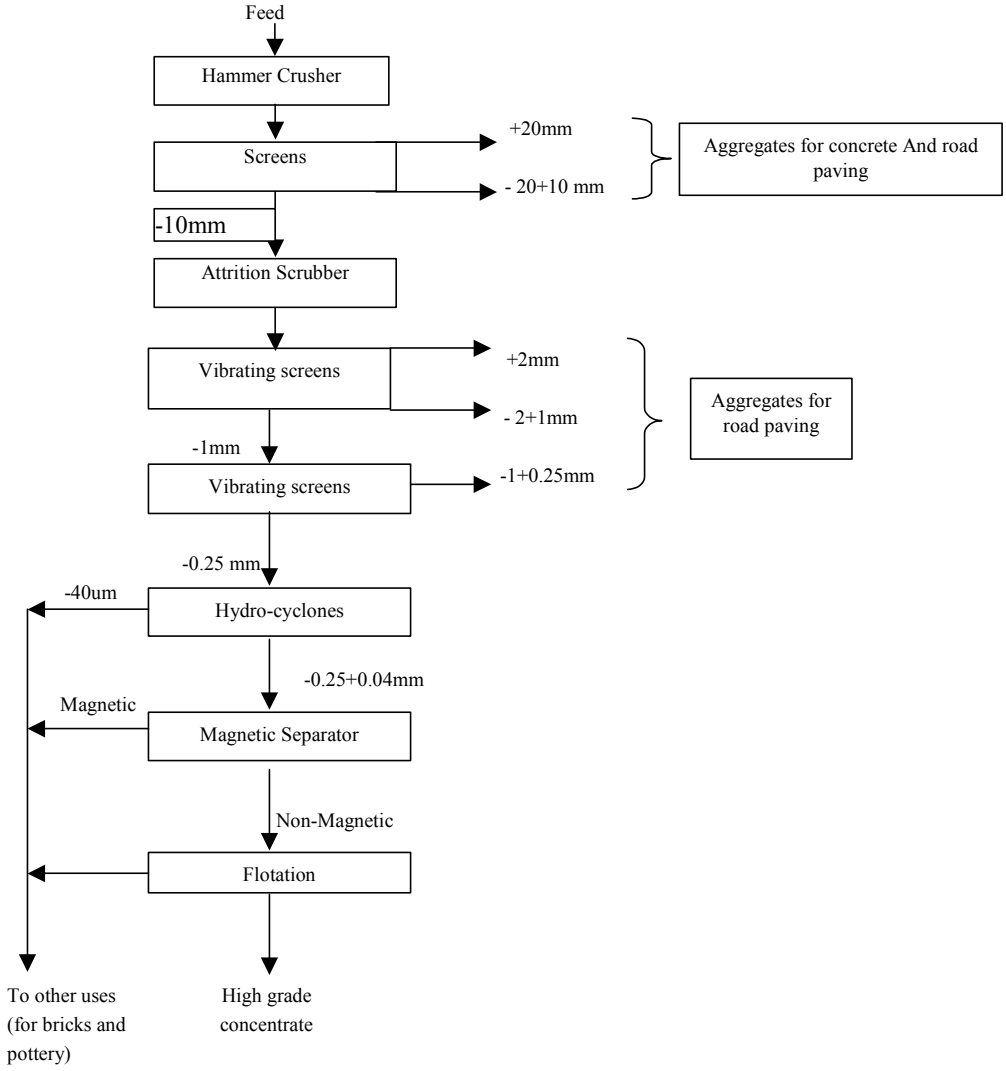

Fig.2. Proposed flow sheet for flotation of Sebaeya low grade phosphate

DIRECT USE OF PHOSPHATE WASTE IN AGRICULTURE

Egyptian soils are normally alkaline, therefore, the low availability of P to plants is common, especially in highly calcareous soils. Maximum phosphorus availability occurs at pH value of 6 to 7. Below this pH range, iron and aluminum phosphate were formed, but above this pH range, minimum solubility of calcium phosphate is formed.

Organic manures can increase the availability of P-forms for the growing crops, by rapid decomposition and liberation of large quantities of carbon dioxide, which dissolves in water to form carbonic and other acids. Organic manures can help to lower the pH of alkaline soil and increase the availability of phosphate to the succeeding crop. On the other hand, phosphate dissolving microbes solubilize insoluble P by producing various organic acids. This available P is taken up by plants.

SUMMARY

1. Approximately 1.5 megagrams (Mg) of coarse waste (-80 mm) and 1.0 Mg of slimes averaging 22 % and 15 % P_2O_5 respectively have been stock piled at El-Mahameed area (East Sebaeya) rejects from the phosphate processing plant.
2. Laboratory-scale tests revealed the technical feasibility of retreatment of the coarse waste to produce a concentrate of more than 30% P_2O_5 at over 90% recovery. The proposed flow-sheet comprises crushing, attrition scrubbing, desliming and direct flotation of phosphate using oleic acid or rice bran oil as collectors. Some equipment of the existing plant may be used in the proposed retreatment mill.
3. Full-scale tests proved the possibility to produce fired bricks from a blend of 90% phosphate slimes and 10% shale with acceptable properties concerning compressive strength, bulk density and slake durability. The same mix could be used for the production of pots and jars of reasonable quality.
4. The coarse phosphate waste can be utilized as aggregates in concrete mix to obtain concrete of more than 240 kg/cm^2 compressive strength as well as the construction of low volume roads.
5. The ultra-fine fraction (-40 micrometers) discarded from the flotation process feed proved to be a suitable raw material for pottery and brick making.
6. Green house experiments showed the possibility of direct application of phosphate tailings in both sandy and calcareous soils at high levels of phosphate uptake which is comparable to commercial super phosphate fertilizers.

REFERENCES

ABOUZEID, A-Z.M., 2008, "*Physical and thermal treatment of phosphate ores-An overview"* Int. J. Miner. Process. vol. 85, no. 4, 58-89.

DOWN, C.G.; and STOCKS, J., May 1977 *" Methods of tailings disposal"* , Mining Magazine, 345-359.
DOWN C.G.; and STOCKS J., July 1977*" Environmental problems of tailings disposal"* , Mining Magazine, 25-33.
Internet communication, 2003 *"Unbound granular materials for road pavements"*
Lancsaster., 1974 *"Bricks, their properties and use" The* construction press LTD, part1, 3-10
NEGM A.A., Feb. 2001 *"Environmental pollution control in mining and mineral processing Plants"*, the 7th Int. Conf. on Min., Pet. and Metall. Eng., (MPM), Assiut, Egypt, vol. 4, 58-62.
NEGM, A.A.; ABOUZEID,A-Z.M., 1977 *"Application of mineral processing technology for Environmental protection and recycling.* 5th Int. Conf. (MPM) Suez, Egypt, 127-145.
NASH, W.G., 1966 *"Brick work 1", Hutchison Technical Education , London, 1-13.*
ROBERTSON, D.J., *1986," Evaluation of phosphate clay and other wastes for construction Products"* Florida Inst. of Phosphate Research, 1-12.
RODRIGUEZ , H.; and FRAGA.R. 1999 " *Phosphate solublizing bacteria and their role in plant growth* promotion. Biotech. Adv., 319-339.
SHAFIC,H.H.; RAMPACEK, C.,1980 *" Resources potential of mineral and metallurgical wastes", Proc. of the Int. Symp. of fine particles processing, AIME, Vol. 2, 1709-1729.*

Negm A.A., Abouzeid A.-Z. M., *Wykorzystanie odpadów stałych po przeróbce fosforytów*, Physicochemical Problems of Mineral Processing, 42 (2008), 5-16 (w jęz. ang)

Większość skał fosforytowych ma niską zawartość fosforu i wymagają one wzbogacania prze wykorzystaniem. Dlatego duże ilości odpadów stałych o podwyższonej zawartości P_2O_5 są generowane w zakładach przerabiających fosforyty. Są one szkodliwe dla środowiska oraz źródłem zanieczyszczania powietrza, wody oraz gleby, a także generują koszty związane z usuwaniem odpadów. Wykorzystanie odpadów przeróbczych staje się więc obecnie codzienną praktyką dla uniknięcia zanieczyszczenia środowiska oraz dla zwiększenia ekonomiki zakładów przeróbczych. W pracy z powodzeniem wykorzystano odpady fosforytowe z zakładu przeróbczego Sebaeya w Górnym Egipcie do produkcji wysokiej jakości materiałów do produkcji kamieni stosowanych do utwardzania dróg oraz produkcji składników cementu, cegieł oraz fajansu, a także bezpośredniego wykorzystania do nawożenia gruntów rolniczych.

słowa kluczowe: fosforyty, odpady, kamienie drogowe, składniki cementu, cegły, fajans, grunty rolnicze

Physicochemical Problems of Mineral Processing, 42 (2008), 17-28
Fizykochemiczne Problemy Mineralurgii, 42 (2008), 17-28

Heba Amin∗, Ashraf Amer*, Anwer El Fecky*, Ibrahim Ibrahim∗∗

TREATMENT OF TEXTILE WASTE WATER USING H_2O_2/UV SYSTEM

Received February 14, 2008; reviewed; accepted July 31, 2008

Treatment of textile wastewater with the Advanced Oxidation Process (AOP) is based on using the H_2O_2/UV system. The optimum condition for treatment of an effluent sample was determined by experimenting on a synthetic dye solution prepared using the blue sulfur dye. Different parameters that affect the reaction rate were tested (UV intensity of 18, 36 and 54 W, initial dye concentration of 70, 80, 90 and 100 ppm, pH 3, original pH of the solution equal to 7.29 and 10 as well as the catalyst dose). Absorbance was measured to determine the decolorization efficiency and then the total organic carbon was measured for the reactions at optimal conditions to assure that decolorization is accompanied by degradation.

key words: wastes processing, waste water, water purification, decolorization

INTRODUCTION

Textile industry ranks top among most consumers. This is due to its raw materials, namely cotton, wool and man-made fibers, which are considered as sources of wealth (Hebiesh, 2000). In Egypt, this industry employs about one million manpower and the lives of many Egyptian families are connected with the textile industry (agriculture, trade and services). Furthermore, many research institutes and large companies are associated with the textile industry.

In Egypt, the textile production emerged thousand of years ago and it was founded on scientific basis in 1927. Egypt became an exporter of textile yarn in 1949. In the past the textile production had depended on the export especially to the European Union. Currently, the trade and export of textile is a complex business, in which many

∗ Environmental Science Department, Faculty of Science, Alexandria University, Alexandria, Egypt
∗∗ Central Metallurgical Institute for Research and Development, El Tabbin, Cairo, Egypt

different aspects, such as marketing, access to the right distribution channels and compliance with the national legislation of the country to which goods will be exported, must be taken into account.

The problems start with the use of pesticides during the cultivation of the natural fibers or by emission during the production of synthetic fibers. Textile raw materials, essentially, cotton, wool, and synthetic fibers pass through several mechanical and chemical stages before reaching the consumer in the form of fabrics or ready-made garment. Certain chemicals which are used in the textile production chain can cause environmental and health problem. These problems may occur during the production process. With respect to emission or occupational health problem e.g., statistical significance RR-4.7 (RR, is a relative risk of individual substance, i.e., the frequency of adverse effects in relation to cumulated doses) was established for exposure to aromatic amines. For those contacting with aniline dyes the relative risk (RR) made up 2.4. The risk to develop bladder cancer in powder shops (RR-3.2) was attributed to the hazards of dyes and diphenylamine. In leather-shoe shops and textile industry the exposure to dyes is not safe (RR-6.1) (Nizamova, 1991; and Kampan et al., 2000). Other problems related to the chemicals used, which appear in the final product and cause, for instance, allergic skin reactions or even cases of cancer.

Textile wastewaters exhibit low BOD to COD ratios (<0.1) indicating non-biodegradable nature of dyes (Pagga and Brown, 1986; Reife, 1993). Fifteen percent of the total world production of dyes is lost during dyeing process and is released in the textile effluents. The release of those colored wastewaters in the ecosystem is a dramatic source of esthetic pollution, eutrophication, and perturbations in aquatic life. As international environmental standards are becoming more stringent (EPA, 1998), technological systems for the removal of organic pollutants, such as dyes, have been recently developed. Among the heterogeneous photocatalysis is the Advanced Oxidation Process or AOP, which can be successfully used to oxidize many organic pollutants present in aqueous systems.

Decolorization of dye effluents has therefore acquired increasing attention. During the past two decades, the treatment of spent textile dyeing wastewater by traditional methods has proven to not be effective for many wastewater treatment facilities. Conventional activated sludge treatment is the typical treatment used today, though activated sludge was not originally used for treatment of industrial wastes, particularly textile wastes containing dyes and surfactants (Yang et al., 1998). Additional textile treatment methods such as combination of biological, physical, and chemical methods including coagulation/flocculation, electrochemical oxidation and activated carbon adsorption, reverse osmosis, ozone and oxidative/reductive chemical processes are all techniques that can be used for treating textile wastewater. Biological processes are not effective enough to decolorize dyes of high photostability while ordinary physical/chemical processes are not strong enough to decompose dye. Hence sludge generations are the principal weakness of these processes (Slokar and Majcen, 1998). The AOP decomposes the chromophore of the dye (Ferrero, 2000; Kurbus et al.,

2002) and consequently realizes complete decolorization, so advanced oxidation processes are being considered as emerging technology to handle large volumes of textile waste water.

The concept behind the AOP is exposure of a strong oxidizing agent to ultraviolet (UV) light generates hydroxyl free radicals, which are stronger than any other oxidants (Bolton and Cater, 1994). The hydroxyl radicals generated after activation have a higher oxidation potential (2.8 V) than hydrogen peroxide (1.78 V) and so dye decolorization is feasible. Advanced oxidation is one of the potential alternatives to decolorize and reduce recalcitrant wastewater loads from textile dyeing and finishing effluents. This process implies generation and subsequent reaction of hydroxyl radicals, which are the most powerful oxidizing species after fluorine (Legrini et al., 1993).

When a water or wastewater containing H_2O_2 is irradiated with UV, hydroxyl radicals are formed which are very powerful oxidizing species (Shu et al., 1994; Namboodri and Walsh, 1996). Furthermore, the H_2O_2/UV process has an additional advantage in that there is no sludge formation during any stage of the treatment (Galindo and Kalt, 1999).

MATERIALS AND METHODS

To experiment on the efficiency of the H_2O_2/UV method, the Bleu-N-RM-2114 dye was purchased from the Engineering Company of Textile (Tenth of Ramadan City). The dye was classified as the sulfur dye. It was used directly as received from the textile industry without further purification. The synthetic dye solutions were prepared by dissolving a defined quantity of the dye into a 1-dm^3 Erlenmeyer flask and diluting it with tap water. They were protected from the light and kept in dark. The registration number of the dye is K3-01-0004, the trade name is Bleu-N-RM-2114, and the IUPAC nomenclature of the dye is sodium-1-amino 4-(2-methyl-5- (methyl phenyl sulfamyl amino) phenyl amino) arthraquinone-2-sulphamate.

Before the oxidation experiments were conducted, it was necessary to choose the appropriate concentration of the dye solution. A standard curve was drawn and concentrations of 70, 80, 90 and 100 ppm were selected for experimentation. The decolorization of the dye solution and wastewater was monitored spectrophotometrically with a UV-visible diffuse reflectance Cecil 7200 spectrometer, the maximum absorbance peak was determined by scanning the dye solution with 4000 nm/mm speed, band width 2 nm, and wavelength range from 190 to 900 nm. The maximum absorbance peak was at wavelength 576 nm for the synthetic dye solution and 462 nm for the effluent sample. In order to evaluate the extent of mineralization, total organic carbon measurements were performed using a "Phoenix 8000" Total Carbon Analyzer.

The wastewater sample used in the present study was effluent from the final clarifier at the Engineering Company of Textile (Tenth of Ramadan City). The effluent

was a murky, orange/maroon color and relatively free of particulate matter and it was directly analyzed for absorbance, total organic carbon, metals and the temperature was measured. Irradiation was performed in a cylindrical Pyrex batch reactor of volume 350 cm^3, fitted with a chamber for the UV lamp to be placed in it. A low-pressure mercury-vapor fluorescent discharge lamp of 18 W consisting of a tubular glass envelope, emitting short-wave ultraviolet radiation (Philips Pl-S, with emission 253.7 to 350 nm), was used. The lamp was placed horizontally in the specified chamber. The cylindrical Pyrex had a source of aeration, to assure continuous homogenization of the dye solution with the reactant and also continuous supply of oxygen.

TREATMENT BY H_2O_2/UV

Synthetic dye solutions were injected in the reactor and dosed with different H_2O_2 volumes (2.5, 5, 7 and 10 cm^3) to study the effect of H_2O_2 concentration on the dye degradation. Also experiments were conducted by changing the pH conditions (3, 7.29, 9 and 11), the initial dye concentrations (70, 80, 90 and 100 ppm) and varying UV intensities (18 W, 36 W and 54 W) to study the effect of these factors on the degradation efficiency. Furthermore, samples were taken every 10 minutes and analyzed for UV/visible absorbance to study the decolorization of the solution and the kinetics of the reaction. Afterwards the most optimal conditions for degradation and decolorization of the synthetic dye solution were chosen and then applied on the wastewater sample. As previously mentioned, 300 cm^3 of the wastewater was placed in the reactor, and treatment took place using the optimal condition. The samples were withdrawn at defined time intervals and analyzed for UV/visible absorbance to determine the decolorization efficiency and the kinetic of reaction. At the end of the reaction time, a each sample was taken and analyzed for the total organic carbon content in order to assure mineralization of the wastewater.

RESULTS AND DISCUSSION

EFFECT OF H_2O_2 DOSE

The effect of H_2O_2 dosage (ranging from 3 cm^3 to 10 cm^3) on the decolorization efficiency was investigated while stabilizing all the conditions of the reaction and altering the H_2O_2 doses. The conditions of the treatment experiment are listed as follows: UV power 18 Wt, dye concentration 70 ppm, reaction time 3hrs, pH 7.29, volume of the dye solution 300 cm^3, room temperature. The effect of the H_2O_2 dose on the decolorization efficiency is shown in Figure 1. It can be observed that the decolorization efficiency increases with increasing hydrogen peroxide dose up to a point where it reaches a maximum and then starts to decrease, where the decolorization efficiency

reached 90.69% at H_2O_2 dose equal to 10 cm^3 (3.9 wt %), whereas above this dose the decolorization efficiency decreased to 82.3% when the applied dose was 12 cm^3 (4.8 wt %) which is consistent with the available literature (Stefan et al.,1996, Chu, 2001 and Ghaly et al., 2001). Daneshvar et al., (2004) reported that in the decolorization of AO7 the same behavior is observed. This behavior is due to the fact that hydrogen peroxide is a scavenger for hydroxyl radicals according to the reaction given in the following equation (Buxton, 1988; Dionysiou et al., 2004):

$$OH^{\bullet} + H_2O_2 \rightarrow HO_2^{\bullet} + H_2O$$
$$2\,HO_2^{\bullet} \rightarrow H_2O_2 + O_2^{\bullet}$$
$$OH^{\bullet} + OH^{\bullet} \rightarrow H_2O_2.$$

When enough hydrogen peroxide is present in the solution, it starts to compete with the dye for reaction with hydroxyl radicals since $HO_2^{\bullet}$ is less reactive than the $OH^{\bullet}$ radical. An increased level of hydrogen peroxide has a diminishing effect on the reaction rate (Aleboyeh et al., 2005). In addition, the $OH^{\bullet}$ radicals generated at a high local concentration will readily dimerize to H_2O_2. Therefore, it is important to optimize the applied dose of hydrogen peroxide to maximize the performance of the UV/H_2O_2 process and minimize the treatment cost. The optimum dose for this experiment is 10 cm^3 (3.9 wt %) where the decolorization efficiency reached 90.69%, whereas above this dose the decolorization efficiency decreased to 82.3%, when the applied dose was 12 cm^3 (4.8 wt %). The hydrogen peroxide concentration is an important parameter to adjust and control the decolorization of dyes in the UV/H_2O_2 reactor. Degradation of the color is due to the hydroxyl radicals generated upon photolysis of hydrogen peroxide (Namboodri and Walsh, 1996; Arslan and Balcioglu, 1999). Several studies have proposed different reaction mechanisms for this photolysis. It is widely accepted that the main interaction between H_2O_2 with UV radiation and free radicals are well represented by the following reactions (Alfano et al., 2001).

Propagation

$$H_2O_2 + OH^{\bullet} \rightarrow O_2H^{\bullet} + H_2O_2$$
$$H_2O_2 + O_2H^{\bullet} \rightarrow OH^{\bullet} + H_2O.$$

Termination

$$OH^{\bullet} + OH^{\bullet} \rightarrow H_2O_2$$
$$O_2H^{\bullet} + O_2H^{\bullet} \rightarrow H_2O_2 + O_2$$
$$OH^{\bullet} + O_2H^{\bullet} \rightarrow H_2O + O_2\,.$$

The powerful oxidizing hydroxyl radicals react with the dye molecules resulting in the destruction of their intrinsic color.

Decomposition

$$RX + OH^{\bullet} \rightarrow \text{products}$$
$$RX + O_2H^{\bullet} \rightarrow \text{products}.$$

The $OH^{\bullet}$ radicals are capable of oxidizing organic compounds mostly by hydrogen *abstraction*

$$RH + OH^{\bullet} \longrightarrow R^{\bullet} + H_2O.$$

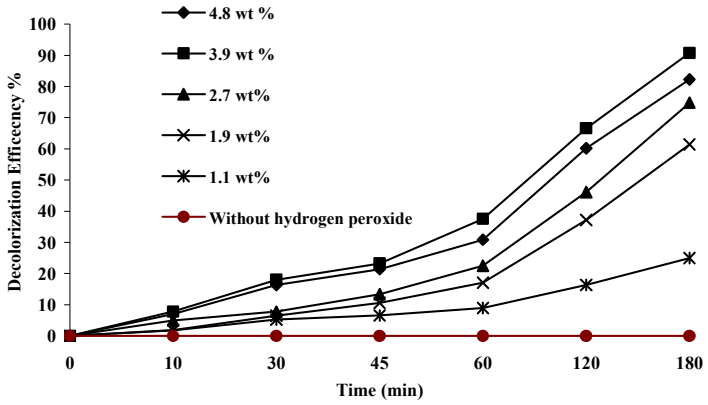

Fig.1. Effect of H_2O_2 concentration on the decolorization efficiency of dye solution using H_2O_2/UV system

This reaction generates organic radicals which by addition of molecular oxygen yield peroxyl radical. These intermediates initiate thermal chain reactions of oxidative degradation leading finally to carbon dioxide, water and inorganic salts. Electrophilic addition of $OH^{\bullet}$ radicals to organic π (double bond) systems constitutes another mechanism of oxidative degradation.

EFFECT OF UV POWER

The effect of the UV power on the decolorization efficiency was also studied, by testing UV intensities of 18, 36 and 54 W. The experiments were performed as mentioned earlier, while stabilizing all the other conditions. These conditions are: H_2O_2 dose 3.9 wt %, dye concentration 70 ppm, reaction time 3hrs, pH 7.29, volume of dye solution 300 cm^3. As shown in Figure 2, when the UV power was 18 W, the decolorization efficiency was 7.84% after 10 min, and then, at the end of the 3 hrs of decolorization, the efficiency reached 90.69%. By increasing the UV power to 36 W, the decolorization efficiency became 21.84% after 10 min, and finally the decolorization efficiency reached 94.7% at the end of the 3 hrs. The UV power was further increased to 54 W to study its effect on the decolorization efficiency. The data showed that after 10 min the decolorization efficiency was 24.93% after 10 min, then at the end of the 3 hrs the decolorization efficiency was 100%. This reveals that increasing the UV power from 18 to 54 W the removal efficiency increased from 90.69% to

100%. This increase in decolorization is due to increased production of hydroxyl radical. At low UV power, the rate of photolysis of H_2O_2 into hydroxyl radical ($H_2O_2+h\upsilon \rightarrow 2^{\bullet}OH$) is reduced (Yang et al., 1998).

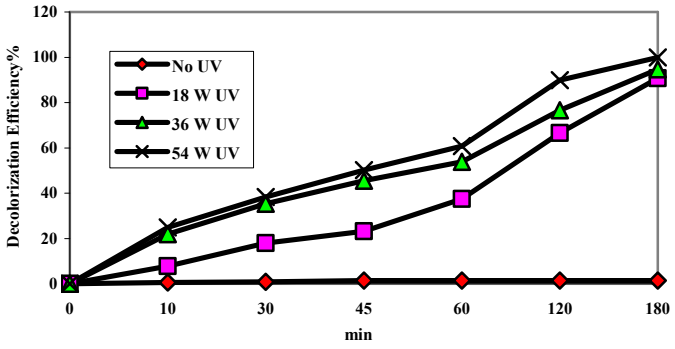

Fig. 2. Effect of UV power on decolorization efficiency

Therefore, the best optimal condition for the experiment is utilizing the UV power of 54 W, because it yields the maximum decolorization percentage.

EFFECT OF THE INITIAL DYE CONCENTRATION ON THE DECOLORIZATION EFFICIENCY

After studying the effect of the two previous factors, another factor was studied which is the effect of the initial dye concentration on the decolorization efficiency. This factor was studied by stabilizing all the other conditions as follows: H_2O_2 dose 3.9 wt %, reaction time 3 hrs, pH 7.29, UV power 54 W, volume of the dye solution 300 cm^3, room temperature. The results show that by increasing the initial dye concentration from 70 ppm to 100 ppm the removal efficiency decreased from 100% to 70.5%.

Hydroxyl radical is mainly responsible for dye decolorization and its concentration remains constant for all dye concentration. The increase in dye concentration increases the number of dye molecules and not the hydroxyl radical concentration and therefore the removal rate decreases. The increase in dye concentration may also induce a rise of the internal optical density and the solution becomes more and more impermeable to UV radiation. Then, hydrogen peroxide can only be irradiated by a smaller portion of UV light to form less free radicals and the color degradation rate decreases (Aleboyeh et al., 2005). Aleboyeh et al., (2003) obtained similar results for the acid orange 8, acid orange 7, and methyl orange dyes.

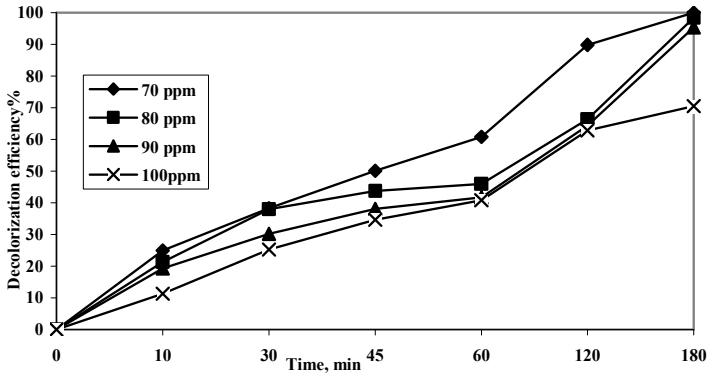

Fig.3. Effect of initial dye concentration on the decolorization efficiency of the blue dye solution using H_2O_2/UV

EFFECT OF pH ON DECOLORIZATION EFFICIENCY

The effect of pH on the decolorization efficiency of the blue dye solution was studied by stabilizing all the other conditions and only changing the pH of the dye solution where H_2O_2 dose was 10 cm^3, reaction time 3 hrs, UV power 54 W, dye concentration 70 ppm, volume of dye solution 300 cm^3. As shown in Figure 4, the decrease of the pH from the original conditions of the dye solution (pH=7.29) to 3.03 has slightly decreased the removal efficiency from 100% to 98.75% while increasing the pH from the original conditions of the dye solution (7.29) to 11.11 led to a decrease in the removal efficiency from 100% to 86.96%. It can be concluded that the pH increase leads to a decrease in the decolorization efficiency. This can be explained by the fact that part of H_2O_2 is used for the oxidation of alkalis (NaOH) during the decolorization forming sodium peroxide (Na_2O_2). As a result, less hydrogen peroxide is available for the formation of hydroxyl radicals and consequently the degradation of the dye decreases. This behavior is especially noticeable at higher concentration of NaOH as follows:

$$2NaOH + H_2O_2 + 6\ H_2O \rightarrow Na_2O_2 + 8H_2O.$$

Oxidation with H_2O_2 should therefore be performed in acidic medium, but acidification and neutralization increase the cost of such processes. Fortunately in our case there was no great effect of acidification on the decolorization efficiency of the synthetic dye solution.

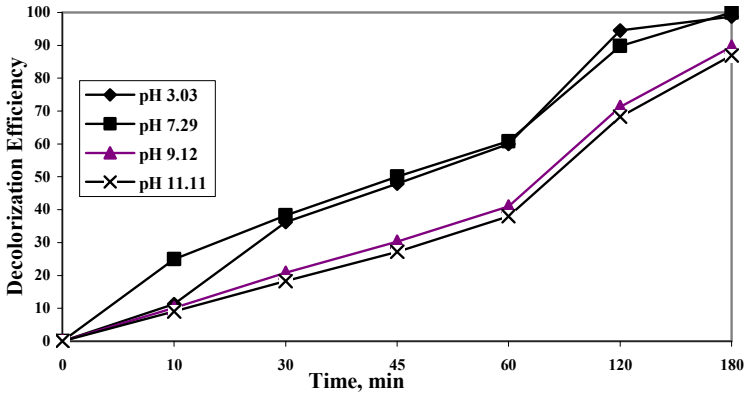

Fig.4. Effect of pH variation on the decolorization efficiency of the blue dye solution using H_2O_2/UV

The most favourable conditions which give a full decolorization rate are as follows: H_2O_2 dose 10 cm^3 (3.9 wt %), pH 7.29, initial dye concentration 70 ppm, UV intensity 54 W. The total organic carbon or TOC, a measure of the quantity of organically bound carbon that can be oxidized to CO_2, was analyzed before and after the decolorization process to prove that the decolorization of the solution is accompanied by degradation and mineralization of organic matter. It was found that the TOC of the original dye solution was 62 mg/dm^3 and after treatment it reached 4.34 mg/dm^3 (removal efficiency 93%). It can be concluded that although the decolorization efficiency reached 100% but the TOC removal did not reach that percentage. This may be attributed to the destruction of the dye into intermediates that are no longer visible and need smaller amounts of oxygen to completely oxidize, while at the same time these intermediates cause higher TOC values (Kurbus et al., 2002).

TREATING THE EFFLUENT SAMPLE USING H_2O_2/UV SYSTEM

First, TOC was determined (700 mg/dm^3) before applying the H_2O_2/UV treatment method, then the treatment was carried under the optimum conditions of the H_2O_2/UV system: H_2O_2 dose 10 cm^3 (3.9 wt %), pH 7.29, initial dye concentration 70 ppm, UV intensity 54 W. After 5 hours the TOC was determined as 105 mg/dm^3 (removal efficiency 85%).

CONCLUSIONS

It can be concluded that although the decolorization efficiency reached 100% but the TOC removal did not reach that percentage. This may be attributed to the destruction of the dye into intermediates that are no longer visible and need smaller amounts

of oxygen to completely oxidize while at the same time these intermediates cause higher TOC values (Kurbus et al., 2002). It can be noticed that the TOC removal percentage in the effluent sample is less than removal efficiency of the synthetic dye solution (except for the ozone system). This can be explained by two reasons:

1. presence of other than dyes refractory materials
2. increase in alkalinity which may be due addition of sodium carbonate.

Sodium carbonate is the common auxiliary chemical employed in textile processing operations where it is used in the dyeing path in order to adjust the pH of the bath as it plays an important role in fixing the dye on the fabrics and in the fastness of color.

The decrease in the degradation of the sample in the presence of carbonate ions is due to the hydroxyl scavenging property of carbonate ions which can be accounted from the following reactions:

$$OH^{\cdot} + CO^{2-}_3 \longrightarrow OH^- + CO_3^{-\cdot}$$
$$OH^{\cdot} + HCO^-_3 \longrightarrow H_2O + CO_3^{-\cdot}.$$

It can also be noticed that the TOC removal is incomplete while the color has completely disappeared. This phenomenon may be due to the destruction of the chromophore of the dye which is responsible for the color appearance and transforming it into smaller fragments of molecules (intermediates). Extending the reaction time should completely eliminate the TOC.

REFERENCES

ALEBOYEH, A. ALEBOYEH, H. and MOUSSA, Y., 2003. Critical effect of hydrogen peroxide in photochemical oxidative decolorization of dyes: acid orange 8, acid blue 74 and methyl orange. Dyes and pigments. Vol. 57, pp. 67-75.

ALEBOYEH A., MOUSSA Y. ALEBOYEH H., 2005. The effect of operational parameters on UV/H_2O_2 decolourisation of Acid Blue 74. Dyes and Pigments, Vol. 66, pp. 129-134.

ALFANO, O.M., BRANDI, R.J., CASSANO, A.E., 2001. Degradation kinetics of 2,4-D in water employing hydrogen peroxide and UV radiation. Chem. Eng., Vol. 82, pp. 209–218.

Arslan, I. and Balcioglu, A.I., 1999. Degradation of commercial reactive dyestuffs by heterogenous and homogenous advanced oxidation processes: a comparative study. Dyes and Pigments, Vol. 43, pp. 95–108.

BUXTON G.V., GREENSTOCK, C.C., HELMAN ,W.P., ROSS, A.B., 1988. Chemical review of rate constants for the reaction of hydrated electrons, hydrogen atoms and hydroxyl radicals in aqueous solution. Phys. Chem., Vol. 17, pp. 513-586.

CHU, W., 2001. Modeling the quantum yields of herbicide 2,4-D decay in UV/H_2O_2 process. Chemosphere, Vol. 44, pp. 935–941.

DANESHVAR, N., RABBANI, M., MODIRSHAHLA, N. BEHNAJADY, M.A., 2004. Photooxidative degradation of Acid Red 27 (AR27): modeling of reaction kinetic and influence of operational parameters. J. Environ. Sci. Health A, Vol. 39, 2319–2332.

DIONYSIOU D.D., SUIDAN T.M., BAUDIN I. LAIN´E J.M., 2004. Effect of hydrogen peroxide on the destruction of organic contaminants-synergism and inhibition in a continuous-mode photocatalytic

reactor, Appl. Catal. B, Environ. Vol. 50, pp. 259–269.
FERRORO, F., 2000. Oxidative degradation of dyes and surfactant in the Fenton and photo-Fenton treatment of dye house effluents. JSDC., Vol. 116, pp. 148- 153.
GALINDO C., JACQUES P. KALT A., 1999. Total mineralization of an azo dye (Acid Orange 7) by UV/H_2O_2 oxidation. J. Adv. Oxid. Technol., Vol. 4, No.4, PP.400–407.
GHALY, M.Y., H◡RTEL, G., MAYER, R., HASENEDER, R., 2001. Photochemical oxidation of p-chlorophenol by UV/H $_2O_2$ and photo-Fenton process: a comparative study. Waste Management, Vol. 21, pp. 41–47.
HEBIESH A., 2nd edn., 2000. Social town environmental problem for textile industry development, National Research Center, Egypt. p. 381.
KAMPAN, V., MERGET, R. BAUR, X., 2000. Occupational airway sensitizers, American Journal of Industrial Medicine, USA. Vol., 38, pp. 164-218.
KURBUS, T., SLOKAR M.Y. MAJCEN LE MARECHAL, A., 2002. The study of the effects of the variables on H_2O_2/UV decolorization of vinylsulphone dye: II. Dyes and Pigments, Vol., 54, pp. 67-78.
LEGRINI, O., OLIVEROS, E., BRAUN, A.M., 1993. Photochemical processes for water treatment. Chem. Rev., Vol. 93, pp. 671–98.
NAMBOODRI, C.G. WALSH, W.K., 1996. Ultraviolet light/hydrogen peroxide system for decolorizing spent reactive dyebath waste water. American Dyestuff Reporter.
NIZAMOVA, R.S., 1991. Occupational hazards and bladder cancer, Urol Nefrol, Russian. Vol., 5, pp. 35-38.
PAGGA, U., BROWN, D., 1986 .The degradation of dyestuffs part II: behaviour of dyestuffs in aerobic biodegradation tests. Chemosphere, Vol. 15, No. 4, pp. 479-491.
REIFE A., 1993. Dyes environmental chemistry. In Kirk. (ED). Othmer encyclopedia of chemical technology. Vol 8. 4th ed. New York: John Wiley and sons Inc: 1993. p. 753-84.
SHU, H., HUANG, C., CHANG, M. 1994. Decolorization of Mono-Azodyes in wastewater by Advanced Oxidation Processes: A Case Study of Acid Red 1 and Acid Yellow 23. Chemosphere, Vol. 29, pp. 2597-2607.
SLOKAR, Y.M. MAJCEN LE MARECHAL, A., 1998. Methods of decoloration of textile wastewaters. Dyes and Pigments, Vol., 37, pp. 335-356.
STEFAN, M.I., HOY, A.R. BOLTON, J.R., 1996. Kinetics and mechanism of the degradation and mineralization of acetone in dilute aqueous solution sensitized by the UV photolysis of hydrogen peroxide. Environmental Science and Technology, Vol. 30, pp. 2382–2390.
YANG M., HU J., ITO K., 1998. Characteristics of Fe^{2+}/H_2O_2/UV oxidation process. Environ. Technol., Vol. 19, pp. 183-191.

Amin H., Amer A., El Fecky A., Ibrahim I., *Przeróbka wody odpadowej za pomocą sytemu H_2O_2/UV*, Physicochemical Problems of Mineral Processing, 42 (2008), 17-28 (w jęz. ang)

Przeróbka wód odpadowych przemysłu farbiarskiego metodą Advanced Oxidation Process (AOP) jest oparta na układzie H_2O_2/UV. Określono eksperymentalnie optymalne warunki przerobu odcieków dla syntetycznego barwnika *blue sulfur*. Badano parametry które wpływają na szybkość reakcji (intensywność UV na poziomie 18, 36 oraz 54 W, początkowe stężenie barwnika 70, 80, 90 oraz 100 ppm, pH 3 oraz naturalne wynoszące od 7.29 do 10, jak również ilość katalizatora). Mierzono absorbancję dla określenia wydajności odbarwiania orz całkowitą ilość węgla organicznego dla optymalnych warunków reakcji zapewniających rozpadu barwnika w trakcie jego dekoloryzacji.

słowa kluczowe: przeróbka odpadów, wody odpadowe, oczyszczanie wód, dekoloryzacja

Physicochemical Problems of Mineral Processing, 42 (2008), 29-36
Fizykochemiczne Problemy Mineralurgii, 42 (2008), 29-36

Katarzyna Rotuska*, Tomasz Chmielewski*

GROWING ROLE OF SOLVENT EXTRACTION IN COPPER ORES PROCESSING

Received May 15, 2008; reviewed; accepted July 31, 2008

Heap leaching of oxide copper ores and cathode copper recovery by solvent extraction (SX) and electrowinning (EW) has been well established as a primary low-cost hydrometallurgical copper recovery method. Subsequently, hydrometallurgy was also gradually developed and applied for sulphidic ores and concentrates. Presently, more than 20 % of total world production of copper is achieved through the solvent extraction route. The success of this method led to a significant revival in the development of hydrometallurgical processes to recover copper from ores both sulphidic and oxidized. This work reviews the major problems related to solvent extraction from pregnant leach solutions (PLS) after leaching oxide and sulphide copper minerals.

key words: heap leaching, extraction, electrowinning, copper oxide, copper ore, sulfides

INTRODUCTION

At present, there are basically two main methods employed world wide in order to process copper ores for metal production. The most important one is the "conventional" - pyrometallurgical method, comprised numerous types of shaft and flash technologies, which consists of crushing, grinding, flotation, smelting-refining and electro-refining. This method is applied to sulphide flotation concentrates rather than ores and is economically feasible for copper rich feed and for large scale operations.

A second method, "hydrometallurgical", is applied to the rest of the world's primary copper production. Hydrometallurgy consists of crushing, leaching (non-oxidative leaching, atmospheric leaching and pressure leaching), solvent extraction and electrowinning. Hydrometallurgical processing can be effectively applied for oxi-

* Chemical Metallurgy Division, Department of Chemistry, Wroclaw University of Technology, Wybrzeże Wyspiańskiego 23, 50-370 Wroclaw, Poland, tomasz.chmielewski@pwr.wroc.pl

dized ores, containing CuO, Cu_2O, carbonates and some silicates, as well as for sulphide ores with chalcopyrite as a predominant copper mineral. Hydrometallurgical methods are used in countries having readily available deposits with low copper content and with surplus of oxidized forms at the same time (USA, Chile, Australia, and Peru). Recently, observed is a considerable intensification in research and development of hydrometallurgical ore, by-product and concentrate treatment as alternative to traditional pyrometallurgical processes for sulphidic ores and concentrates, particularly for small scale production and for remote metal resources - not acceptable by pyrometallurgy.

Hydrometallurgy has been used for copper recovery for more than 300 years. The most important development in copper hydrometallurgy, with respect to the growing number of its applications as well as for its future potential, has been solvent extraction. It became the achievement which revolutionized copper production all over the world and enabled to introduce hydrometallurgy for industrial scale. First SX small scale plants started in 1968 and already in 1974 copper production was expanded to a large scale of about 0.1 Tg/year (Szymanowski, 1996).

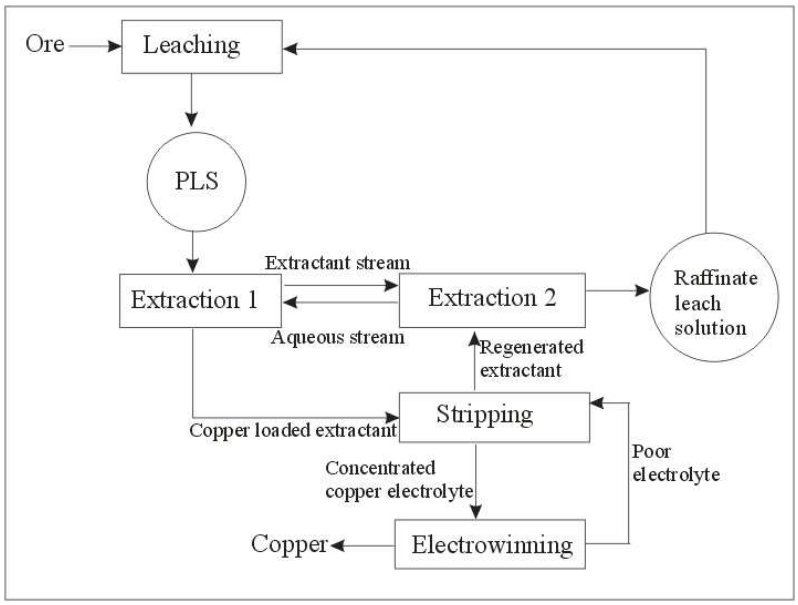

Fig. 1 Typical flow-sheet diagram of LX/SX/EW plant (Bergh and Yianatos, 2001)

Figure 1 shows a typical flow-sheet of hydrometallurgical copper processing, which consists of three fundamental unit operations:

- leaching of copper ore with a week acidic solution, which usually is sulfuric acid,

- solvent extraction, in which the aqueous pregnant leach solution (PLS) is vigorously mixed with an organic solvent, selectively recovers copper from PLS, being acidic or ammonia solution. The organic solvent is then separated and the copper stripped from it with a fresh acidic solution to produce a highly concentrated, relatively pure copper liquor suitable for the final step–electrowinnig or precipitation,
- electrowinning, where copper-rich solution is filtered to remove entrained organics, heated, and then passed through a series of electrolytic cells to form high quality cathodes, which are the market deliverable product (Bartos, 2002).

According to International Copper Study Group data, during the last decade world copper mine production increased by 30 %, from 11.5 Tg (million metric tones) in 1997 to 15 Tg in 2006. Simultaneously, production of copper in concentrates rose by 24 % while production by solvent extraction–electrowinning (SX/EW) rose as high as by 63 % (Fig. 2) (ICSG, 2007).

Furthermore, world mine production in 2007 increased by 3 % to 15.5 Tg and it is expected to increase in 2008 by 6 % to 16.4 Tg, and in 2009 of 1.5 Tg (9 %) to 17.9 Tg owing to mine developments and increased capacity utilization. For 2007–2009 higher growth rates are expected for SX/EW production (about 4.5 Tg in 2009) (ICSG, 2008).

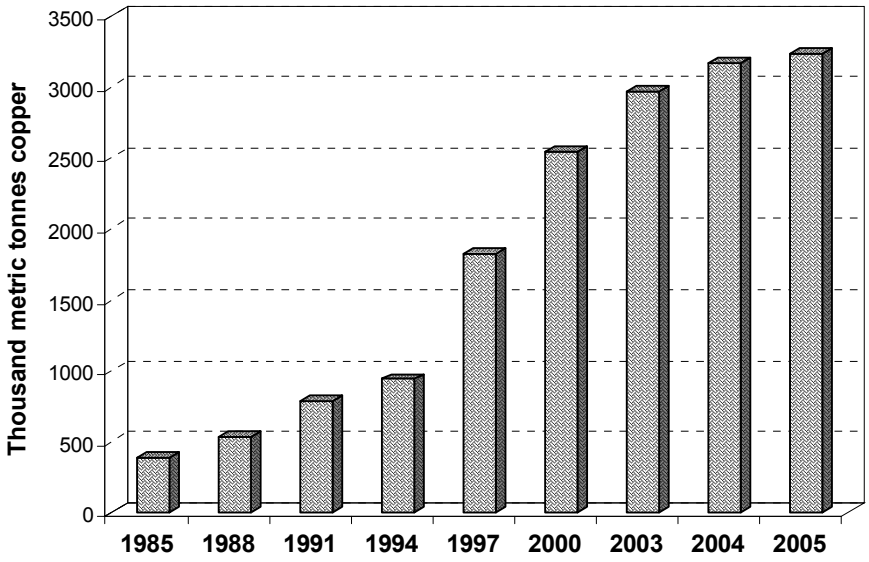

Fig. 2. World trends in SX capacities for copper from 1985 to 2005

Therefore, an enormous role of solvent extraction in growing copper production can be clearly seen. Moreover, the application of SX/EW technique for processing of waste oxide copper ores appeared to be the most economical process for copper pro-

duction in the world. Typical cash operating costs for mine/heap leach/SX/EW operations are in the range of $0.40-0.55 US/lb Cu, depending on ore grade, mining costs, Cu recovery, acid requirements and power costs (Peacey et al., 2008)

RESEARCH AREA

Implementation of hydrometallurgical technique for copper production, using solvent extraction on an industrial scale, has strongly stimulated studies on synthesis of novel extractants as well as on the extraction process. Solvent extraction provides a possible process whereby a pure feed to electrowinning could be obtained if an appropriate copper extractant is available. Until now, the most popular and unbeatable copper extractants are hydroxyoximes. It results from a number of their advantages in terms of fast extraction kinetics and high extractant strength, allowing the extraction of copper from highly acidic PLS with good selectivity over iron(III). However, increasing the extractant strength increases the acid strength required for stripping. Thus, it is not acceptable to most copper producers because the acid concentration is too high for electrowinning purposes.

To overcome these difficulties different types of modifiers can be added. Although, it ought to be mentioned, that the use of modified extractants results in more SX circuit cross –contamination and worse selectivity than it was reported for unmodified extractants. High Cu/Fe rejection ratio is very desirable feature of all copper extractants, because the appearance of iron in the tankhouse results in low current efficiency for the cathodic deposition of copper.

All advantages and disadvantages must be taken into account when selecting the best copper extractant for any particular application. It is important that each reagent should accomplish the basic requirements, listed below:

- good ability to extract the metal at the required pH
- selectivity for the required metal and rejection of undesired metals
- acceptable rates of extraction, scrubbing and stripping
- good solubility in the organic phase and restricted solubility in the aqueous phase
- high stability throughout the principal stages.

Besides finding an appropriate extractant, there are also other problems related to SX plants, like crud formation and entrainment. There is still no possible to fully eliminate these problems but scientists still work on minimizing the unwanted effects on extraction efficiency.

At present, the most up-to-date problem is application of solvent extraction for copper processing from sulphide ores. The success of SX plants in the copper recovery system results from easy leachability of oxide ores, while the main obstacle for

application of hydrometallurgy for sulphide ores processing is difficulty of their leaching, relevant to scarce solubility of copper sulphides, particularly chalcopyrite. Therefore the efforts of scientists are focused mainly on finding the best efficient leaching method and then liquid-liquid extraction from received pregnant leach solutions.

DISCUSSION

At the beginning, hydrometallurgy based on solvent extraction, could not compete with conventional copper recovery methods based on smelting because the quality of copper produced was lower than that produced by smelting followed by electrorefining. By 1977, the SX/EW process had improved to such extent that most production now resulted in high-quality cathode that could be directly used by wire rod plants, without further refining. This made the SX/EW process superior to cement copper in terms of product quality and costs, production of SX/EW copper rapidly increased. When the major breakthrough of a flexible extractant was developed, there rapidly followed a whole series of minor improvements, all of which contributed significantly to SX/EW's overall productivity. New organic extractants greatly reduced iron adsorption and allowed for a much wider range of copper concentrations (Bartos, 2002).

The greatest contribution in achievements of solvent extraction provided extractants based on hydroxyoximes. As they were synthesized there were no better copper extractants, and since then all investigations were performed in order to improve their properties. The very important issue for researchers has been an increase of extractant strength and consequently an improvement of stripping efficiency. Initially, different mixtures of extractants were used, for example Cognis reagent LIX 64N (blend of LIX 64 and LIX 63). LIX 64 alone was able to extract copper selectively from iron in the pH range 1.5-2.5, but with the disadvantage of slow rate of extraction. This was solved by the addition of a small amount of LIX 63. The mixture, LIX64N, for many years was the extractant of choice for commercial copper extraction from acidic leach solution (Szymanowski, 1993).

Other extractants, based on organophosphorus compounds (Cyanex series of extractants), were also widely tested for copper recovery, but the results could not be accepted for further applications. It was shown that in order to achieve a reasonable level of copper stripping from Cyanex 302 13.5M acid was required, and in the case of Cyanex 301 even the use of concentrated (18M) H_2SO_4 did not strip copper from organic phase (Sole, Hiskey, 1995). From other paper it was clear that among all Cyanex series only Cyanex 272 can be successfully used in hydrometallurgy but only for the separation and recovery of cobalt from nickel (Flett, 2005).

As mentioned previously, to solve problems related to stripping performance the addition of modifiers to organic phase was necessary. Such modified "blend" results in a mixture that is a weaker extractant while at the same time it is easier to strip with

conventional electrowinning electrolytes. As an example Avecia with their Acorga reagents have showed that addition to the hydroxyoxime of nonyl phenol, tridecanol or alkyl esters improves the stripping performance, with only little effect on extraction (Cox, Musikas, Chopin, 2004). However, what should be strongly pointed, some deleterious problems appeared, related to addition of modifiers. The very important ones are crud formation and entrainment, which result in greater contamination of electrolyte with leach solution, greater losses of extractant and solvent from the extraction circuit and worse selectivity (Merigold, 1996).

To cope with these problems a new innovation was established by Outokumpu Oyj in Finland – the Vertical Smooth Flow (VSF^{TM}), mixers which have been extensively piloted at Chuquicamata and are said to significantly reduce the amount of entrainment in the raffinate stream. The basic idea of the VSF^{TM} technology is to maintain smooth agitation throughout the SX plant to avoid oxidation of organic and development of overly small droplet size in dispersion. These principles give Outotec's SX plant the flexibility to run in widely varying conditions and to have high trough output with very little organic losses and crud formation (Outotec Oyj., 2007).

All the issues discussed above, were related to solvent extraction from solutions after leaching oxide ores. The real question is what will differ in the case of sulphide ores? If there will be any new problems, what should be taken into account? Copper sulphide minerals are not readily leached by conventional heap leach methods and require more vigorous or non-conventional conditions (the presence of oxidant or bacteria) for effective copper recovery. To solve this problem a lot of processes using different leaching agents (bacteria, sulphate, sulphate/chloride, and halides) have been developed in order to process sulphide copper ores: BioCop, Bactech/Mintek, CESL, Albion, Sepon, Mt. Gordon, HydroCopper (Peacey et al.; Dreisinger, 2006). There is, however, no hydrometallurgical technology which could be directly used for processing sulphidic copper ore, by-product or concentrate from each deposit.

At present a lot of attention is bestowed upon bioleaching methods. There are several examples of industrial bioleaching operations in Chile (Quebrada Blanca operation), USA and Australia (Girilambone Mine) (Dresher, 2004). Other solution was provided in Konkola Deeps sulphide deposit in Zambia (Avecia Notes, 2003). The sulphide material was concentrated by flotation up to 40-45 % Cu and then subjected to a high pressure acid leach. The autoclave liquid discharge contained 60 g/dm^3 Cu and 5 g/dm^3 H_2SO_4. This enabled the pregnant leach solution to be purified directly by means of SX. Another method applied for sulphide ores is total pressure oxidation process (commercialized by Phelps Dogde in 2007), which uses high temperature and pressure oxidation conditions to oxidize all sulfide minerals. The autoclave stream is merged with stockpile leach solution stream to provide a combined PLS feed to the SX/EW facility. The process has been commercially demonstrated at a large-scale and should be regarded as a "proven" technology (Dreisinger, 2006).

The development of new leaching technologies for sulphide ores has also necessitated requirements for solvent extraction of copper from more concentrated feed solu-

tions. Until recently, typical leach solutions contained 0.5 to 8 g/dm^3 Cu at 15 to 25 °C. Leaching of high grade copper sulphide ores and copper concentrates result in leach solutions having 15 - 60 g/dm^3 Cu and 2-50 g/dm^3 sulphuric acid, at high temperatures. Therefore, significantly higher reagent strengths are required to achieve recoveries comparable to those obtained for conventional heap or dump leach liquors.

Other challenges for the solvent extraction reagents can include higher impurity levels and higher solution temperatures tolerance (Kordosky et al., 2006). The best reagent to achieve this for a number of years was Acorga P - 5100 but in recent years it has been replaced with new Acorga reagents such as M5640 and PT5050 both of which exhibit better selectivity and higher recovery characteristics. This new class of modified aldoxime extractants has greatly contributed to the growth trend in SX/EW technology. Extensive pilot plant studies and existing operations have demonstrated that current copper solvent extraction reagents are suitable for use with concentrated feed solutions but further investigations are necessary to establish optimal conditions of solvent extraction processes in copper ore processing.

SUMMARY

The leaching and SX/EW technique has been rapidly developing world-wide technology for copper production in recent years. For many years this technology was related mostly to oxide copper ores, but recently we can observe a growing interest in application of this method also for sulphide ores, by-products and concentrates processing. The success could not be obtained if there will be no good leaching method for this sulphidic material. With the recently developed technologies that are now under investigations in demonstration plants and ongoing research into improved technologies, we can safely predict that solvent extraction will eventually contribute to an increasing fraction of the copper produced each year not only from oxide but also from sulphide ores.

REFERENCES

Acorga Notes, 2003, Solvent Extraction of Copper form High Concentration Pressure Acid Leach Liquors, Acorga Notes, 8, 4 - 6, www.cytec.com

BARTOS P. J., 2002, SX-EW copper and technology cycle, Resources Policy, 28, 85-94.

BERGH L. G., YIANATOS J. B., 2001, Current status and limitations of copper SX/EW plants control, Minerals Engineering, 14 (9), 975 - 985.

COX M., MUSIKAS C., CHOPPIN G., 2004, Solvent extraction Principles and Practise, Second edition, Marcel Dekker Inc., New York.

DREISINGER D., 2006, Copper leaching from primary sulfides: Options for biological and chemical extraction of copper, Hydrometallurgy 83, 10 – 20.

DRESHER W. H., 2004, Copper applications in mining & extraction. Producing Copper Nature's Way:

Bioleaching, www.copper.org
FLETT, D.S., 2005, Solvent extraction in hydrometallurgy: the role of organophosphorus extractants, Journal of Organometallic Chemistry, 690, 2426 – 2438.
ICSG Press Release, 2007, Release of ICSG 2007 Statistical Yearbook, www.icsg.org
ICSG Press Release, 2008, ICSG Forecast 2008 - 2009, www.icsg.org
KORDOSKY G., VIRNING M., BOLEY B., 2006, Equilibrium Copper Strip Points as a Function of Temperature and Other Operating Parameters: Implications for Commercial Copper Solvent Extraction Plants, Tsinghua Science & Technology, 11, (2), 160 – 164.
MERIGOLD C.R., 1996, Copper Extractants Modified and Unmodified Oximes, A Comparison, BGRIMM Annual Technical Seminar.
Outotec Oyj., 2007, Copper SX-EW technology, www.outotec.com/36285.epibrw
PEACEY J., GUO X.J., ROBLES E., 2008, Copper Hydrometallurgy – Current Status, Preliminary Economics, Future Direction and Positioning versus Smelting, www.hatch.ca
SOLE K.C., HISKEY J.B., 1995, Solvent extraction of copper by Cyanex 272, Cyanex 302 and Cyanex 301, Hydrometallurgy 37, 129-147.
SZYMANOWSKI J., 1993, Hydroxyoxymes and Copper Hydrometallurgy, CRC Press Inc., Boca Raton Florida.
SZYMANOWSKI J., 1996, Copper hydrometallurgy and extraction from chloride media, Journal of Radioanalytical and Nuclear Chemistry, 28 (1), 183-194.

Rotuska K., Chmielewski T.*„Rosnąca rola ekstrakcji rozpuszczalnikowej w przetwarzaniu rud miedzi,* Physicochemical Problems of Mineral Processing, 42 (2008), 29-36 (w jęz. ang)

Ługowanie na hałdzie (heap leaching) tlenkowych rud miedzi i odzysk miedzi w postaci katodowej na drodze ekstrakcji rozpuszczalnikowej (SX) i elektrolizy (EW) zostało uznane za podstawowy i ekonomicznie atrakcyjny hydrometalurgiczny sposób wytwarzania metalu. Hydrometalurgia miedzi została mocno rozwinięta w ostatnich latach również do przetwarzania siarczkowych rud i koncentratów. Obecnie, ponad 20 % światowej produkcji miedzi ma miejsce przy zastosowaniu metod hydrometalurgicznych, stosujących ekstrakcje rozpuszczalnikową. Osiągnięcia nowych technologii hydrometalurgicznych doprowadziły do znacznego ożywienia badań nad alternatywnym do hutniczego odzyskiwaniem miedzi z jej surowców tlenkowych i siarczkowych. Niniejsza praca jest przeglądem zasadniczych problemów związanych z ekstrakcją miedzi z roztworów po ługowaniu tlenkowych i siarczkowych minerałów miedzi.

słowa kluczowe: ługowanie na hałdzie, ekstrakcja, tlenki miedzi, ruda miedzi siarczki

Physicochemical Problems of Mineral Processing, 42 (2008), 37-46
Fizykochemiczne Problemy Mineralurgii, 42 (2008), 37-46

Małgorzata Pacholewska*, Beata Cwalina**, Karolina Steindor***

THE INFLUENCE OF FLOTATION REAGENTS ON SULFUR-OXIDIZING BACTERIA *ACIDITHIOBACILLUS THIOOXIDANS*

Received May 4, 2008; reviewed; accepted July 31, 2008

It has been demonstrated that various flotation reagents influence, in a different manner, the metabolic activity of the sulfur-oxidizing bacteria *Acidithiobacillus thiooxidans* (strain C1 being isolated from the Fe-Zn tailings water) growing in the Waksman/Joffe (W/J) liquid culture medium that contains thiosulfate as a sole energy source for bacteria growth. The ethyl- and amyl xanthates as well as the frothing reagent stimulated, to a limited extent, the tested C1-bacteria metabolic activity. The very well documented bacterially-influenced acidification of the W/J solution supplemented with the ethyl- or the amyl xanthates suggests the possibility of these substances effective acid-degradation in the post-industrial environments rich in various flotation reagents, mainly xanthates. Both the activator containing the carbamate ethyl-derivative and the modifier composed of Cu(II)-ions caused a complete inactivation of the *A. thiooxidans* C1-metabolism. It is suggested that some unexpected chemical reactions may proceed in the tested systems, as a result of interactions between the culture medium components, flotation reagents, their decomposition products, and also the products of bacterial metabolism.

key words: Acidithiobacillus thiooxidans, metabolic activity, flotation reagents, xanthates, frother, activator, Cu(II)-ions

INTRODUCTION

Flotation is a method used for enrichment of millions tons (Tg, teragrams) of mineral raw materials, including 80-90% of non-ferrous metal ores mined in the world. In

* Department of Metallurgy, Silesian University of Technology, Krasinskiego 8, 40-019 Katowice, Poland, e-mail: Malgorzata.Pacholewska@polsl.pl
** Environmental Biotechnology Department, Silesian University of Technology, Akademicka 2, 44-100 Gliwice, Poland, e-mail: Beata.Cwalina@polsl.pl
*** Faculty of Biology and Environmental Protection, University of Silesia, Jagiellońska 26/28, 40-032 Katowice, Poland.

Poland, nearly 30 Tg of copper ores as well as about 5 Tg of zinc-lead ores are concentrated by this method. In the minerals processing, flotation is one of the most important physicochemical methods of the mineral raw materials enrichment (Drzymała, 2007; Laskowski and Łuszczkiewicz, 1989). This method is also of high efficiency in the zinc and lead sulfide minerals selective separation from crude ores. No chemical changes in the ore mineral components take place during flotation processes. Initial stage of the ore enrichment in the heavy media with either ferrosilicon or magnetite makes possible the barren dolomite separation from the heavier aggregates. The dolomite gangues are widely used as the aggregate in building materials. The pre-enriched ore is milled, and then floated, using many flotation reagents including:

- collector reagents - mainly xanthates (ethyl, butyl, amyl), alkyl sulfates, and aliphatic amine hydrochlorides
- frothing reagents - octanol and diacetone alcohol mixtures with the mesityl oxide
- modifying reagents - activators, depressors, pH regulators.

A number of flotation reagents remain in the post-flotation waste materials, which are composed mainly of the carbonate gangues (70%), Fe sulfides (pyrite and marcasite, 15-20%), non-floatable small fractions of the Pb and Zn sulfide minerals, as well as Zn, Pb, Cd, As and Tl oxide minerals. The post-flotation tailings resulting from processing of the Zn-Pb ores originated from the Pomorzany, Olkusz and Bolesław mines are stored in the Olkusz region. Here, the post-mining grounds and storage yards (containing both present and historic waste materials) occupy an area of about 2000 ha.

Chemical stability of the flotation reagents such as xanthates depends mostly on pH of the environment. Significant increase in acidity (pH 3-5) leads to xanthates degradation according to overall reaction: $ROCS_2H \rightarrow ROH + CS_2$ (Zhongxi and Forsling, 1999).

The sulfide minerals present in the post-flotation waste materials form a habitat favorable to the acidophilic sulfur bacteria growth (Cwalina and Jaworska-Kik, 2008; Pacholewska et al., 2007). Their ability to oxidize sulfur compounds leads to environment acidification. Thus, the xanthates decomposition may result from the sulfur-oxidizing bacteria metabolic activity, although the biological degradation of flotation reagents is rather attributed to the bacterium *Bacillus polymyxa* action (Deo and Natarajan, 1998). On the other hand, it seemed to be probable that xanthates could be used as sulfur-bearing substrates for the sulfur-oxidizing bacteria growth due to chemical composition of these substances group (Fig. 1). Although it has been demonstrated by Hoon and Madgwick (1995) that ethyl, amyl and isobutylxanthates cause inhibition of the *Acidithiobacillus ferrooxidans* bacteria growth, but we observed a high metabolic activities of the *A. ferrooxidans* and *Acidithiobacillus thiooxidans* strains isolated from the flotation tailings rich in various flotation reagents including xanthates (Pacholewska et al., 2007; Cwalina and Jaworska-Kik, 2008). This finding pointed to

these bacteria adaptation to such environment and suggested possibility of xanthates use for their growth.

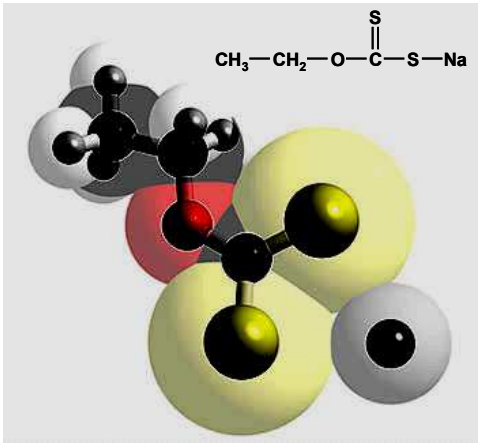

Fig. 1. Sodium ethyl xanthate structure (after http://www.3dchem.com; with modification)

The aim of present work was to study the influence of various flotation reagents on the metabolic activity of the sulfur-oxidizing bacteria *Acidithiobacillus thiooxidans* being isolated from the Fe-Zn tailings water. The main question was, whether or not the tested bacteria metabolic activity is stimulated or depressed by the flotation reagents. On the other hand, it seems to be probable that the biogenic sulfuric acid resulted from the high metabolic activity of the *A. thiooxidans* bacteria may cause the flotation reagents degradation. Both the flotation reagents as well as their decomposition products appear to have effect on the bacteria growth and activity. This activity has been evaluated basing on acidifying the Waksman/Joffe (W/J) liquid culture medium (Waksman and Joffe, 1922) that contains thiosulfate as the sole energy source for bacterial growth.

MATERIALS AND METHODS

Investigations have been carried out using C1 strain of *Acidithiobacillus thiooxidans* bacteria (Fig. 2) of high metabolic activity, being able to oxidize sulfur and its inorganic compounds (Cwalina and Jaworska-Kik, 2008; Pacholewska et al., 2007). This bacteria strain has been isolated from the acid water sampled from the piezometer P1 installed in the Fe-Zn tailings pond (HMN Szopienice, Katowice). Bacteria were cultured in the W/J liquid medium (Waksman and Joffe, 1922) containing (g/dm^3): $Na_2S_2O_3 \cdot 5H_2O$ - 5.0; KH_2PO_4 - 3.0; $MgCl_2 \cdot 6H_2O$ - 0.1; $CaCl_2 \cdot 6H_2O$ - 0.25; NH_4Cl - 0.1; $FeSO_4 \cdot 7H_2O$ - traces; pH 4.0. The culture medium was supplemented with the flotation reagents being used for the Zn-Pb ores enrichment during their in-

dustrial processing in the Olkusz mine. The reagents have been obtained from the Ores Enrichment Plant ZGH Bolesław S.A. Additives were introduced into the W/J liquid medium to provide concentrations proportional to those occurring under industrial conditions, taking into account the pulp density used in the experiments, i.e. 5 g of waste material in 100 cm^3 of the solution. Additions of the flotation reagents were as follows:

1. collector, amyl xanthate - 0.4 cm^3/100 cm^3 of W/J solution
2. collector, ethyl xanthate - 0.2 cm^3/100 cm^3 of W/J solution
3. frothing reagent, Corflot - 0.04 cm^3/100 cm^3 of W/J solution
4. activator/collector, Selkol 1981 - 0.01 cm^3/100 cm^3 of W/J solution
5. modifying reagent, the industrial solution $CuSO_4$ - 0.32 cm^3/100 cm^3 of W/J solution.

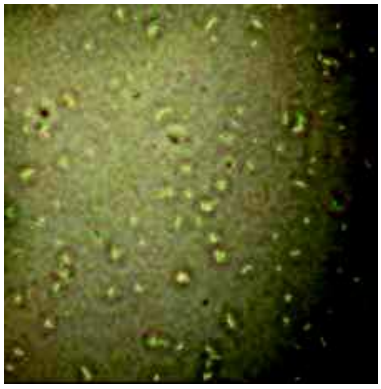

Fig. 2. Cells of *Acidithiobacillus thiooxidans* bacteria (strain C1) in the Waksman/Joffe (W/J) liquid culture medium. Optical microscope; picture taken at magnification 1000×

The liquid culture of the *A. thiooxidans* C1 bacteria strain growing in the W/J solution without flotation reagents as well as the sterile W/J media without or with flotation reagents have been used as the control systems. Bacteria were introduced as 2cm^3 aliquots of inoculum containing *A. thiooxidans* C1 population in the exponential phase of growth. Experiments were carried out at temperature of 20^oC, under mechanical shaking. The suspensions' pH has been measured using a combined glass electrode, type ERH 111 (Hydromet), and Slandi SP300 electronic pH-meter.

RESULTS AND DISCUSSION

A. THIOOXIDANS ACTIVITY IN THE PRESENCE OF XANTHATES

The results presented in Fig. 3 reflect the xanthates influence on *A. thiooxidans* (strain C1) metabolic activity. Only inconsiderable differences are visible between C1

cultures grown in W/J solutions without and with xanthates. The lowest and very similar values of pH (1.7-2.2) have been measured in all solutions inoculated with C1 bacteria after their culturing for 96 hours and longer (up to 192 hours). Besides, some beneficial effect of xanthates on the bacteria activity has been observed after 72 hours of the C1-strain growth in the W/J liquid medium supplemented with these flotation reagents, where the solution acidification was more intensive as compared with the xanthate-free bacterial culture. These results suggest that the *A. thiooxidans* bacteria metabolic activity was influenced by xanthates only to a small extent and that their presence was not disadvantageous for bacterial populations being used in the experiment. As a result, considerable acidification of the W/J solution occurred in all liquids inoculated with the *A. thiooxidans* C1 strain, leading to form favorable conditions for the xanthates degradation. Sterile W/J solution supplemented with the ethyl xanthate indicates no changes in its acidity throughout the experiment duration whereas some inconsiderable pH-increase has been observed in the W/J solution containing the amyl xanthate.

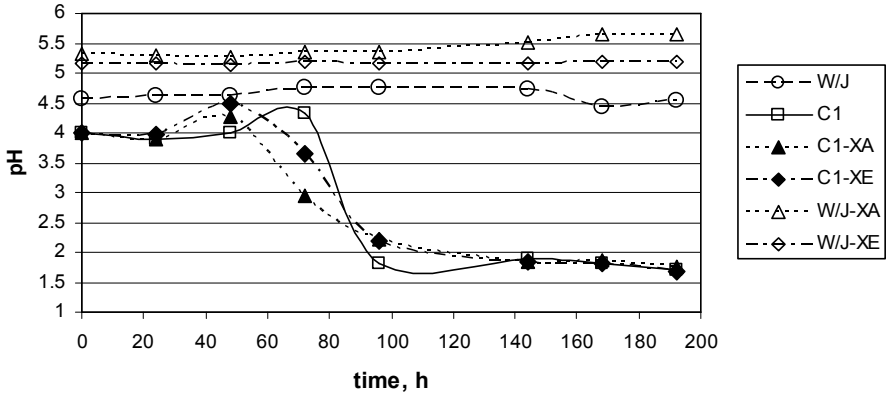

Fig. 3. The influence of xanthates on *A. thiooxidans* (strain C1) metabolic activity; W/J - sterile Waksman/Joffe liquid culture medium; C1 - W/J+C1 strain; XA - amyl xanthate; XE - ethyl xanthate

A. THIOOXIDANS ACTIVITY IN THE PRESENCE OF FROTHING REAGENT

The influence of the Corflot frothing reagent on metabolic activity of the *A. thiooxidans* bacteria (strain C1) has been shown in Fig. 4. It is worth to denote that dynamic curves indicating the W/J liquid culture medium acidification by C1 bacteria growing without and with the frothing reagent tested were almost identical. The Corflot frothing reagent did not cause the pH-changes in the W/J sterile solution.

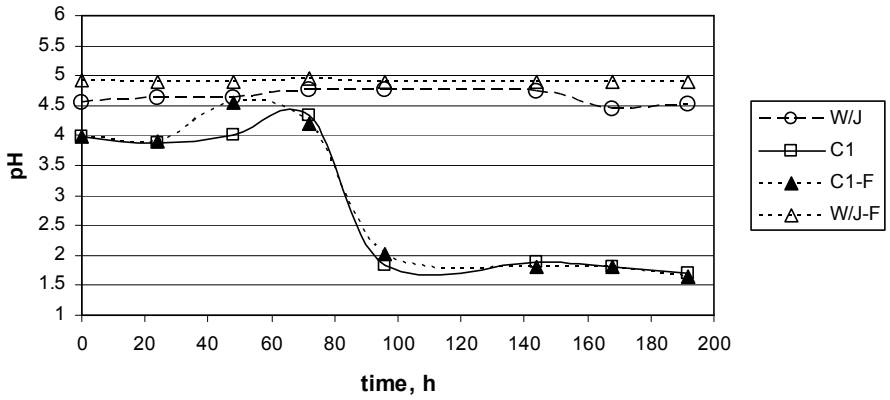

Fig. 4. The influence of frother on *A. thiooxidans* (strain C1) metabolic activity; W/J - sterile Waksman/Joffe liquid culture medium; C1 - W/J+C1 strain; F - frother

A. THIOOXIDANS ACTIVITY IN THE PRESENCE OF ACTIVATOR

Figure 5 summarizes results concerning the Selkol activator influence on the *A. thiooxidans* bacteria (strain C1) metabolic activity. Unfavorable effect of this flotation reagent is very essential and clear. No acidification took place in the C1-bacteria culture growing in the W/J liquid medium supplemented with Selkol. This flotation agent caused the bacteria metabolism inactivation from the beginning of bacteria culturing. The toxic effect of the Selkol activator is probably due to the presence in it of very toxic carbamate ethyl-derivative. The Selkol activator had no effect on pH of the W/J sterile solution.

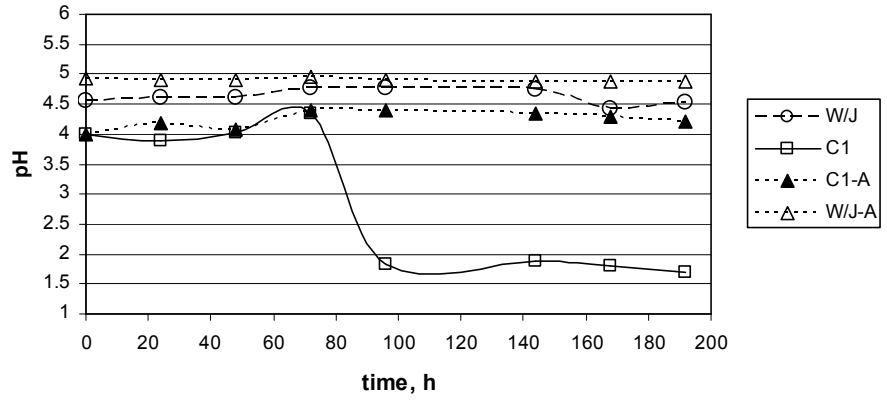

Fig. 5. The influence of activator on *A. thiooxidans* (strain C1) metabolic activity; W/J - sterile Waksman/Joffe liquid culture medium; C1 - W/J+C1 strain; A - activator

A. THIOOXIDANS ACTIVITY IN THE PRESENCE OF MODIFIER - Cu(II)

The results presented in Fig. 6 show the influence of Cu(II)-ions (being used in flotation processes as the modifying reagent) on the pH-changes in the W/J liquid culture media - both sterile and inoculated with *A. thiooxidans* bacteria (strain C1). No acidification has been denoted in the bacterial solution supplemented with copper ions. On the contrary - pH-changes towards the solution alkalization have been observed. This points to a highly toxic effect of these ions on the investigated bacteria strain. The *A. thiooxidans* bacteria sensibility to various metal ions, including Cu(II), will be presented in the separate paper.

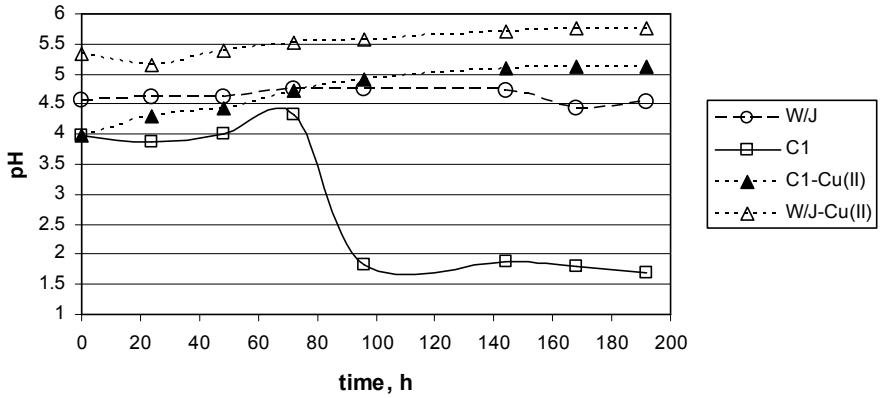

Fig. 6. The influence of Cu(II)-ions on *A. thiooxidans* (strain C1) metabolic activity; W/J - sterile Waksman/Joffe liquid culture medium; C1 - W/J+C1 strain; Cu(II) - $CuSO_4$

Apart from the *A. thiooxidans* C1-metabolism complete inactivation, an increase in the pH values being observed during the process run under sterile conditions suggests possibility of the thiosulfate destabilization due to the Cu(II)-ions chemical reaction (Senanayake, 2005).

THE OVERALL ANALYSIS OF FLOTATION REAGENTS INFLUENCE ON THE *A. THIOOXIDANS* METABOLIC ACTIVITY

The mean values of the rates of H^+-concentration changes in pure W/J liquid medium as well as in the media supplemented with selected flotation reagents, both sterile and inoculated with *A. thiooxidans* bacteria (strain C1), have been presented in Table 1. It may be stated that the bacteria presence in the W/J solution leads to about 10000-fold increase in the protons concentration - from about $2.0 \cdot 10^{-3}$ mmol/dm^3 up to 20.3±2.3 mmol/dm^3. Calculated values of the mean rates of H^+-production due to the bacteria activity were 2.52±0.25 mmol/dm^3/d, indicating the variability coefficient not exceeding 10%. All flotation reagents tested did cause some decrease in the H^+ con-

centration in the W/J solution. This effect seems to be more significant in solutions supplemented with the activator and the Cu(II)-ions, especially in the presence of bacteria. In this experimental system, the rate of H^+ concentration decrease was about 10-fold higher as compared with a parallel sterile solution. These results may point to both toxic effects of the activator and modifier on the bacteria metabolic activity as well as to chemical reactivity modification of these substances by the bacteria metabolites or the cells' lysis products liberated into the solution. On the other hand, it has been demonstrated for the first time that the ethyl and amylxanthates as well as the frothing reagent studied in this work may stimulate, to a limited extent, the metabolic activity of the bacteria *Acidithiobacillus thiooxidans* (Fig.3, 4; Tab. 1), but their role in the activation effect has not been studied as yet.

Table 1. Changes in H^+ concentration in pure Waksman/Joffe (W/J) liquid medium and in the media (sterile and inoculated with *A. thiooxidans* strain C1) containing flotation agents

Sample symbol	Addition of C1-bacteria and flotation agents (FA) to W/J solution	H^+ concentration increase (+) or decrease (-) [mmol/dm^3]	Rate of change in H^+-concentration [mmol/dm^3/d]
W/J	W/J sterile, without FA	$+2.0\cdot10^{-3}$	$+2.5\cdot10^{-4}$
C1	C1 without FA	+20.3	+2.5
C1-XA	C1 + amyl xanthate	+17.3	+2.2
C1-XE	C1 + ethyl xanthate	+20.8	+2.6
C1-F	C1 + frother	+22.8	+2.8
C1-A	C1 + activator	$-4.2\cdot10^{-2}$	$-5.3\cdot10^{-3}$
C1-Cu(II)	C1 + $CuSO_4$	$-9.5\cdot10^{-2}$	$-1.2\cdot10^{-2}$
W/J-XA	W/J + amyl xanthate	$-2.5\cdot10^{-3}$	$-3.2\cdot10^{-4}$
W/J-XE	W/J + ethyl xanthate	$-4.5\cdot10^{-4}$	$-5.6\cdot10^{-5}$
W/J-F	W/J + frother	$+5.5\cdot10^{-4}$	$+6.9\cdot10^{-5}$
W/J-A	W/J + activator	$+1.2\cdot10^{-3}$	$+1.5\cdot10^{-4}$
W/J-Cu(II)	W/J + $CuSO_4$	$-1.5\cdot10^{-2}$	$-1.8\cdot10^{-3}$

CONCLUSIONS

1. Various flotation reagents influence, in a different manner, the metabolic activity of the sulfur-oxidizing bacteria *Acidithiobacillus thiooxidans* (strain C1 being isolated from the Fe-Zn tailings water) growing in the Waksman/Joffe (W/J) liquid culture medium that contains thiosulfate as a sole energy source for bacteria growth.
2. It has been demonstrated that the ethyl- and amyl-xanthates as well as the frothing reagent stimulated, to a limited extent, the tested C1-bacteria metabolic activity.

3. The very well documented bacterially influenced acidification of the W/J solution supplemented with the ethyl- or the amyl-xanthates suggests the possibility of effective acid-degradation of these substances in the post-industrial environments, rich in various flotation reagents, mainly xanthates.
4. Both the activator containing the carbamate ethyl-derivative and the modifier composed of Cu(II) ions caused complete inactivation of the *A. thiooxidans* C1-metabolism.
5. It is suggested that some unexpected chemical reactions may proceed in the systems tested. They may result from interactions between the culture medium components, the flotation reagents, their decomposition products, and also the products of bacterial metabolism.

ACKNOWLEDGEMENTS

This work was supported by Commissioned Research Project PBZ-KBN-111/T09/2004 from the Polish Funds for Science, 2005-2008.

REFERENCES

CWALINA B., JAWORSKA-KIK M.: Sulfur–oxidizing activity of bacteria isolated from Zn-Pb flotation tailings. Ecological Chemistry and Engineering, 2008, 15 (in press)

DEO N., NATARAJAN K.A.: Biological removal of some collector reagents from aqueous solutions and mineral surfaces. Minerals Engineering, 1998, 11 (8), 717-738.

DRZYMAŁA J.: Mineral processing. Foundations of theory and practice of minerallurgy. Oficyna Wydawnicza Politechniki Wrocławskiej, 2007, http://www.dbc.wroc.pl/Content/2070 /Drzymala.pdf

HOON YIN LOON, MADGWICK J.: The effect of xanthate floatation reagents on bacterial leaching of chalcopyrite by *Thiobacillus ferroxidans*. Biotechnology Letters, 1995, 17 (9), 997-1000.

LASKOWSKI J, ŁUSZCZKIEWICZ A.: Fossil processing (in Polish), Wydawnictwo Politechniki Wrocławskiej, Wrocław, 1989.

PACHOLEWSKA M., CABAŁA J., CWALINA B., SOZAŃSKA M.: Environmental conditions of the metals (bio)leaching from zinc-lead post-flotation taillngs (in Polish). Rudy i Metale Nieżelazne, 2007, 52 (6), 337-342.

SENANAYAKE G.: Role of copper(II), carbonate and sulphite in gold leaching and thiosulphate degradation by oxygenated alkaline non-ammoniacal solutions. Minerals Engineering, 2005, 18 (4), 409-426.

WAKSMAN S.A., JOFFE J.S.: Microorganisms concerned in the oxidation of sulfur in the soil. II. *Thiobacillus thiooxidans*, a new sulfur oxidizing organism isolated from the soil. Journal of Bacteriology, 1922, 7: 239-256.

ZHONGXI S., FORSLING W.: The degradation kinetics of ethyl-xanthate as a function of pH in aqueous solution. Mineral Engineering, 1999, 10 (4), 389-400.

Pacholewska M., Cwalina B., Steindor K., *Wpływ odczynników flotacyjnych na utleniające siarkę bakterie Acidithiobacillus thiooxidans,* Physicochemical Problems of Mineral Processing, 42 (2008), 37-46 (w jęz. ang)

Wykazano, że różne odczynniki flotacyjne oddziaływały w różny sposób na aktywność metaboliczną utleniających bakterii siarkowych *Acidithiobacillus thiooxidans* (szczep C1 izolowany z wody szlamów Fe-Zn) rosnących w pożywce płynnej Waksmana/Joffe (W/J) z tiosiarczanem jako podstawowym źródłem energii dla wzrostu bakterii. Ksantogeniany: etylowy i amylowy, jak również odczynnik spieniający stymulowały w ograniczonym zakresie aktywność metaboliczną testowanych bakterii C1. Bardzo dobrze udokumentowane, spowodowane przez bakterie zakwaszenie roztworu W/J zawierającego dodatek ksantogenianów: etylowego lub amylowego sugeruje możliwość efektywnej kwaśnej degradacji tych substancji w środowiskach poprzemysłowych bogatych w różne odczynniki flotacyjne, głównie ksantogeniany. Zarówno aktywator zawierający etylową pochodną karbaminianu, jak i modyfikator zawierający jony Cu(II) powodowały zupełną inaktywację metabolizmu *A. thiooxidans* C1. Sugeruje się, że w testowanych systemach mogą przebiegać pewne nieoczekiwane reakcje chemiczne, jako rezultat interakcji między składnikami pożywki, odczynnikami flotacyjnymi, produktami ich rozkładu, a także produktami metabolizmu bakterii.

słowa kluczowe: Acidithiobacillus thiooxidans, aktywność metaboliczna, odczynniki flotacyjne, ksantogeniany, spieniacz, aktywator, jony Cu(II).

Physicochemical Problems of Mineral Processing, 42 (2008, 47-56
Fizykochemiczne Problemy Mineralurgii, 42 (2008, 47-56

Elżbieta Grządka*, Stanisław Chibowski *

INFLUENCE OF A KIND OF ELECTROLYTE AND ITS IONIC STRENGTH ON THE CONFORMATION CHANGES OF POLYACRYLIC ACID DURING ITS COMING FROM THE BULK SOLUTION TO THE SURFACE OF MnO_2

Received July 8, 2008; reviewed; accepted July 31, 2008

Changes in PAA 2000 macromolecules conformation in the bulk solution as well as on the surface of MnO_2 as a function of a kind of electrolyte (NaCl, $CaCl_2$), electrolyte ionic strength (I=0.01, 0.1) and pH (3, 6, 9) of the solution were measured. In order to determine the influence of electrolyte on PAA conformation in the bulk solution the expansion coefficient (α) was measured. Such quantities as: the square root of the mean of the square distance between ends of polymer chain ($\sqrt{r^2}$), the square root of the mean of square radius of polymer coil rotation ($\sqrt{s^2}$) and hydrodynamic radius of polymer coil in the bulk solution (R_h) were measured to describe changes in PAA macromolecule conformation during its coming from the bulk solution to the surface of MnO_2. Moreover, PAA adsorption layer thickness in the presence of two various electrolytes, NaCl and $CaCl_2$ (I=0.01, 0.1) was measured. From the obtained results it is clearly visible that researched factors: kind of electrolyte, its ionic strength and pH of a solution have great influence on the conformation of the polymer macromolecules.

Key words: polymer conformation, polymer adsorption, expansion coefficient, adsorption layer thickness

INTRODUCTION

Research on the polymer adsorption on the solid surfaces is carried out in two aspects: theoretical and practical (Fleer et al., 1993; Markovic, 1996; Pan et al., 2001).

* Uniwersytet M. Curie-Skłodowskiej, Wydział Chemii, Zakład Radiochemii i Chemii Koloidów, Plac M. Skłodowskiej-Curie 3, 20-031 Lublin, PL, egrzadka@wp.pl

Interest in the polymers adsorption on the metal oxide/polyelectrolyte solution interface results from the fact that the mechanism of polymer adsorption is completely different from the mechanism of small particles and ions adsorption. Polymer chains may form lots of different conformations in both the bulk of solution and in the interface, while the ions and the small particles have invariable, defined shape (Cohen Stuart et al., 1991). Changes in the polymer conformation in the bulk solution and at the interface as well as changes in the structure of polymer chain during its coming from the solution to the surface of the solid are the most important problems in the description of polymers adsorption process. In the bulk solution polymer chains are flexible. It helps them to create coil type structures. The shapes and the dimensions of above-mentioned structures depend on a few factors. Among them the most important ones are interactions between polymer segments and solvent particles, molecular weight of used polymer and polymer concentration. Moreover, polymer coils might permeate each other. The result of that is a very complicated and hard to explain thermodynamic system. When polymer particles are being adsorbed on the surface of the adsorbent, their conformation changes radically. Because of the fact that the concentration of the polymer is always higher in the surface layer than in the bulk solution, the co-permeating process of polymer chains takes place in by-surface layer. The evidence for that is the presence of trains, loops and tail structures. Trains are whose segments that are adjoined to the surface of the adsorbent. Loops and tails are so called spacious polymer structures. They can interact with each other and there are two effects of this interaction: one is their expansion towards the bulk of the solution and the second one is the creation of closely packed polymer coils. The kind of produced polymer conformation has the influence on some parameters describing polymer macromolecule in the solution as well as on the surface. The above-mention parameters are: expansion coefficient (α), thickness of adsorbed polymer layer (δ), square root of the mean of the square distance between ends of polymer chain ($\sqrt{\overline{r^2}}$), square root from the mean of square radius of polymer coil rotation ($\sqrt{\overline{s^2}}$), hydrodynamic radius of polymer coil in the bulk solution (R_h).

Polyacrylic acid was used as a polyelectrolyte because of wide range of its practical applications (Szlezyngier, 1998). It is used as supplement to surfactants, compound used in the production of paper, inhibitor of fur formation, concentrators in cosmetics and components of drugs, artificial tears. There are also some measurements which explain the fact of stability changes of phase colloids in the presence of polyacrylic acid.

Manganese dioxide was chosen as an adsorbent. This oxide is chemically inert, insoluble and stable in a broad pH range. These features as well as well-defined interface allow to use it as an adsorbent. Manganese dioxide finds applications in the production of matches, in glass-making industry to decolourization of glass and as a depolarizer in voltaic cells (Trzebiatowski, 1979).

EXPERIMENTAL

MnO_2 produced by POCh-Gliwice was used as an adsorbent in all measurements. The specific surface area of manganese dioxide, calculated using the BET (Brunauer, Emmet, Teller) method was 38 $m^2 g^{-1}$ and the average diameter of this oxide particles equalled 280 nm. Before the measurements MnO_2 was washed with doubly distilled water until the conductivity of the supernatant smaller than 2μS cm^{-1}.

NaCl, and $CaCl_2$ were used as background electrolytes. Polyacrylic acid (molecular weight 2000) produced by Aldrich was used as a polyelectrolyte.

PAA expansion coefficient (α) in the presence of NaCl and $CaCl_2$ as background electrolytes was determined using the viscosity method (Porejko et al., 1974). Viscosity of the polymer solutions with various concentrations was measured by a rotary rheometer (CVO 50, Bohlin Instruments). On the basis of above mentioned the reduced viscosity (η_r) for all samples was calculated using the formula:

$$\eta_r = \frac{\eta_{sp}}{c} = \frac{\eta_{rel} - 1}{c} = \frac{\frac{\eta_l}{\eta_0} - 1}{c} \tag{1}$$

where: η_{sp} - the specific viscosity, η_{rel} - the relative viscosity, η_l - the polymer solution viscosity, η_0 - the solvent viscosity and c is the polymer solution concentration.

From the dependence between the reduced viscosity of polymer solution and its concentration, the reduced viscosity of the polymer solution at a given temperature ($[\eta]$) was determined using the extrapolation method ($[\eta] = \lim_{c \to 0} \eta_r$). These measurements were made for various ionic strengths of the solution (0.01, 0.1) and for various pH values (3, 6, 9). The expansion coefficient of PAA chains was calculated from the following formula:

$$\alpha = \left(\frac{[\eta]}{[\eta_\Theta]} \right)^{1/3} \tag{2}$$

where: $[\eta]$ - the reduced viscosity of the polymer solution at a given temperature, $[\eta_\Theta]$ - the reduced viscosity of the polymer solution at the Θ temperature (PAA Θ temperature ≈ 14° C).

From the viscosity measurements some qualities describing polymer coil during its coming from the bulk solution to the surface of the solid were obtained. $\sqrt{r^2}$ - square root from the mean of the square distance between ends of polymer chain was estimated using the Flory - Fox equation:

$$[\eta] = \frac{\Phi\left(\overline{r^2}\right)^{3/2}}{M} \tag{3}$$

where: $[\eta]$ - reduced viscosity of the polymer solution, Φ - Flory-Fox constant = 2.1×10^{21}, M - molecular weight of measured polymer.

From $\sqrt{\overline{r^2}}$ square root of the mean of square radius of polymer coil rotation ($\sqrt{\overline{s^2}}$) was calculated using the formula:

$$\left(\overline{s^2}\right) = \frac{\left(\overline{r^2}\right)}{6}\,. \tag{4}$$

Hydrodynamic radius of polymer coil in the bulk solution (R_h) was estimated from the equation:

$$R_h = f\sqrt{\overline{s^2}} \tag{5}$$

where: f - polymer constant for PAA = 0.66.

Thickness of PAA adsorption layer (δ) was also measured by the viscosity method (Pandou et al., 1987), using a rheometer. The MnO_2 suspensions with its various volumetric fractions (ϕ_0) were prepared. The volumetric fraction of the solid was determined from the formula:

$$\phi_0 = \frac{m}{dv} \tag{6}$$

where: m - the solid mass, d - the solid specific gravity, v - the reference solution volume.

Next, the suspensions were shaken for 24 hours and their viscosity (η) as well as that of the reference solutions (η_0) were measured using a rheometer. In this way, the influence of ϕ_0 on η/η_0 was calculated (calibration curve). In the same way the viscosity of the suspensions with the adsorbed polymer (η_p) as well as that of the polymer solution (η_{p0}) was measured and the influence of η_p/η_{p0} was determined. Next, from the calibration curve the volumetric fraction of a solid (ϕ_p) was estimated. When the radius of MnO_2 particles is known, the thickness of the adsorption layer can be calculated from the following formula:

$$\delta = r\left[\left(\frac{\phi_p}{\phi_0}\right)^{1/3} - 1\right] \tag{7}$$

where: r - the radius of the metal oxide particle, ϕ_p - the volumetric fraction in the presence of polymer, ϕ_0 - the volumetric fraction in the absence of the polymer.

Thickness of the polymer adsorption layer (δ) on the metal oxide in the presence of NaCl and $CaCl_2$ for various electrolytes ionic strengths (0.01, 0.1) and for various pH values (3, 6, 9) was determined.

RESULTS AND DISCUSSION

Table 1 shows the obtained values of the expansion coefficient (α) of PAA 2000 in the presence of NaCl and $CaCl_2$ (I= 0.01, 0.1). Measurements were made for various pH values (3, 6, 9) of the solution.

Table 1. PAA expansion coefficient in the presence of NaCl and $CaCl_2$

	pH	0.01M NaCl	0.1M NaCl	0.003M $CaCl_2$	0.033M $CaCl_2$
PAA 2000	3	1.33	1.16	1.42	1.23
	6	1.34	1.32	1.45	1.32
	9	1.45	1.45	1.51	1.48

Analysis of the obtained data, which describe the dimensions of a singular polymer coil in the bulk solution, shows that the expansion coefficient is always higher in the presence of $CaCl_2$. This situation might be explained by the influence of divalent cations on the degree of carboxylic group dissociation. In the presence of Ca^{2+} PAA is more dissociated than in the presence of monovalent cation. Because of a larger number of negatively charged carboxylic groups which repel each other, polymer coil becomes more stretched and the expansion coefficient of PAA increases.

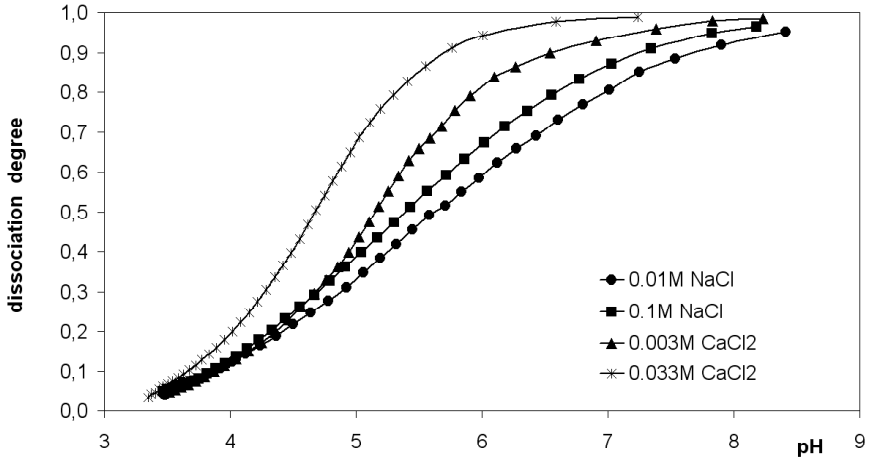

Fig. 1. PAA 2000 dissociation degree as a function of pH in the presence of NaCl and $CaCl_2$.

Linear dimensions of polymer coil also increase with the increase of pH. This fact is a consequence of the increasing number of carboxylic groups in the polymer chain with the increase of pH of the solution. The repulsion forces between $-COO^-$ groups cause the stretching of the polymer chain and the increase of PAA expansion coefficient.

Table 2. The ratio of concentration of neutral/ionized groups in PAA 2000 chain as a function of solution pH in the presence of NaCl and $CaCl_2$

pH	$(1-\alpha_d)/\alpha_d$=[COOH]/[COO^-]			
	0.01M NaCl	0.1M NaCl	0.003M $CaCl_2$	0.033M $CaCl_2$
3.5	25	17	20	14
4.5	3.5	2.8	3.3	1.3
5.5	1.2	0.8	0.51	0.15
6.5	0.43	0.26	0.11	0.095
7.5	0.13	0.09	0.042	0.031
8.5	0.033	0.020	0.014	0.011

One of the most surprising facts is that the increase of ionic strength causes the decrease of α. This fact is a consequence of three factors: the increase of dissociation of carboxylic groups (Chibowski et al., 2003), the decrease of PAA solubility and the increase of carboxylic groups screening effect by electrolyte cations. The first from the above-mentioned effects causes the increase of α while two others cause the decrease of this value. It seems that the summary effect of the influence of these factors on the expansion coefficient causes small decrease of α values.

Table 3 presents PAA 2000 adsorption layer thickness on the surface of MnO_2 in the presence of NaCl and $CaCl_2$.

Table 3. PAA 2000 adsorption layer thickness on the surface of MnO_2 in the presence of NaCl and $CaCl_2$

electrolyte	pH	δ [nm]	electrolyte	pH	δ [nm]
0.01 M NaCl	3	1.8	0.003 M $CaCl_2$	3	5.1
	6	2.4		6	8.4
	9	3.5		9	12.6
0.1M NaCl	3	2.5	0.033 M $CaCl_2$	3	8.0
	6	3.5		6	13.6
	9	7.0		9	15.3

Analysis of the data presented in Table 3 confirms that both the kind of used electrolyte and its ionic strength have the influence on the adsorption layer thickness. Comparison between these data leads to the conclusion that the presence of divalent metal chloride as the electrolyte causes larger increase of the adsorption layer thickness than in the presence of NaCl. This fact is a consequence of a few phenomena.

Firstly, PAA dissociation degree is higher in the presence of $CaCl_2$ than in the presence of NaCl as the background electrolyte. Because of larger number of dissociated carboxylic groups and because of their repulsion, polymer forms conformation expanded towards the bulk of solution what leads to the increase of polymer adsorption layer thickness. Secondly, divalent metal cations have the tendency to creation of bidental complexes with carboxylic groups from the polymer chains (Vermöhlen et al., 2000), therefore that polymer conformation is rich in loops and tails structures and the adsorption layer thickness increases. The last effect influences the adsorption layer thickness values is the competitive adsorption between Ca^{2+} cations and polymer segments. It is known that there is constant number of active places on the surface of the adsorbent. If some of them are blocked by metal cations, polymer is forced to create conformation on the rest of them. Such a conformation is always rich in loops and tails structures, what increases the PAA adsorption layer thickness (Chibowski, 1988). Moreover, there is an increase of the adsorption layer thickness with the increase of pH. The explanation of such an adsorptive behavior of PAA is the influence of pH on PAA dissociation degree as well as on a kind and the concentration of the metal surface groups. It is known that the increase of pH causes the increase of PAA dissociation degree. When pH of the solution is higher than pK value of polyacrylic acid ($pK_{PAA} = 4.5$) the increase of the number of dissociated carboxylic groups is observed. The consequence of that is the increase of repulsion between negatively charged carboxylic groups and the increase of the polymer adsorption layer thickness. Because PAA adsorption is higher in low pH values and lower in higher ones (Chibowski et al., 2005) some conclusions about PAA conformation on the interface solid/polyelectrolyte solution might be drawn. If the increase of pH causes straightening of PAA coils, adsorption of negatively charged polymer chain on the negative surface takes place only by a few groups. The rest of the polymer chain stays in the solution and forms brush type conformation. Such a conformation is characterized by low amount of adsorbed polymer but a thick adsorption layer. On the other hand, for low pH values, besides the hydrogen bond type, there are electrostatic attraction forces between positively charged surface and dissociated negatively charged carboxylic groups (Solberg et al., 2003). Under such conditions the polymer adsorption layer is closely packed what leads to lower values of polymer adsorption layer thickness.

The influence of ionic strength on the thickness of PAA adsorption layer can be analyzed from the data presented in Table 3. It can be seen that the increase of electrolyte ionic strength accompanies the increase of adsorption layer thickness. It is a consequence of the fact that in high salt concentration repulsion between the surface groups of metal oxide as well as between polymer segments is better screened by metal cations. The effect of this phenomenon is not only the increase of PAA adsorption amount but also the increase of the polymer adsorption layer thickness. Another reason for the increase of PAA adsorption layer thickness with the increase of electrolyte ionic strength is the above-mentioned competitive adsorption between polymer segments and metal cations. It also should be noticed that the increase of salt concen-

tration leads to the increase of flexibility of polymer chain (Steitz et al., 2000; Adachi et al., 2002). That conduces the increase of the polymer adsorption layer thickness.

Tables 4-5 present characteristics of PAA 2000 macromolecules during their coming from the bulk of electrolyte solution to the surface of MnO_2.

Table 4. Characteristic of PAA 2000 particles during their coming from the bulk of NaCl solution to the surface of MnO_2.

	pH	$\sqrt{\overline{\mathbf{r^2}}}$ [nm]	$\sqrt{\overline{\mathbf{s^2}}}$ [nm]	R_h [nm]	δ [nm]
0.01 M NaCl	3	14.4	8.9	9.1	1.8
	6	20.5	11,3	11.3	2.4
	9	33.4	17.5	15.2	3.5
0.1 M NaCl	3	16.4	10.8	10.9	2.5
	6	23.1	11.8	12.7	3.5
	9	35.6	17.2	15.9	7.0

Table 5. Characteristic of PAA 2000 particles during their coming from the bulk of $CaCl_2$ solution to the surface of MnO_2

	pH	$\sqrt{\overline{\mathbf{r^2}}}$ [nm]	$\sqrt{\overline{\mathbf{s^2}}}$ [nm]	R_h [nm]	δ [nm]
0.003 M $CaCl_2$	3	26.8	13.3	11.7	5.1
	6	35.9	17.6	14.5	8.4
	9	49.2	22.8	20.1	12.6
0.033 M $CaCl_2$	3	33.5	16.2	16.1	8.0
	6	46.3	21.7	18.3	13.6
	9	59.8	27.5	24.0	15.3

A comparison between data presented in Table 4 and 5 allows to draw some conclusions about the influence of a kind of electrolyte and its ionic strength on the conformational changes of PAA chain during its coming from the bulk solution to the surface of MnO_2. First of all, R_h values in the presence of $CaCl_2$ are higher those in the presence of NaCl. This fact comes from high affinity of Ca^{2+} cations to PAA carboxylic groups and Ca^{2+} tendency to creation of bidental complexes. In the presence of divalent metal cations dimensions of PAA macromolecule are higher not only in the solution but also on the metal oxide surface (δ values in the presence of $CaCl_2$ are also higher). Changes in $\sqrt{\overline{\mathbf{s^2}}}$, R_h, and δ values strongly prove that PAA conformation is changed during its coming from the bulk solution to the surface of the solid. The polymer chains are being adsorbed on the surface of the solid by a few number of functional groups, what dramatically changes their conformation. Because of this fact polymer adsorption layer thickness is lower than the dimensions of polymer macromolecule in the bulk solution. Moreover, because δ values are lower than the polymer

coil diameter in the solution ($2x\sqrt{\overline{s^2}}$), it evidences that adsorbed polymer chains may permeate each other. Such a situation leads to closely packed conformation of PAA in the adsorption layer. It can also be seen from the data presented in Tables 4-5 that not only pH values but also electrolyte ionic strength increase the values of the parameters which characterized the polymer macromolecule during its coming from the bulk solution to the surface of the metal oxide. This is a consequence of the influence of above-mentioned factors on the PAA dissociation degree. As it was said above, the increase of pH and the increase of electrolyte ionic strength both cause the increase of the PAA dissociation degree.

CONCLUSIONS

1. PAA expansion coefficient is always higher in the presence of $CaCl_2$ and at higher pH values. This fact results from larger number of negatively charged carboxylic groups.
2. α of PAA decreases with the increase of ionic strength. This is a summary consequence of three factors: the increase of dissociation of carboxylic groups, the decrease of PAA solubility, and the increase of carboxylic groups screening effect by counterions.
3. The polymer adsorption layer thickness is higher in the presence of divalent metal chloride. There are three explanations of this phenomenon: larger number of dissociated carboxylic groups, creation of bidental complexes between carboxylic groups, and divalent metal cations and competitive adsorption between Ca^{2+} cations and the polymer segments.
4. α of PAA increases also with the increase of pH. The reasons for that are changes in PAA dissociation degree and changes in a kind and a concentration of the metal surface groups.
5. The increase of electrolyte ionic strength accompanying the increase of PAA adsorption layer thickness. It is a consequence of better screening effect in the presence of salt.
6. Changes in $\sqrt{\overline{r^2}}$, $\sqrt{\overline{s^2}}$, $_{Rh}$, and δ values in the presence of different electrolytes strongly prove that PAA conformation is changed during its coming from the bulk solution to the surface.

REFERENCES

ADACHI Y., MATSUMOTO T., COHEN STUART M.A., (2002), Effects of hydrodynamic mixing intensity coupled with ionic strength on the initial stage dynamics of bridging flocculation of polystyrene latex particles with polyelectrolyte, Coll. Surf., 207, 253.

CHIBOWSKI S., (1988), Effect of the ionic composition of the solution on the polyvinyl alcohol adsorp-

tion on the surface of Al_2O_3, Mater. Chem. Phys., 20, 65.
CHIBOWSKI S., WIŚNIEWSKA M., MARCZEWSKI A.W., S. PIKUS S., (2003), Application of the SAXS method and viscometry for determination of the thickness of adsorbed polymer layers at the ZrO_2–polymer solution interface, J. Coll. Interface Sci., 267, 1.
CHIBOWSKI S., OPALA MAZUR E., PATKOWSKI J., (2005), The influence of ionic strength on an adsorption and electrokinetical properties of dispersed aluminum oxide in a presence of polyacrylic acid', Mater. Chem. Phys., 93, 262.
COHEN STUART M.A., FLEER G.J., LYKLEMA J., NARDE W., SCHEUTJENS J.M.H.M., (1991), Adsorption of ions, polyelectrolytes and proteins, Adv. Coll. Inter. Sci., 34, 477.
FLEER G.J., COHEN STUART M.A., SCHEUTJENS J.M.H.M., COSGROVE T., VINCENT B., (1993), Polymers at Interfaces, Chapman & Hall, London.
MARKOVIC B., (1996), Ph.D. Thesis, University of Zagreb, Croatia.
PAN Z., CAMPELL A., SOMASUNDORAN P., (2001), Polyacrylic acid adsorption and conformation in concentrated alumina suspensions, Coll. and Surf., 191, 71.
M'PANDOU A., SIFFERT B., (1987), Polyethyleneglycol adsorption at TiO2-H2O interface: Distortion of ionic structure and shear plane position, Coll. Surf. 24, 159.
POREJKO S., FEJGIN I., ZAKRZEWSKI L., (1974), Chemia Związków Wielkocząsteczkowych, WNT, Rzeszów.
SOLBERG D., WAGBERG L., (2003), Adsorption and flocculation behavior of cationic polyacrylamide and colloidal silica, Coll. Surf., 219, 161.
STEITZ R., LEINER V., SIBRECHT R., KLITZING R., (2000), *Influence of the ionic strength on the structure of polyelectrolyte films at the solid/liquid interface*, Coll. Surf., 163, 63.
SZLEZYNGIER W., (1998), Tworzywa Sztuczne, WOF, Rzeszów.
TRZEBIATOWSKI W., (1979), Chemia nieorganiczna, PWN, Warszawa.
VERMÖHLEN K., LEWANDOWSKI H., NARRES H-D., SCHWUGER M.J., (2000), Adsorption of polyelectrolytes onto oxides - the influence of ionic strength, molar mass, and Ca^{2+} ions, Coll. Surf., 163, 45.

Grządka E., Chibowski S.,*Wpływ rodzaju elektrolitu i jego siły jonowej na zmiany konformacyjne kwasu poliakrylowego podczas jego przechodzenia z głębi roztworu na powierzchnię MnO2.* Physicochemical Problems of Mineral Processing, 42 (2008), 47-56 (w jęz. ang)

Zbadano wpływ rodzaju elektrolitu (NaCl i $CaCl_2$) i jego siły jonowej (0.01, 0.1) na zmiany konformacyjne kwasu poliakrylowego PAA 2000 w głębi roztworu, na powierzchni adsorbentu (MnO_2) jak i w trakcie przechodzenia makrocząsteczek z głębi roztworu na powierzchnię ciała stałego. W tym celu przeprowadzono pomiary wiskozymetryczne następujących wielkości: współczynnika ekspansji kwasu poliakrylowego (α), grubości warstewek adsorpcyjnych (δ) oraz parametrów charakteryzujących makrocząsteczkę w trakcie przechodzenia z głębi roztworu na powierzchnię ciała stałego czyli: pierwiastka kwadratowego ze średniej kwadratu odległości między końcami łańcucha ($\sqrt{r^2}$), pierwiastka kwadratowego ze średniej kwadratu promienia obrotu kłębka polimerowego ($\sqrt{\mathbf{s}^2}$) oraz promienia hydrodynamicznego (R_h). Przeprowadzone pomiary pozwoliły uzyskać informacje na temat charakterystyki konformacyjnej PAA w zależności od rodzaju i stężenia elektrolitu podstawowego.

słowa kluczowe: konformacje polimerowe, adsorpcja polimeru, współczynnik rozszerzalności , grubość warstwy adsorpcyjnej

Physicochemical Problems of Mineral Processing, 42 (2008), 57-66
Fizykochemiczne Problemy Mineralurgii, 42 (2008), 57-66

Anita Sędłak*, Władysław Janusz*

SPECIFIC ADSORPTION OF CARBONATE IONS AT THE ZINC OXIDE/ELECTROLYTE SOLUTION INTERFACE

Received May 15, 2008; reviewed; accepted July 31, 2008

A study of adsorption of carbonate ions at the interface of ZnO/aqueous solution of $NaClO_4$ is presented. The concentration range of carbonate ions was $1 \cdot 10^{-6}$ to $1 \cdot 10^{-3}$ M. The shape of adsorption of carbonate ions plot vs. pH is characteristic for anions adsorption onto metal oxides and is called the "adsorption envelope". In order to prevent carbon dioxide access to solution, all measurements must have been taken in special chamber in nitrogen atmosphere.

key words: zinc oxide, carbonate ions, adsorption

INTRODUCTION

Practical application is the most important aspect for experimental study of properties of the electrical double layer. Zeta potential measurements give important information concerning the properties of the diffuse part of the edl. Measurements include surface charge, ion adsorption, and zeta potential. Zinc oxide occurs in nature as zincite and is widely used in technology (Bolewski, 1982). Recently, ZnO is considered as a biosensing material. This explains the need for theoretical and experimental studies involving the oxide/electrolyte interface. In order to obtain precise research results the measurements were carried out using ZnO with rigorously defined properties. A higher solubility of this oxide in comparison to either TiO_2 or Fe_2O_3 complicates potentiometric titration because dissolution processes also compete significantly for added acid or base.

* Department Radiochemistry and Colloid Chemistry Maria Curie Skłodowska University, pl. M.C. Skłodowskiej 3, 20-031 Lublin, Poland, wjanusz@hermes.umcs.lublin.pl

Zinc oxide is a white powder with exceptional and unique properties. Partly due to its various applications in electronic, cosmetics and medicine devices, zinc oxide has been a subject of many studies. ZnO is one of important ceramic materials and has been found to have diversified applications in electronic devices such as gas sensors, varistors and transducers. The adsorption process of ions at the metal oxide/water solution interface and its influence on the electrical double layer structure is well described in literature. However, in real dispersed systems, for instance in many technological processes or aqueous environment, the composition of the solid phase as well as of the solution is rich in many organic and inorganic substances.

EXPERIMENTAL

MATERIALS AND METHODS

All measurements were carried out on commercial (Aldrich) zinc oxide (zincite structure). The specific surface of the powder, determined by the Braunauer Emmet Teller (BET) method (nitrogen adsorption - desorption) was 5.7 m^2/g. BJH (Barret, Joyner, Halenda) cumulative desorption volume of pores between 1.7 and 300 nm was 4.59 cm^3/g, which means that the sample was porous with an average pore diameter of 12.80 nm. Polydispersity coefficient (by PCS method) is equal to 0.02 means that the investigated zinc oxide is monodispersed. X-ay diffraction data revealed the crystalline zincite structure of oxide. XRF data showed that zinc oxide was pure without any contaminations. All reagents (NaOH, sodium carbonate , analytical grade, supplied by Polskie Odczynniki Chemiczne, Gliwice, Poland; $NaClO_4$, analytical grade, supplied by Aldrich) were dissolved in doubly-distilled water. The surface charge of zinc oxide was calculated by comparison of the potentiometric titrations curve of the oxide suspension and the background electrolyte. These titrations of oxide suspensions were carried out in a thermostatic teflon vessel under free of CO_2 nitrogen atmosphere at 25°C with 0.1°C accuracy (Julabo Refrigerated/Heating Circulator model F10) in a special chamber that isolates titration vessel from the outer environment. During experiments the nitrogen pressure in the chamber was slightly higher than that in the outside chamber.

Measurements were performed using a PHM 240 Radiometer Research pH-meter with a glass electrode and calomel reference electrode. The whole titration procedure (e.g. addition of titrant by Dosimat 665) and data acquisition from pH-meter during measurement was controlled by a computer. Potentiometric titration was carried out with the use of an automatic burette (Dosimat 665. Metrohm). For adsorption and potentiometric titration experiments, sample of ZnO (1.0 g) was added to 50 cm^3 of solution.

The background electrolyte concentrations were $1 \cdot 10^{-1}$, $1 \cdot 10^{-2}$ and $1 \cdot 10^{-3}$ M, respectively. The concentration range of carbonate ions in the system was from $1 \cdot 10^{-6}$ to $1 \cdot 10^{-3}$ M. Adsorption measurements of carbonate ions from the $NaClO_4$ solution were carried out with and ^{14}C isotopes as the radiotracer. The radioactivity of samples was measured with a LS5000 TD Beckman beta counter.

The measurements were limited to narrow pH range (from 10 to 6) because of relatively high solubility of zinc oxide ($1 \cdot 10^{-5}$ M and higher).

The ζ potential measurements were carried out for concentration ranging from $1 \cdot 10^{-6}$ to $1 \cdot 10^{-3}$ M. The ζ potential was measured with Malvern 3000 Standard Zetasizer. Each survey of the ζ potential was repeated five times.

RESULTS AND DISCUSSION

The surface charge is formed on the metal oxide as a result of ionization and complexation reaction of surface hydroxyl groups. Surface charge density as a function of pH is very important characteristic of the surface properties of the metal oxide/electrolyte solution. pH_{pzc} position depends on the alkali-acid character of surface hydroxyl groups. For zinc oxide, the value of this parameter is in a very wide range of 6.9 – 9.8 (Kosmulski, 2001).

In aqueous solution ZnO dissolution takes place according to following reactions:

$$Zn^{2+}_{(aq)} + OH^- \Leftrightarrow Zn(OH)^+_{(aq)} \quad (1)$$

$$Zn(OH)^+_{(aq)} + OH^- \Leftrightarrow Zn(OH)_{2(s)} \quad (2)$$

$$Zn(OH)_{2(s)} \Leftrightarrow Zn(OH)_{2(aq)} \quad (3)$$

$$Zn(OH)_{2(s)} \Leftrightarrow Zn^{2+}_{(aq)} + 2\ OH^- \quad (4)$$

$$Zn(OH)_{2(s)} + OH^- \Leftrightarrow Zn(OH)^-_{3\ (aq)} \quad (5)$$

$$Zn(OH)_{2(s)} + 2\ OH^- \Leftrightarrow Zn(OH)^{2-}_{4\ (aq)} \quad (6)$$

$$ZnO_{(s)} \Leftrightarrow Zn^{2+} + O^{2-} \quad \mathbf{(7)}$$

$$ZnO_{(s)} + H_2O \Leftrightarrow Zn^{2+} + 2OH^- \quad pK=16,4 \quad (8)$$

$$ZnO_{(s)} + H_2O \Leftrightarrow ZnOH^+ + OH^- \quad pK=12,0 \quad (9)$$

$$ZnO_{(s)} + H_2O \Leftrightarrow ZnO_2H^- + H^+ \quad pK=17,0 \quad (10)$$

$$ZnO_{(s)} + H_2O \Leftrightarrow ZnO_2^{2-} + 2H^+ \quad pK=29,7 \tag{11}$$

The solubility diagram for zinc oxide in equilibrium with an aqueous solution at varying pH is shown in Fig. 1 (Blok and de Bruyn, 1970). The minimum solubility is at pH=9.9 – 12.3.

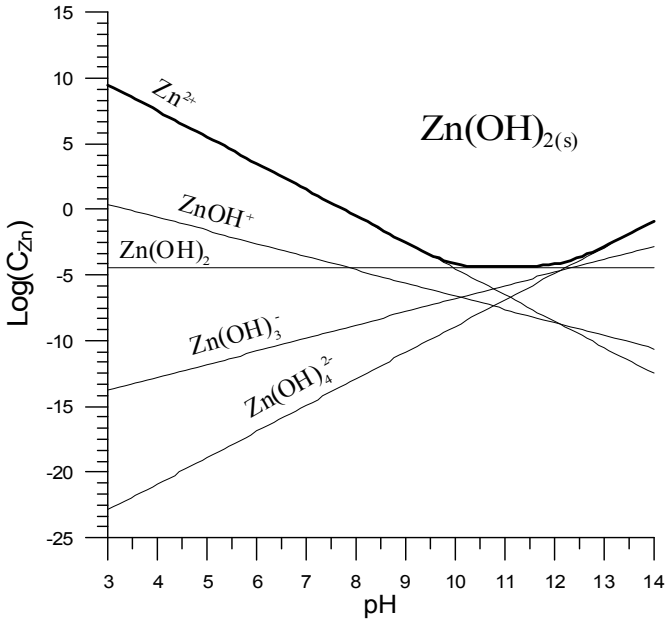

Fig. 1. Solubility diagram for zinc oxide

The surface charge density dependence on pH for ZnO/aqueous solution of the $NaClO_4$ shows that pH_{pzc} is equal to 8.0, however, the ζ potential pH_{iep}= 8.7 (Fig. 2). It seems that the difference between these points may arise from particle size of ZnO dispersion that was used in the potentiometric titration and electrophoretic measurements. In the last method, fine particle were used while in potentiometric titrations aggregates of zinc oxide particles were present.

The ζ potential of ZnO as a function of pH in the presence of carbonate ions is shown in Fig. 3. As one can see, the isoelectric point of ZnO is equal to pH=8.7 in the absence of carbonate ions and shifts towards lower pH in presence of carbonate ions with increase of their concentration. At the initial concentration of 0.001M carbonate ions the pH_{iep} is equal to 8.3.

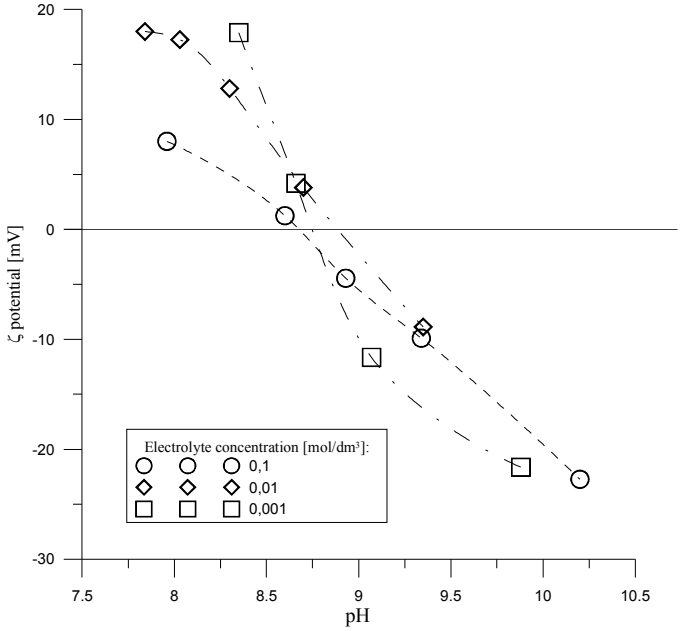

Fig. 2. The ζ potential of ZnO as a function of pH

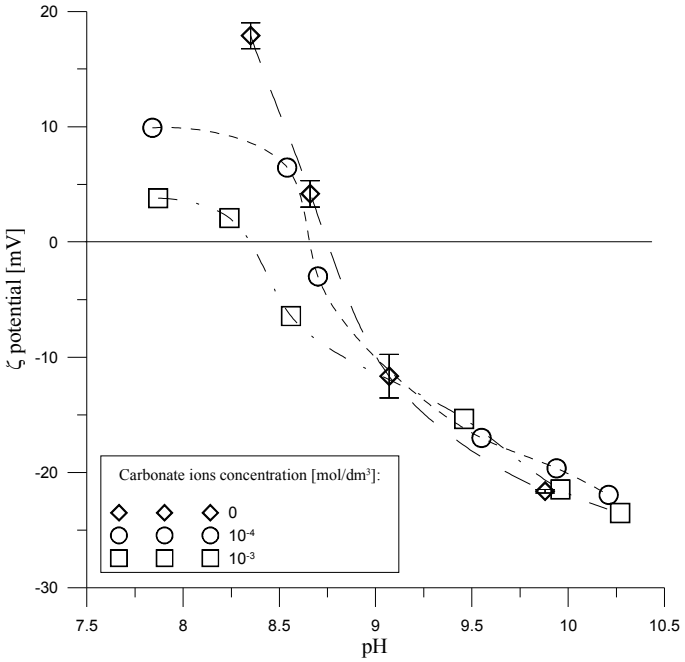

Fig. 3. The ζ potential of ZnO as a function of pH in 0.001 M $NaClO_4$ solution in presence of carbonate ions

Specific adsorption of anions at the metal oxide/electrolyte interface leads to a decrease of pH_{iep} due to the increase of concentration, complexed by anions, positively charged groups at the ZnO/electrolyte interface, eg. $\equiv ZnOH_2^+HCO_3^-$ and simultaneous decrease of concentration of ionized positively charged forms like $\equiv ZnO_2^+$. Because the diffuse layer charge is proportional to algebraic sum of negatively and positively charged groups, the decrease of concentration of positively charged groups leads to the formation of negatively charged ions, and to the decrease of zeta potential and shift of pH_{iep} towards low pH.

The adsorption densities and equilibrium concentrations of carbonate ions as a function of pH are depicted in Figs 4, 5, 6 and 7.

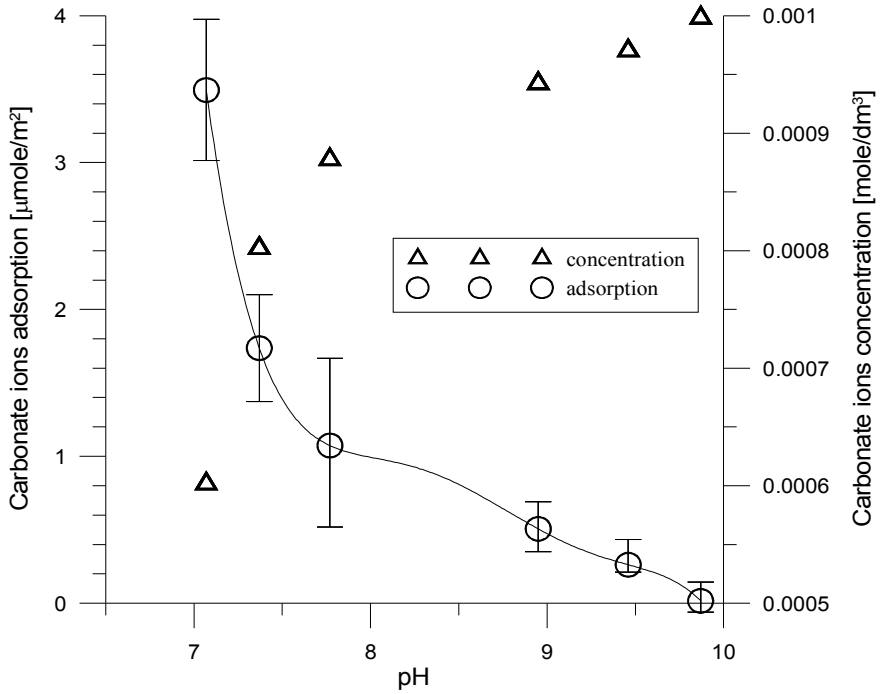

Fig. 4. Adsorption density as a function of pH solution in the Zn/0.001M $NaClO_4$ + 0.001 M HCO_3^- system

The initial concentration of carbonate ions was from $1 \cdot 10^{-3}$ M to $1 \cdot 10^{-6}$ M, respectively. The shapes of adsorption of carbonate ions plot vs. pH are characteristic for anions adsorption onto metal oxides and are called “adsorption envelope”. One can observe an increase of adsorption and decrease of concentration of carbonate ions with a decrease of pH of the electrolyte. That progress of adsorption is characteristic for specific anion adsorption onto metal oxides.

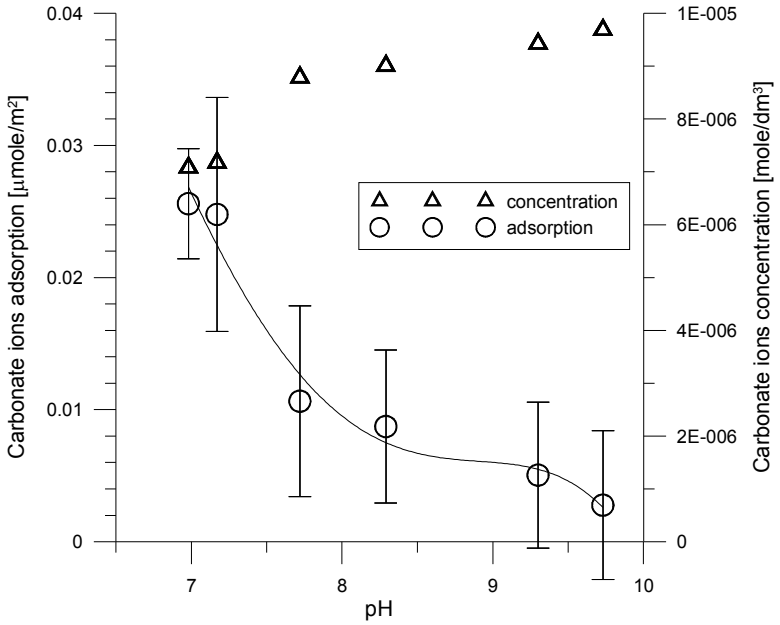

Fig. 6. Adsorption density as a function of pH solution in the Zn/0.001M $NaClO_4$ + 0.0001 M HCO_3^- system

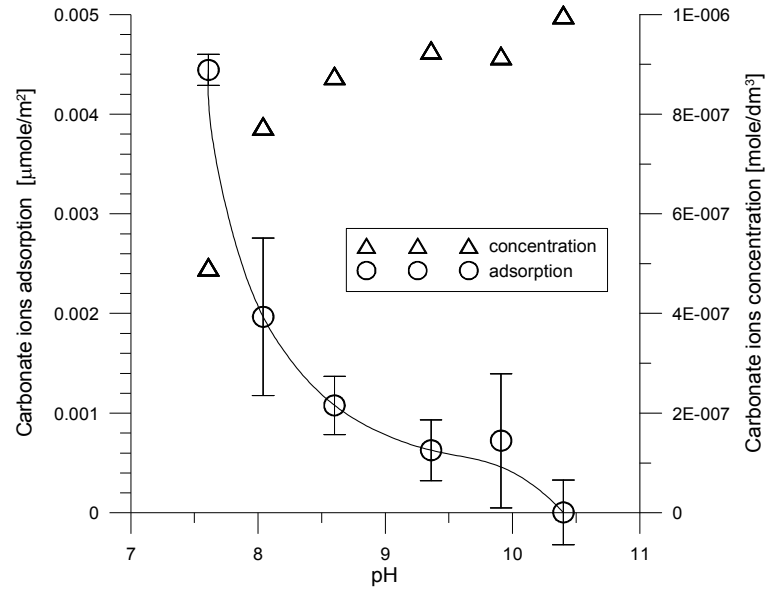

Fig. 7. Adsorption density as a function of pH solution in the Zn/0.001M $NaClO_4$ + 0.000001 M HCO_3^- system

The edge of adsorption moves to acidic environment with the increase of the concentration of the carbonate ions. That means that the carbonate ions adsorption may go through exchange of hydroxyl groups with innersphere complex formation (Eq. 7) or through hydrogen ions consumption with outersphere complex formation (Eq. 8). According to both equations, the increase of pH causes a decrease of carbonate ions adsorption.

$$-\mathrm{ZnOH} + \mathrm{HCO_3^-} \Leftrightarrow -\mathrm{ZnCOH} + \mathrm{OH^-} \tag{7}$$

$$2-\mathrm{ZnOH} + \mathrm{H^+} + \mathrm{HCO_3^-} \Leftrightarrow \left(-\mathrm{ZnOH_2^+}\right)_2 \mathrm{CO_3^{2-}} \tag{8}$$

The decrease of adsorption of carbonate ions with increase of pH is result of the following reaction:

$$\equiv \mathrm{ZnOH} + \mathrm{H^+} + \mathrm{HCO_3^-} \Leftrightarrow \equiv \mathrm{ZnOH_2^+HCO_3^-} \tag{9}$$

As one can conclude from Eq. 9, the decrease of pH will support the formation of carbonate groups at the zinc oxide surface. The concentration of carbonate ions in the solution decreases but even at the end of adsorption process it is still high, and can be a result of a small affinity of carbonate ions towards the surface of zinc oxide.

Table 1. Zinc oxide's surface parameters before and after adsorption of 0.001 M carbonate

Parametr	ZnO	ZnO+0.001M HCO_3^-
BET surface area	5.74 m^2/g	6.37 m^2/g
Langmuir surface area	7.89 m^2/g	9.08 m^2/g
BJH cumulative adsorption pore volume of pores 1,7nm<d<300nm	0.014 cm^3/g	0.016 cm^3/g
BJH cumulative desorption pore volume of pores 1,7nm<d<300nm	0.012 cm^3/g	0.014 cm^3/g
Average pore diameter	6.62 nm	8.68 nm
BJH adsorption average pore diameter	12.80 nm	8.83 nm
BJH desorption average pore diameter	12.94 nm	7.57 nm

From Table 1 one can see that the surface area of the zinc oxide increased after adsorption of the carbonate ions. This may be a result of the surface fluffing because the XRD measurements did not showed any formation of new structural phases. In Figs 8 and 9 the results of measurement of the ZnO particle size before and after adsorption of carbonate ions (concentration of carbonates equaled 0.001 M) are shown. The results proved that the average size of particles decreased. It can be explained by disaggregation of the zinc oxide particles.

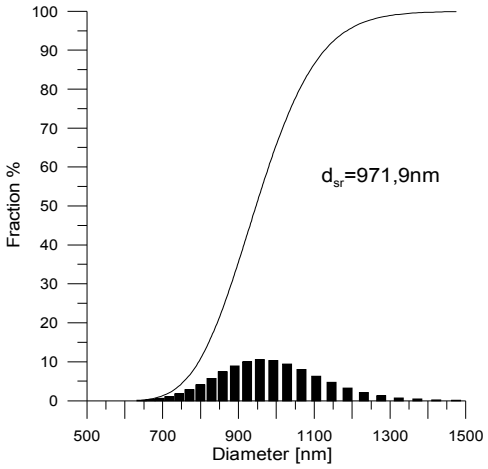

Fig. 8. Particle size of ZnO

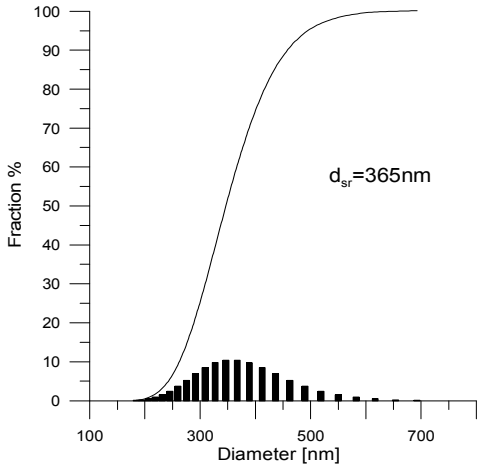

Fig. 9. Particle size of ZnO after adsorption of 0.001M carbonate ions

CONCLUSIONS

Carbonate ions adsorption causes exchange of surface groups with carbonate groups that cause an increase of negatively charged groups on the surface of zinc oxide and in consequence a decrease of ζ. The shapes of adsorption of carbonate ions plot vs. pH are characteristic for anions adsorption onto metal oxides and are called "adsorption envelope". One can observe an increase of adsorption and decrease of concentration of carbonate ions with a decrease of pH of the electrolyte. Adsorption on the zinc oxide is not complete because of small affinity of carbonate ions to the zincite surface.

REFERENCES

ADAMSON A.W., GAST A.P., (1997) Physical Chemistry of Surface, 6th ed., Wiley, New York,

BLOK L., DE BRUYN I P.L, (1970), „ *The ionic Double Layer at the ZnO/Solution Interface. I The Experimental Point of Zero Charge"*, J. Colloid Interface Sci., 32, 518-526.

BLOK L., DE BRUYN I P.L, (1970), „ *The ionic Double Layer at the ZnO/Solution Interface. II Composition Model of the Surface"*, J. Colloid Interface Sci., 32, 527-532.

BLOK L., DE BRUYN I P.L, (1970), „ *The ionic Double Layer at the ZnO/Solution Interface. III Comparison of calculated and Experimental Differential Capacities"*, J. Colloid Interface Sci., 32, 533-538.

BOLEWSKI A., (1982), Mineralogia szczegółow*a,* Wydawnictwa Geologiczne.

CRAWFORD R.J., HARDING I.H, MAINWARING D.E., (1996), „*The Zeta Potential of Iron and Chromium Hydrous Oxides during Adsorption and Coprecipitation of Aqueous Heavy Metals* ", J.

Colloid Interface Sci. 181, 561-570.
HAYES, K.F. KATZ L.E., (1996), Physics and Chemistry of Mineral Surfaces, Bardy, P.V. ed, CRC Press, New York, p.147.
JANUSZ W.; (2002) *„Electrical Double-Layer at Oxide Solution Interface"s,* , Encyclopedia Colloid and Surface Sci., (A. Hubard ed.) M. Dekker Inc., New York 2002, pp. 1687-1703.
KOSMULSKI M., (2001), Chemical Properties of Material Surfaces, Surfactant Sci. Series v. 102, M. Dekker Inc.
LU CH., YEH CH., (2000), Ceramics International 26, 351-357,
ROBERTSON A. P., LECKIE J. O., (1997), *„ Cation Binding Predictions of Surface Complexation Models: Effects of pH, Ionic Strength, Cation Loading, Surface Complex, and Model Fit "*, J. Colloid Interface Sci., 188, 444–472.
SIGOLI F.A., DAVOLOS M.R., JAFELICCI M., (1995), J. Alloys and Compounds, 262-263, 292-295.
SPRYCHA R, JABLONSKI J., MATIJEVIC E., (1992), „ *Zeta Potential and Surface Charge of Monodispersed Colloidal Yttrium (III) Oxide and BASIC carbonate*", J. Colloid Interface Sci. 149, 561-568.
TAHA F., EL-ROUDI A.M., ABD EL GABER A.A., (1990), Rev. Roum. Chim. 35, 503-509.
WANG R., SLEIGHT A.W., (1996), J. Solid State Chem., 122, 148-150.

Sędłak A., Janusz W., *Adsorpcja specyficzna jonów węglanowych na granicy faz tlenek cynku/roztwór elektrolitu,* Physicochemical Problems of Mineral Processing, 42 (2008), 57-66 (w jęz. ang)

Badania nad adsorpcją jonów węglanowych na granicy faz tlenek cynku/wodny roztwór $NaClO_4$ są przedstawione w niniejszej pracy. Zakres stężenia jonów węglanowych, dla których przeprowadzono pomiary wynosi od 10^{-6} do 10^{-3} M. Kształt krzywych adsorpcji względem pH jest charakterystyczny dla adsorpcji anionów na tlenkach metali i jest nazywany „obwiednią" adsorpcji. W celu wyeliminowania dostępu dwutlenku węgla do układu badanego wszystkie pomiary były przeprowadzone w specjalnej komorze.

Słowa kluczowe: telenek cynku, jony węglanowe, adsorbcja

Physicochemical Problems of Mineral Processing, 42 (2008), 67-74
Fizykochemiczne Problemy Mineralurgii, 42 (2008), 67-74

Beata Kurc∗, Teofil Jesionowski*, Andrzej Krysztafkiewicz*

FORMATION AND PHYSICOCHEMICAL PROPERTIES OF SILICA FILLERS PRECIPITATED IN EMULSION MEDIUM

Received May 15, 2008; reviewed; accepted July 31, 2008

The studies were performed on production of silica particles in emulsion medium. Precipitation of silicon dioxide was performed from aqueous solutions of sodium metasilicate and hydrochloric acid. A non-ionic surfactant (Rokanol K7) was applied as the emulsifier. Heptane formed the organic phase. Optimum compositions of emulsion and appropriate parameters of silica precipitation were determined. Particle size and morphology of the formed dispersions were examined using scanning electron microscopy (SEM). Dispersion character of the examined colloids was also defined using the non-invasive back scattering method (NIBS). Moreover, studies were conducted on sedimentation and wettability of the products with water and, at the final stage, adsorptive analysis was conducted.

Key words: silica fillers, emulsion systems, polydispersity, adsorption, sedimentation and wettability
Słowa kluczowa:

INTRODUCTION

In recent years increasingly high quality requirements have to be met by polymer composites. Selection of appropriate filler represents an important variable which shapes composite properties. The most important criteria in classification of inorganic fillers include their physicochemical properties dispersion and morphological properties in particular (Yatsuyanagi 2001, Chen 2005, Mathew 2004).

Modern silica fillers have to exhibit highly uniform particles, a relatively well developed specific surface area (particularly the outer surface area) and a specific-chemical character of their surface (Wu 1997, Gun'ko 2002). Among several types of

∗ Poznan University of Technology, Institute of Chemical Technology and Engineering, Pl. M. Skłodowskiej-Curie 2, 60-965 Poznan, Poland, btepper@interia.pl

silica, synthetic colloidal silicas deserve huge attention. They are obtained mainly by combustion of silicon halides (flame technique) (Barthel 1995), by acidic agent-induced precipitation from aqueous solutions of sodium metasilicate (Jesionowski 2002a, Zhang 1997, Jesionowski 2002b), and also using the technique of Stöber (alkoxysilane hydrolysis and condensation) (Stöber 1968, Esquena 2001).

In this study we suggest an alternate way of formation of nanometric monodisperse silicas in emulsion medium using heptane as an organic phase. The precipitated silicas manifest a strictly defined morphological and dispersion character. Moreover, the numerous active chemical centres present at silica surface may participate in formation of bonds in the polymer-filler system. The principal aim of the study involved selection of optimum precipitation parameters (in emulsion medium) and a comprehensive physicochemical characterization of the produced silica fillers.

EXPERIMENTAL

MATERIALS

Silicas were obtained by precipitation from aqueous solutions of sodium metasilicate (Vitrosilicon S.A.) and hydrochloric acid (POCh S.A.). The organic phase was formed by heptane (POCh S.A.) while oxyethylenated fatty alcohol, Rokanol K7 (PCC Rokita S.A.) was used as an non-ionic emulsifier.

METHODS OF STUDIES

The silica precipitation process was preceded by preparation of two emulsions, of which one, the alkaline one (E1), contained appropriate volume of sodium silicate solution and heptane. The other, acidic emulsion (E2), contained hydrochloric acid and an organic solvent. The third component of both emulsion involved the same emulsifier, added to the emulsions in various amounts. Emulsion E2 was placed in a reactor and emulsion E1 was dosed to while the entire reactor content was mixed using a homogenizer. The precipitated silica was destabilized and, then, the organic solvent was distilled off.

Silica powders dispersion studies were performed, including determination of silica particle size distribution, with appropriate attention given to band intensity and particle volume, using the non-invasive back scattering method (NIBS) and employing Zetasizer Nano ZS (Malvern Instruments Ltd.). Silica particle shape and surface morphology were examined using scanning electron microscopy (Size VO40). Moreover, the course of sedimentation and wettability with water of the precipitated silicas were documented using K100 tensiometer (Krüss). At the last stage, specific surface

area (BET) was estimated for selected silicas using ASAP 2010 (Micromeritics Instruments Co.).

RESULTS AND DISCUSSION

The results of the physicochemical tests of the obtained silicas fillers are presented in Table 1.

Table 1. Mean particle diameter and polydispersity of silica related to content of emulsifiers

Sample No.	Emulsifier content (g)		Range of particle diameters (nm)		Polydispersity
	E1	E2	by intensity	by volume	
1	3.0	1.0	459-955; 2670-5560	396-1110; 2670-6440	0.261
2	2.5	0.8	220-295; 615-1110; 4150-5560	190-342; 531-1280; 3580-6440	0.520
3	2.0	0.7	106-122; 164-190; 342-396; 3090-5560	106-220; 295-459; 2670-6440	1.000
4	3.0	0.8	1110-2670	955-3090	0.751

The evaluated results documented negative effects of insufficient amounts of the applied emulsifier in preparation of the two emulsions on the number of bands which appeared in the particle size distributions. Taking into account either band intensity of particle volumes, the multimodal particle size distribution was confirmed by the value of polydispersity, which amounted to 1.000 (Table 1). Much better physicochemical parameters were manifested by silicas precipitated in the presence of augmented amounts of surfactants (samples 1 and 4).

The silica of most advantageous parameters and physicochemical properties was obtained in sample 1. The respective particle size distributions are shown in Fig.1, taking into account the relationship between particle diameter and either band intensity (Fig.1a) or volume share (Fig.1b).

In Fig. 1a the intense band of primary agglomerates (aggregates) of silica particles could be noted in the diameter range of 459-955 nm, with maximum intensity of 24.8 for the particles of 615 nm in size. The other band, of a much lower intensity, reflected the presence of secondary agglomerates and showed maximum intensity of 14.1 which corresponded to agglomerate diameter of 4100 nm. In turn, in the particle size distribution which took into account volume share of the particles, domination of secondary agglomerates was observed (Fig.1b). In the precipitated silica the highest share was formed by particles of 2670-6440 nm in diameter. Approximate volume shares of the two bands may indicate that such conditions silica precipitation in emulsions resulted in a product of a highly uniform character, which was confirmed by the polydispersity value of 0.261.

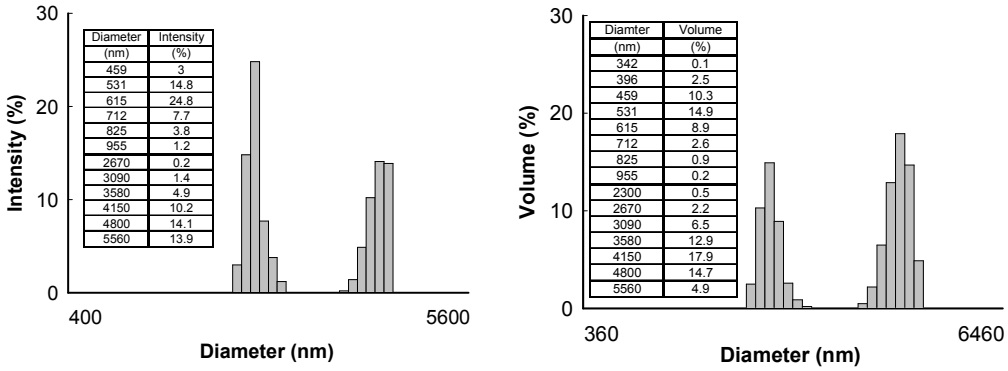

Diameter (nm)	Intensity (%)
459	3
531	14.8
615	24.8
712	7.7
825	3.8
955	1.2
2670	0.2
3090	1.4
3580	4.9
4150	10.2
4800	14.1
5560	13.9

Diamter (nm)	Volume (%)
342	0.1
396	2.5
459	10.3
531	14.9
615	8.9
712	2.6
825	0.9
955	0.2
2300	0.5
2670	2.2
3090	6.5
3580	12.9
4150	17.9
4800	14.7
5560	4.9

(a) (b)

Fig.1. Particle size distribution of silica precipitated in sample 1 (a) by intensity and (b) by volume

Electron micrograph of silica precipitated in sample 4 is shown in Fig. 2.

The silica precipitated under conditions listed in Table 1 manifested only one intense band, representing particles of 1110-2670 nm in diameter. The SEM photograph confirmed the near uniform character of the sample and low tendency to form larger accumulations of the particles while polydispersity of the sample amounted to 0.751.

Silica particle sedimentation profile in water is shown in Fig. 3 as a function weight gain with time for the samples precipitated using heptane as the organic solvent of the emulsion system.

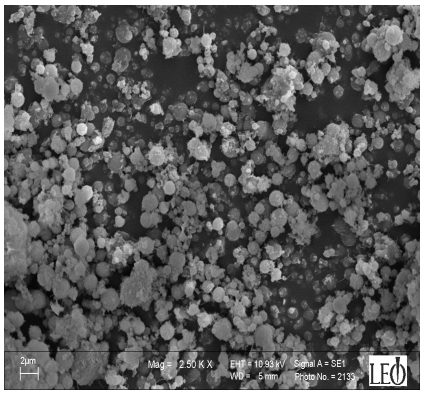

Fig. 2. Electron micrograph (SEM) of silica precipitated in sample 4

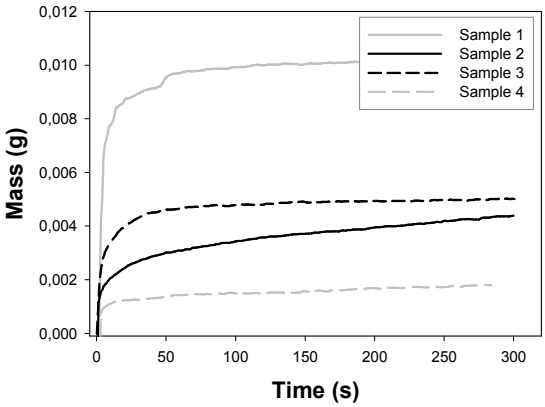

Fig. 3. Sedimentation profile for obtained silicas

Course of the curves permitted to note that the lowest weight increased vs. time was shown by silica precipitated in sample 4. Slightly more particles sedimented in silicas precipitated in samples 2 and 3. The weight increased in time was reciprocally

related to the amount of applied emulsifier: it was increasing in line with decreasing weight share of the surfactant applied in preparation of the two emulsions.

Curves of wettability with water for selected silicas are shown in Fig.4.

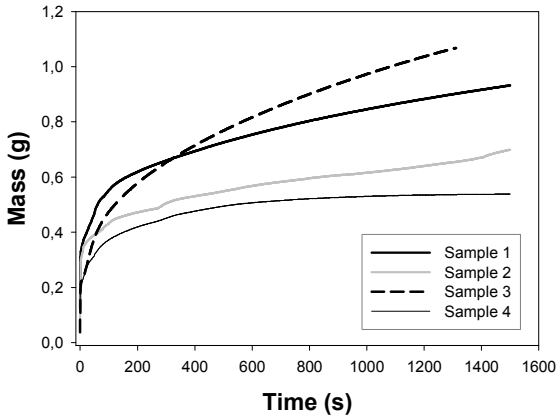

Fig. 4. Wettability with water for selected silicas

Studies conducted on wettability of the analyzed products with water demonstrated that the most hydrophilic silica was obtained when the added emulsifiers comprised the lowest weight share (sample 3). The silica manifested complete wetting before the time set at 1500 s. Silicas precipitated in samples 1, 2, 4 manifested a relatively slower wetting. The curve of wetting for silica precipitated in the latter sample, diverged most from a hydrophilic type (mass of the wetted silica amounted to just 0.5 g in the course of entire measurement).

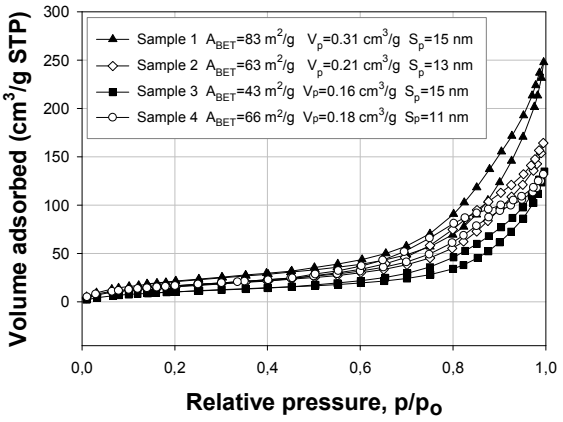

Fig. 5. Nitrogen adsorption/desorption isotherms for selected silicas precipitated in emulsion medium

Results of adsorption studies and isotherms of nitrogen adsorption/desorption for selected silicas are shown in Fig.5.

As indicated by the data of Fig.5, silicas precipitated in an emulsion medium demonstrated similar specific surface areas and depended upon the amount of added surfactant in the course of emulsion preparation. In the range of relative pressures p/p_0 = 0.0-0.7 the amount of adsorbed nitrogen increased only slightly. When the pressure was exceeded, however, the amount of adsorbed nitrogen abruptly increased to reach the highest value of 250 cm^3/g at p/p_0=1 in silica precipitated in sample 1. The graph indicated also that the range of hysteresis loop was the highest for the product, which was confirmed by the high value of BET specific surface area equal 83 m^2/g.

CONCLUSIONS

Silica of best dispersive and morphological properties was obtained, with optimized amounts of emulsifier (Rokanol K7), amounting to 3 g for emulsion E1 and 1.0 g for emulsion E2. Just a slight increase in weight of the added surfactant in emulsion E2 resulted in markedly higher polydispersity, in appearance of larger particle clumps and particle shape diverged slightly from the ideal, spherical one. Sedimentation curves demonstrated that weight of the sedimenting silica particles increased in line with decreasing amounts of added of emulsifiers added in the course of silica precipitation. Silicas precipitated under the suggested conditions were, in general, well wettable with water. Adsorption studies showed that the obtained silicas manifested a moderately developed specific surface area (BET: 40-85 m^2/g) and showed mesoporous character.

ACKNOWLEDGEMENTS

This work was supported by the Ministry for Science and Higher Education research grant No. R08 034 01 (2006-2008).

REFERENCES

BARTHEL H., 1995, Surface Interactions of dimethylsiloxy group-modified fumed silica, Colloids Surf., 101, 217-226.

CHEN G., ZHOU S., GU G., YANG H., WU L., 2005, Effects of surface properties of colloidal silica particles on redispersibility and properties of acrylic-based polyurethane/silica composites, J. Colloid Interface Sci., 281, 339-350.

ESQUENA J., SOLANS C., 2001, Phase changes during silica particle formation in water-in-oil emulsions, Colloids Surf.A, 183-185, 533 – 540.

GUN'KO V.M., SHEERAN D.J., AUGUSTINE, S.M., BLITZ, J.P., 2002, Structural and energetic char-

acteristics of silicas modified by organosilicon compounds, J. Colloid Interface Sci., 249, 123-133.
JESIONOWSKI, T., 2002a, Synthesis of organic–inorganic hybrids via adsorption of dye on an aminosilane-functionalised silica surface, Dyes Pigm., 55, 133-141.
JESIONOWSKI T., ŻURAWSKA J., KRYSZTAFKIEWICZ A., 2002b, Surface properties and dispersion behaviour of precipitated silicas, J. Mater. Sci., 37, 1621-1633.
MATHEW G., HUH M.-Y., RHEE J.M., LEE M.-H., NAH C., 2004, Improvement of properties of silica filled styrene-butadiene rubber composites through plasma surface modification of silica, Polym. Adv. Technol. 15, 400-408.
STÖBER W, FINK A, BOHN E., 1968, Contolled growth of monodisperse silica spheres in the micron size range, J. Colloid Interf. Sci., 26, 62-69.
WU G., KOLIADIMA A., HER Y.-S., MATIJEVIC E., 1997, Adsorption of dyes on nanosize modified silica particles, J. Colloid Interf. Sci. 195, 222-228.
ZHANG K., GAN L.M., CHEW C.H., GAN L.H, 1997, Silica from hydrolysis and condensation of sodium metasilicate in bicontinuous microemulsions, Mater. Chem. Phys., 47, 164.
YATSUYANAGI F., SUZUKI N., ITO M., KAIDOU H., 2001, Effects of secondary structure of fillers on the mechanical properties of silica filled rubber systems, Polym., 42, 9523-9529

Kurc B., Jesionowski T., Krysztafkiewicz A., *Otrzymywanie i charakterystyka fizykochemiczna napełniaczy krzemionkowych strącanych w środowisku emulsji,* Physicochemical Problems of Mineral Processing, 42 (2008), 67-74 (w jęz. ang)

W przedstawionej pracy podjęto próbę uzyskania napełniaczy krzemionkowych metodą strąceniową w układzie emulsyjnym z roztworu metakrzemianu sodu i kwasu solnego, z zastosowaniem heptanu jako fazy organicznej oraz z dodatkiem Rokanolu K7. Otrzymane krzemionki poddano badaniom sedymentacji i zwilżaniu, określono wielkość powierzchni właściwej BET, a następnie wyznaczono rozkłady wielkości cząstek oraz dokonano obserwacji morfologii i mikrostruktury. Kolejnym etapem było omówienie i porównanie wyników świadczących o odpowiednim doborze parametrów, podczas syntezowania krzemionek. Badania dowiodły, że osiągnięto podstawowy cel, uzyskano wysoko zdyspergowane sferyczne krzemionki z układów emulsyjnych dla zastosowanej fazy organicznej. Użycie heptanu jako medium organicznego pozwoliło otrzymać krzemionkę o odpowiednich właściwościach fizykochemicznych, a uzyskane produkty mogą mieć szerokie zastosowanie w różnych gałęziach przemysłu, między innymi jako napełniacze wzmacniające w produktach elastomerowych, nośniki czynników zabezpieczających plony (nośniki konserwantów) oraz w środkach ochrony roślin, czynniki wybielające i czyszczące w pastach do zębów, pigmenty do produkcji papieru, czy też jako wypełniacze w farbach i lakierach itp.

słowa kluczowa:wypełniacze krzemionkowe, systemy emulsyjne,polidyspersja, adsorpcja, sedymentacja, zwilżalność

Physicochemical Problems of Mineral Processing, 42 (2008), 75-84
Fizykochemiczne Problemy Mineralurgii, 42 (2008), 75-84

Jan Drzymała*

ATLAS OF UPGRADING CURVES USED IN SEPARATION AND IN MINERAL SCIENCE AND TECHNOLOGY PART III

Received April 27, 2008; reviewed; accepted July 31, 2008

The present Atlas (Part III) is the last from a series of articles on upgrading curves relating quality and quantity of products of separation. In this Atlas 12 additional upgrading curves were presented while 30 curves were presented in Parts I and II. In the previous papers the curves were grouped into categories: A_I (α-insensitive curves with triangle or near triangle area accessible for plotting) A_o (α-insensitive curves with square area available for plotting) B_I (α-sensitive curves with triangle plotting area, B_o (α-sensitive curves having square plotting area), C_I (α-insensitive curves for $\beta > \alpha$ and triangle area for plotting), and C_o (α-insensitive curves for $\beta > \alpha$ or $\beta < \alpha$ and square area) where β stands for the content of a component in concentrate while α is the content of a component in the feed. In this Part III more complex upgrading curves were presented and an additional class of upgrading curves was introduced with irregular area for plotting. It was again stressed that all the upgrading curves contain the same information but in a different, specific for a given curve form. The use of upgrading curves depends on the needs and preferences of users. An appropriate matching of an upgrading plot with a set of separation results allows to approximate the curve with a suitable mathematical formula which can be used for characterizing separation. As previously, the readers are kindly asked to report unmentioned hitherto upgrading curves to jan.drzymala @pwr.wroc.pl for their future publication in the Internet http://www.ig.pwr.wroc.pl/minproc/krzywe%20wzbogacania.html

Key words: separation, upgrading, upgrading curves, separation efficiency

INTRODUCTION

Many aspects of separation and analysis of separation results have been discussed in detail in the previous parts of this series of papers. In Parts I and II 30 separation

* Wrocław University of Technology, Wybrzeże Wyspianskiego 27, 50-370 Wrocław, Poland, jan.drzymala@pwr.wroc.pl

curves were presented. It was claimed there that there is unlimited number of separation curves. It will be shown here that it results from the principles of separation and considering the upgrading process as a relationship between quantity and quality of separation products.

During separation the feed is split into two products, that is concentrate and tailing. When more products are created, the system always can be treated as a two-product separation by considering certain product as the first product while the mixture of remaining products as the second product.

The principal equation, also called the separation mass balance, for a selected component (1) in the feed and in the products of separation is:

$$100\%\alpha_1 = \gamma_1\beta_1 + \gamma_2\vartheta_1 \tag{1}$$

There are other equations valid for the considered separation system:

$$\alpha_1 + \alpha_2 = 100\% \tag{2}$$

$$\beta_1 + \beta_2 = 100\% \tag{3}$$

$$\vartheta_1 + \vartheta_2 = 100\% \tag{4}$$

$$\gamma_1 + \gamma_2 = 100\% \tag{5}$$

where symbol 2 stands for the second component, that is everything except component 1. In the case of γ, symbol 1 means product 1 and symbol 2 means product 2. Equations 1-5, when combined, provide a modification of Eq.1, that is the mass balance for component (2):

$$100\%\alpha_2 = \gamma_1\beta_2 + \gamma_2\vartheta_2 \tag{1b}$$

In Eqs 1-5 α, β, ϑ stand for content of a component in the feed, concentrate and tailing, respectively, while γ_1 means yield of concentrate while γ_2 means yield of the tailing.

Thus, there are 8 unknowns and 5 equation in the separation systems considered as upgrading. Therefore, three values are needed for a complete solution of the balance of separation system. These unknowns can be taken from experimental data (for instance α_1, β_1, and ϑ_1 or γ_1, β_2, and ϑ_2, etc.).

When the separation involves many sets of separation data, it is very convenient to plot the separation result as upgrading curves. Still, for each set of data we need the values of three parameters from the list of 4 variables (α, β, ϑ, γ). In the case when all three selected parameters vary, a 3D plot is needed to represent the results of separation (Tumidajski et al., 2007). However, frequently one of the variables is constant. Usually, it is the content of the valuable component in the feed (α_1 = const) while we have all needed separation data for the remaining two variables. Then, it is convenient

to plot the results of separation as a map in a x-y Cartesian system as a relationship between two variables (any other parameter can be calculated). Plotting the results for only two parameters of separation provide a map of results. Sometimes, if there is a law governing separation, we can get, instead of a cloud-shape scattered data, a linear relationship, but this case will be discussed a little further.

The results of separation cannot be represented by any number because there are limits of separation. The limits are: ideal separation, ideal mixing (when the 100% pure component under question, which forms concentrate, starts to be diluted with the unwanted component), and no separation. Then, equations 1-5 should be solved for:

$$\alpha_1 = \beta_1 \text{ (lack of separation)} \tag{6}$$

$$\beta_1 = 100\% \text{ (ideal separation)} \tag{7}$$

$$\gamma_1\beta_1/\alpha_1 \ (=\varepsilon_1=\text{recovery,}) = 100\% \text{ (ideal mixing)} \tag{8}$$

For instance, for the plot relating yield (γ) and content (β), also know as the Henry curve, the limiting area is complex (Atlas, Part I) with its upper side represented by a hyperbolic $1/\beta$ curve.

When the separation results, drawn on a separation plot, form a line or curve which can indicate that there is a law governing the separation, the three "missing" equation are:

a) α_1 = const

b) for instance β_1 = certain value or values

c) law governing separation, that is equation relating any two variables (for instance $\gamma = a/\beta + b$ (Tumadajski *et al*., 2007) or $\vartheta = a\beta + b$ (Stepinski, after Pudlo, 1971) and many other formulas (Drzymala and Hussin, 2005).

Since the law governing separation, as a rule, introduces new unknown or unknowns, in fact we have to use not three but four or more equations, depending on how many adjustable parameters are used by the law expressed as equation. The additional equations are:

d) constant(s) of the equation representing the law.

The separation governing law is a convenient tool for characterizing separation results provided that the equation contains only one adjustable parameter. Then, for separation systems obeying the law, a comparison of the separation results can be based on comparison of the one-adjustable parameter of separation.

As it was demonstrated, any separation system, considered as upgrading, consists of 8 parameters. In addition to that, these parameters can be combined into unlimited number of new parameters called indices, factors, numbers, ratios, efficiencies, etc. Each new parameter provides both a new equation and a new unknown. Thus, introducing new parameters does not provide any new information about the system. How-

ever, frequently the new parameters are very useful. For instance recovery in concentrate (ε) is defined as:

$$\varepsilon_1=\gamma_1\beta_1/\alpha_1 \tag{9}$$

where subscript 1 means component 1. Recovery indicates , usually in %, how much of component's mass was transferred to a given product. Parameters are the enrichment ratio (β/α) and the Hancock efficiency of separation $E=\varepsilon_{1,1}-\varepsilon_{2,1}$ or $E=\frac{10^4(\alpha-\vartheta)(\beta-\alpha)}{(\beta-\vartheta)(100-\alpha)\alpha}$ (see Fig. 1) (Taggart, 1943; Jowett, 1975). Numerous equivalent formulas for the Hancock efficiency parameter were given by Barskij and Rubinstein (1970). Many other separation parameters were presented in Parts I and II of the Atlas.

All the upgrading parameters can be grouped into pairs providing infinitive number of upgrading curves which represent the same data but in a different esthetical and graphical form. The usefulness of a given upgrading curve depends, to a great extent, on personal preferences.

UPGRADING BALANCE

For plotting upgrading curves, the same hypothetical results of separation (Table 1) were considered as in Atlas Parts I and Part II (Drzymala, 2006, 2007). It was assumed that the feed contains only two components, that is component 1 and component 2 (rest of material). Only principal parameters, that is feed grade (α), yield of products (γ), content of component 1 (β), and recoveries ε of both components are presented. Other parameters can be calculated using the formulas given in the axes of the upgrading curves.

Table 1. Upgrading balance of a hypothetical separation. The data were used for calculation of upgrading curves

Product	yield, γ (%)	content of component 1, β, %	recovery of component 1 $\varepsilon=\gamma\beta/\alpha$, %	recovery of component 2 $\varepsilon=\gamma\beta/\alpha$, %
K_1	12.06	81.70	64.00	2.00
K_1+K_2	20.14	60.40	79.01	9.43
$K_1+K_2+K_3$	42.27	32.44	89.07	33.71
$K_1+K_2+K_3+K_4$	70.14	21.73	98.99	63.92
Tailing	29.86	0.52	1.01	36.08
Feed	100.00	15.40=α	100.00	100.00

UPGRADING CURVES

In the previous paper the upgrading curves were classified into three categories: A (α-insensitive), B (α-sensitive), C (α-insensitive but covering limited range of variables). There were additional symbols for the shape of the area available for plotting (/ for triangle area and *o* for square area). The same classification was used in this Atlas III. A new class of separation curves B_u was added for α-sensitive curves with irregular shape available for plotting. The upgrading curves considered in this Atlas are shown in Fig. 1.

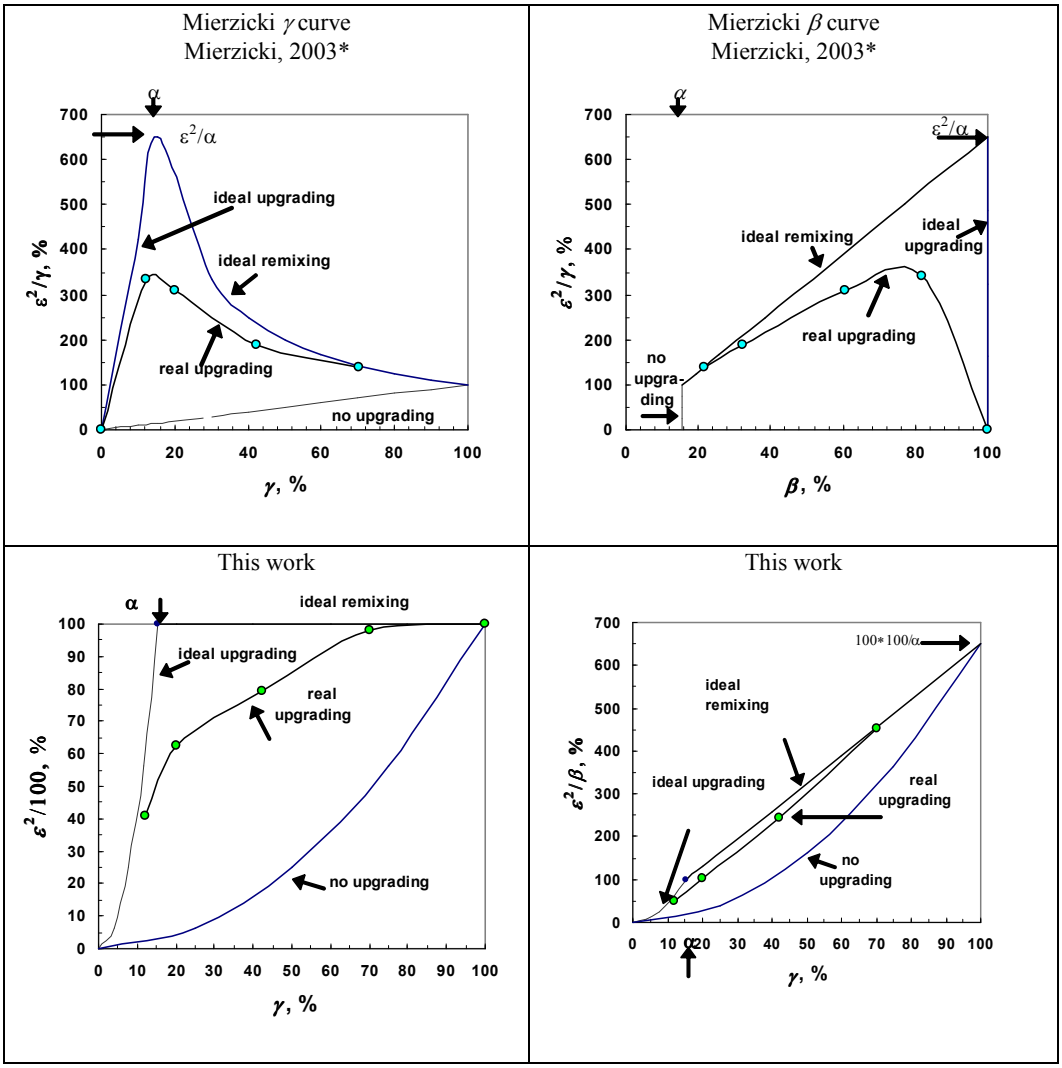

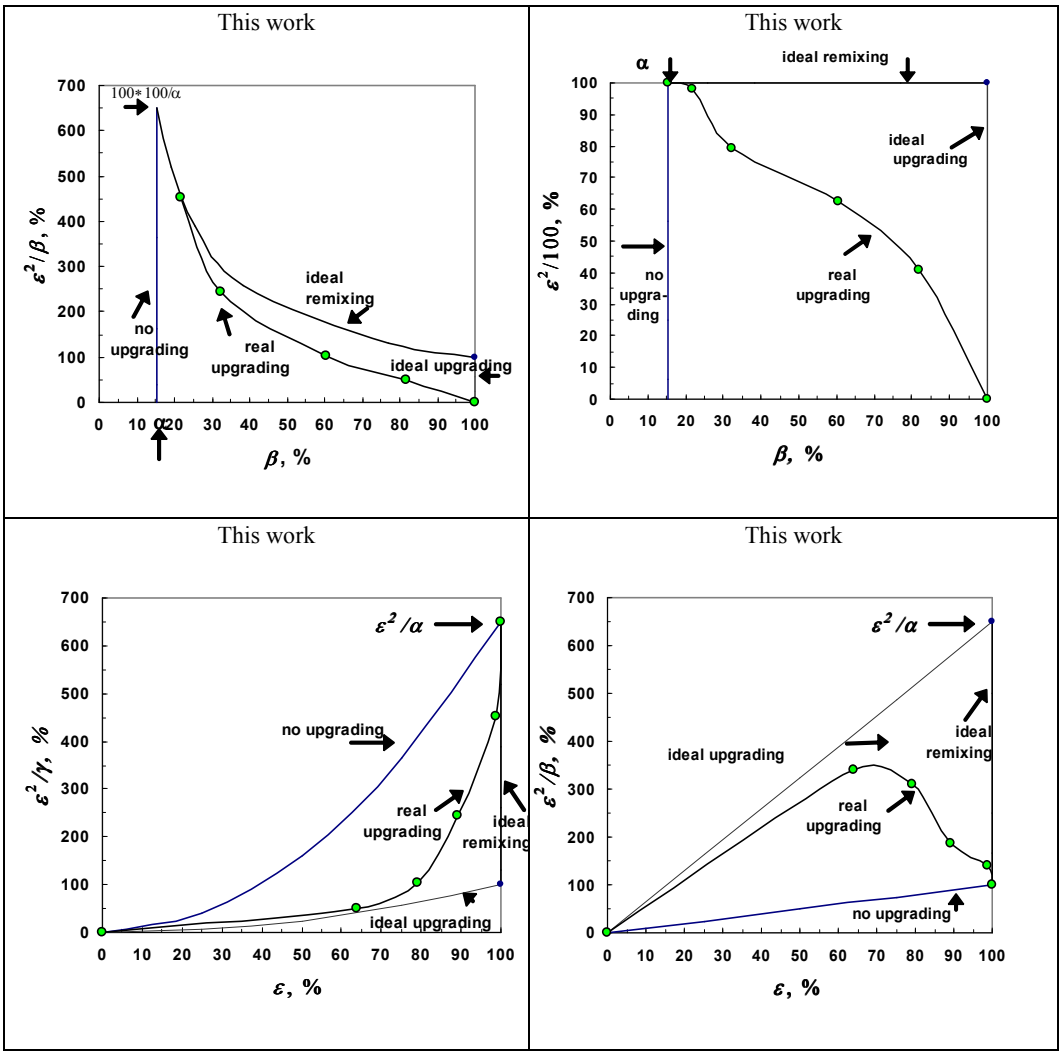
This work
100*100/α
no upgrading
real upgrading
ideal remixing
ideal upgrading
α
ε²/β, %
β, %
This work
α
ideal remixing
ideal upgrading
no upgra-ding
real upgrading
ε²/100, %
β, %
This work
ε² /α
no upgrading
real upgrading
ideal remixing
ideal upgrading
ε²/γ, %
ε, %
This work
ε² /α
ideal upgrading
ideal remixing
real upgrading
no upgrading
ε²/β, %
ε, %

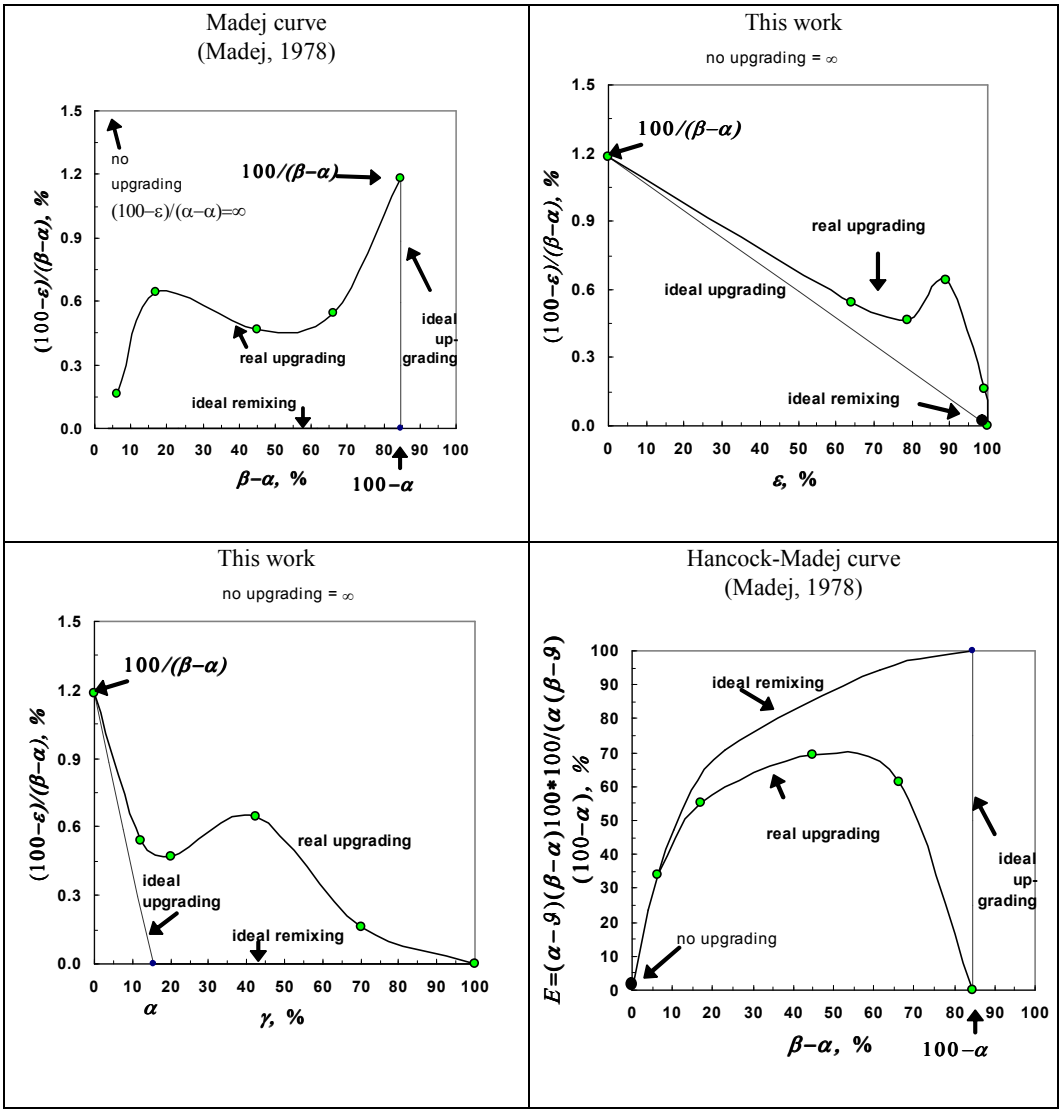

*Mierzicki (2003) considered the following upgrading curves: $\gamma^2\beta^3 = f(\gamma)$, $\gamma\beta^2 = f(\gamma)$, $\gamma\ \beta^2/\alpha^2 = f(\gamma)$, $\frac{\alpha^3}{\gamma^2\beta^2} = f(\gamma)$, $\frac{\alpha^3}{\gamma^2\beta^2} = f(\beta)$, $\gamma^2\beta^3 = f(\beta)$, and $\gamma\beta^2 = f(\beta)$.

Fig.1. Different upgrading separation curves considered in this Atlas (Part III).
All the curves are B_u type (α-sensitive and irregular shape of area available for plotting), expect the $\varepsilon^2/100$ vs β curve which is of B_o type

CONCLUSIONS

The present Atlas (Part III) is a final part in a series of papers providing different upgrading curves relating quality and quantity of the products of separation. In all three parts of the Atlas 42 curves were shown and characterized. This number of curves is still not great in comparison to unlimited number of possible upgrading curves. The new curves presented in this paper and the ones which will be generated in the future, as a rule, are very complex and can be applied only for very special purposes.

ACKNOWLEDGEMENTS

Financial support from the Ministry of Science and Higher Education (zlec. 342-865) is gratefully acknowledged.

REFERENCES

BARSKIJ L.A., RUBINSTEIN J.B., 1970. Cybernetic methods in mineral processing, Nedra, Moscow, 1970, in Russian.

DRZYMALA, J., AHMED, H.A.M., Mathematical equations for approximation of separation results using the Fuerstenau upgrading curves, Int. J. Miner. Process., 76, 55-65, 2005

DRZYMALA, J., Atlas of upgrading curves used in separation and mineral science and technology, Physicochemical Problems of Mineral Processing, 40, 19-29, 2006

DRZYMALA, J., Atlas of upgrading curves used in separation and mineral science and technology (Part II), Physicochemical Problems of Mineral Processing, 41, 27-35, 2007

JOWETT, A. Formula for the technical efficiency of mineral separation, Int. J. Min. Process. 2, 1975, 287-301

MADEJ, W., Ocena procesów wzbogacania, Prace Instytutu Metali Nieżelaznych, tom VII, nr 3/78, 1978, 105-113

MIERZICKI M., Właściwości krzywych wzbogacania wyższego rzędu, Engineer Thesis, Wrocław University of Technology, Mining Engineering Faculty, 2003

PUDŁO, W., O pewnej metodzie aproksymowania krzywych wzbogacalności, Zeszyty Problemowe Górnictwa PAN., Z.2, v. 9., 1971, 83-103

TAGGART, A.F. Handbook of mineral dressing. Wiley, New York, 1943,

TUMIDAJSKI T., SARAMAK D., NIEDOBA T.: *Matematyczne aspekty opisu i oceny wzbogacalności rud miedzi*. Górnictwo i Geoinżynieria, z. 4, 2007, s. 97-106

Drzymala J., *Atlas krzywych wzbogacania do opisu separacji stosowanych w nauce i w przemyśle mineralnym*. Część III, Physicochemical Problems of Mineral Processing, 42 (2008), 75-84 (w jęz. ang)

Obecny Atlas (cześć III) jest ostatnią z serii prac o krzywych wzbogacania wiążących ilość i jakość produktów separacji. W obecnym atlasie przedstawiono 12 dodatkowych krzywych wzbogacania,

podczas gdy poprzednio w częściach I i II pokazano 30 krzywych wzbogacania. W poprzednich artykułach krzywe były pogrupowane na kategorie: $A_{/}$ (α-nieczułe z trójkątnym lub blisko trójkątnym obszarem dostępnym do rysowania) A_o (α- nieczułe krzywe z kwadratowym obszarem dostępnym do rysowania), $B_{/}$ (α-czułe krzywe z trójkątnym lub blisko trójkątnym obszarem rysowania, B_o (α-czułe krzywe z kwadratowym obszarem dostępnym do rysowania), $C_{/}$ (α-nieczułe krzywe dla $\beta > \alpha$ i trójkątnym obszarem rysowania), C_o (α-nieczułe krzywe dla $\beta > \alpha$ lub $\beta < \alpha$ i kwadratowym obszarem rysowania), gdzie β oznacza zawartość składnika w koncentracie podczas gdy α oznacza zawartość rozpatrywanego składnika w nadawie. W części III Atlasu zaprezentowano bardziej skomplikowane krzywe wzbogacania tworzące nowa klasę krzywych, które zostały określone symbolem B_u oznaczającym czułość na α oraz nieregularny obszar dostępny do rysowania. Podkreślono ponownie, że wszystkie krzywe wzbogacania zawierają te same informacje, ale w innej, specyficznej dla danej krzywej formie. Zastosowanie danej krzywej wzbogacania powinno zależeć od preferencji użytkownika. Wykazano, że odpowiednie połączenie krzywej wzbogacania z rezultatami separacji pozwolić może na wyznaczenie równania matematycznego, które może pełnić rolę prawa rządzącego separacją. Podobnie jak poprzednio, czytelnicy proszeni są o nadsyłanie nieopisanych dotąd krzywych wzbogacania pod adres jan.drzymala@pwr.wroc.pl dla ich opublikowania w Internecie pod adresem http://www.ig.pwr.wroc.pl/ /minproc/krzywe%20wzbogacania.html.

słowa kluczowe: separacja, wzbogacanie, krzywa wzbogacania, efektywność wzbogacania

Physicochemical Problems of Mineral Processing, 42 (2008), 85-90
Fizykochemiczne Problemy Mineralurgii, 42 (2008), 85-90

Danuta Szyszka*, Ewa Glapiak*, Jan Drzymała*

ENTRAINMENT-FLOTATION ACTIVITY OF QUARTZ IN THE PRESENCE OF SELECTED FROTHERS

Received April 27, 2008; reviewed; accepted July 31, 2008

Flotation is used for separating mineral particles. Flotation is accompanied by entrainment of hydrophilic particles which is an undesirable process. Flotation and entrainment depend on numerous parameters, among them the presence and concentration of frother. This work was devoted to investigate the borderline between entrainment and flotation of quartz particles in the so-called monobubble Hallimond tube in the presence of varying concentrations of selected frothers. The following frothers were used: octyl alcohol, isoamyl alcohol, α-terpineol, tricosene-ethyleneglycol 1-hexadecanoic ether and corflot (a mixture of butyl ethers of di-, tri- and tetraethylene glycols). Entrainment of the quartz particles in pure water has also been conducted as a reference test. The work has confirmed that entrainment depends on particle size. It also confirmed the role of the frother used. Two of the frothers: tricosene-ethylene glycol 1-hexadecanoic ether and octyl alcohol have exhibited both frothing and collecting properties.

key word: mechanical recovery, frother, entrapment, surface phenomena, quartz, flotation

INTRODUCTION

Flotation is accompanied by undesirable phenomena, such as particle aggregation and entrainment, taking place usually during fine particles flotation. Entrainment has been investigated by numerous researchers including Ross (1991), Drzymała (1994), Łukaszewska (1998), Hrycyna (1999), Konopacka (2005) and Szyszka (2007), with the use of flotation machines or the so-called Hallimond tubes. In spite of extensive research on the subject, the phenomenon is not yet well understood, especially the

* Wrocław University of Technology, Wybrzeże Wyspianskiego 27, 50-370 Wrocław, Poland, danuta.szyszka@pwr.wroc.pl

issue when a frother becomes collector in flotation. The purpose of this work was to study this aspect of flotation.

EXPERIMENTAL

Microlaboratory tests were performed with quartz obtained from Osiecznica (Poland) using five frothers: octyl alcohol, isoamyl alcohol, α-terpineol, tricosene-ethyleneglycol 1-hexadecanoic ether and corflot (a mixture of butyl ethers of di-, tri- and tetraethylene glycols). In order to obtain the desired quartz particles it was crushed in a laboratory rock disintegrator and separated by wet screening into size fraction using 0.5, 0.2, 0.1 and 0.0071 mm screens. The square-shaped screens were provided by Metallweberei (Germany). After screening, the quartz samples were dried and individual particle size fractions were use for flotation-entrainment tests.

The stock aqueous solution of frothers were 1% by weight. The amount of frother for each concentration was established on the basis of its molecular weight.

The flotation experiments were conducted in a Hallimond tube shown in Fig. 1. Prior to each experiment, 0.35 g of quartz had been added to 120 cm^3 of aqueous frother solution in a glass beaker. Then, the mixture was agitated for 1.5 min, poured into the Hallimond tube and subjected to flotation with an air flow of 0.625 cm^3/s. The air flow was measured with the use of a Brooks Rotametr Co. (US). The air bubbles in pure water were 3.1 mm in diameter.

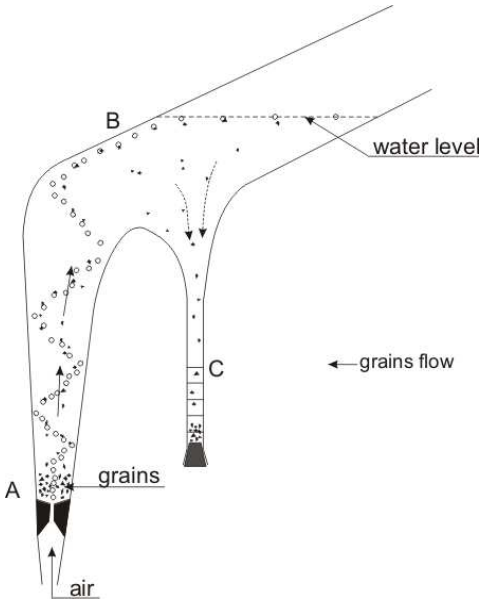

Fig. 1. Hallimond tube used in the experiments

The tested material was placed in part B of the Hallimond tube. The air bubbles and some mineral particles were moving to the water surface (C) where the particles were falling to the calibrated glass tube D. This enabled a continuous measurement of the percentage of the material floating and entrained as a function of time. The recovery of particles were read every 3 minutes throughout the whole flotation time of 15 minutes.

RESULTS AND DISCUSSION

As a result of the tests, conducted for all quartz size fractions, it was possible to determine the amount of particles entrained with air bubbles with time. On the basis of the results, kinetics of flotation-entrainment were plotted for different frothers and for pure water. Next, an average particle size was calculated for each size fraction as an arithmetic mean of the largest and the smallest particles in a given fraction. Having such data, it was possible to draw curves to show a relationship between the maximum recovery and average particle size. The way frothers affect flotation has been presented in Tables 1-5.

Table 1. The results obtained for air bubbles passing through the Hallimond tube filled with 0.5-0.2 mm quartz particles

Time t, min	Cumulative recovery, Σε, %					
	water	α-terpineol	isoamyl alcohol	octyl alcohol	Ether $C_{16}E_{23}$	corflot
0	0	0	0	0	0	0
3	0.3	0.5	0.5	0.5	2	0.5
6	0.5	0.5	0.5	0.5	4	0.5
9	0.5	0.8	1	1	8	0.5
12	0.5	0.8	1	1	9	0.5
15	0.5	0.8	1	1	9	0.5

Table 2. The results obtained for air bubbles passing through the Hallimond tube filled with 0.2-0.1 mm quartz particles

Time t, min	Cumulative recovery, Σε, %					
	water	α-terpineol	isoamyl alcohol	octyl alcohol	Ether $C_{16}E_{23}$	corflot
0	0	0	0	0	0	0
3	1	2	2.5	5	17	1
6	1.5	3	3.5	8	32	1.5
9	2	4	4.5	9	40	2
12	2.5	4.5	5	10	43	3
15	3	4.5	5.5	10	44	4

Table 3. The results obtained for air bubbles passing through the Hallimond tube filled with 0.1-0.071 mm quartz particles

Time t, min	Cumulative recovery, Σε, %					
	water	α-terpineol	isoamyl alcohol	octyl alcohol	Ether $C_{16}E_{23}$	corflot
0	0	0	0	0	0	0
3	9	7	8	15	48	5
6	16	10	11	28	70	12
9	19	15	16	40	78	20
12	23	19	20	49	80	26
15	28	21	25	52	81	30

Table 4. The results obtained for air bubbles passing through the Hallimond tube filled with <0.071 mm quartz particles

Time t, min	Cumulative recovery, Σε, %					
	water	α-terpineol	isoamyl alcohol	octyl alcohol	Ether $C_{16}E_{23}$	corflot
0	0	0	0	0	0	0
3	10	12	10	19	25	10
6	22	23	16	33	40	20
9	31	30	26	41	48	28
12	36	34	30	47	54	34
15	38	38	32	51	59	39

Table 5. Cumulative quartz recovery $\Sigma\varepsilon_{max}$ for each size fraction

Average-sized particles, $d_{śr}$	Cumulative recovery, Σε, %					
	water	α-terpineol	isoamyl alcohol	octyl alcohol	Ether $C_{16}E_{23}$	corflot
0.35	0.5	0.8	1	1	1	0.5
0.15	3	4.5	5.5	10	10	4
0.086	28	21	25	52	52	30
0.036	38	38	32	51	51	39

The work was focused on investigating frothing and collecting properties of frothers. During the experiments, pure water was used as the reference. The research results indicate that the collecting properties towards hydrophilic quartz particles depends on the frother type.

A comparison of the results obtained (Fig. 2.) has led to an observation that tricosene-ethylene glycol 1-hexadecanoic ether and to a lesser extent octyl alcohol show collective properties towards quartz. The remaining frothers were responsible merely for the quartz particle entrainment, since the amount of entrained particles was

comparable with the amount obtained when the flotation cell was filled only with water.

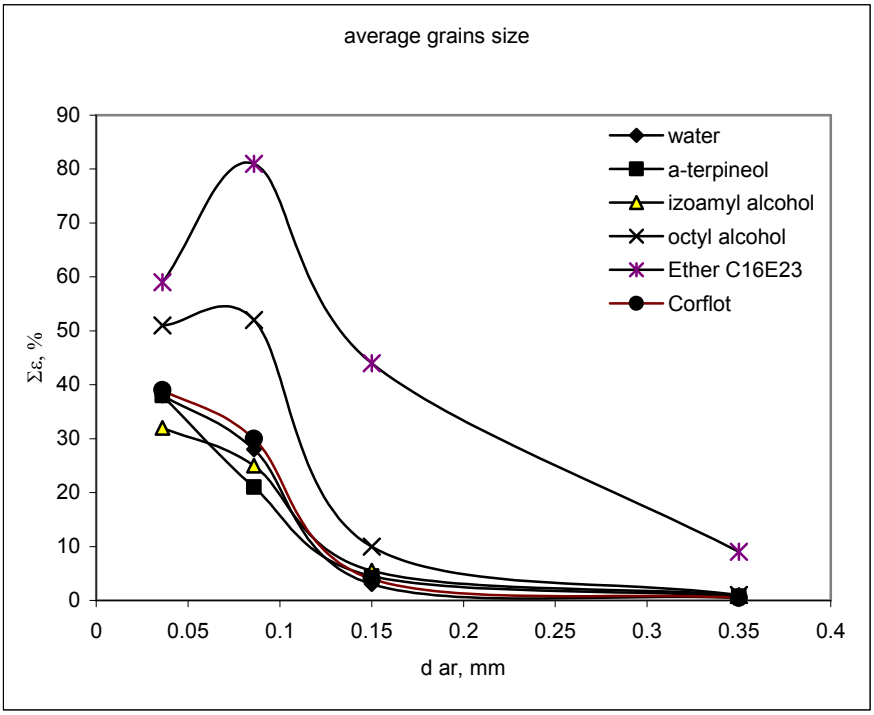

Fig. 6. Quartz cumulative recovery (Σε) after 15 minutes of flotation (plateau) vs. size of quartz particles

CONCLUSIONS

Among the five frothers used tricosene-ethyleneglycol 1-hexadecanoic ether, and to a lesser extent octyl alcohol, produced quartz flotation, with the particle recovery greater than the entrainment. The remaining frothers (isoamyl alcohol, α-terpineol and corflot) acted as proper frothers, with entrainment being equal to that observed in water containing no frother. Thus, such a simple Hallimond tube experiment can be used for testing frothers to establish whether they are pure entraining non-collecting frothers or they have tendency to float the particles. The frothers which partially collect (float) particles may significantly contribute to reduced flotation selectivity.

REFERENCES

DRZYMAŁA J., 1994. Characterization of materials by Hallimond tube flotation. Part 1: maximum size of entrained particles. Int. J. Miner. Process., 42: 139-152

ROSS V. E., 1991. Comparision of methods for evaluation of true flotation and entraiment. Trans. Inst. Min. Metall. (Sec. C: miner. Process. Extr. Metall.), 100: C121-C126

ŁUKASZEWSKA I., 1998. Flotation in the Hallimond tube., Wroclaw University of Technology, Department of Geoengineering, Mining and Geology, Wroclaw

HRYCYNA E., 1999. Entrainment of particles in the mechanobr laboratory flotation machine. M.Sc. thesis, Wroclaw University of Technology, Department of Geoengineering, Mining and Geology, Wroclaw

KONOPACKA Ż., 2005. The entrainment of flotation. Oficyna Wydawnicza Politechniki Wrocławskiej, Wrocław, in Polish

SZYSZKA D., 2007. Entrainment of particles flotation only frothers. Gornictwo i Geoinżynieria, Rok 31, Zeszyt 4

Szyszka D., Glapiak E., Drzymała J., *Właściwa i mechaniczna aktywność flotacyjna kwarcu w obecności różnych spieniaczy,* Physicochemical Problems of Mineral Processing, 42 (2008), 85-90 (w jęz. ang.)

Flotacja jest stosowana do rozdziału drobnych ziarn mineralnych. Każdej flotacji towarzyszy zjawisko niepożądane pogarszające jakość końcowego produktu, którym jest wyniesienie mechaniczne ziarn (flotacja mechaniczna). Na flotacje właściwą i mechaniczną wpływa wiele parametrów, które nie zostały całkowicie poznane. W pracy badano flotację mechaniczną ziarn kwarcu w monopęcherzykowym flotowniku Hallimonda w zależności od rodzaju stosowanych spieniaczy. W testach zastosowano takie spieniacze jak: alkohol oktylowy, alkohol izoamylowy, α-terpineol, eter jednoheksadekanowy trikozanoetylenowy oraz corflot (mieszanina eterów butylowych glikoli di, tri i tetraetylenowych). Przeprowadzono także badania dla czystej wody, które obrano jako punkt odniesienia w stosunku do pozostałych wyników testów. W pracy stwierdzono, że eter jednoheksadekanowy trikozanoetylenowy ($C_{16}E_{23}$) oraz alkohol oktylowy wykazały nie tylko właściwości spieniające, ale również zbierające.

słowa kluczowe: wyniesienie mechaniczne, spieniacze, właściwości powierzchniowe, kwarc, flotacja

Physicochemical Problems of Mineral Processing, 42 (2008), 91-106
Fizykochemiczne Problemy Mineralurgii, 42 (2008), 91-106

Iwona Kupich*, Janusz Girczys*

SLUDGE UTILIZATION OBTAINED FROM Zn-Pb MINE WATER TREATMENT

Received May 15, 2008; reviewed; accepted July 31, 2008

The paper describes the possibilities for utilization of sludge obtained during the treatment of mine water discharged from the Zn-Pb ore mines. These possibilities were analyzed based on the results from the study on the properties of sludge from the treatment of mine water discharged from the mines of the Bytom Basin area. The fine-grained texture and chemical content of sludge result in the properties typical for very fine-grained limestone. Small quantities of unprocessed $Ca(OH)_2$ increase the activity of sludge in comparison to pure $CaCO_3$. Due to these properties the sludge may be applied in many environmental engineering processes aiming at limitation of heavy metal migration and SO_2 emissions, and also neutralization of waste acids from used accumulator processing.

key words: zinc and lead mining, water discharged, water treatment, sludge utilization

INTRODUCTION

The sludge from the treatment of water discharged from ore mining belongs to a specific category of waste and can often display significantly different properties. These differences are mainly the result of the diversity of the content of discharged water, and accordingly impose a suitable treatment method (Adamczyk, 1990; Adamczyk and Haładus, 1996; Kropka, 1995; Kryza at al., 1995). However, since the main goal of treatment is to discharge the water to the environment in a safe manner, it is expected that the sludge produced during mechanical separation should also be environmentally safe. This assumption was verified by the study of sludge from the treatment facility for mine water discharged from the "Bolko" shaft. Water subjected to treatment in this facility comes from drainage caused by the closed ore mines lo-

* Instytut Inżynierii Środowiska, Politechniki Częstochowskiej, ikupich@is.pcz.czest.pl

cated in the area of the Bytom Basin (Kropka at al., 1995; Kropka at al., 1994; Kropka, 1996).

The technology applied in the "Bolko" shaft generates about 2 Gg (2 000 tones) of sludge per year. The properties and chemical content of sludge are similar to the natural raw materials exploited for economic purposes. Based on those assumptions and current legal requirements the analysis of utilization methods for sludge from mine water treatment was performed. In view of physical and chemical properties of sludge only the main directions of sludge utilization were analyzed. The advantages of sludge utilization can be manifold, including limitation of natural resources exploitation, improvement of environment protection and reduction of landfill areas.

Production of the sludge is the consequence of the needs to dewater old and closed Zn-Pb ore mines located in the Bytom Basin.

THE ORIGIN OF SLUDGE

DISCHARGED WATER

It is estimated that about 370,000 m^3 of mine water per day is discharged from Zn-Pb ore mines in Poland. Approximately 45% of this quantity is used for drinking and industrial applications (Adamczyk, 1990; Adamczyk and Haładus, 1996; Kropka, 1997). Water discharged from the closed ore mines in the area of the Niecka Bytomska, which contributes to about 8% of total quantity of discharged mine water, does not comply with the standards for drinking and industrial water (Kropka, 1995; Grabowska and Sowa, 2000; Kupich, 2005). The sludge generated in the process of mine water treatment is discharged to the Brytnica River (Hydrolog S.C Operat…., 2000; Girczys and Sobik – Szołtysek, 2003).

Due to the formation of an extensive depression cone on the large areas of ore mining the chemical content of water undergoes changes including an increase in the concentration of different constituents, mainly sulfates, calcium and heavy metals (Girczys and Sobik – Szołtysek, 2002; Informacje i dokumentacje "Bolko"; GIG, 1994).

Migration of heavy metals is strongly affected by the geochemical properties of the environment in which underground water transport occurs. The occurrence of carbonate rocks (i.e. dolomite and limestone) causes slightly alkaline reaction, and thus in natural conditions the bicarbonate ions predominate (Girczys and Sobik – Szołtysek, 2002). Under specific conditions it leads to a significant reduction of heavy metal migration.

Sludge from the treatment process is loaded with substances which can infiltrate to water from the surface to the intake in the shaft sump. Therefore, it contains insignifi-

cant or trace quantities of constituents typical for a given mining area (Grabowska and Sowa, 1996; Różkowski and Ziemiański, 1995).

SLUDGE SEPARATION

The mine water discharged from the Bytom Basin is treated by means of coagulation with the application of lime carbide residue which as lime milk is fed into the mine water pipelines. Intensive stirring of lime milk with mine water occurs in the pipeline and the well below the settling tank. The water is then discharged to the settling tanks where the suspended matter in the water undergoes coagulation and sedimentation. The application of lime carbide residue in the process of mine water treatment generates significant quantities of suspension that is well dispersed and difficult to sediment. To shorten the time the process of clarification of treated water the polyelectrolyte S-216 was applied. After the completion of a working cycle the accumulated sludge is removed from the settling tank whereas cleared water is discharged through a set of drainage channels to the Brynica River (figure 1).

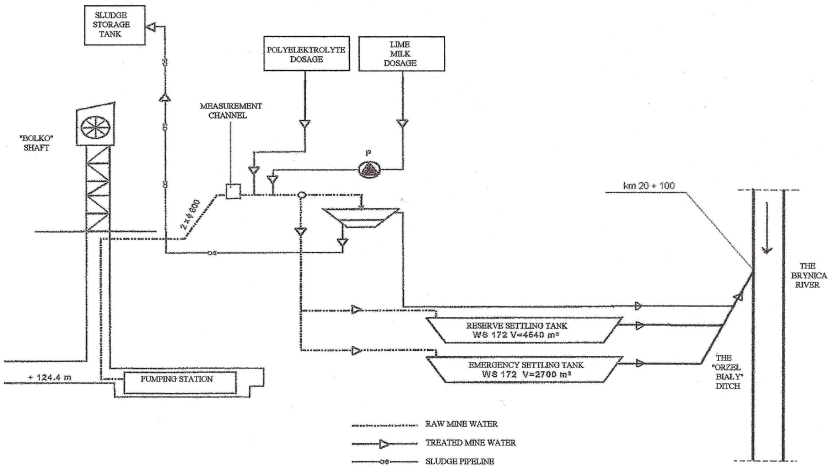

Fig. 1. Schematics of mine water discharge process

The content of lime carbide residue (dosed in a quantity of 250÷400 g/m^3) is presented in the table 1.

Due to the activity of lime carbide residue the water in the overfall of the settling tank is almost completely free of Pb, Cd and Cu. The concentration of Zn decreases from 12 mg/dm^3 in raw water to less then 2 mg/dm^3 in the overfall water.

Table 1. The content of lime carbide residue applied in the process of coagulation, (wt %)

H_2O	$Ca(OH)_2$	$CaSO_4$	$CaCO_3$	Pb	Fe	SiO_2	Al_2O_3
Up to 20	84÷90	0.5÷3	5÷9	0.02÷0,5	0.1	1÷3	0.02÷1

The addition of $Ca(OH)_2$ leads to the following chemical reactions:

$$Ca(HCO_3)_2 + Ca(OH)_2 = 2CaCO_3 + 2H_2O \quad (1)$$

and

$$Zn^{2+} + 2OH^- = Zn(OH)_2 \quad (2)$$

The main components of sludge are the calcium carbonate with the excess lime carbide residue formed during above reactions, and the suspended matters are. The sludge is a white, alkaline (pH ~ 9,8), and quite moist substances (40÷70%).

SLUDGE PROPERTIES

METHODS

The sludge separated from discharged water and the sludge water extracts were subjected to chemical analysis by atomic spectrometry methods (i.e. ICP and ASA). The phase composition was determined basing on the thermogravimetric analysis with a derivatograph (model Labsys, manufactured by SETARAM).

The analysis of grain size for material of the grain size < 200 μm was conducted by a laser grain size analyzer (model LAU – 10). Prior to this analysis the material with the grain size > 200 μm was removed.

The reactivity test (Szymanek 2000; Bis, Radecki 2002) was used to evaluate the potential of sludge as a sorbent for dry de-SO_x methods. This test allows to determine the absolute sorption (CI – capacity index) and reactivity of calcium sorbent (RI – reactivity index) indexes from the change in sulfur mass and content in the calcium sorbent exposed to exhaust gas containing CO_2, O_2 and SO_2 in the standard conditions. The total content of sulfur was determined with LECO SC-144 analyzer.

The absolute sorption index (CI) was calculated from [Alsthrom Pyropower…, 1995]:

$$CI = \frac{1000 \cdot \left[\frac{C_{S_p} - C_{S_b}}{100} + \frac{M_{CO_2}}{M_C} \left(\frac{C_{C_p} \cdot C_{S_b} - C_{C_b} \cdot C_{S_p}}{10000} \right) \right]}{1 - \frac{M_{CO_2}}{M_C} \cdot \frac{C_{C_p}}{100} - \frac{M_{SO_3}}{M_S} \cdot \frac{C_{S_p}}{100}} [gS/kg] \quad (3)$$

and the reactivity coefficient (RI) was calculated from [Alsthrom Pyropower…,1995]:

$$RI = \frac{\frac{C_{Ca}}{100}\cdot\frac{M_S}{M_{Ca}}\left(1-\frac{M_{CO_2}}{M_C}\cdot\frac{C_{C_p}}{100}-\frac{M_{SO_3}}{M_S}\cdot\frac{C_{S_p}}{100}\right)}{\frac{C_{S_p}-C_{S_b}}{100}+\frac{M_{CO_2}}{M_C}\left(\frac{C_{C_p}\cdot C_{S_b}-C_{C_b}\cdot C_{S_p}}{10000}\right)}\left[mol\,Ca/mol\,S\right] \quad (4)$$

were:

C_{Ca}, C_{Cp}, C_{Sp}, C_{Cb}, C_{Sb} are the contents of calcium, carbon and sulfur in the sample after the test, carbon and sulfur before the test respectively [%],

$M_S, M_{Ca}, M_C, M_{CO_2}, M_{SO_3}$ - molar mass of sulfur (32,064 g/mol), calcium (40,08 g/mol), carbon (12,01 g/mol), carbon dioxide (44,01 g/mol), sulfur trioxide (80,06 g/mol).

The hydraulic permeability was determined from analysis of a seasoned sample of sludge (moisture content about 10%). An apparatus with a filtration chamber and a pressure tube was used to measure the velocity of filtration. The hydraulic permeability was calculated knowing the volume of the liquid in the pressure tube before and after each test in a given timeframe. The filtration coefficient for a given temperature (T) was calculated from:

$$k_T = \frac{a\cdot l}{A\cdot t}\log\frac{h_1}{h_2} \qquad \text{[m/s]} \quad (5)$$

where:

a – cross-sectional area of a tube, m^2,

l – height of a sample bed, m,

A – cross-sectional area of a sample, m^2,

t – filtration time, s,

h_1, h_2 – maximum and minimum levels of liquid in the tube (measured from the top level of the outlet), m.

RESULTS

Chemical and phase content

The results of tests performed are presented in the Table 2.

Table 2. The content of sludge after coagulation (d.m., wt %)

$Ca(OH)_2$	$CaCO_3$	$CaSO_4$	Zn	Pb	Cu	Fe
14÷15	60÷85	5÷7.5	1.7÷4	0.05÷1	0.002÷0.008	0.4÷1.3

The quantities of the remaining constituents are insignificant and the average contents determined by random tests in the past years are as follows (Table 2B):

Table 2B. The content of sludge after coagulation (d.m., wt %)

MgO	Mn	SiO_2	S	Sb	As	Cd
1.5	0.22	3.4	1.0	0.015	0.1	0.004

The water extracts of sludge was characterized by high alkalinity and low content of heavy metals. No trace of mercury was detected either in the sludge or in the water extracts, and the concentration of radionuclides was below the average content in the lithosphere.

The results of the tests did not confirm significant concentration of hazardous substances in the sample since those may be easily washed out to the environment. The concentrations of heavy metals are within the corresponding limits for first class inland surface water cleanness.

The data of the leaching test indicate an increased concentration of sulfates. The concentration was 3-fold higher than the corresponding standard limits for the wastewater discharged to water and soil.

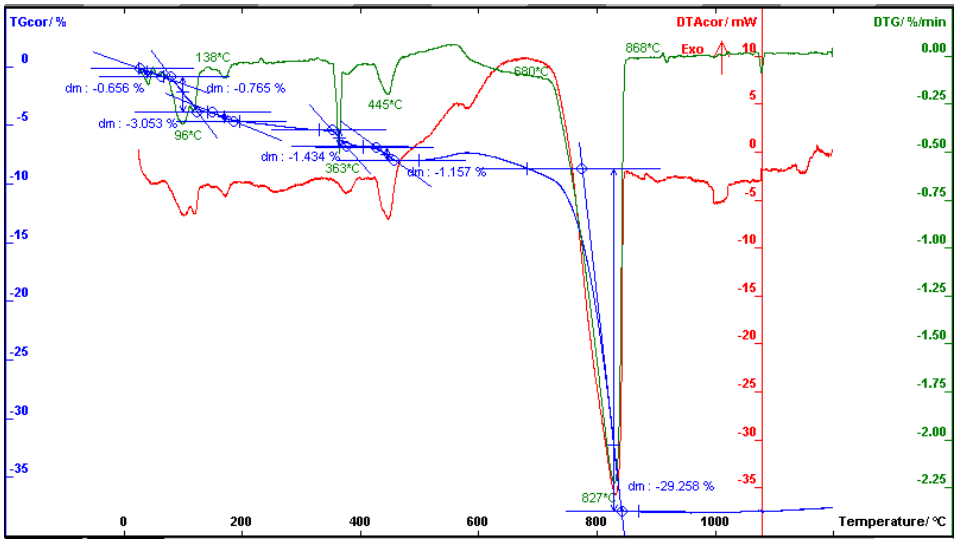

Fig. 2. Derivatographic analyses, sample No.1

The primary content of seasoned sludge samples in the settling tank during the recent years was determined by thermo gravimetric analysis and the results were presented in Table 3. The gravimetric transformations resulted from the effect of temperature on the sludge are shown in the Figure 3 (sample No. 1 sampled from the settling tank). With the reference to the thermo gravimetric data, the content of calcium hydroxide in the seasoned sludge sample (table 4) decreased at the expense of crys-

tallization of gypsum, while the content of magnesium, as $Mg(OH)_2$, slightly increased (table 2).

Table 3. The content of the investigated samples (d.m.) – thermo gravimetric analysis

Sample No.	Ca CO_3 [%]	$Ca(OH)_2$ [%]	$Mg(OH)_2$ [%]	$CaSO_4 \cdot 2H_2O$ [%]	$Fe_2O_3 \cdot H_2O$ [%]
1	70.22	5.07	4.86	15.42	4.43
2	60.53	6.44	4.03	29.0	-
3	72.95	6.92	4.96	15.26	-

With the reference to the thermo gravimetric data, the content of calcium hydroxide in the seasoned sludge sample (table 4) decreased at the expense of crystallization of gypsum, while the content of magnesium, as $Mg(OH)_2$, slightly increased (table 2).

Technical analysis

The investigated material was white, and the moisture retained under the intergranular pores was alkaline of pH~9,8. The results also demonstrated that the sludge was fine-grained. Prior to the analysis the sample was washed out and the fraction of material with the grain size > 200 μm (which was 3% of the total mass sample) was not typical for sludge separated during the treatment of discharged water, and thus removed. The grain size distribution for the sample No. 3 was presented in Figure 3 and is consistent with the results obtained for the remaining sludge sampled from the settling tank.

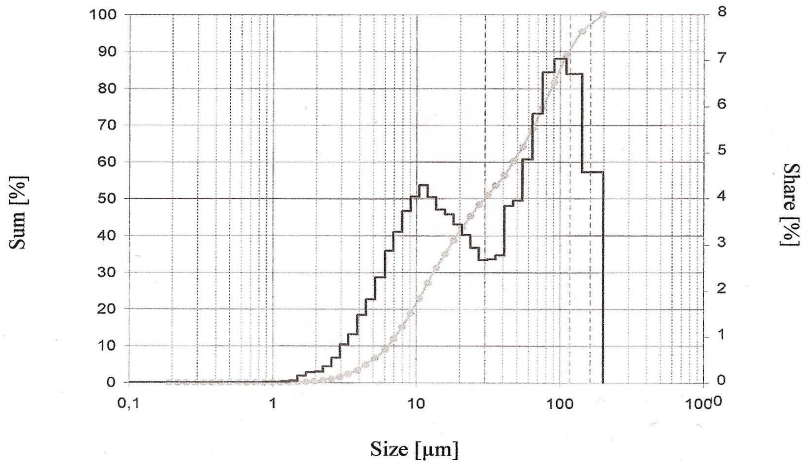

Fig. 3. Particle size distribution, sample No. 3

In the investigated material two fractions of particles of the size ~ 10 μm and 100 μm were observed. The fraction of grains with size less than 20 μm constituted over 40% of the total mass. This resulted in the expansion of the surface area estimated at about 2000 cm^2/g. The average grain density of ~ 2 g/cm^3 corresponds to the average grain size of ~ 15 μm.

Sorption capacity of sludge is one of the most important properties of this material. The chemical content and particle size distribution of sludge indicate that it may sorb heavy metals from solutions and SO_2 from gas phase. Even the total depletion of $Ca(OH)_2$, does not remove the sorptive properties, because $CaCO_3$ remains still active. The mechanism of heavy metals sorption in liquid phase is based on the processes of hydrolysis and dissociation, and can be described by a simplified equation:

$$Ca\,CO_3 + 2\,H_2O \rightarrow H_2CO_3 + Ca^{2+} + 2\,OH^-. \quad (6)$$

It has to be pointed out that this equation is general and all products in this reaction undergo further dissociation, hydrolysis and precipitation of slightly soluble compounds.

The carbonic acid dissociates according to the following equations:

$$H_2CO_3 \leftrightarrow HCO_3^- + H^+ \quad K_1 = 4.5 \cdot 10^{-7} \quad (7)$$

$$HCO_3^- \leftrightarrow CO_3^{2-} + H^+ \quad K_2 = 4.7 \cdot 10^{-11} \quad (8)$$

The ionic activity of CO_3^{2-} calculated from Eqs 7 and 8 can be presented with the formula:

$$\log a\,(CO_3^{2-}) = 2\,pH + \log a\,(H_2CO_3) + \log K_1 K_2 \quad (9)$$

In the state of equilibrium of the seasoned sludge sample (in which calcium carbonate is the main component) the pH was ≈ 9 and the activity (calculated from Eqs 6-8)
$a\,H_2CO_3 \approx 0{,}04$. Based on those calculations the activity of CO_3^{2-} (Eq. 9) becomes:

$$a\,CO_3^{2-} = 8.4 \,.\, 10^{-3} \quad (10)$$

Table 4. The results of sorption of seasoned sludge samples

Sample No.	RI [*mol Ca/mol S*]	CI [*gS /kg sorbent*]
1	4.1	57
2	4.5	51
3	4.2	55

This activity exceeds the solubility of the majority of heavy metal carbonates by several orders of magnitude. Therefore heavy metal ions precipitate and the concentration of those ions in the leachate is insignificant. However, high concentration of Ca^{2+}, Mg^{2+} and SO_4^{2-} ions is observed. The verification of SO_2 sorption in the gas phase indicated (Table 4) that the sludge produced during the treatment of discharged

water is a promising SO_2 sorbent, even though some active substances were removed from sludge due to its storage in unfavorable conditions.

Hydraulic permeability

The hydraulic permeability of sludge was determined in the ambient temperature, and then recalculated to hydraulic permeability at 10 ºC. At this temperature the filtration coefficient was calculated from the formula:

$$k_{10} = \frac{1.359 \cdot k_T}{1 + 0.0337 \cdot T + 0.00022 \cdot T^2} \qquad \text{[m/s]} \qquad (11)$$

The calculated coefficient of $7.0 \cdot 10^{-8}$ m/s was typical for powdery clay, aggregated mud and mudstone which are semi-permeable in horizontal and slightly insulating in vertical filtration (Marciniak et al., 1998). This combined with the sorptive properties makes sludge a perfect material for construction of active insulation barriers.

TECHNOLOGIES OF SLUDGE UTILIZATION

With the reference to the properties of sludge investigated in the presented study as well as the current state of legislation (Girczys, 2007; Prawo Ochrony Środowiska) several utilization technologies in which sludge can be a substitute for natural resources are suggested. The sludge generated in the treatment of mine water discharged from the „Bolko" shaft has properties similar to fine-grained limestone with small quantities of $Ca(OH)_2$, $Mg(OH)_2$ and iron hydroxides.

Suggested applications of sludge include three technological forms:

- an alkaline suspension for SO_2 sorption or H_2SO_4 neutralization
- an inert mineral layer for landfilling of various waste
- a filling material for post-mining voids or landfilling.

The first two forms can be obtained from sludge that was stored in conditions preventing from conversion of active substances into gypsum. Time for stabilization should not exceed several months. To ensure the required properties of sludge it should be extracted from a settling tank and air dried (e.g. under an umbrella roof).

The technology of wet removal of sulfur from exhaust gas is considered as the most technologically advanced. Sludge from the "Bolko" installation may be used for preparation of sorbent (Fig. 4). Without prior preparation sludge can be fed into a hydrocyclone (5) – unlike limestone it does not require milling. From the mine limestone is delivered to the warehouse by trains (1), and then it is transported by a belt conveyer to day storage bins (2) adjacent to the mills. From the day storage bins the limestone is fed to a ball grinder for grinding. Wet ball grinders are the most frequently applied. After grinding, the suspension with the limestone concentration of 70% is stored in a mill tank (4) where the suspension is diluted with water. Then, the

suspension is transferred to a system of hydrocyclones (5) for grain size grading. Larger grains are fed back to the mill whereas the suspension with the required grain size is transferred to a buffer tank (6), then conveyed by a pipeline and fed to an absorber depending on, e.g. the concentration of SO_2 in the exhaust gas.

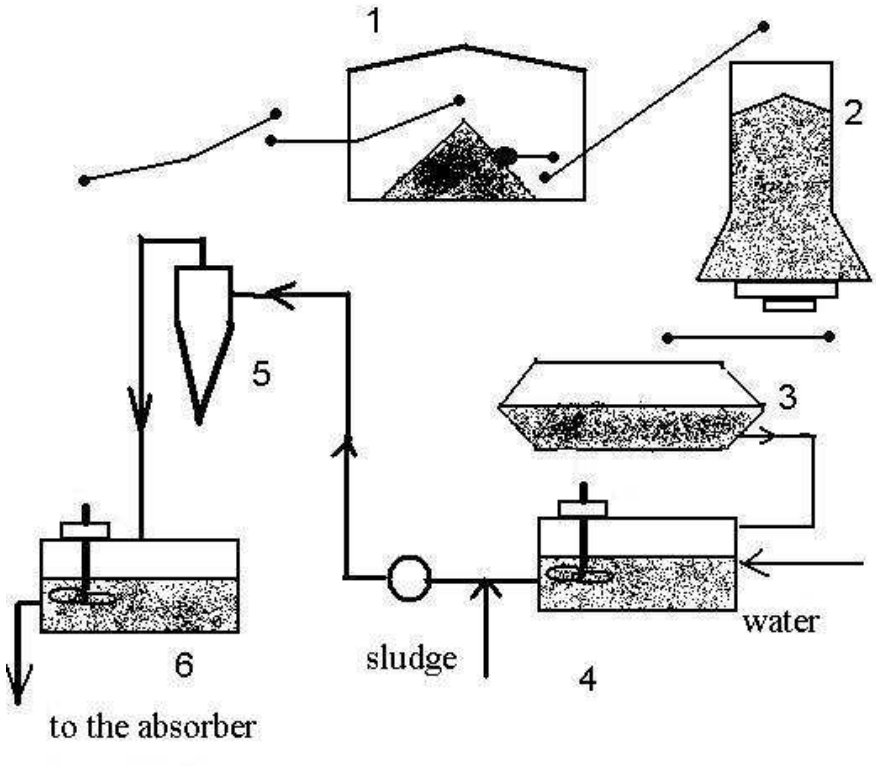

Fig. 4. Schematics of for limestone sorbent production technology

The sludge suspension also meets the requirements for alkalifying agents and can be used directly in the process of neutralization of sulfuric acid from used (old) car butteries (accumulators). The schematics of that process is shows in Fig. 5.

In landfilling municipal waste it is a prerequisite to apply inert layers in construction of a landfill. The layers can be made of debris, cullet, slag, ash, sand or other fine-grained mineral materials (Oleszkiewicz, 1999). Sludge from the "Bolko" shaft can be also used for building inert layers. Prior to this, the water needs to be removed to ensure proper distribution in the surface area. More over, the inert layers built with sludge can facilitate the processes of heavy metal sorption and alkalization of leachate.

The properties of sludge allow for technical reclamation of industrial waste landfills, particularly for construction of a subsoil inert layer. The primary operations in technical reclamation of existing dumping grounds include:

- land levelling to form the required shape of the surface
- compacting the upper layer (i.e. surface layer)
- applying a cover layer for plant vegetation.

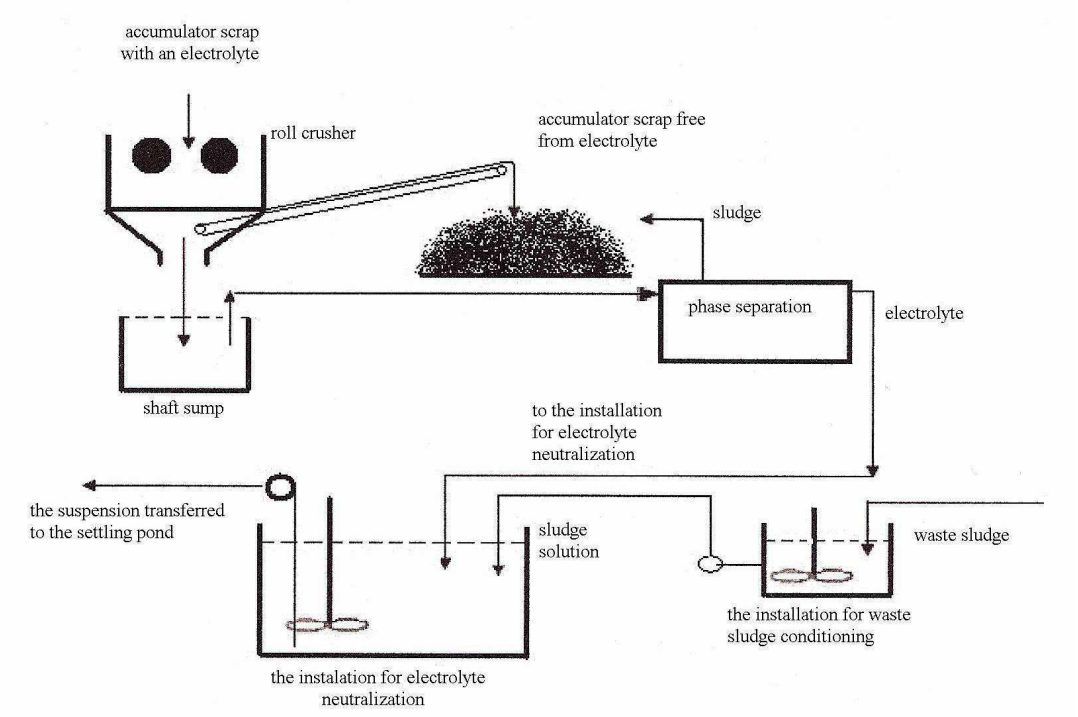

Fig. 5. Schematics of recovery and neutralization of sulfuric acid from the used car batteries (accumulators)

Due to various properties sludge generated in the treatment of mine water can be used as a subsoil layer that insulates soil from the impact of hazardous waste and ensures proper conditions for plant vegetation.

Generally, the addition of sludge expands the area for landfilling and facilitates protection of the environment resulting from:

- improved compaction of waste in a landfill body
- favorable changes in chemical properties of a landfilled material.

The compaction of landfilled material can be improved by fulfilling the intergranular voids of waste coarse grain structure with sludge. This will efficiently reduce the processes of:

- water infiltration causing migration of metals

- oxidation leading to water and air contamination or even fires.

As a neutralizing material sludge can be applied for currently generated waste. Satisfactory results are achieved mainly in landfilling sludge blended with various types of slag, generated e.g. in the Dörschl's furnace, during melting of lead from accumulator scrap or ebonite from spent accumulator processing.

High quantities of $CaCO_3$, which constitutes about 80% of sludge dry matter, applied to waste with high content of heavy metals, allows for immobilization of these metals in the landfill body due to various chemical reactions. The value of solubility product for carbonates of heavy metals is lower by several orders of magnitude. This shifts the reaction equilibrium towards the formation of insoluble carbonates of these metals which are removed from infiltrating water.

The ratio of sludge and coarse grained waste in the mixtures depends on the size of intergranular voids. Sludge should be added in the quantity which allows to fulfill these voids. Under this condition the addition of sludge can be calculated from:

$$M_S = \frac{(\rho_W - \rho_N) \cdot \rho_S}{\rho_W} \tag{12}$$

where:

M_S – mass of sludge [Mg]
ρ_w – density of hazardous waste [Mg/m^3]
ρ_N – bulk density of hazardous waste [Mg/m^3]
ρ_S – density of sludge added to 1 m^3 of hazardous waste [Mg/m^3].

Another condition for estimating the ratio of sludge in mixtures is the content of $CaCO_3$. The addition of sludge should ensure that the quantity of $CaCO_3$, when dissolved in water, will balance stechiometrically all metals present in hazardous waste. This allows for efficient water protection in the infinite timeframe as the mechanism of carbonated mineral formation in nature (e.g. siderite, smithsonite, cerrusite) will be restored. Formation of these minerals in nature does not pose any threat to water.

CONCLUSIONS

The properties of sludge generated during coagulation of mine water discharged from the Zn-Pb ore mines were extensively studied. The knowledge of these properties allowed to develop suitable concepts for sludge utilization. It is estimated that the quantity of sludge generated annually in next few years will be at the same or slightly lower order than the current quantity. However, a due to silting-up, natural attenuation, formation of flow streams or technical activity in water regulation a strong tendency to reduce the quantity of sludge over time is expected.

In the view of the potentials for economic applications of the sludge the following conclusions may be formulated:

1. The sludge generated during treatment of mine water discharged from the "Bolko" shaft does not show any characteristics typical for hazardous waste.
2. With reference to the chemical composition and grain composition the sludge may be applied as a substitute of fine-grained limestone.
3. From technical and organizational point of view, the most suitable application of the sludge is its landfilling at areas designated for hazardous waste from used accumulator processing as an agent for removal of heavy metal ions from the car butteries (accumulators).
4. Another suitable application of the sludge is construction of mineral layers at municipal waste landfills. However, this can be done only at landfills employing advanced technologies.
5. The utilization of sludge for neutralization of a used electrolyte in butteries scrap processing does not require the implementation of new technical solutions. The sludge will partially substitute lime carbide residue.
6. After field-testing, sludge can be use as a SO_2 sorbent in sulfur removal from exhaust gas irrespective of applied technology.

The sludge can be also applied as a filling material for restoring post-mining voids. This should not pose any technical difficulties due the properties of sludge. However, prior to this application a number of formal requirements need to be fulfilled.

ACKNOWLEDGEMENTS

This work was supported by the Częstochowa Technical University internal grant BS 401/302/08

REFERENCES

ADAMCZYK A. F., Wpływ górnictwa rud cynku i ołowiu w rejonie olkuskim na wody podziemne i powierzchniowe, Zesz. Nauk. AGH, Sozologia i Sozotechnika z. 32, Kraków 1990.

ADAMCZYK A.F., HAŁADUS A., Zmiany jakości wód kopalnianych odprowadzanych kanałami ZGH Bolesław, Gospodarka Surowcami Mineralnymi 1996, nr 3, s. 479-505.

Alsthrom Pyropower Reactivity index, 1995 r.

BIS Z., RADECKI M., Alternatywne sorbenty wapniowe do odsiarczania spalin w kotłach fluidalnych, IX Konferencja Kotłowa nt.: Aktualne problemy budowy i eksploatacji kotłów, str. 59-72, 2002.

GIRCZYS J., Charakterystyka szlamów odpadowych z instalacji uzdatniania wód zrzutowych z szybu „Bolko" wraz z technologią ich utylizacji, Bytom 2007.

GIRCZYS J., SOBIK–SZOŁTYSEK J., Odpady przemysłu cynkowo – ołowiowego, Wydawnictwa Politechniki Częstochowskiej, Częstochowa 2002.

GIRCZYS J., SOBIK–SZOŁTYSEK J., 2003, Wpływ na stan wody Brynicy zrzutu ścieków i wód dołowych, Inżynieria i Ochrona Środowiska, t.6, nr 3-4, s.441-453.

Główny Instytut Górnictwa, Ocena możliwości obniżenia stężenia siarczanów w wodach kopalnianych

odprowadzanych za pomocą pompowni Bolko z nieczynnych wyrobisk porudnych ZGH „Orzeł Biały" S.A. oraz skutków społecznych uzasadniających potrzebę tego odwadniania, Katowice 1994.
GRABOWSKA K., SOWA M., Agresywność siarczanowa wód dołowych z wybranych kopalń północnozachodniej części GZW, Prace naukowe GIG, Seria: konferencje 2000, nr 35, s. 113-120.
GRABOWSKA K., SOWA M., Charakterystyka składowisk odpadów poflotacyjnych ZGH „Orzeł Bialy" w aspekcie ekologicznym, Materiały VI Konferencji nt.: Problemy geologii w ekologii i górnictwie podziemnym, Ustroń 1996, s. 285-297.
HYDROLOG S.C., Operat wodnoprawny na odprowadzenie wód kopalnianych z nieczynnych wyrobisk porudnych Zakładu Górniczego – Centralnej Pompowni „Bolko" w Bytomiu do rzeki Brynicy w km 20+100, Katowice 2000.
Informacje i dokumentacje Centralnej Pompowni „Bolko" sp. z o.o.
KROPKA J., 1996, Drogi krążenia, zasoby i zagospodarowanie wód podziemnych w triasowym zbiorniku „Bytom" w warunkach aktywnej działalności górnictwa, Przegląd Geologiczny, vol.44, nr 8, s. 845-849.
KROPKA J., DALIBÓG J., MOJ H., Pięcioletnie (1990-1994) doświadczenia związane z centralnym odwadnianiem wyrobisk kopalń rud Zn-Pb w niecce bytomskiej, Współczesne problemy hydrogeologii, t. VII, cz. 2, Kraków –Krynica 1995.
KROPKA J., DALIBÓG J., ZDYBIEWSKA K., Zawodnienie i likwidacja kopalń rud cynku i ołowiu w niecce bytomskiej, Przewodnik LXV Zjazdu PTG Sosnowiec, Wyd. Uniw. Śląskiego, Katowice 1994, s. 253-262.
KROPKA J., Występowanie cynku i ołowiu w wodach dołowych kopalń rud Zn-Pb rejonu bytomskiego, Współczesne problemy hydrogeologii, Tom VII cz..2, Kraków – Krynica 1995, s. 87-92.
KRYZA A., MOTYKA J., SZUWARZYŃSKI M., KRAM M., Anomalia hydrochemiczna w kopalni TRZEBIONKA, Współczesne problemy hydrogeologii, T. VII, CZ.2, Kraków – Krynica 1995, S. 101- 106.
KUPICH I., Praca doktorska: Ograniczenie zawartości jonów metali ciężkich i siarczanowych w zrzutowych wodach dołowych kopalń rud Zn – Pb, Politechnika Częstochowska, Wydział Inżynierii i Ochrony Środowiska, 2005.
MARCINIAK M., PRZYBYŁEK J., HERZIG J., SZCZEPAŃSKA J., Laboratoryjne i terenowe oznaczanie współczynnika filtracji utworów półprzepuszczalnych, Wyd. Sorus, Poznań 1998 r.
Oleszkiewicz J., Eksploatacja składowiska odpadów. Poradnik decydenta, Lem Projekt s. c. Kraków 1999.
Prawo Ochrony Środowiska, www.ochronaśrodowiska.com.pl, wersja aktualizowana
RÓŻKOWSKI A., ZIEMIAŃSKI A., Mapa ognisk zanieczyszczeń wód podziemnych Górnośląskiego Zagłębia Węglowego i jego obrzeżenia, Państwowy Instytut Geologiczny, Warszawa 1995.
SZYMANEK A., Badania modyfikowanych sorbentów wapniowych do suchego odsiarczania spalin, Rozprawa doktorska, Politechnika Wrocławska, Wydział Mechaniczno-Energetyczny, 2000.

Kupich I., Girczys J., *Utylizacja szlamów pozyskiwanych w procesie oczyszczania wód dołowych kopalń Zn-Pb,* Physicochemical Problems of Mineral Processing, 42 (2008), 91-106 (w jęz. ang)

Przedstawiono możliwości gospodarczego wykorzystania szlamów odpadowych z oczyszczania wód zrzutowych kopalń rud Zn-Pb. Samo wytwarzanie tego odpadu jest konsekwencją wynikającą z konieczności odwadniania nieczynnych już kopalń rud cynkowo-ołowiowych niecki bytomskiej. Przeznaczone do usunięcia z wody metale ciężkie, w wyniku hydrolizy i działania jonów węglanowych, występują w postaci cząsteczkowej, dlatego podstawą oczyszczania jest koagulacja wapnem. Ubocznym efektem tego procesu jest wytrącanie dużych ilości $CaCO_3$. Powstające osady mają właściwości fizyczne i skład chemiczny taki, jak materiały naturalne wykorzystywane gospodarczo.

Proponowane kierunki zagospodarowania szlamu mieszczą się w trzech grupach technologicznych:

- jako zawiesiny alkalicznej w sorpcji SO_2 lub neutralizacji H_2SO_4
- wykonywanie warstwy mineralnej, inertnej w stosunku do środowiska w procesie składowania różnych odpadów
- wypełnianie pustek poeksploatacyjnych górnictwa lub składowanie.

Wykorzystanie technologiczne odpadu z uzdatniania wód może przynieść wymierne oszczędności surowców naturalnych, poprawić warunki ochrony środowiska w obszarze składowisk i rozwiązać problemy z pozyskiwaniem terenu pod składowanie.

słowa kluczowe: górnictwo cynku i ołowiu, wody zrzutowe, uzdatnianie wody, utylizacja odpadów

Physicochemical Problems of Mineral Processing, 42 (2008), 107-118
Fizykochemiczne Problemy Mineralurgii, 42 (2008), 107-118

Eisa S. Mosa*, Abdel-Hady M. Saleh*, Taha A. Taha.*, Anas M. El-Molla**

EFFECT OF CHEMICAL ADDITIVES ON FLOW CHARACTERISTICS OF COAL SLURRIES

Received February 10, 2008; reviewed; accepted July 31, 2008

In the present paper, the effect of chemical additives or reagents on rheological characteristics of coal-water slurry (CWS) was investigated. The power-law model was applied to determine the non-Newtonian properties of coal slurries. Three types of dispersants namely, sulphonic acid, sodium tri-polyphosphate and sodium carbonate were studied and tested at different concentrations ranging from 0.5 to 1.5% by weight from total solids. Sodium salt of carboxymethyl cellulose (Na-CMC) and xanthan gum were tested as stabilizers at concentrations in the range of 0.05 to 0.25 % by weight from total solids. It was found that apparent viscosity and flow properties of CWS are sensitive to the use of chemical additives (dispersants and stabilizers). Among studied dispersing agents, sulphonic acid recorded the best performance in modification and reducing CWS viscosity. The best dosage of all tested dispersants was found to be as 0.75 % by wt of solids. With regard to studied stabilizers, Na-CMC recorded better performance than xanthan gum. The best dosage of investigated stabilizers was found to be as 0.1 % by wt. from total solids.

key words: coal slurry, viscosity, dispersants, carboxymethylcellulose, gum guar, sulphonic acid, tri-polyphoshate

INTRODUCTION

Xiao-an et al.,(1994) stated that the surface nature of coal is very important in the preparation of high solid/liquid ratio coal-water suspensions (CWS). In this investigation, two kinds of additives were used. The first was a non-ionic surfactant while the second was a mixture of two anionic polyelectrolytes. The first was a polyalkylene glycol ether derivative prepared in the laboratory and the second was a mixture of sodium humate and naphthalene-sulphonic acid formaldehyde condensate. By proper

* Mining & Petroleum Eng. Dept., Faculty of Engineering, Al-Azhar University, Cairo, Egypt
** Civil Eng. Dept., Faculty of Engineering, Al-Azhar University, Cairo, Egypt

selection of surfactant and treatment of coal powders, the authors obtained a high solid concentration, up to 70% by weight, of the CWS. Boylu et al.(2004) studied the effect of sodium polystyrene sulphonate (SPS) as a dispersing agent on rheology of coal water slurries. It is a product of Japanese Com and Lion Corporations with molecular weight of 14 and 95% sulfonation degree. Encouraging results were obtained at a dispersant dosage less than 1 wt. % of the solids. Nigle and Neil (2003) cited that reducing friction in non-settling slurry pipe flow is obtained by reducing the viscosity of this slurry by adding suitable chemicals or additives. In this work, the effects of different chemical additives have been studied on a number of mineral slurries including drilling mud slurries (using sodium acid pyrophosphate and sodium hexametaphosphate), phosphate rock slurries (using caustic soda), limestone cement feed slurries (using a combination of sodium tripolyphosphate and sodium carbonate). The work aimed to reduce the viscosity of investigated slurries to facilitate long-distance pumping and reducing energy requirements. Meikap et al., (2005) studied the relation between shear rate and shear stress for microwave-treated and untreated reject coal samples. In this work, all suspensions were found to follow pseudoplastic behavior, which is higher at higher concentrations. The shear stress for untreated reject coal was higher than that of microwave-treated coal. This was explained on the basis of changing surface characteristics of microwave-treated coal. Also, it was found that untreated clean coal suspensions of 30 to 40 wt. % solid concentrations are pseudoplastic.

Another work by Boylu et al.,(2005) involved a study illustrating the effect of carboxymethyl cellulose (CMC) on the stability of the coal-water slurry using different coal ranks. The experimental results showed that polymeric anionic CMC agent has higher effect on the stability of CWS, in particular, that prepared from bituminous coal. Casassa et al.,(1984) studied rheological behavior, sedimentation stability and electrophoretic mobility of four bituminous coals in water and in solutions of simple well-characterized surfactants. The list of surfactants included cationic hexadecyltrimethyl ammonium bromide, anionic sodium dodecyl sulfate and Aerosol OT. It was found that slurry rheology and stability depend on coal particle surface charge. It was claimed that additives may be chosen to modify the surface charge and hence improve slurry rheology. Huynh et al.,(2001) illustrated the effect of dispersants on the rheological properties of copper concentrate slurry. The reagents used include phosphate, naphthalene sulphonate formaldehyde condensate (NSF), sodium orthophosphate (Na_3PO_4), sodium tripolyphosphate ($Na_5P_3O_{10}$) and a polyphosphate sample with different degree of polymerization. The range of studied degree of polymerization was from 1 to 19 with an average value of 10. In comparing the effect of the different rheological modifiers investigated, the greatest reduction in the yield stress was obtained with the phosphates, while an equivalent mass concentration of NSF produced an inferior result. Mingzhao et al.,(2004) reported some guidelines in selecting

dispersants in order to have a suitable chemically controlled viscosity. These guidelines include: a) dispersant must be adsorbed by enough solid surfaces to affect slurry viscosity, b) slurry viscosity must be as high that the utilization of the dispersant can help reducing or control slurry viscosity, c) dispersant must be consistent in its ability to decrease viscosity as a function of changing dispersant concentration, pH value and water quality, d) dispersant must be nontoxic and degradable, and e) dispersant must not adversely affect or contaminate downstream operations, such as flotation, thickening etc.

COMMON RHEOLOGICAL SLURRY MODELS

Among numerous rheological models, the power law has a wide application (Chhabra and Richardson, 1999; George et al., 1984). The model can mathematically expressed as

$$\tau = k\,\gamma^{n}\,. \tag{1}$$

The apparent viscosity can be estimated from the power-law model as

$$\mu_a = \tau\ /\ \gamma = k\,(\gamma)^{n-1}, \tag{2}$$

where μ_a is the apparent viscosity (Poise), τ shear stress (dyne/cm^2), γ shear rate, (s^{-1}), k consistency coefficient of fluid (Pa/s) (the higher the value of k the more viscous the fluid), and n is the flow behavior index, which is a measure of the degree of departure from the Newtonian fluid behavior. Depending on the value of n, Lester (1994) has identified that the power law describes three flow behaviors. These behaviors include pseudoplastic (n<1.0) - the effective viscosity decreases with shear rate, Newtonian (n=1.0) - the viscosity does not change with shear rate and dilatant (n>1.0), the effective viscosity increases with the shear rate. This model was selected and applied throughout this work to estimate the apparent viscosity of considered slurries. Other flow models such as Bingham (Nigel, 1999) plastic and Herschel-Bulkley (Bahn, 2002) models were also suggested elsewhere.

EXPERMENTAL WORK

SAMPLE AND ITS PREPARATION

The material used in this paper was a low rank coal. It was obtained from the main coal seam of El–Maghara coal mine, Northern Sinai, Egypt. The chemical analysis of head sample is shown in Table 1.

Table 1. Chemical analysis of the head sample

Proximate analysis		Ultimate analysis	
Test	Value	Test	Value
Moisture content,%	3.90	Carbon %	66.16
Volatile matter %	43.10	Hydrogen%	5.88
Ash %	20.76	Nitrogen %	1.16
Fixed carbon %	32.24	Sulfur %	4.13
		Oxygen %	11.00

COAL-WATER SLURRY (CWS) SAMPLES PREPARATION

The particle size of raw coal sample was initially reduced to less than 3 cm using jaw crusher and then dry ground by a laboratory-size disc mill. The discharge space between the two discs of mill was controlled to obtain a suitable product which was tested to obtain a feed sample characterized by whole particle size distributions of -250 μm maximum size. The solid concentration was kept constant at 40% solids by weight through all tests. The procedure of preparation of the CWS was standardized for all tested samples. Weighed amount of tap water was transferred into a 500 cm^3 glass beaker, and then the weighed coal sample was slowly transferred into the beaker. The contents were stirred by magnetic stirrer for about 20-30 minutes after adding all the coal sample. The CWS was then allowed to stand in the beaker for about 10 hours to ensure release of entrapped air. Before testing, the slurries were always thoroughly mixed by hand shaking and stirring to ensure homogeneity of the slurry. The same procedure was repeated with different test conditions.

Three dispersants were used in this study namely, sulphonic acid, sodium tripolyphosphate and sodium carbonate at dosages range from 0.5 to 1.5 wt. % of solids. Two types of chemicals were tested as stabilizers, namely, sodium salt of carboxy methyl cellulose (CMC) and xanthan gum. They tested at dosages range from 0.05 - 0.25 % by wt. of the solids. The selected additives (dispersant and stabilizers) were prepared in the predetermined ratio and dissolved in a little amount of water before adding them to the coal slurry. Stabilizers were tested always in conjunction with dispersants while dispersants were tested also alone.

RHEOLOGICAL MEASUREMENTS

Laboratory rheological data were obtained with Chandler Engineering viscometer Model 3500LS^+ which measure the rheological properties of tested slurries by measuring shear stress at specific shear rates. It considered as a concentric cylinder rotational viscometer with a wide shear rate range, i.e, from 0.17 to 1022 S^{-1} (Chandler Engineering, 2003).

RESULTS AND DISCUSSION

EFFECT OF DISPERSANTS

Figure 1 illustrates the relationship between shear stress and shear rate for the 250 μm particle size sample at 40% solids by wt. using different dosages of sulphonic acid as a dispersant agent. The dispersant dosage was expressed as percentage of total solids. It can be seen that the shear stress decreases with the increase in the amount of sulphonic acid, i.e, from 0.50 % to 0.75 % and then increases with increasing sulphonic acid concentration from 0.75 % to 1.5 % wt. of solids. The best sulphonic acid dosage is 0.75% as it gives the lowest shear stress at all studied shear rates.

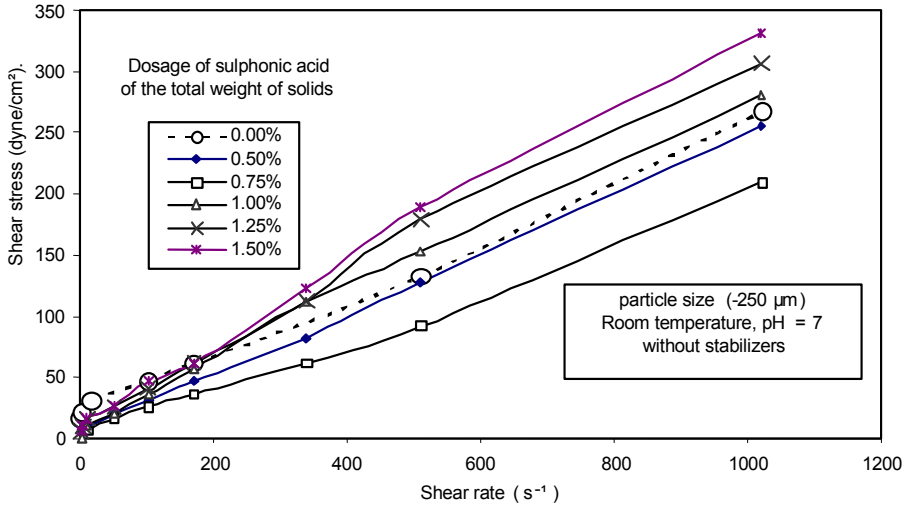

Fig. 1. Relation between shear stress and shear rate for -250 μm particle sizesample at different dosages of sulphonic acid as a dispersing agent and at solid concentration 40% by wt.

The same results were obtained (Fig. 2 and 3) using sodium tripolyphosphate and sodium carbonate as dispersing agents. These figures showed also that the best dosage of these reagents is 0.75% wt of solids. Increasing the dosage of dispersant behind this value does not lead to an improvement in flow properties of considered slurries. The effect of dispersant type and dispersant dosage on the apparent viscosity of -250 μm particle size sample at 40% wt. is presented in Fig. 4. From this figure can be observed that the lowest value of viscosity is attained at 0.75 % by wt. of coal for all

three tested dispersing agents. At reagent concentration less than 1% the best dispersant is sulphonic acid but at higher concentrations sodium tripolyphosphate is the best.

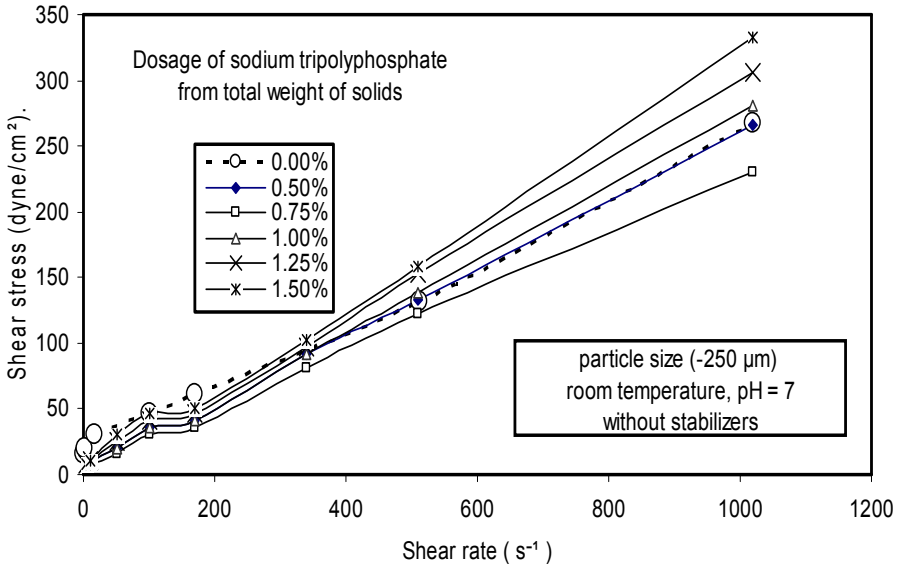

Fig. 2. Relation between shear stress and shear rate for -250 µm particle size sample at different dosages of sodium tripolyphosphate as a dispersing agent and at solid concentration 40% by wt.

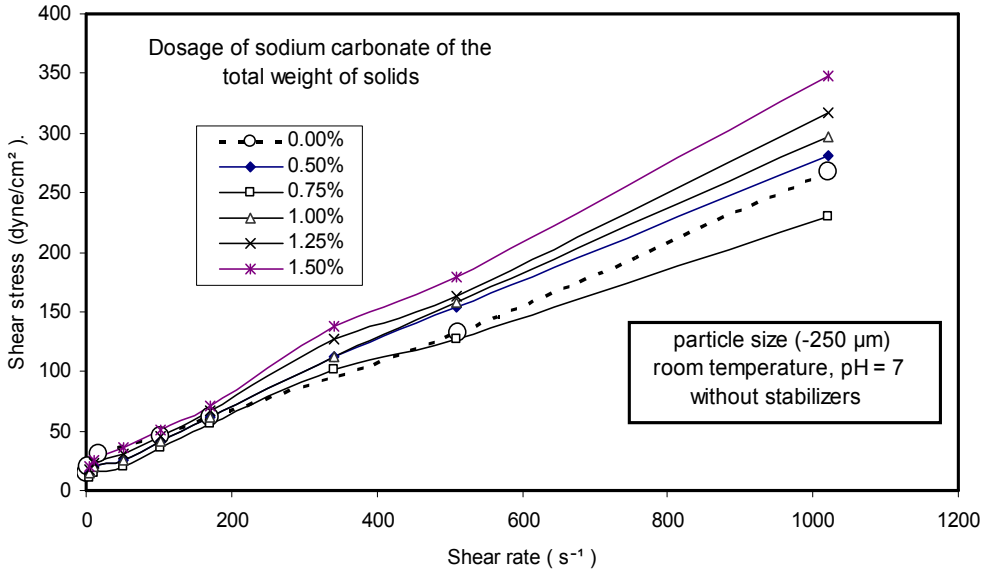

Fig. 3. Relation between shear stress and shear rate for -250 µm particle size sample at different dosages of sodium carbonate as a dispersing agent and at solid concentration 40% by wt.

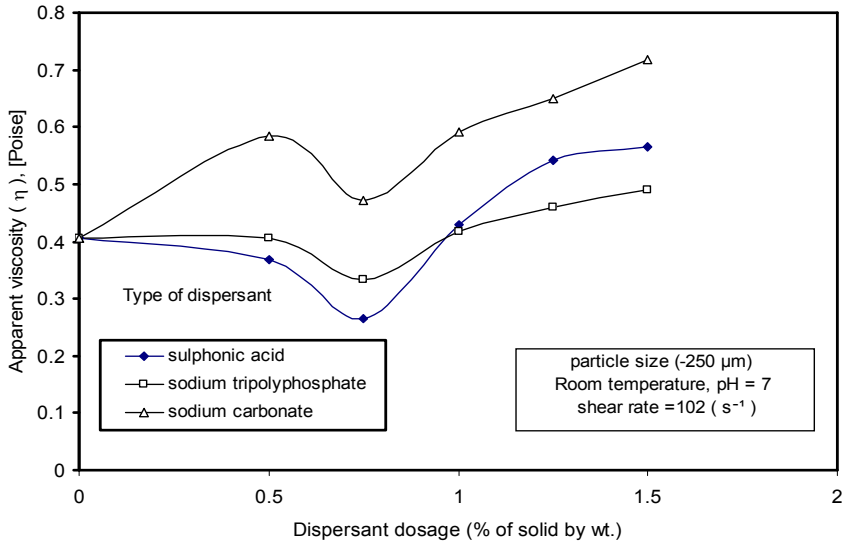

Fig. 4. Effect of dispersant dosages on apparent viscosity of -250 µm particle size at 40% solid by wt.

EFFECT OF STABILIZERS

It is worth to mention that all stabilizers were tested in the presence of sulphonic acid as a dispersing agent at concentration equal to 0.75% of total solids.

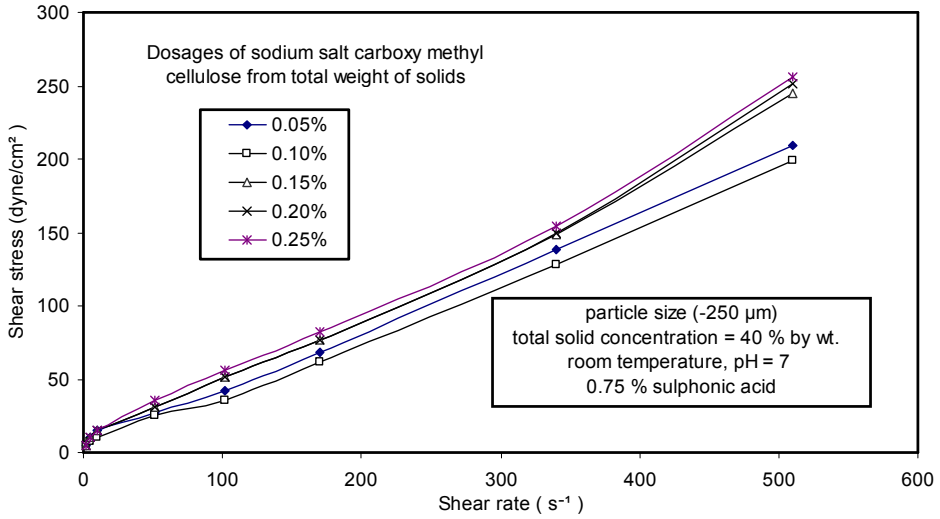

Fig. 5. Relation between shear stress and shear rate for -250 µm particle size sample at different dosages of sodium salt of carboxymethyl cellulose as a stabilizer and 0.75% sulphonic acid as a dispersing agent

Figure 5 illustrates the relationship between shear stress and shear rate for -250 μm particle size, at 40% solids by wt. using different dosages of sodium salt of carboxymethyl cellulose (CMC-Na) as a stabilizing agent. It can be seen that the shear stress decreases with the increase of the amount of sodium salt of carboxymethyl cellulose, from 0.05 % to 0.1 % wt. of solids. With CMC-Na concentration increase from 0.1 % to 0.25 % wt. of solids the shear stress increases.

Figure 6 illustrates the relationship between shear stress and shear rate for -250 μm particles at 40% solids by wt. using different dosages of xanthan gum as a stabilizing agent. It can be seen that the shear stress increases with the increase of xanthan gum dosage for all studied range of reagent dosage (i.e, from 0.05 % to 0.25 % wt. of solids).

Figure 7 shows the relationship between the apparent viscosity and stabilizer dosage for both CMC-Na and xanthan gum at 102 S^{-1} shear rate. Viscosity increases with increasing stabilizer dosage. This increase is more remarkable with xanthan gum. It can be seen that the CMC-Na is more effective than xanthan gum where less viscosity is obtained at all stabilizer dosages. The comparison between the use CMC-Na and xanthan gum at 0.1 % concentration and at different shear rates was carried out. These results are presented in Fig. 8. As it is observed from this figure, the type of stabilizer is an important factor affecting the rheological properties of the slurry. It is shown that the use of CMC-Na is better than xanthan gum because the slurry becomes less viscous at all studied shear rates.

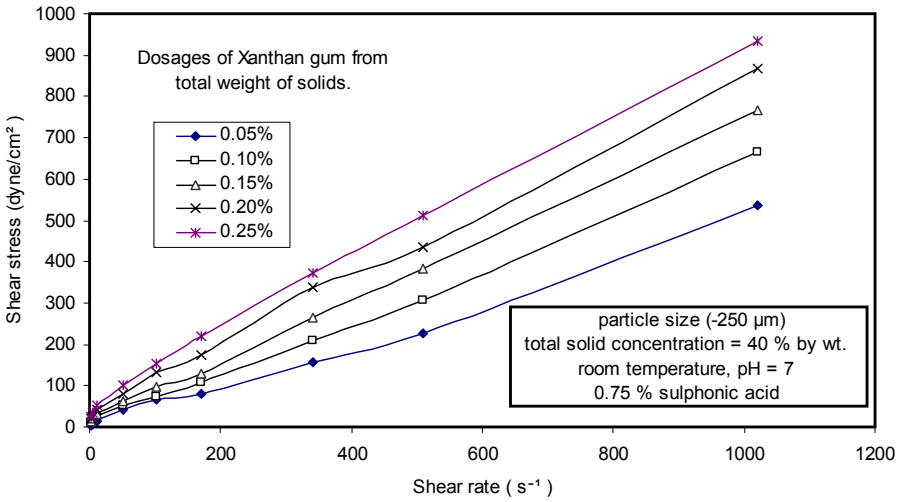

Fig. 6. Relation between shear stress and shear rate for -250 μm particle size sample at different dosages of xanthan gum as a stabilizer and 0.75% sulphonic acid as a dispersing agent

In the paper, flow properties of coal slurry samples in presence and absence of chemical additives were investigated. The applied dispersant was sulphonic acid at

0.75% wt of solids. The mentioned stabilizers, i.e, CMC-Na and xanthan gum were used at 0.1% wt of solids.

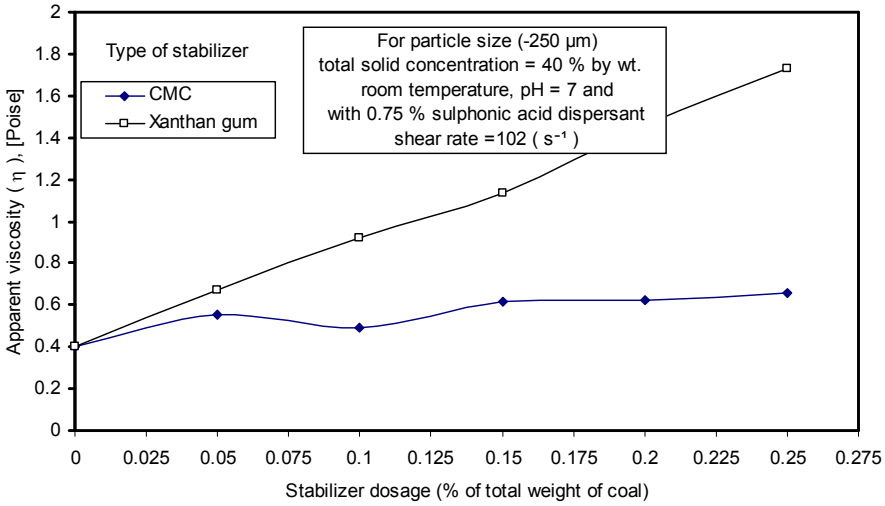

Fig. 7. Effect of stabilizer type and dosage on apparent viscosity for -250 μm particle size in presence of 0.75% sulphonic acid

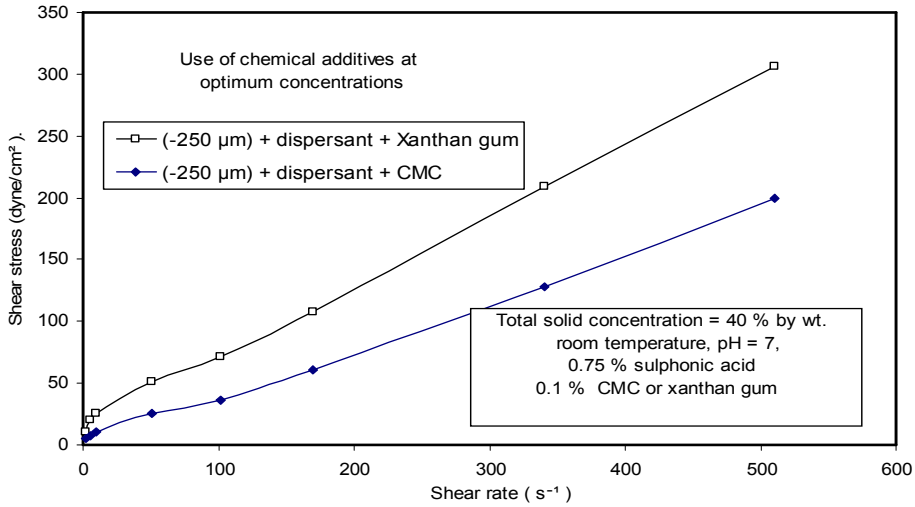

Fig. 8. Relation between shear stress and shear rate for -250 μm particle size sample using 0.75% sulphonic acid and 0.1% from total solids stabilizer dosage at different shear rates

The results are presented in Fig. 9. It is clear that the dispersant (sulphonic acid) addition is an important factor for improving the rheological properties of the coal slurry. The viscosity of the slurry increases by use of CMC-Na and xanthan gum. This increase is more remarkable at high shear rates. CMC-Na recorded better performance than xanthan gum as lower shear stress was obtained at all investigated shear rates.

Hence, it seems like that obtaining a slurry of low viscosity and at the same time of good stability is a difficult task. Alternatively, one may select or achieve slurry of low viscosity and acceptable stability.

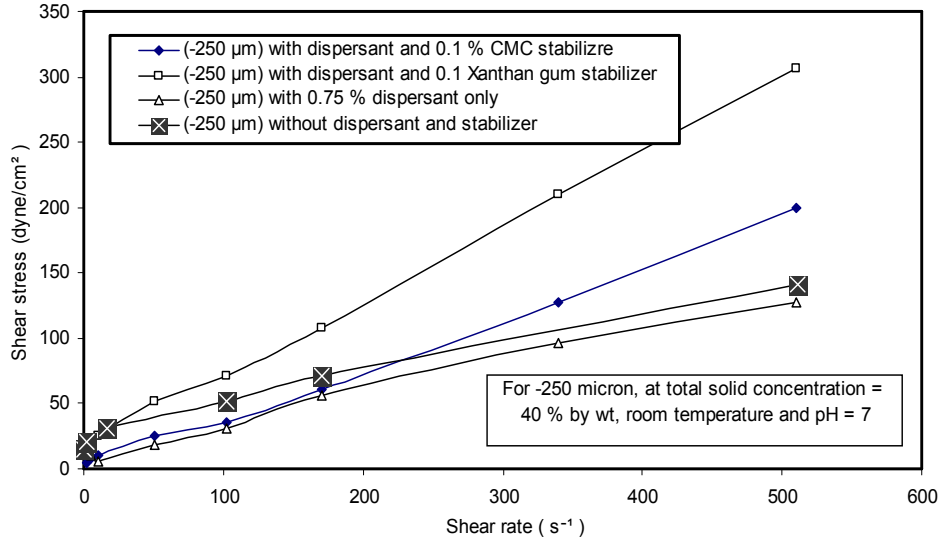

Fig. 9. Relation between shear stress and shear rate for -250 µm particle size sample with and without using different types of chemical additives.

Generally, particulate slurries exhibit non-Newtonian flow behaviour because of the interparticle forces that act between the particles in these chemically complex systems. Various chemical treatments are used to alter the surface chemistry and then the interactions between particles within the slurry. It is expected that the surface chemistry (forces) of particles affect rheological behaviour of the slurry to a great extent. These surface forces arise from chemistry of solid-solution interface and dominate the interaction between neighboring particles. Hence the surface species will dictate the interparticle forces (which are responsible for the rheological properties) between coal particles in the slurry. When the electrostatic repulsive forces between the particles are weak and insufficient, the aggregation of the particles occurs and the result is an aggregated slurry with increase in rheological parameters (yield stress and viscosity). However, when the electrostatic repulsion between particles are sufficient to prevent the Van der Waals attractive forces from operation, a well dispersed slurry with reduced rheological parameters is obtained. Such surface forces (attraction or repulsion) depend on adsorption of reagent ions on solid surfaces which, in turn, depend on slurry pH. A study of the surface chemistry of the slurry by X-ray photoelectron spectroscopy (XPS) under considered chemical treatments is recommended in future work to describe the observed changes in the rheological properties. Hence, it is expected that the rheological behaviour of the slurry may be favorably altered by successful

manipulation of the surface chemistry of the particle surface via alteration of solution conditions (e.g. pH) or addition of reagents (rheology modifiers).

CONCLUSION

The test results clearly indicate that the coal water slurry (CWS) rheology depends on chemical additives applied such as dispersants and stabilizers. It was found that the flow properties and the apparent viscosity of the CWS are very sensitive to the use of chemical additives. Using a dispersant agent is very important as it reduces the apparent viscosity of CWS. Three dispersants, namely, sulphonic acid, sodium tripolyphosphate and sodium carbonate were tested throughout this study. Among these dispersants, sulphonic acid recorded the best performance. The best dosage of all tested dispersants was found to be as 0.75 % wt. of solids. Two stabilizers were tested in conjunction with sulphonic acid dispersant, namely, sodium carboxyl methyl cellulose (CMC-Na) and xanthan gum. With respect to the effect of tested stabilizers on the slurry viscosity, it was found that they increase slurry viscosity. CMC-Na recorded better performance compared to xanthan gum. The best dosage of (CMC-Na) as a stabilizer was found as 0.1 % wt. of solids. Although stabilizers increase viscosity of slurry, they sometimes are applied to improve stability of the slurry against sedimentation. Hence, one may conclude that stabilizers must be used in a small concentration to obtain better flow properties with reasonable stability. It seems like that obtaining a slurry of low viscosity and at the same time of high stability is a difficult task to obtain but instead one can obtain a slurry with low viscosity and acceptable stability.

REFERENCES

XIAO-AN, F., YU-CHENG, S., SHAO-BING, H., LIN, Z. LONG J., "Influence of pitch coal surface treatment on the beneficiation of high water content coal and the rheological properties of CWS" Fuel, Vol. 73, No. 11, 1994, pp (1772-1775).

BOYLU, F., DINCER, H. ATESOK, G. "Effect of coal particle size distribution, volume fraction and rank on the Rheology of coal–water slurries". Fuel Processing Technology, 85 (2004), pp 241– 250

NIGEL, I. H. NEIL, J. A., "Developments in slurry pipeline technologies, update your knowledge of modeling, optimizing and controlling slurry pipeline flows" Solid/ Liquid Handling, www. Cepmagazine.org, April 2003 CEP.

MEIKAP, B. C., PUROHIT, N. K. MAHADEVAN, V. "Effect of microwave pretreatment of coal for improvement of rheological characteristics of coal–water slurries" ,Journal of Colloid and Interface Science, 281 (2005), pp 225–235.

BOYLU, F., ATESOK, G. DINCER, H. "The effect of carboxymethyl cellulose (CMC) on the stability of coal-water slurries", Fuel, Vol.84, no 2-3 January/ February 2005, pp 315-319.

CASASSA, E. Z., PARFFIT, G. D., RAO, A. S. TOOR, E. W. "Effect of surface active additives on coal / water slurry rheology" American Society of Mechanical Engineers (paper), 1984, ASME, New York, NY, USA ,10p 84, WA/HT-96.

HUYNH, L., PAUL, J. JOHN, R. "The rheological properties of copper concentrate slurry: from surface chemistry to pipeline transport" 2001

MINGZHAO, H., YANMIN, W. FORSSBERG, E. "Slurry rheology in wet ultrafine grinding of industrial minerals: a review", Powder technology, Vol. 147, November 2004, pp (94-112).

CHHABRA R. P. RLCHARDSON J. F., "Non-Newtonian flow in the process industries, fundamentals and Engineering Applications " Butterworth Heinemann, Oxford, 1999, Chap. 1,2,3,4 and 8.

GEORGE, R. G., DARLEY, H. C., WALTER F. R., "Composition and properties of Oil well drilling fluids", Fourth Edition, Gulf Publishing company, Houston, Texas, 1984, Chap. 1, 2,3 and 5. pp (3-239).

LESTER C. B., " Hydraulics for pipeliners " Vol. 1, Fundamentals, Second Edition Gulf Publishing company, Houston, Texas, London, Paris, Tokyo, 1994, Chapter 3,4.

NIGEL I. H, "Designing for the storage and conveying of slurries", Chemical Engineering progress, Sept. 1999**,** pp. (21-41).

BAHN E. A. "Slurry systems handbook" Mc Graw-Hill, New york, Chicago, 2002.

Chandler engineering, L.L.C. 3500LS^{+} , Direct indicating viscometer, 2003/03/20, www.chandlereng.com

Mosa E. S., Saleh A.-H. M., Taha T. A., El-Molla A. M., *Wpływ reagentów chemicznych na charakterystykę przepływu zawiesin węglowych*, Physicochemical Problems of Mineral Processing, 42 (2008), 107-118 (w jęz. ang)

W pracy badano wpływ odczynników na charakterystykę reologiczną zawiesin wodno-węglowych (CWS). Zastosowano model potęgowy do wyznaczenia nieniutonowkich właściwości zawiesin węglowych. Badano trzy typy dyspersantów: kwas sulfonowy, tripolifosforan sodu oraz węglan sodu przy różnych ich stężeniach od 0.5 to 1.5% wagowego. Zastosowano sól sodową carboksymetylocelulozy (Na-CMC) oraz gumę guarową jako stabilizatory zawiesin używając ich w ilości od 0.05 to 0.25 % wagowego. Stwierdzono, że pozorna lepkość i charakterystyka przepływu CWS są podatne na użyte dyspersanty i substancje stabilizujące. Wśród badanych dyspersantów, kwas sulfonowy odznaczał się najlepszym działaniem i wysoka redukcją lepkości CWS. Ilość użytych dyspersantów wyniosła 0.75 % wagowego. Wśród substancji stabilizujących lepszą okazała się Na-CMC niż guma guarowa. Najodpowiedniejsza ilość stabilizatora to 0.1 % wagowego.

słowa kluczowe: zawiesiny węglowe, lepkość, dyspersanty, karboksymetyloceluloza, guma guarowa, kwas sulfonowy, tripolifosforan

Physicochemical Problems of Mineral Processing, 42 (2008), 119-130
Fizykochemiczne Problemy Mineralurgii, 42 (2008), 119-130

Abdel-Hady M. Saleh*, Atef M. Ramadan *, Mohamed R. Moharam*

BENEFICIATION OF EGYPTIAN ABU-SWAYEL COPPER ORE BY FLOTATION

Received March 15, 2008; reviewed; accepted July 31, 2008

In this study, an attempt was made to recover copper from Abu-Swayel deposit. A reverse flotation technique was applied leading to flotation of the accompanying oxide and sulfide minerals and gathering copper oxide minerals in the sink product. The results showed that the application of such technique is possible under the optimum flotation conditions. Studying the main factors that affect such flotation system indicated that the optimum flotation conditions are at 1.5 kg/t oleic acid as the collector, pH=10, air flow rate=7 l/min and 5 min flotation time. In the context, about 90% of copper recovery with 10% copper grade was obtained. It was also found that the copper mineral particles lost in the froth product by mechanical carryover mechanism can be recovered through concentrate cleaning under the same flotation conditions. Hence, one may conclude that the results of this study are useful and may help in reassessment of exploitation of such copper deposit.

key words: flotation, upgrading, copper ore, copper minerals, copper oxides

INTRODUCTION

The application of flotation in copper ore treatment plants is used on a wide scale. Hosten and Tezcan (1990) used kinetic analysis and separation efficiency factors for comparison of frother performance in flotation of a massive copper sulfide ore. The studied frothers included polyglycols, pine oil and methyl isobutyl carbinol (MIBC). No obvious differences in the frother selectivity were observed. However, polypropylene glycol frother gave the highest flotation rate. Heyes and Trahar (1977) studied natural floatability of chalcopyrite. It appeared that the particle surface is rendered hydrophobic in an oxidizing environment and hydrophilic in a reducing environment. They stated that the principal side effect of grinding in an iron mill is the strongly cre-

* Mining & Petroleum Eng. Dept., Faculty of Engineering, Al-Azhar University, Cairo, Egypt

ated reducing environment. Such environment suppresses the normal floatability of chalcopyrite which can be reestablished by raising the pulp potential either by aeration or by addition of oxidants.

The electrokinetic behavior of copper sulfide ores and their flotation response was investigated by many authors (Acar and Somasundaran, 1992; Uribe-Salas, 2000; Leppinen, 1998; Hanson and Fuerstenau, 1991) . The results obtained by Acar and Somasundaran (1992) showed that covellite and millerite exhibit two charge reversals, one from negative to positive in the neutral pH range, and another from positive to negative in the alkaline pH range. Uribe-Salas, et al.,(2000) studied the selective flotation of chalcopyrite contained in a fine-grained complex ore by increasing the pulp potential using hydrogen peroxide. The results showed that the recovery of chalcopyrite flotation occurs near Eh = 0.3V. Leppinen et al., (1998) found that the grinding medium had a strong effect on electrode potential and flotation results. Copper recovery increased by 80% within a narrow potential range in the flotation of an "easy" ore type whereas only 15% increase in copper recovery occurred in the flotation of "difficult" copper ore. Hanson and Fuerstenau (1991) studied the electrochemistry and wetting behavior of chalcocite in aqueous solutions of potassium salts of octyl hydroxamate and ethyl xanthate. The results showed that hydroxamate may be promising as a collector, not only for copper sulfide ores but also for oxidized copper ores. It was concluded that the selective separation of copper minerals (sulfides and/or oxides) may be possible by controlling the flotation pulp potential.

Evaluation of flotation collectors for copper sulfides was performed by Ackerman et al.,(1987) and Senior et al. (2006) using criteria of recovery and flotation rate. The flotation of copper sulfides with sulphydryl collectors was found to follow the order: xanthate > dithiophosphate = thionocarbamate > dixanthogen. Separability curves in the form of mineral recovery versus yield have been used to characterize the copper flotation process both at batch laboratory scale and industrial plant scale Yianatos et al.,(2003). A comparison was made at the maximum separation efficiency point in both operations. The results showed a good consistency for scaling up the rougher flotation recovery from batch tests to industrial within 1 percentage point error range. Laboratory experiments carried out on flotation of copper oxides by Aplan and Fuerstenau (1984) demonstrated that chrysocolla and malachite can be floated with a mercaptan collector. Higher xanthate homolog (hexyl, dodecyl), when used in large quantities, will float malachite but not chrysocolla. In the presence of finely ground gangue particles, an addition of the mercaptan to the grinding mill gave superior recoveries over its addition to flotation cell. A model for the attachment of the mercaptan to the chrysocolla surface is proposed which involves a reaction of mercaptan molecules with copper sites which leads to the formation of insoluble copper mercaptide and splitting off water molecule at the surface.

The Abu–Swayel ore deposit is located at about 185 km south of Aswan, near the Wadi Haimour (Egypt). The ore body includes both massive and disseminated mineralization hosted in a lens–like body of amphibolite. The amphibolite lens is sur-

rounded by biotite–garnet schist of basic origin Hussein (1990). The deposit consists of copper, nickel, and iron minerals in the form of oxides and sulfides and is not exploit. A few studies was carried out on the extraction of copper from this deposit by heap and agitation leaching (Fathy, 2005; Abbas, 1983).

An important problem facing the copper industry in the world is the recovery of oxide copper minerals because they float poorly. It is expected that the reverse flotation technique may be appropriate to recover such oxide copper minerals from the accompanying mineral oxides/sulfides.

This work aimed to separate or recover copper mineral oxides in the sink product and other minerals in float product by reverse flotation technique. Hence, a study that adds information and/or investigates the effect of various parameters on such flotation is of a great interest.

EXPERIMENTAL

MATERIAL

The experimental work was carried on a sample of Abu-Swayel copper ore deposit. This deposit consists of copper, nickel and iron minerals in the form of oxides and sulfides. The mineralogical composition of this deposit was studied by X-ray diffraction and microscopic examination (Fathy, 2005; Abbas 1983), and the founding are shown in Table 1. A bulk sample was collected from some outcropping areas of the deposit. A representative sample was taken to determine the percentage of copper in the flotation feed. The experiments showed that it contains about 6% Cu. The chemical analysis of other elements, carried out in the laboratory of Egyptian Geological Survey and Mining Authority (EGSMA) are shown in Table 2 (Abbas 1983).

Table 1. Mineralogical composition of Abu-Swayel ore deposit

Mineral	Chemical formula	Mineral	Chemical formula
chalcopyrite	$CuFeS_2$	violarite	$(Ni_2\ Fe)SO_4$
malachite	$CuCO_3(OH)_2$	ilmenite	$FeTiO_3$
calcanthite	$CuSO_4.5H_2O$	goethite	FeOOH
brochiantite	$Cu_4\,(SO_4).(\ OH)_6$	hematite	Fe_2O_3
bravoite	$(NiFe)S_2$		

Table 2. Chemical analysis of the representative sample

Chemical constituent	Si	Fe	Mg	Ca	Ni	L.O.I
Percentage, %	20.14	16.86	9.16	1.20	1.80	8.50

Oleic acid was used as collector and pine oil at fixed dosage of 250 mg/dm^3 was applied as a frother.

METHODS

The raw material was received as coarse lumps. These lumps were crushed in a laboratory jaw crusher to 1 mm size. The product from jaw crusher was dry ground in a closed circuit disk crusher to a –0.5 mm size. After each run, the product was screened on a 0.5 mm screen using Ro-tap shaker. The +0.5 mm fraction was returned to the mill while the -0.5 mm fractions were collected to form the flotation feed.

Flotation tests were carried out in a laboratory subaeration mechanical flotation machine equipped with 1 dm^3 capacity cell. Flotation tests were carried out using tap water at 20% pulp density (i.e., 20% solids by wt.). The sample was agitated for 5 min to ensure complete wetting of particle surface. The pulp was conditioned for 5 min with collector and for 1 min with frother. The parameters studied and their ranges of study are shown in Table 3.

Table 3. Parameters studied and their ranges of study

Parameter	Range of investigated parameter
collector dosage (oleic acid)	0.5 - 3.0 kg/Mg
pH	6 - 12
air rate	3 - 15 l/min
flotation time	1 - 5 min

In the tests designed to study the effect of time, the concentrate was collected after 1, 2, 3, 4, and 5 min flotation time. However, one concentrate was collected after the barren bubbles were observed. The time was measured from the moment at which the air is introduced into the cell. The pulp density and impeller speed (1000 rpm) were kept constant during all tests. pH was controlled using HCl and NaOH solutions. The pulp level was kept constant by adding more water during flotation.

A given tested parameter was changed or studied at the mentioned range while other parameters were fixed or kept constant. The concentrate (float) as well as the tailing (sink) were filtered in a vacuum filter and dried in an electric drier at 80 – 100^{o}C, weighed with a balance and analyzed for copper content.

Although the type of flotation machine has a self–inducing aerator, in which the gas flow rate is dependent on the impeller speed, the gas flow rate to the machine was controlled and measured to study its effect. The applied system in this work was a batch system consisting of water–air–solid phases.

RESULTS AND DISCUSSION

It is worth to mention that all tests were carried out at 200 g in one dm^3 i.e. at 20% solid/liquid ratio by wt., 250 mg/dm^3 pine oil as a frother and at1000 rpm impeller speed. Four groups of tests were considered. The first aimed to study the effect of collector dosage. In this group a selective values for pH and air flow rate (8 and 6 dm^3/min) were considered. The second illustrates the effect of pH value on the considered flotation system where the optimum collector dosage from the first group and 6 dm^3/min flow rate were considered. The third investigates the effect of air flow rate as the optimum collector dosage from the first group and optimum pH value from the second group were considered. The fourth aimed to study the effect of optimum flotation time. In this fourth group, the optimum values obtained for collector dosage, pH and air flow rate were considered to determine the optimum flotation time. Except the fourth group of tests, the flotation was continued until barren bubbles were observed.

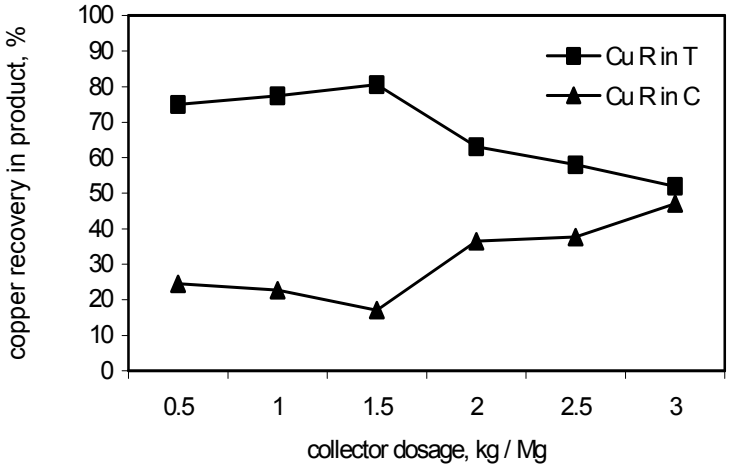

Fig. 1. Effect of collector dosage on copper recovery in flotation concentrate and tailing

Figure 1 shows the effect of collector dosage on copper recovery in flotation concentrate and tailing. Figure 2 reflects the same information with regard to product grade, i.e. copper content % in concentrate and tailing products. It is clear that the recovery of copper in the float product (concentrate) is low at low collector dosage (< 1.5 kg/Mg) and increases as the collector dosage increase (> 1.5 kg/Mg). The concentrate grade decreases to about 1.5 kg/Mg collector dosage and then begins to increase at higher dosages. The recovery of copper as well as the product grade are higher in the sink product than float product. This means that the floatability of copper minerals is poor with oleic acid collector. The increase in copper recovery in float product at high collector dosages may be related to mechanical carryover mechanism

or overdosage of collector which must be added in starving amounts in these flotation systems.

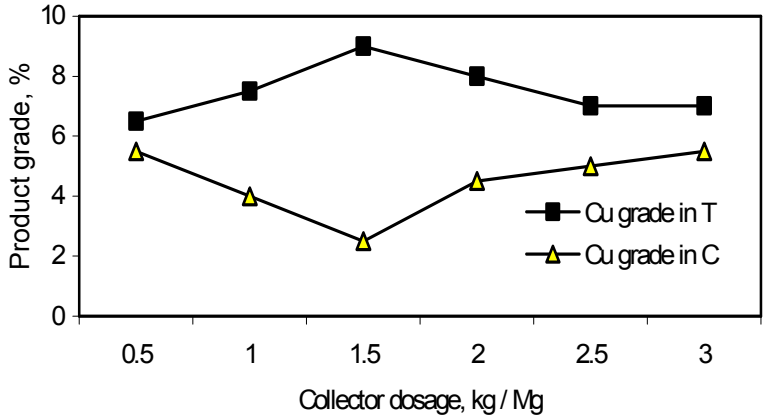

Fig. 2. Effect of collector dosage on copper grade in flotation concentrate and tailing.

It is expected that the accompanied minerals in feed, i.e, other oxides such as Fe_2O_3 or SiO_2 have been floated leaving copper oxide minerals in the tailing product. It is clear that the best collector dosage is about 1.5 kg/Mg, which gave the highest copper recovery (≈80%) in the sink product and at the same time a high copper grade. Hence, one may conclude that the recovery of copper minerals from such an ore is possible with reverse flotation.

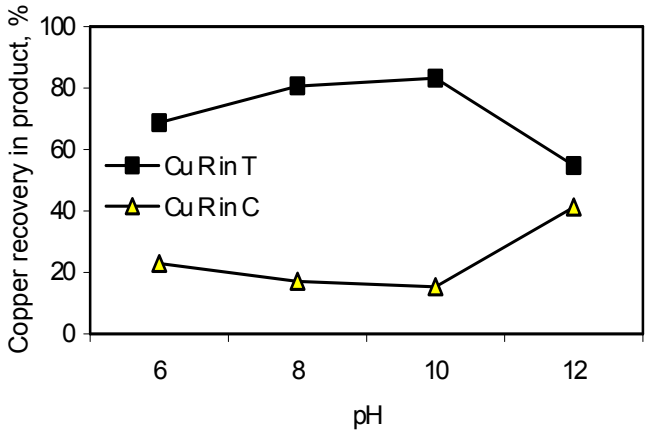

Fig. 3. Effect of pH on copper recovery in flotation concentrate and tailing

Figures 3 and 4 illustrate the effect of pH on the reverse flotation concentrating copper minerals in the sink product. The recovery of copper increases with increasing

pH from 6 to 10, then it decreases above pH 10. The recovery of copper is about 84% at pH 10 which represents the highest value. The highest product grade, ~ 10% is obtained at the same pH. This means that the optimum pH to float other accompanying oxides from copper minerals is about pH 10. Such a pH is similar to the pH applied in floating iron oxides and silica.

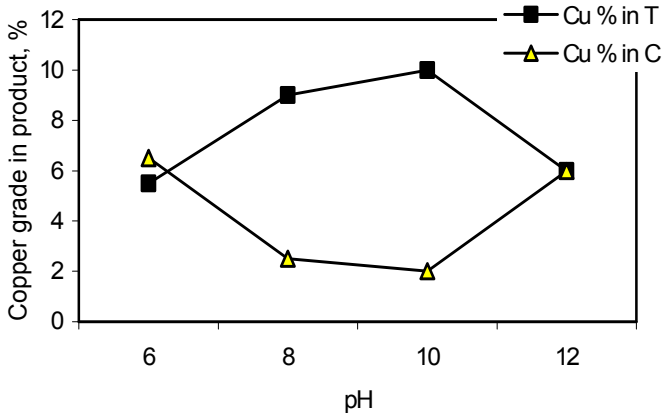

Fig. 4. Effect of pH on copper grade in flotation concentrate and tailing

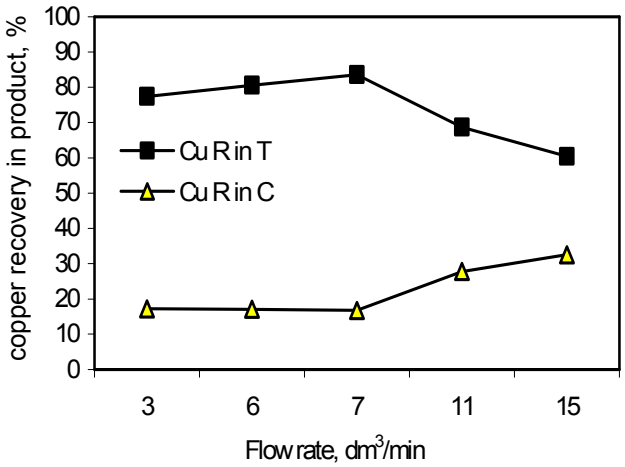

Fig. 5. Effect of air flow rate on copper recovery in flotation concentrate and tailing

Figures 5 and 6 show the effect of air flow rate with regard to copper recovery and copper grade in float and sink products. Below 7 dm^3/min, the copper recovery increases slightly in the sink product and still, more or less, constant in the float product. Above 7 dm^3/min flow rate, the copper recovery decreases in the sink product and increases in the float product. Similar trends are obtained for copper grade in froth

and sink products. It is obvious that the best flow rate is about 7 dm^3/min as the highest copper recovery and copper grade are attained in sink product at this value.

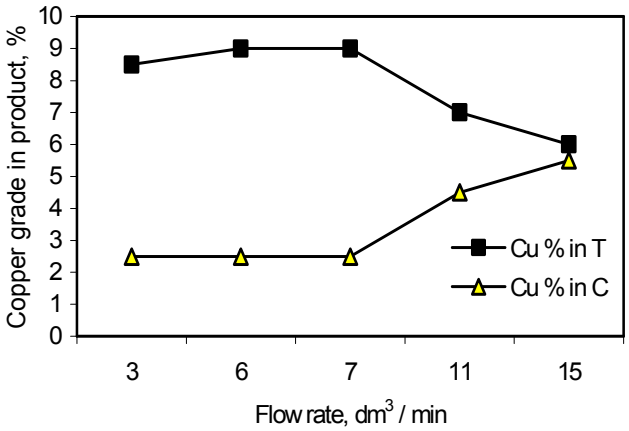

Fig. 6. Effect of air flow rate on copper grade in flotation concentrate and tailing

This result is in agreement with the results mentioned in flotation literature which state that the flotation recovery of floating particles increases with flow rate increase until a definite limit (optimum flow rate), and then begins to decrease. An increase of the copper recovery and copper content in the float product (concentrate) which is accompanied with a decrease in the copper recovery and grade in the sink product at high flow rates (> 7dm^3/min) may be due to a mechanical carryover mechanism and not due to a real flotation mechanism. It is well known in the flotation literature, that the mechanical carryover mechanism does not distinguish between hydrophobic and hydrophilic particles.

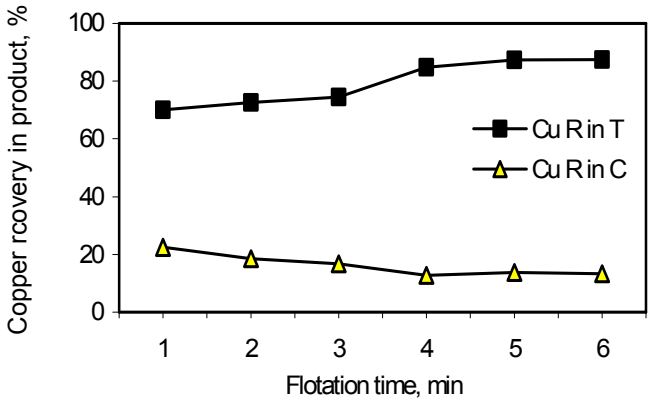

Fig. 7. Effect of flotation time on copper recovery in concentrate and tailing

Figure 7 represents the effect of flotation time on the recovery of copper in concentrate (float product) and in tailing. This test aimed to illustrate the optimum flotation time. The recovery of copper increases in the sink product and decreases in the float product until 5 min flotation time. It is clear from this figure that the optimum flotation time is about 5 min as after such time the recovery of copper in sink product becomes constant.

The reverse flotation of copper minerals at the optimum flotation conditions obtained previously, i. e, at 1.5 kg/Mg collector dosage, pH =10, 7 dm^3/min air flow rate and 5 min flotation time is considered. This experiment was carried out at 800 g in 4 dm^3 flotation cell capacity, i. e, at 20% by wt solid/liquid ratio. The obtained results indicated that about 90% of copper is recovered in the sink product at about 11% Cu content. The froth product (float) from this test was found to have about 1.5 % Cu content. An attempt was carried out also to recover such a small amount of copper from the concentrate product (float).

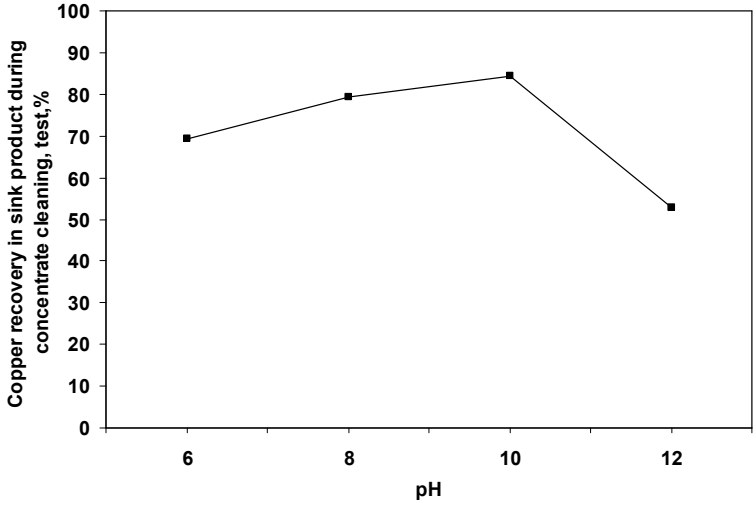

Fig. 8. Effect of pH on Cu recovery in sink product during concentrate reverse flotation cleaning test

Figure 8 shows the effect of pH on such cleaning test, i.e, recovering copper mineral particles present in the froth product (concentrate) during reverse flotation. The reverse flotation technique and the optimum flotation conditions obtained above were applied except that of collector dosage and pulp density. The pulp density in this test was 10% by wt solid/liquid ratio and the applied collector dosage was 0.5 kg/Mg. It was found that the recovery of copper increases as pH increases until pH 10, and then begins to decrease.

At pH 10, about 90% of copper in the concentrate (float) of the first flotation stage is recovered in the sink product of the second flotation stage. This test is beneficial in illustrating the possibility of waste treatment of copper processing plants and recover-

ing such an important element. Also, it may be useful for environment protection by removing such a heavy metal from discarded plant wastes.

CONCLUSION

In this study, the recovery of copper from Abu–Swayel (Eastern Desert, Egypt) ore deposit by reverse flotation was attempted. The copper minerals contained in this copper deposit are mainly copper oxide minerals. The important factors that affect such flotation system were studied to determine the optimum conditions. The results showed that the flotation response of copper minerals is poor and it is difficult to recover such copper minerals in froth or float product (concentrate) by direct flotation technique. The reverse flotation technique was applied to float the minerals accompanying minerals such as hematite, silica and others (as a float) and obtaining copper minerals in the sink product. Oleic acid was used as the collector and pine oil was applied as the frother. Encouraging results were obtained since about 90% of copper content at 10% copper grade have been recovered in sink product. The optimum flotation conditions for such a reverse flotation system were obtained and recorded at 1.5 kg/Mg oleic acid collector dosage, pH =10, 7 dm^3/min air flow rate, and 5 min flotation time. Also, it was found that the copper mineral particles which have been lost in the float product (concentrate) due to mechanical carryover mechanism may be recovered by concentrate cleaning under the same flotation conditions.

The results of this work are promising because it may help exploitation of such copper deposit and hence obtaining a high value industrial element. It may be useful also for environment protection since enables removal of heavy metal from discarded wastes.

REFERENCES

ABBAS, M. H., “Extraction of copper from the Egyptian copper ore of Abu – Swayel”, Ph.D. Thesis, Mining & Pet. Dept., Faculty of Engineering, Alazhar University, Cairo, 1983.

ACAR, S. SOMASUNDARAN, P. "Effect of dissolved mineral species on the electrokinetic behaviour of sulfides", Minerals Engineering, Vol.5, No 1, 1992, 27-40.

ACKERMAN, P. K. , HARRIS, G. H., KLIMPEL, R. R. APLAN , F.F., "Evaluation of flotation collectors for copper sulfides and pyrite" , Inter. J. of Mineral Processing, 21 (1987), 105 – 127.

APLAN, F. F. FUERSTENAU, D. W.," The flotation of chrysocolla by mercaptan reagents", Inter. J. of Mineral Processing, Vol. 13, issue 2, August 1984, 105 – 115.

FATHY, W.M., “Application of heap leaching technique in hydrometallurgical treatment of Abu – Swayel copper oxide ore”, Msc. Thesis, Mining & Pet Dept., Faculty of Engineering, Alazhar University, Cairo, 2005.

HANSON, J.S. FUERSTENAU, D. W., "The electrochemical and flotation behavior of chalcocite and

mixed oxide / sulfide ores" , Inter. J. of Mineral Processing, Vol. 33, issue 1-4, Novemmber 1991, 33 – 47.

HEYES , G.W. TRAHAR , W.J., " Natural floatability of chalcopyrite" , Inter. J. of Mineral Processing, 4 (1977), PP. 317 – 344.

HOSTEN, C., TEZCAN, A. "The influence of frother type on flotation kinetics of a massive copper sulfide ore", Minerals Engineering, Vol.3, No 6, 1990, PP. 637-640.

HUSSEIN, A. A., " Mineral deposits of Egypt", In: Geology of Egypt, Said, R. (ed), Balkema Pub. Com., Amsterdam, 1990, 511.

LEPPINEN, J.O., HINTIKKA, V.V., KALAPUDAS, R.P., "Effect of electrochemical control on selective flotation of copper and zinc from complex ores ", Minerals Engineering, Vol. 11, Issue 1, January 1998, 39 –51.

SENIOR, G. D., GUY, P.J., BRUCKARD, W.J., "The selective flotation of energite from other copper minerals – Asingle mineral study in relation to beneficiation of Tampakan deposit in the Philippines", Inter. J. of Mineral Processing, Vol. 81, issue 1, October 2006, 15 – 26.

URIBE-SALAS, A., MARTINEZ, CAVAZOS, T.E., NAVA – ALONSO, F.C., MENDEZ- NONELL, J., LARA – VALENZUELA, C. "Metallurgical improvement of lead / copper flotation by pulp potential control" , Inter. J. of Mineral Processing, Vol. 59, issue 1, Apr. 2000, 69 – 83.

YIANATOS, J.B., BERGH, L.G., AGUILERA , J., " Flotation scale up : use of separability curves", Minerals Engineering, Vol.16, issue 4, April 2003, 347 – 352.

Saleh A.-H. M., Ramadan A. M., Moharam M. R., Wykorzystanie Egipskiej rudy miedziowej z Abu-Swayel metodą flotacji, Physicochemical Problems of Mineral Processing, 42 (2008), 119-130 (w jęz. ang)

W pracy podjęto próbę odzysku miedzi z egipskiego złoża Abu-Swayel. Zastosowano flotację odwrotną polegającą na flotacji towarzyszących tlenków i siarczków, gromadząc minerały tlenkowe miedzi w produkcie tonącym. Stwierdzono, że technika ta jest użyteczna, ale w warunkach optymalnych. Badania głównych czynników wpływających na stosowany układ flotacyjny wskazują, że optymalne warunki flotacji to 1.5 kg/Mg kwasu oleinowego jako kolektora, pH=10, przepływ powietrza 7 dm^3/min a czas flotacji to 5 minut. W tych warunkach otrzymano 10% koncentraty miedziowe przy uzysku około 90%. Stwierdzono także, iż ziarna minerałów miedzi stracone w produkcie pianowym są wynoszone mechanicznie i mogą być odzyskiwane przez czyszczenie koncentratu w tych samych warunkach flotacji. Można zatem powiedzieć, że wyniki tych badań są pozytywne i mogą pomóc przy ponownej ocenie możliwości eksploatacji złóż miedziowych tego typu.

słowa kluczowe: flotacja, wzbogacanie, ruda miedzi, minerały miedzi, tlenki miedzi

Physicochemical Problems of Mineral Processing, 42 (2008), 131-140
Fizykochemiczne Problemy Mineralurgii, 42 (2008), 131-140

Teresa Szymura*

DEPOSITS IN WATER - BASED COOLING SYSTEMS

Received April 11, 2008; reviewed; accepted July 31, 2008

The paper discusses phenomena that cause scale and sludge formation in water-based cooling systems. Results of experimental research into cooling water treatment in an industrial cooling installation with the application of ammonium salts of strong acids have been presented. It has been found that a stoichiometric dose causes carbonate hardness removal. Adequately higher doses bring about crumbling and insignificant dissolving of the scale. Simultaneous application of an inhibitor of corrosion and incrustation prevents corrosion losses and advantageously influences water treatment.

key words: cooling water, water treatment, scale, cooling system, inhibitors

INTRODUCTION

Cooling water systems operate practically in all sectors of the industry. In the year 2001 total consumption of water in Poland amounted to 7.308 km^3, out of which 55% has been used in the power engineering industry and most (about. 95%) of the water consumed by that sector has been applied for cooling purposes (Statistical Yearbook of 2003; Spoz, 2000). Situation illustrated by those data is typical for majority of industrialized countries (Veil, 1999).

In Poland, cooling systems apply raw water that, due to the lack of treatment or inhibitor additives, exhibits aggressively corrosive and deposit-forming properties. It results from a considerable flow-capacity of those systems, which causes excessive consumption of the water and creates an economic barrier for its rational treatment. This unfavorable situation can be improved by replacing once-through systems by recirculating ones. At the same time it is possible to apply multi-functional inhibitor preparations that could protect the systems against such phenomena as corrosion, de-

* Institute of Building Engineering, Department of General Construction Engineering, Lublin University of Technology, t.szymura@pollub.pl

posit formation and development of microorganisms, even at a high condensation degree of the recycled water.

It is important to reduce water consumption in Poland because fresh water resources are extremely poor there. In Europe an average fresh water amount per capita is 4560 m^3, while in Poland it is by three times less.

At late 90-ties of the 20^{th} century fresh water consumption in Poland has been reduced by 25% owing to shutdowns of cooling systems. The mentioned water consumption reduction has unquestionably contributed to the improvement of water quality in Polish rivers (Spoz,2000).

COOLING SYSTEMS

Although in the pertinent literature many kinds of cooling systems are described all of them can be classified into three principal types: once-through systems, open recirculating and closed recirculating ones (Ahmed, 2000).

CORROSIVE AND DEPOSIT-FORMING PROPERTIES OF WATER

Properties of water that is commonly used in industrial cooling installations cause corrosion and incrustation, which brings about many technical problems and considerably raises operation costs of those installations.

Depending on the water quality and construction materials the following weakly or firmly adherent deposits can form on heat exchange surfaces,

- corrosion products forming as a result of the reaction of water or its components with metal
- incrustation products that form so-called *scale* composed mostly of sparingly soluble calcium compounds
- suspended solids in the form of *sludge* resulting from the sedimentation of mineral and biological particles that are present in cooling water.

The deposits impair operation of cooling water installations by bringing about such disadvantageous phenomena as:

- frequent and difficult repairs
- costly overhauls and related system outages
- induced use of oversized apparatus
- increased water consumption
- energy losses following from additional resistance to the water flow due to the formed deposit layers.

CORROSION OF WATER COOLERS

Corrosion processes occurring in metals that heat exchangers are made of depend on a composition of the construction material as well as on the cooling water composition. Standard cooling water installations usually are made of carbon steel, zinc-coated steel, copper and brass. Oxygen in the cooling water makes the most frequent corrosive agent. Metal elements corrode in oxygenated neutral water when the metal oxidation potential is more negative than the equilibrium potential of cathode depolarization:

$$O_2 + 2H_2O + 4e = 4OH^-$$

Corrosion rate grows along with the increase of:

- temperature (value of the oxygen diffusion coefficient grows)
- oxygen concentration in water
- water flow rate (decrease of the diffusion layer also called boundary layer).

In specific conditions carbon steel exchangers can undergo passivation, although an increase of oxygen concentration in water at higher temperatures and in the presence of chlorides can lead to the occurrence of strong pitting corrosion (Kubicki, 1994).

Carbon dioxide makes another corrosion-accelerating agent in cooling systems.

The effect of various salts dissolved in water on corrosion depends on the kind of salts. Chlorides and sulfates considerably intensify corrosion processes, while phosphates, silicates, and carbonates cause passivation of carbon steel.

Significant share in the total of corrosion damages has the activity of various kinds of microorganisms that destroy the apparatus, armature, constructions, and protective coats on their surfaces.

INCRUSTATION PROCESSES

In the case when cooling water does not meet the chemical requirements it can cause precipitation of the following kinds of deposits:

- mineral crystalline
- mineral amorphous.

The main reason for the mentioned precipitation is high carbonate hardness and excessive salinity of cooling water. Salts that are dissolved in the water get condensed as water evaporation proceeds and usually precipitate when the solubility product gets exceeded. The process runs in heat exchangers (and in cooling installations) that make an advantageous environment for the beginning of solid phase crystallization.

Scale deposits that form in cooling water systems are polycrystalline porous substances with amorphous inclusions. Their physical - chemical and mechanical properties are variable depending on many factors such as:

- the kind and concentration of substances contained in the recycled water - both pollutants and substances purposefully added to enhance properties of the water
- local heat load
- the kind of crystallization base
- hydrodynamic conditions
- contact with polluted atmospheric air
- corrosive power of water against construction materials
- development of biological life in water.

Depending on the prevailing content of carbonate, sulfate or silicate compounds-three main types of scale can be distinguished (Stańda, 1999):

- carbonate scale that contains mainly calcium and magnesium carbonates as well as magnesium hydroxide
- sulfate scale (gypsum), that contains more than 50% of calcium sulfate
- silicate scale whose basic components are calcium and magnesium silicates and aluminosilicates.

Considerable content of calcium bicarbonate in raw water that is used for cooling purposes, its low solubility and favorable conditions in recirculating cooling systems are the reason why carbonate scale occurs the most frequently and its basic component is calcium carbonate which can form as a result of:

- temperature increase in the system
- pH changes
- concentration increase following from the solution condensation.

COOLING SYSTEM PROTECTION AGAINST DEPOSIT PRECIPITATION

Methods for preventing scale formation can be developed in the two following directions:

- introduction of supplementary water with most of the scale-generating pollutants removed
- treatment of the recycled water by adding inhibitors.

INHIBITOR PROTECTION

An analysis of the pertinent literature reports of the recent 10 years and opinions based on practical experience leads to the conclusion that inhibitor protection, sometimes also coupled with biocide, makes the most effective and economical method for preventing scale formation and corrosion in industrial cooling water systems of the recirculating type.

The key to elaborate a good program for the cooling water treatment in recirculating systems is its chemical composition when it gets condensed.

The best regulator for the economics and reliability of the applied chemical treatment method is the recycled water reaction.

According to Ascolese Ch.It R., (1998) water treatment programs can be classified into two groups:

- a neutral program in the operation conditions of $6.8 < pH < 7.8$
- an alkaline program when $7.8 < pH < 9.0$.

Till recent times many inorganic metallic compounds such as chromates, molybdates and zinc compounds as well as some non–metallic ones like phosphates (polyphosphates and orthophosphates), silicates, nitrites and also azoles that effectively protect copper alloys have been applied as corrosion inhibitors.

Disadvantages of inorganic inhibitors such as: toxicity (chromates), low stability (silicates and polyphosphates) or selective protective action (nitrites) as well as increasingly rigid ecological standards, have turned the interest of researchers to the application of organic compounds as potential inhibitors of multifunctional properties (Amjad, 1997).

Within the 10 recent years, many water treatment technologies based on phosphonate acid compounds have been elaborated. They exhibit relatively high efficiency both in inhibiting corrosion of ferrous metals as well as in water treatment and preventing scale formation.

REMOVAL OF DEPOSITS AND PREVENTING THEIR FORMATION IN INDUSTRIAL COOLING INSTALLATION

The testing has been performed in a recirculating cooling installation *Lacpol* in Gdynia. The installation has been composed of four shell-and-tube ammonia condensers of the SRS type and fan coolers. All condenser and cooler elements that contact water have been made of ST3 steel. Surfaces of heat exchangers have been covered with scale layer of 3mm of average thickness.

REFERENCE CONDITIONS

Chemical analysis of the scale has shown that it has contained 95% of $CaCO_3$, about 3% of iron compounds, and 2% of HCl-insoluble components (including organic ones). Table 1 presents properties of the cooling water It follows from the analyses of the feeding and recycled waters that condensation coefficients have the values given in the last column of Table 1. The condensation coefficient of chlorides (the best soluble salts) that almost 2-fold exceeds the condensation value of general and carbonate hardness proves the occurrence of precipitation of calcium and magne-

sium carbonates. As *t/n* is 0.75, it can be calculated that 25% of hardness introduced to the system precipitated in the form of scale.

Table 1. Properties of the cooling water

No	Indicators	Makeup water	Recycled water	Condensation coefficient
1	pH	7	8.5	
2	general hardness, mval/dm^3	6.6	7.92	1.2 (t)
3	carbonate hardness, mval/dm^3	4.8	5.4	1.2
4	Cl- content, mg/dm^3	36.2	58.2	1.5 (n)
5	SO42- content, mg/dm^3	80.0	124.8	1.56

The average water consumption prior to the treatment application:

- in the summer season - 202 m^3/day
- in the winter season - 110 m^3/day.

In a one-year time, a scale deposit of 3 mm thickness has accumulated and has been mechanically removed every year.

DESCRIPTION OF THE COOLING WATER TREATMENT PROCESS AND DESCALING

A water treatment method elaborated according to the Polish patent No. 102516 (Zagórski et al., 1978) has been applied. Ammonium salt of a strong acid (ammonium chloride and sulfate) has been used as the pH regulator. Sodium polyphosphate (the trade name - *Polifos*) with the addition of zinc sulfate has been applied as the corrosion and incrustation inhibitor while sodium lignosulfonate (known in the market under name of *Klutan*) has acted as a dispersion agent (Szymura et al., 2005).

Because of a great amount of scale in the installation a preliminary dose of ammonium salts of 1.7 of the stoichiometric dose with respect to carbonate hardness has been applied. The proportions of ammonium sulfate and chloride have been calculated in such a way for not to exceed the gypsum solubility product. Analyses of the feeding and recycled waters have been performed twice a week.

An additional system has been elaborated and applied to supply chemicals to the feeding water pipe and direct them together directly to the condenser. The system has been automated. When the salinity meter indication for the recycled water has exceeded by three times the value for the feeding water with chemicals a valve for supplementary water has been opened. It has made it possible to maintain an assumed level of the recycled water condensation. Figure 1 presents a schematic diagram of the cooling installation together with the metering system.

Graph in Fig. 2 presents a course of the cooling water treatment process realized in the discussed installation. Values of the *t/n* ratio illustrate the decarbonization reac-

tion process (t/n =1). The t/n values of that are higher than unity indicate scale dissolution.

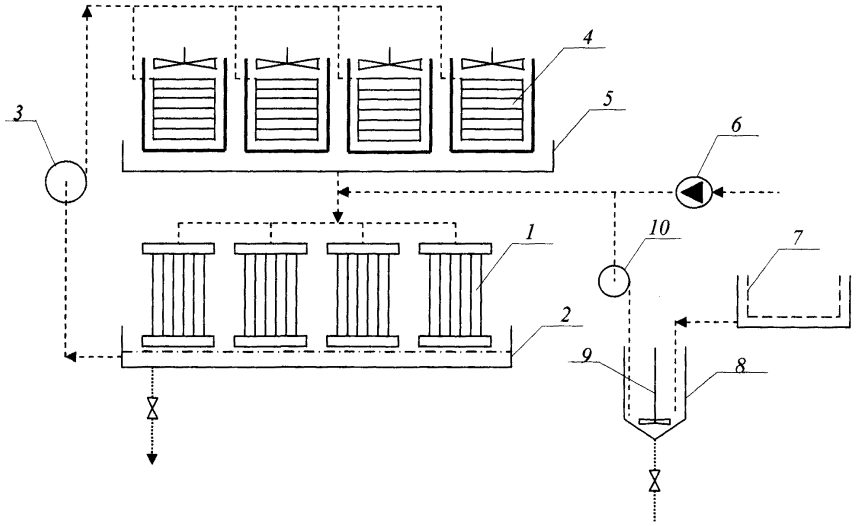

Fig. 1. Diagram of the cooling installation *Lacpol* in Gdynia. 1 -shell-and-tube condenser, 2 - tank under condensers, 3 - recycled water pump, 4 - fan coolers, 5 - trays under coolers, 6 - water meter, 7 - tank with a screen for dissolving chemicals, 8 -mixer, 9 - stirrer, 10 - volumetric pump

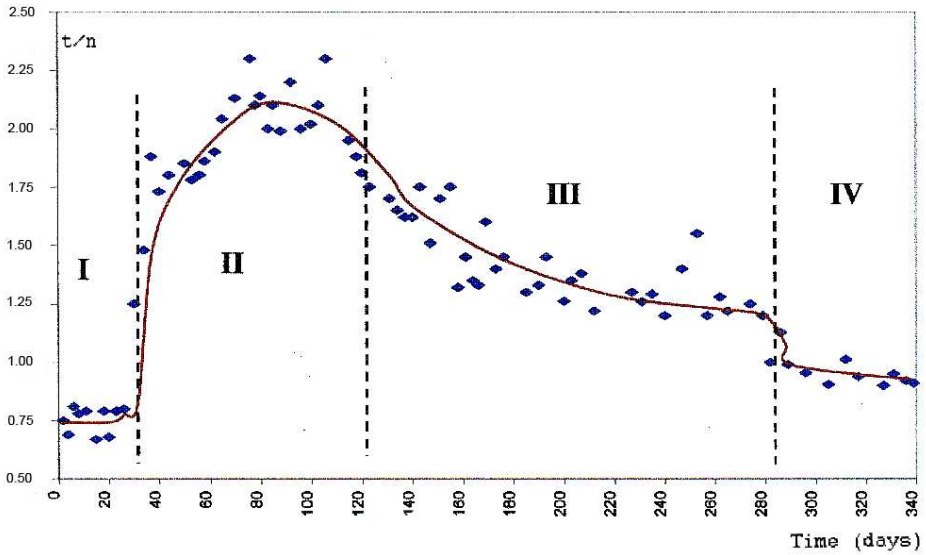

Fig. 2. Variations of the t/n ratio during the application of ammonium sulfate in the Cold Store *Lacpol* installation in Gdynia

DISCUSSION

In Fig.2, a one-month period when the preparation has not been applied is denoted as I. The ratio $t/n \approx 0.75$ indicates scale deposition in the installation.

During the second two-month period (II) the preparation dose of 1.7 of the stoichiometric value has been applied. The *t/n* has increased even up to 2, but low pH (close to 6.2) has made authors reduce the preparation dose. Scale has kept softening and dropping off metal surfaces in great quantities.

Over the third period (III) a dose equal to 1.5 of the stoichiometric value has been applied and the recycled water pH has increased up to 6.5 ÷ 6.8. The mentioned procedures have been applied for four months and then it has been decided to stop the installation for a short time to remove sludge and pieces of dropped-off scale from trays under coolers and condensers.

After 330 days of the preparation application, in the fourth period (IV) it has been decided to reduce the preparation dose down to 1.2 of the stoichiometric value because the scale has practically been removed from the installation. The *t/n* ratio has been close to 1, and the carbonate hardness (alkalinity *m*) has been of fractional value, which confirmed decarbonization of the water.

The water treatment process in the discussed installation has been controlled for the next 10 years. By that time the recycled water pH has been maintained within the range of 6.5 ÷ 7.5. When the pH has been getting lower than 6.5 the dose of ammonium salts has been reduced by 10%, and when it has reached values higher than 7.5 - the dose has been increased by 10%. The installation has operated according to the expectations - scale deposit has not grown.

At the same time, a research into the corrosive effect of water on ST3 steel has been carried out as well as microbiological tests. Results of those investigations will be the subject of separate reports.

REFERENCES

AHMED S., BAYERS J., 2000. *Design basics for cooling systems*: Chemical Engineering, 1, 78-83.

AMJAD Z., PUGH J., ZIBRIDA J., 1997. *Polymer performance in cooling water:* The Influence of Process Variables, Chemical Treatmant Materials Performances, 1, 32-38.

ASCOLESE CH.R., BAIN D.J., 1998. *Take advantage of effective cooling-water –treatment programs*: Chemical Engineering Progress, 3, 49-54.

KUBICKI J., 1994. *Wybrane problemy korozyjne w instalacji wody chłodzącej*, Prace Nauk. I-26, 41, Wyd. Politechnika Wr., Wrocław, 46-57.

Rocznik Statystyczny R.P., 2003.

SPOZ J., 2000. *Potrzeby wodne elektrowni cieplnych w latach 1955-1995*, Gospodarka Wodna, 4, 136—138.

STAŃDA J., 1999. *Woda do kotłów parowych i obiegów chłodzących siłowni cieplnych*, WNT, Warszawa.

SZYMURA T., POMORSKA K., 2005. *Zastosowanie soli amonowych w układach wody chłodniczej*, Chłodnictwo, 1-2, 22-27.

VEIL J.A., PUDER M.G., LITTLETON D.J., HOSES D.O.: Cooling Water use Patterns at US Nonutility Electric Generation Facilitis, Environmental Science & Policy, 2, 1999

ZAGÓRSKI K., WARSZAWA Z., SZYMURA T., 1978. *Sposób usuwania węglanowego kamienia kotłowego i zapobieganie jego powstawaniu w wodno-chłodniczych instalacjach przemysłowych,* Patent Polski nr 102517.

Szymura T., *Osady w układach z wodą chłodzącą*, Physicochemical Problems of Mineral Processing, 42 (2008), 131-140 (w jęz. ang)

W pracy przedyskutowano zjawiska, które powodują tworzenie się kamienia kotłowego oraz osadów w układach z użyciem wody chłodzącej. Zaprezentowano wyniki badań dotyczących modyfikowania wody chłodzącej w instalacjach przemysłowych z zastosowaniem soli amonowych silnych kwasów. Stwierdzono, że stechiometryczna dawka powoduje usuwanie twardości węglanowej. Odpowiednio wyższa dawka powoduje rozpad kamienia i niewystarczające się jego rozpuszczanie. Jednoczesne zastosowanie inhibitora korozji i inkrustacji zapobiega stratom korozji i dodatnio wpływa na przeróbkę wody.

słowa kluczowe: kamień kotłowy, chłodzenie, przeróbka wód, korozja, twardość wody, sole amonowe, inhibitory korozji

Physicochemical Problems of Mineral Processing, 42 (2008), 141-152
Fizykochemiczne Problemy Mineralurgii, 42 (2008), 141-152

Katarzyna Siwińska-Stefańska*, Andrzej Krysztafkiewicz*, Teofil Jesionowski*

EFFECT OF INORGANIC OXIDES TREATMENT ON THE TITANIUM DIOXIDE SURFACE PROPERTIES

Received May 15, 2008; reviewed; accepted July 31, 2008

Studies were conducted involving evaluation of titanium white, surface-coated with inorganic oxides. The studies aimed at determining dispersion properties, i.a. particle size distribution and polydispersity index. Moreover, microscopic observation allowed to evaluate surface morphology of the modified TiO_2 particles. Colourimetric data of titanium white was measured and the specific surface area was estimated using BET method. Effect of the surface modification with oxides on electrokinetic properties and zeta potential were appraised. Increased amounts of aluminium oxide and silicon dioxide used for modification of titanium dioxide surface deteriorate uniform character of the sample and results in an increase in diameter of pigment particles. The titanium white pigments belong to mesoporous adsorbents. Value of the isoelectric point (IEP) depends on the amounts of aluminium oxide and silica used for surface processing of titanium white.

key words: titanium dioxide, surface modification, PSD, surface morpholgy, zeta potential, adsorption/desorption isotherm

INTRODUCTION

Titanium dioxide particles crystallize mosty in two polymorphic forms: rutile and anatase. Anatase, as a metastable phase, is chemically and optically active, thus is suitable for catalysts and supports (Ding 1997) while rutile, the thermodynamically stable polymorph, has the highest refractive index and ultrafiolet absorptive and is widely used as white pigments (Zhao 1998). It has been extensively demonstrated that the physicochemical properties of TiO_2 are strongly dependent on its crystal structure and morphology as well as grain size (Cozzali 2003).

* Poznan University of Technology, Institute of Chemical Technology and Engineering Pl. M. Sklodowskiej-Curie 2, 60-965 Poznan, Poland, teofil.jesionowski@put.poznan.pl

Many methods such as sol-gel process (Zhang 2003), hydrothermal methods (We 2002), solvothermal methods (Kim 2003) and emulsion precipitation (Ramakrishna 2003) have been developed for the synthesis of titanium dioxide nanoparticles.

The properties of TiO_2, including a hight refractive index (Schmidt 2005), light absorption/scattering (Brand 2003) and photocatalytic activity (Legrini 1993, Paz 1997, Linsebigler 1995, Chen 2004, Hashimoto 2005, Hoffmann 1995, Blade 1999, Hirakawa 2004) have led to the exploitation of titanium dioxide in a variety of fields.

The studies aimed at determining effect of titanium white surface modification, using inorganic oxides, on its dispersion and physicochemical properties.

EXPERIMENTAL

MATERIALS

In the studies pigments of rutile titanium dioxide, TYTANPOL R-210, R-211 and R-213 were used, produced by Chemical Works „Police" S.A. using the sulphate technique. The pigments are surface processed with aluminium and silica compounds and modified using organic compounds of a hydrophilic-hydrophobic character (R-210 and R-211) and a hydrophilic character (R-213).

METHODS OF STUDIES

Size of titanium white particles and the respective particle size distribution were determined using Zetasizer Nano ZS (Malvern Instruments Ltd.) using the non-invasive back light scattering method (NIBS). Particle size distribution permitted to establish polydispersity index (as a measure of uniform character of the pigment). The cumulants analysis give a width parametr known as the polydispersity, or the Polydispersity Index (PDI). The cumulants analysis is actually the fit of a polynomial to the log of the G1 correlation function: $Ln[G1] = a + bt + ct^2 + dt^3 + et^4 + ...$ The value of b is known as the second order cumulant, or the z-average diffusion coefficient. The coefficient of the squared term, c, when scaled as $2c/b^2$ is known as the polydispersity.

A Zetasizer Nano analyzer allowed also to estimate zeta potential on the basis of electrophoretic mobility, using laser Doppler velocimetry (LDV).

The modified titanium whites were also subjected to morphological and microstructural analysis using scanning electron microscopy (Zeiss VO 40) and transmission electron microscopy (Jeol 1200 EX 2). In order to characterize adsorptive properties isotherms of nitrogen adsorption/desorption were determined and parameters such as specific surface area, pore volume and average pore size were determined using ASAP 2010 instrument (Micromeritics Instruments Co.).

Using SPECBOS 4000 colourimeter, colour of the titanium whites was measured. The results were given in L a b colour spaces. Examination in the CIE L a b colourimetric system yields data on colour of a pigment. L* denotes lightness, a* and b* coordinates denote a colour, +a* defining the share of red colour, –a* denoting the share of green colour, +b* representing the share of yellow colour and –b* denoting the share of blue colour. C* indicates colour intensity, h* - shade of the colour while dE is a colour difference representing the resultant of differences for individual components (dE*, da*, db*).

RESULTS AND DISCUSSION

The titanium whites represent pigments of rutile variety, surface processed with aluminium and silica compounds. They differ from each other in the amount of inorganic oxide used for surface modification of TiO_2. Principal properties of the titanium dioxide pigments, are presented in Table 1.

Tabela 1. Principal parameters of commercial titanium dioxide samples TYTANPOL

Sample	Inorganic suface treatment	Organic surface modification, character of organic compound	Content, %		Polydispersity	Content of titanium dioxide, %
			Al_2O_3	SiO_2		
R-210	Al_2O_3, SiO_2	+, hydrophilo-hydrophobic	3.0	1.0	0.174	94
R-211	Al_2O_3, SiO_2	+, hydrophilo-hydrophobic	4.7	2.0	0.170	92
R-213	Al_2O_3, SiO_2	+, hydrophilic	4.7	8.3	0.233	82

In the particle size distribution for R-210 titanium dioxide which took into account band intensity (Fig. 1a) the presence of two bands was noted. The first, more intense band was linked to the presence of particles and primary agglomerates and it fitted the range of 164 – 825 nm (with maximum intensity of 15.2% for particles of 342 nm in diameter). Polydispersity, which is a function of particle diameter scatter, showed the value of 0.174. The band within the range of 3580 – 5560 nm corresponded to secondary agglomerates (maximum intensity of 0.8% corresponded to agglomerates of 5560 nm in diameter). Also in the curve of particle size distribution, which took into account their volume (Fig. 1b) two bands of a similar intensity were present. The first band was linked to the presence of particles of lower diameter and of primary agglomerates. The band demonstrated the range of 142 – 955 nm (with maximum volume of 13.0% for particles with 295 nm in diameter). In the range of diameters the particles comprised almost 70% of the sample. The other band, in the range of 3090 – 6440 nm, reflected the presence of agglomerates with higher diameters (maximum

volume of 10.6% corresponded to agglomerates of 5560 nm in diameter), which comprised 30% of the sample. SEM image (Fig. 1c) confirmed the presence of spherical in shape primary agglomerates, which tended to form clumps. On the other hand, TEM image (Fig. 1d) demonstrated scanty coverage of titanium white surface with the inorganic oxides.

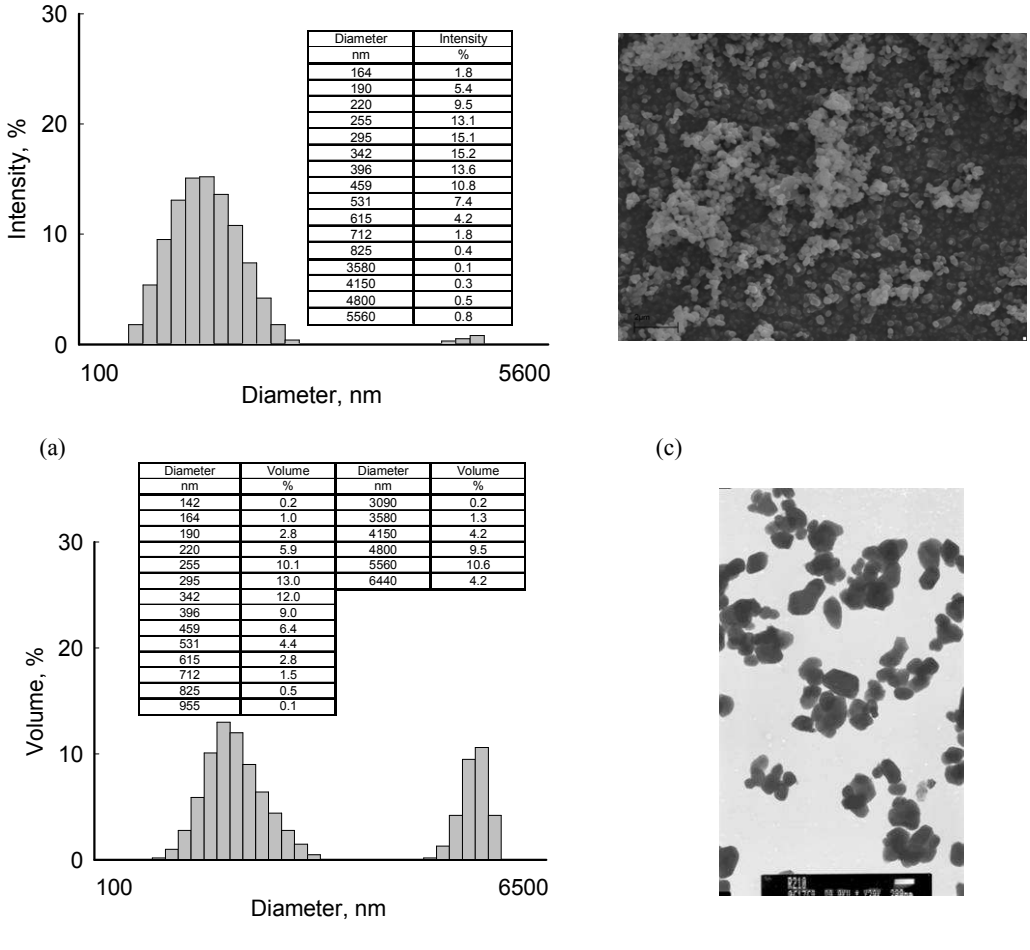

Diameter nm	Intensity %
164	1.8
190	5.4
220	9.5
255	13.1
295	15.1
342	15.2
396	13.6
459	10.8
531	7.4
615	4.2
712	1.8
825	0.4
3580	0.1
4150	0.3
4800	0.5
5560	0.8

Diameter nm	Volume %	Diameter nm	Volume %
142	0.2	3090	0.2
164	1.0	3580	1.3
190	2.8	4150	4.2
220	5.9	4800	9.5
255	10.1	5560	10.6
295	13.0	6440	4.2
342	12.0		
396	9.0		
459	6.4		
531	4.4		
615	2.8		
712	1.5		
825	0.5		
955	0.1		

Fig.1. PSD by (a) intensity, (b) volume and images (c) SEM, (d) TEM of TYTANPOL R-210

In the particle size distribution for R-211 titanium white, which took into account band intensity (Fig. 2a), two bands were noted. The more intense band within the range of 142 – 1280 nm, with maximum intensity of 14.4% for particles of 342 nm in diameter, was linked to the presence of particles and primary agglomerates. On the other hand, the second band reflected the presence of secondary agglomerates in the range of 3090 – 5560 nm in diameter (maximum intensity of 0.5% corresponded to

agglomerates of 4800 and 5560 nm in diameter). The polydispersity amounted to 0.17. The particle size distribution curve which took into account particle volume (Fig. 2b) demonstrated two bands of a similar intensity. The first band was linked to the presence of particles and agglomerates with lower diameters, in the range of 142 – 1280 nm, with maximum volume share of 11.7% for particles of 295 and 342 nm in diameter (particles of the range (142 – 1280 nm) comprised over 70% of the studied sample). On the other hand, the second band reflected the presence of secondary agglomerates in the range of 2300 – 6440 nm (the maximum volume share of 8.4% was comprised by particles of 4800 nm in diameter). The respective SEM image (Fig. 2c) demonstrated the presence of spherical particles with low diameter and few clumps. The TEM image (Fig. 2d) documented coating of titanium dioxide with aluminium and silica oxides, used for surface modification.

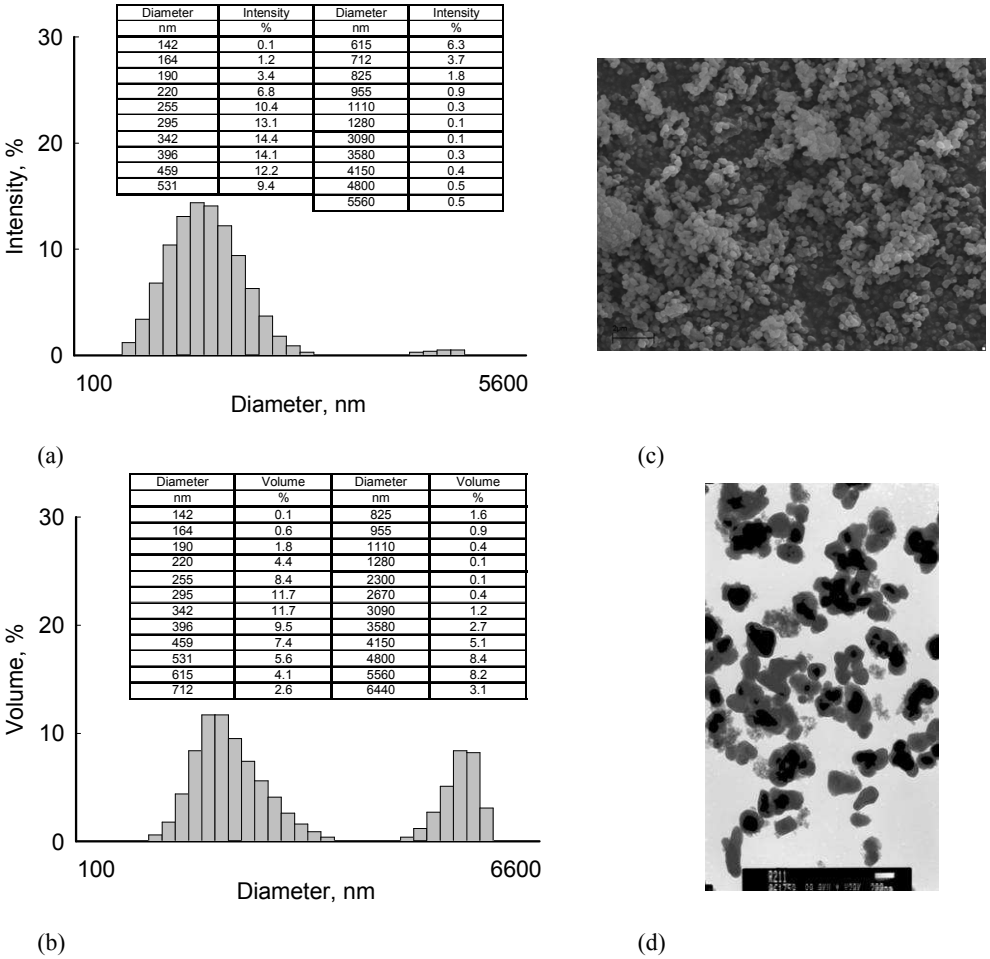

Fig.2. PSD by (a) intensity, (b) volume and images (c) SEM, (d) TEM of TYTANPOL R-211

For R-213 titanium white, the particle size distribution, which took into account intensity (Fig. 3a), a single band was present. The band was linked to the presence of clumps of low and high diameter and it fitted the range of 220 – 5560 nm (with maximum intensity of 11.2% for particles of 615 nm in diameter). On the other hand, on the particle size distribution curve taking volume into account (Fig. 3b) a single band was present. It was linked to the presence of primary and secondary agglomerates and fitted the range of 190 – 6440 nm (with maximum volume of 10.2% for agglomerates of 5560 nm in diameter). The polydispersity manifested value of 0.233. The SEM image (Fig. 3c) manifested the presence of particles spherical in shape which showed a much higher tendency to conglomerate. The TEM image (Fig. 3d) provided an excellent account on the surface processing of titanium white with inorganic oxides.

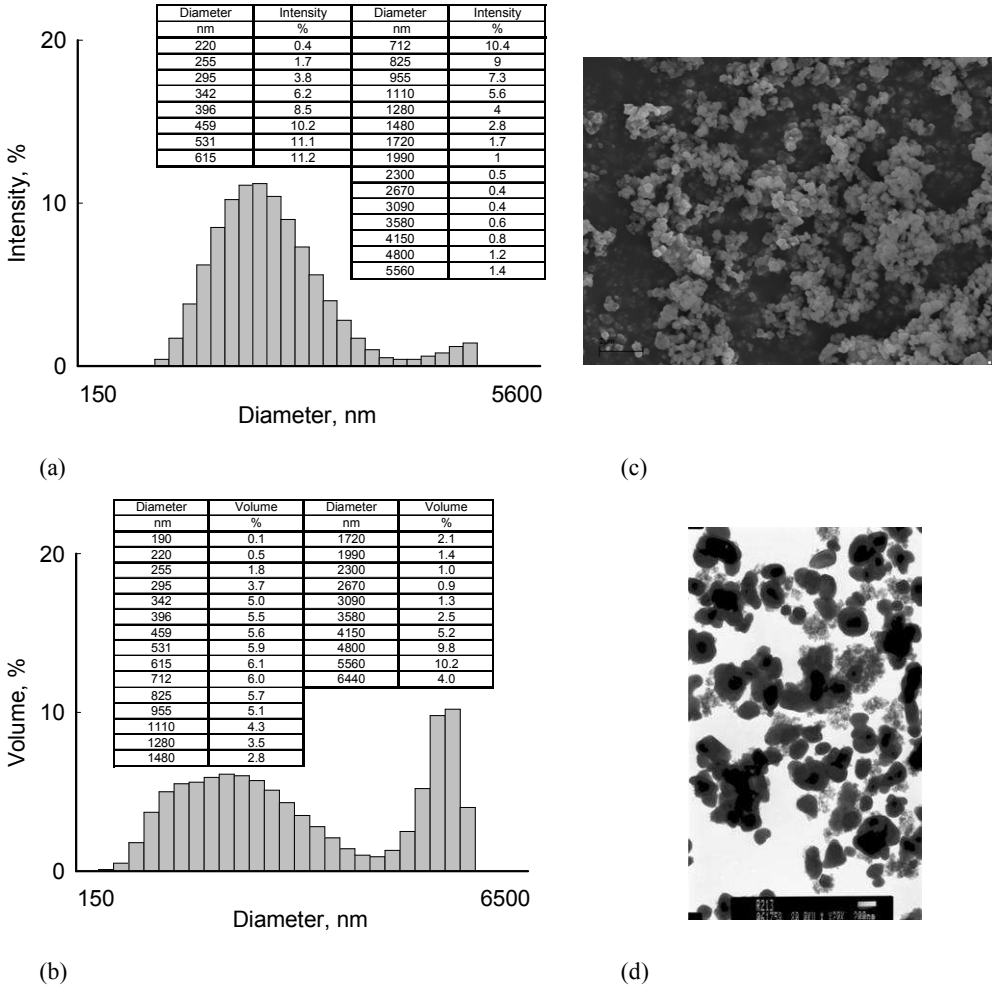

Diameter nm	Intensity %	Diameter nm	Intensity %
220	0.4	712	10.4
255	1.7	825	9
295	3.8	955	7.3
342	6.2	1110	5.6
396	8.5	1280	4
459	10.2	1480	2.8
531	11.1	1720	1.7
615	11.2	1990	1
		2300	0.5
		2670	0.4
		3090	0.4
		3580	0.6
		4150	0.8
		4800	1.2
		5560	1.4

Diameter nm	Volume %	Diameter nm	Volume %
190	0.1	1720	2.1
220	0.5	1990	1.4
255	1.8	2300	1.0
295	3.7	2670	0.9
342	5.0	3090	1.3
396	5.5	3580	2.5
459	5.6	4150	5.2
531	5.9	4800	9.8
615	6.1	5560	10.2
712	6.0	6440	4.0
825	5.7		
955	5.1		
1110	4.3		
1280	3.5		
1480	2.8		

Fig.3. PSD by (a) intensity, (b) volume and images (c) SEM, (d) TEM of TYTANPOL R-213

TYTANPOL R-213 manifested the highest BET surface area (Fig. 4), which amounted to 35 m^2/g, probably reflecting the fact that the pigment was surface coated with the highest amounts of aluminium and silicon oxides, i.e. with 4.7% of Al_2O_3 and 8.3% of SiO_2. For T-213 titanium white, the loop of hysteresis included relative pressures within the scope of $p/p_0 = 0.6 – 1.0$. Pore diameter amounted to 9.8 nm, and the total volume of pores was 0.09 cm^3/g. A lower BET specific surface area was demonstrated by R-211 titanium white, which amounted to 25 m^2/g. A decrease in diameter and volume of pores could also be noted, which amounted to 9.0 nm and 0.06 cm^3/g, respectively. The lowest value of BET specific surface area, of 19 m^2/g, was noted for TYTANPOL R-210. Moreover, the dioxide showed also decreased diameter and volume of pores (8.6 nm and 0.04 cm^3/g, respectively). Processing with inorganic aluminium oxide and silica significantly increased the specific surface area. This was probably associated with the fact that aluminium oxide and, first of all, silica manifested high specific surface areas. In the case of silica, its effect on specific surface area of titanium white clearly depended also on its physicochemical character.

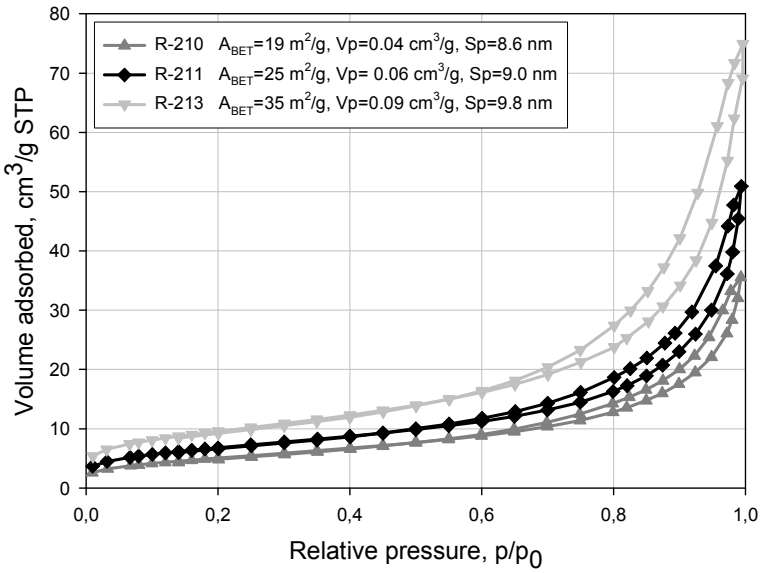

Fig. 4. N_2 adsorption/desorption isotherms of titanium dioxides

Volume distributions and distribution of pore surface as related to pore diameter, presented in Fig.5, demonstrated decrease in both volume and in surface of pores in line with increasing diameter in the studied samples. Effect of such alterations might reflect increasing amounts of inorganic oxides used for surface modification of titanium white samples.

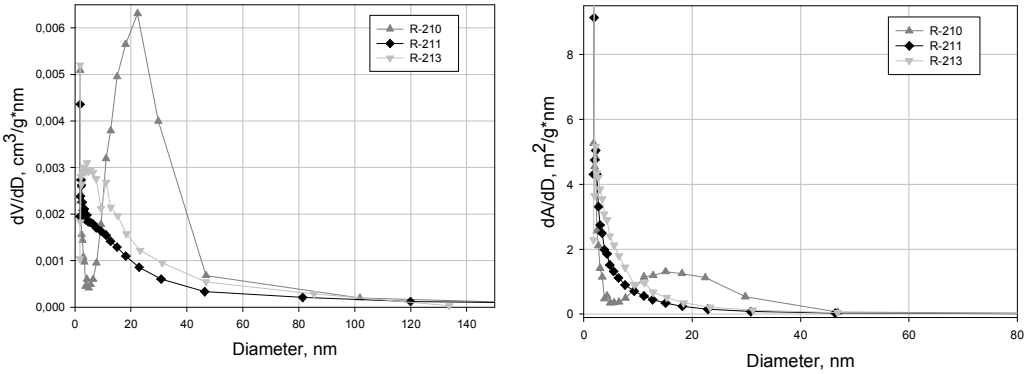

a) b)

Fig. 5. Distribution of pore volumes (a) and of surface area (b) of titanium white samples as related to their particle diameter

In the case of titanium dioxide pigments their lightness could be noted to increase in line with the increasing shares of Al_2O_3 and SiO_2 on TiO_2 surface (respective values of L* amounted to 89.17 for R-210, 92.28 for R-211 and 93.31 for R-213) (Fig. 6).

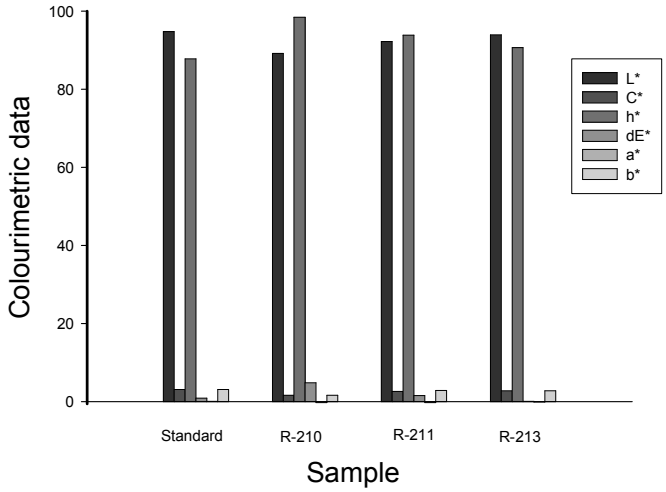

Fig. 6. Colourimetric data of commercial titanium dioxide samples TYTANPOL

In parallel to the increasing content of aluminium oxide and of silica, rising values of C* parameter were also observed, characterizing colour intensity (Table 2).

Table 2. Colourimetric data of commercial titanium dioxide samples TYTANPOL

Sample	Colourimetric data							
	L*	a*	b*	C*	h*	dL*	dH	dE*
Standard	94.79	0.12	3.14	3.14	87.85	0.89	-0.21	0.95
R-210	89.17	-0.25	1.67	1.69	98.45	-4.69	0.32	4.85
R-211	92.28	-0.2	2.93	2.94	93.89	-1.59	0.19	1.6
R-213	93.91	-0.03	2.8	2.8	90.65	0.04	0.02	0.09

All the pigments of titanium dioxide were characterized by low shares of green and yellow colours, which was linked to the method of TiO_2 production. This reflected the presence of contaminations which could not be eliminated during production due to the specificity of the sulphate procedure. As compared to the standard, an increase in the colour shade could also be noted. However, the relationship was inversely related to contents of silica and aluminium oxide (increasing percentage of the oxides content was paralleled by a decrease in the value of colour shade).

Estimation of zeta potential allowed to determine adsorptive properties. The potential was also decisive for stability of dispersion. Indirectly, it allowed to characterize stability of the studied dispersion systems.

Changes in electrokinetic potential, taking place with pH changes, and value of TiO_2 isoelectric point were strongly related to the type and quantity of inorganic substances used for modification. For pure substances the isoelectric point corresponded to pH 4 for titanium dioxide, to pH 2 for silicon dioxide and to pH 9 for aluminium oxide.

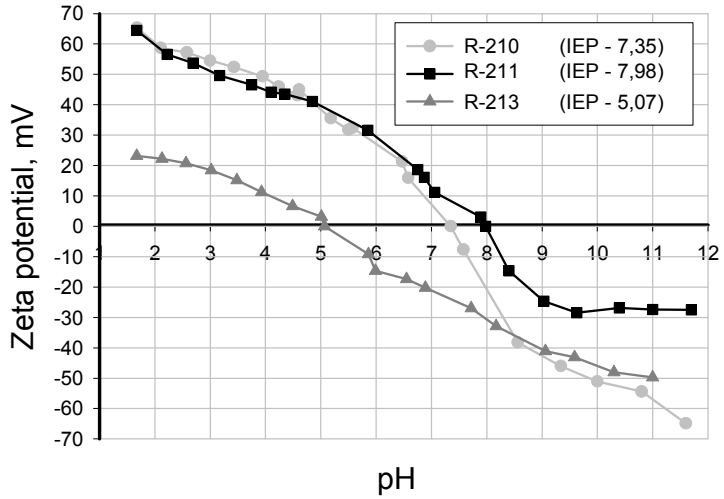

Fig.7. Electrokinetic curves of the examined TiO_2 powders

For TiO_2 pigments of a high SiO_2 content isoelectric point was shifted toward low pH values. On the other hand, involvement of aluminium oxide resulted in a shift of the isoelectric point toward high pH values. Values of isoelectric point amounted to 7.35 for R-210 white, 7.98 for R-211 whit and 5.07 for R-213, respectively (Fig.7).

CONCLUSIONS

The studied TiO_2 samples have demonstrated presence of spherical particles.

The particle size distribution curves have permitted to conclude that surface modification of titanium white using inorganic oxides exerts a significant effect on character and size of pigment particles. We conclude that increased amounts of aluminium oxide and silica used for modification of titanium dioxide surface deteriorate uniform character of the sample and results in an increase in diameter of pigment particles.

The highest adsorptive capacity is manifested by R-213 titanium white. Probably, the size of BET surface area of the white is most pronounced due to the presence of higher number of active centres on the surface.

The titanium white pigments belong to mesoporous adsorbents. Luminosity of titanium dioxide pigments surface modified with inorganic oxides, such as aluminium oxide and silica, increases in parallel to rising share of the oxides. All samples of titanium white are characterized by involvement of yellow and green colours, which results from contaminations introduced during synthesis of the pigments.

Value of the isoelectric point (IEP) depends on the amounts of aluminium oxide and silica used for surface processing of titanium white.

ACKNOWLEDGEMENTS

This work was supported by the Poznan University of Technology Research Grant No. 32-117/08-BW.

REFERENCES

BLAKE D.M., MANESS P.-C., HUANG Z., WOLFRUM E.J., JACOBY W.A., HUANG J., JACOBY W.A., 1999, *Application of the photocatalytic chemistry of titanium dioxide to disinfection and the killing of cancer cells*. Sep. Purif. Methods, 28, 1-50

BRAND R.M., PIKE J., WILSON R.M., CHARON A.R., 2003, *Sunscreens containing physical UV blockers can increase transdermal absorption of pesticides,* Toxicol. Ind. Health, 19, 9-16

CHEN C.-C., LEI P.X., JI H.W., MA W.H., ZHAO J.C., HIDAKA H., SERPONE N., 2004, *Photocatalysis by titanium dioxide and polyoxometalate/TiO_2 cocatalysts. Intermediates and mechanistic study,*Environ. Sci. Technol., 38, 329-337

COZZOLI P. D., KORNOWSKI A., WELLER H., 2003, *Low-temperature synthesis of soluble and proc-*

essable organic-capped anatase TiO_2 nanorods, J. Am. Chem. Soc., 125, 14539-14548
DING X.-Z., LIU X.-H., 1997, *Synthesis and microstructure control of nanocrystalline titania powders via a sol-gel process*, Mater. Sci. Eng., 224, 210-215
HASHIMOTO K., IRIE H., FUJISHIMA A., 2005, *TiO_2 photocatalysis: a historical overview and future prospects*, Jpn. J. Appl. Phys. Part 1, 44, 8269-8285
HIRAKAWA K., MORI M., YOSHIDA M., OIKAWA S., KAWANISHI S., 2004, *Photo-irradiated titanium dioxide catalyzes site specific DNA damage via generation of hydrogen peroxide,* Free Radic. Res., 38, 439-447
HOFFMANN M.R., MARTIN S.T., CHOI W., BAHNEMANN D.W., 1995, *Environmental applications of semiconductor photocatalysis*, Chem. Rev., 95, 69-96
KIM C.-S., BYUNG K.M., PARK J.-H., CHOI B.-C., SEO H.-J., 2003, *Solvothermal synthesis of nanocrystalline TiO_2 in toluene with surfactant*, J. Cryst. Growth, 257, 309-315
LEGRINI O., OLIVEROS E., BRAUN A. M., 1993, *Photochemical processes for water treatment,* Chem. Rev., 93, 671-698
LINSEBIGLER A.L., LU G., YATES J.T., 1995, *Photocatalysis on TiO_2 surfaces: principles, mechanisms, and selected results*, Chem. Rev., 95, 735 – 758
PAZ Y., HELLER A., 1997, *Photo-oxidatively self-cleaning transparent titanium dioxide films on soda lime glass: the deleterious effect of sodium contamination and its prevention*, J. Mater. Res., 12, 2759-2766
RAMAKRISHNA G., GHOSH H.N., 2003, *Optical and photochemical properties of sodium dodecylbenzenesulfonate (DBS)-capped TiO_2 nanoparticles dispersed in nonaqueous solvents,* Langmuir, 19, 505-508
SCHMIDT C., DELP T., SCHOEN S., 2005, U.S. Pat. Appl. Publ., US 2005176850
WU M., LIN G., CHEN D., WANG G., HE D., FENG S., XU R., 2002, *Sol-hydrothermal synthesis and hydrothermally structural evolution of nanocrystal titanium dioxide*, Chem. Mater., 14, 1974-1980
ZHANG Q., GAO L., 2003, *Preparation of oxide nanocrystals with tunable morphologies by the moderate hydrothermal method: insights from rutile TiO_2*, Langmuir, 19, 967-971
ZHAO J., WANG Z., WANG L., YANG H., ZHAO M., 1998, *The synthesis and characterization of TiO_2/wollastonite composite*, Mater. Lett., 37, 149-155

Siwińska-Stefańska K., Krysztafkiewicz A., Jesionowski T., *Wpływ powierzchniowej obróbki tlenkami nieorganicznymi na właściwości dwutlenku tytanu,* Physicochemical Problems of Mineral Processing, 42 (2008), 141-152 (w jęz. ang)

Przeprowadzono badania nad oceną powierzchniowo modyfikowanej bieli tytanowej tlenkami nieorganicznymi. Badania miały na celu określenie właściwości dyspersyjnych, m. in. rozkładu wielkości cząstek oraz indeksu polidyspersyjności. Dokonano ponadto obserwacji mikroskopowych pozwalających na ocenę morfologii powierzchni modyfikowanych cząstek TiO_2. Wykonano pomiar barwy bieli tytanowych oraz określono wielkość powierzchni właściwej metodą BET. Oceniono wpływ powierzchniowej modyfikacji tlenkami na zmianę potencjału zeta. Stwierdzono, że zwiększenie udziału tlenku glinu i krzemionki do modyfikacji powierzchni ditlenku tytanu powoduje pogorszenie jednorodności próbki oraz wpływa na zwiększenie średnic cząstek pigmentu. Pigmenty bieli tytanowej zaliczamy do adsorbentów mezoporowatych. Wartość punktu izoelektrycznego (IEP) zależy od ilości tlenku glinu i krzemionki użytych do powierzchniowej obróbki bieli tytanowej.

słowa kluczowe: dwutlenek tytanu, modyfikacja powierzchni, PSD, morfologia powierzchni, potencjał dżeta, izotermy adsorpcji i desorpcji

Physicochemical Problems of Mineral Processing, 42 (2008), 153-164
Fizykochemiczne Problemy Mineralurgii, 42 (2008), 153-164

Ewa Skwarek*, Marlena Matysek–Nawrocka*, Władysław Janusz*, Vladimir Iljich Zarko**, Vladimir Moiseevich Gun'ko**

ADSORPTION OF HEAVY METAL IONS AT THE Al_2O_3-SiO_2/$NaClO_4$ ELECTROLYTE INTERFACE

Received May 15, 2008; reviewed; accepted July 31, 2008

The study on adsorption of heavy metals (Cd(II), Ni(II) and Pb(II)) at the Al_2O_3-SiO_2/electrolyte solution interface is presented in this paper. The influence of ionic strength, pH, background electrolyte ($NaClO_4$) concentration and composition of metal oxide on adsorption of Cd(II), Ni(II) and Pb(II) from solution of initial concentration ranged from 1×10^{-6} to 1×10^{-3} mol/dm^3 in the mentioned system was investigated. The adsorptions edge parameters ($pH_{50\%}$ and $\Delta pH_{10\text{-}90\%}$) for different concentrations of electrolyte were presented. The adsorption measurements were complemented by the potentiometric titration of Al_2O_3-SiO_2 suspensions and electrophoretic measurements. Charge reversal point (CR2) can be observed for solution concentration of 10^{-3} mol/dm^3 as a result of Cd(II), Ni(II) and Pb(II) ions adsorption.

key words: cation specific adsorption, heavy metals, Cd(II), Ni(II) and Pb(II), electrical double layer, Al_2O_3-SiO_2, zeta potential

INTRODUCTION

Most studies of cations adsorption at metal oxide/electrolyte interface concern the systems where the solid phase is a pure compound. Such systems are convenient for theoretical study, however they differ significantly from real dispersed systems where as a rule, both phases are multicomponent. The adsorption affinity of ions to the surface depends on the basic–acidic properties of the surface hydroxyl groups of metal oxide. Metal atoms surrounding them in the crystal lattice determine the properties of hydroxyl groups. It is known that even simple metal hydroxyl groups change their

* The Department of Radiochemistry and Colloid Chemistry, Maria Curie Skłodowska University, M.C. Skłodowskiej Square 3, 20-031 Lublin, Poland, wjanusz@hermes.umcs.lublin.pl
** Institute of Surface Chemistry, 31 Prospect Nuke, 03680 Kiev, Ukraine

properties with the number of metal atoms in the vicinity of a given surface hydroxyl group. Mixed –two component oxides create greater opportunity of changing properties due to the diversity of metal atoms in the hydroxyl group's surroundings. The adsorption of heavy metal ions at the solid/electrolyte solution interface has been studied to describe processes taking place in environmental systems and for technological purpose to prepare catalysts (Hayes and Katz 1961). Significant amount of anthropogenic heavy metal ions is found in wastewaters from many industries e.g. mining, metallurgical, metal plating, tanneries (Karvelas et al., 2003, Bailey et al.,1999) and in urban inputs like sewage business effluents, atmospheric deposition, and traffic related emissions (Alloway 1995). Because heavy metals are not biodegradable and have a tendency to accumulate in living organisms causing various diseases and disorders, they must be removed from wastewaters. One of the efficient methods of water treatment in order to remove heavy metal is their adsorption at adsorbents type of the metal oxide.

The multivalent ions can be adsorbed specifically on the metal oxide surface on one or two surface sites (hydroxyl groups) via hydrogen exchange, but number of sites usually occupied by a single ion is smaller than two (Schindler et al.,1981) Adsorption such ions may lead to inner-sphere complexes or outer-sphere complexes (when adsorbed cation is separated from surface by water molecule). Usually sharp increase of the cation adsorption from 0% to 100%, with on increase of pH of the electrolyte, is observed. This relationship is called "edge of adsorption" and Robertson and Leckie (1997) have proposed very useful parameters to characterize it, as shown in Table 1.

Table 1. Parameters of adsorption edge

Parameters	Parameters of adsorption edge
$pH_{50\%}$	The value of pH when 50% of initial concentration of cation adsorbs, this parameter characterizes the position of adsorption edge on the pH scale.
$pH_{10\text{-}90\%}$	The range of pH where the adsorption changes from 10% to 90%, it characterizes the slope of the edge.
*d*pMe/*d*pH	Parameter that shows the activity of cations; must vary when pH of the solution changes to maintain the constant adsorption of the cation.

Metal cations belong to ions having a great adsorption affinity to mixed oxide surface and create inner-sphere complexes. DLM and TLM models may describe specific adsorption of ions. According to DLM model, specific adsorption of ions is possible with the creation of inner-sphere complexes, where ions take place inside surface plane. According to TLM (model SCM, *site binding*), also the adsorption of background electrolyte ions may be considered as a specific and nonspecific adsorption. Ions taking part in ionization and complexation reactions, increase the surface charge density on the oxide and adsorb specifically, but ions in diffusion part of edl are adsorbed nonspecifically (Hayes and Katz 1996). In this paper we report the changes of

adsorption affinity Cd(II), Ni(II) and Pb(II) ions with composition of adsorbent and subsequent changes of the parameters of the electrical interfacial layer (EIL) change at the mixed alumina-silica/electrolyte interface.

EXPERIMENTAL

The Al_2O_3-SiO_2 systems were prepared according to the fumed procedure (Gun'ko et al., 2000). The percentage of Al_2O_3 in the samples was as follows: 8, 3 and 1% are denoted as AS8, AS3 and AS1, respectively. Nitrogen adsorption – desorption isotherms in temperature 77,35 K was used to determine the specific surface area and pore radius of studied materials. These parameters are summarized in Table 2.

Table 2. Specific surface area and pore radius of AS samples (Janusz et al.,2007)

Sample	AS1	AS3	AS8
Al_2O_3 [wt %]	1.3	3	8
S_{BET} [m^2/g]	207	188	308
R_p [nm]	3.7	3.8	3.8
pH_{PZC}	4	4	4
pH_{IEP}	<3	<3	<3

The specific adsorption of Cd(II), Ni(II) and Pb(II) ions at Al_2O_3-SiO_2 interface was determined by the means of radioisotope method as a function of Cd(II), Ni(II) and Pb (II) concentration, $NaClO_4$ as a background electrolyte concentration and pH. The initial concentration of the cations ions was ranged from 1×10^{-6} to 1×10^{-3} mol/dm^3, pH was changed from 3 to 10. The $NaClO_4$ solution was used of concentrations 0.1, 0.01, 0.001 mol/dm^3. The adsorption measurements were complemented by the potentiometric titration of Al_2O_3-SiO_2 suspensions and electrophoresis measurements. To remove ionic type contaminations, which might influence the ion adsorption measurements, the Al_2O_3-SiO_2 was washed with double distilled water until conductivity of the supernatant was constant (~2 μS/cm). The adsorption and the surface charge measurements were performed simultaneously in the suspension of the same solid content, to keep the identical conditions of the experiments in a thermostated Teflon vessel at 25°C. To eliminate the presence of CO_2 all potentiometric measurements and adsorption experiments were carried out under the nitrogen atmosphere. The pH values were measured using a set of glass REF 451 and calomel pHG201-8 electrodes with Radiometer assembly. Surface charge density was calculated from the difference of the amounts of added acid or base to obtain the same pH value of suspension as for the background electrolyte. The zeta potential of the Al_2O_3-SiO_2 dispersions was determined by electrophoresis with Zetasizer 3000 by Malvern. The measurements followed the ultrasonication of the suspension containing 100 ppm of the solid.

The adsorption of Cd(II), Ni(II) and Pb(II) ions was determined by radiotracer method using ^{61}Ni, ^{115}Cd, ^{210}Pb radioisotopes respectively. The radioactivity of an electrolyte solution before and after adsorption was measured using liquid scintillation counter LS5000D by Beckman for ^{61}Ni, ^{115}Cd radioisotopes, and using Gamma Counter 5500 for ^{210}Pb.

RESULTS AND DISCUSSION

The surface charge at a mixed metal oxide/electrolyte interface is formed as a result of acid-base reaction of the surface hydroxyl groups (-SOH) and specific interactions these groups with the background electrolyte ions (Wiese et al.,1976, James, Parks 1982). The acid – based properties of hydroxyl groups at the mixed silica-alumina/electrolyte interface are results of type and number of metal surrounding the oxygen in surface hydroxyl groups. Besides, the surface of the mixed oxide may be composed of patches of pure silica or alumina. Table 2 presents all values pH_{PZC} and pH_{IEP} for the electrical double layer at the Al_2O_3-SiO_2/electrolyte solution interface. As it was mentioned above the properties of hydroxyl groups at the surface of mixed oxides depend on a kind of surrounding metal atoms as well as on their number. In the studied adsorbents the surface hydroxyl groups are coordinated by two atoms that might be the same (two Si or two Al) or different ones (one Si atom and one Al atom). Then the properties of these surface hydroxyl groups should differ and therefore the adsorption affinity of cations should also differ. The following reactions are responsible for the adsorption of bivalent cations at the oxide/electrolyte interface:

$$\equiv SOH + Me^{2+} \Leftrightarrow \equiv SO^{-}Me^{2+} + H^{+} \tag{1}$$

$$2(\equiv SOH) + Me^{2+} \Leftrightarrow (\equiv SO^{-})_2 Me^{2+} + 2H^{+} \tag{2}$$

$$\equiv SOH + Me^{2+} + H_2O \Leftrightarrow \equiv SO^{-}MeOH^{+} + 2H^{+} \tag{3}$$

As may be noticed from Eq 1 and 2 the adsorption of cations releases the hydrogen ions from hydroxyl groups, so the increase of pH in the system will favor the adsorption of cations at the metal oxide/electrolyte interface.

Figures 1 (a) and (b) show the adsorption of Cd(II), Ni(II) and Pb(II) ions at the SA1/0.001M $NaClO_4$ system interface for an initial ion concentrations of 1×10^{-6} and 1×10^{-3} mole/dm^3 respectively. Similar dependences of adsorption as a function pH for other studied samples (of different composition) were also observed. The plot of adsorption as a function of pH called as the adsorption edge is characterized by $pH_{50\%}$ and $\Delta pH_{10\text{-}90\%}$ parameters. Basing on the adsorption data, parameters characterizing the adsorption edge ($pH_{50\%}$and $\Delta pH_{10\text{-}90\%}$) were calculated. Figures 2 a and b present

these parameters as a function of an initial concentration of Cd(II), Ni(II) and Pb(II) ions. As it can be seen, the adsorption edge shifts towards higher pH values with an increase of an initial concentration of measured ions. For all studied samples of mixed oxide the following sequence of adsorbed metals was observed:Pb(II)>Cd(II)>Ni(II).

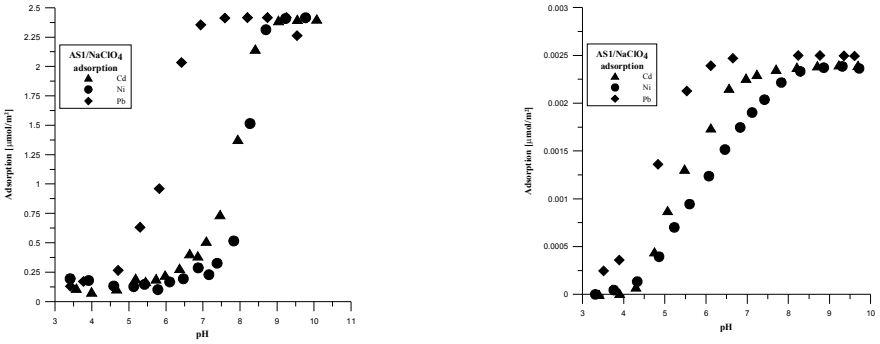

Fig. 1. The adsorption density of Cd(II), Ni(II) and Pb(II) ions as a function of pH in the AS1/0.001M $NaClO_4$ system; the initial ion concentration: (a) 1×10^{-3}; (b) 1×10^{-6} mol/dm^3.

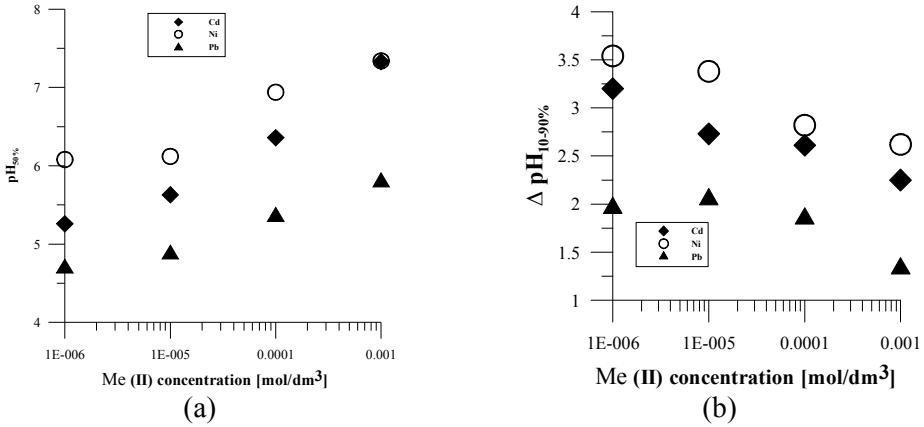

Fig. 2. The parameters of adsorption edge as a function of initial concentration of Cd(II), Ni(II) and Pb(II) for AS1 oxide: (a) $pH_{50\%}$; (b) $\Delta pH_{10\text{-}90\%}$.

The sequence of the adsorption affinity of cations is in an agreement with selectivity series of heavy metal and transition metal ions on the simple metal oxide/electrolyte interface (Hayes and Katz 1996). As it was mentioned above, heavy metal and transition metal cations create inner sphere complexes on the metal oxides. The ability to form inner sphere complexes is connected with the formation of hydrated complexes by respective ions. One can notice certain analogy between the reactions (Hayes and Katz 1996):

$$Me^{2+} + H_2O \leftrightarrow Me(OH)^{+} + H^{+} \tag{5}$$

$$Me^{2+} + \equiv SOH \leftrightarrow SOMe^{+} + H^{+} \quad (6)$$

It is assumed that there is a correlation between the complexation reactions of surface hydroxyl groups and the ability to formation hydrated complexes by metal cations. In Table 3 the values of the first constant of hydrolysis for selected metal cations are presented.

Table. 3. The values of the 1st hydrolysis constant for selected bivalent metal cations (Hayes and Katz 1996).

Cation	pK value
Pb(II)	7.7
Ni(II)	9.9
Cd(II)	10.1

However we observed that the adsorption affinity of Cd(II) ions is higher that Ni(II) ions at low initial concentrations, only for the 0.001 mol/dm^3 adsorption edges cover, so only for this case the correlation discussed above may have place. The parameter charactering the slope of adsorption edge, $\Delta pH_{10\text{-}90\%}$, decreases with an increase of the Cd(II), Pb(II) and Ni(II) ions concentration, which means that the adsorption edge becomes steeper.

Table. 4. The adsorption constants for Cd(II), Ni(II), Pb (II) ions for AS/electrolyte solution system

Concentration [mol/dm^3]	AS1		AS3		AS8	
	Cd (II)					
	pK_1	$p\beta_2$	pK_1	$p\beta_2$	pK_1	$p\beta_2$
10^{-6}	3.45	9.89	4.00	9.95	4.49	9.94
10^{-5}	3.77	9.98	4.34	9.45	4.05	9.84
10^{-4}	3.62	9.56	4.51	9.99	4.15	9.95
10^{-3}	4.00	10.16	6.79	8.89	9.00	9.55
	Ni(II)					
10^{-6}	3.01	9.44	4.44	7.22	3.88	8.15
10^{-5}	3.42	8.96	4.30	8.34	4.00	8.72
10^{-4}	4.72	9.99	4.17	9.33	4.74	9.54
10^{-3}	3.05	8.72	4.00	9.71	4.42	9.99
	Pb(II)					
10^{-6}	2.50	10.5	3.38	10.50	2.90	10.77
10^{-5}	2.42	10.49	3.76	10.90	3.14	9.97
10^{-4}	3.10	10.5	4.31	6.35	3.45	10.88
10^{-3}	3.60	10.5	4.02	6.92	3.86	10.9

We suppose that this phenomenon is caused by influence of increased content of alumina in successive, other samples. According to the reaction 1 and 2, adsorption of metal ions proceeds via exchange of hydrogen ions from one or two surface hydroxyl

groups. For the data presented in Figures 2 the values of adsorption constant of Ni(II), Cd(II) and Pb(II) ions were determined by numerical optimization, using the TLM model. These values are collected in Table 4. For AS1 and AS8 samples the predominant part plays reaction of Pb(II) with one surface hydroxyl group, according reaction 1, while reaction with two surface hydroxyl groups brings a small contribution into adsorption. For higher initial concentration of Pb(II) for AS3 samples the part of reaction 2 in the adsorption process is larger.

Such adsorption mechanism of bivalent metal cations at the high adsorption densities would lead to the overcharging of the compact part of edl and to the presence of the charge reversal point(CR2) on the ζ potential as a function of pH dependence.

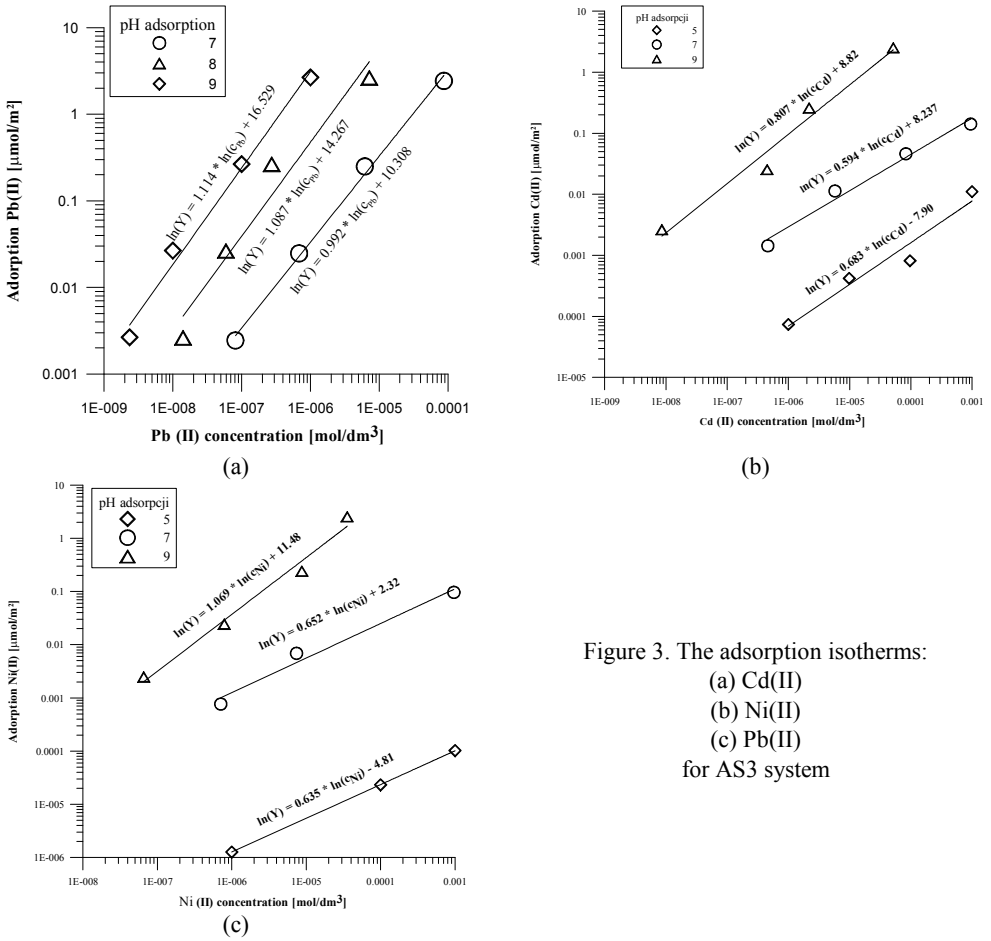

Figure 3. The adsorption isotherms:
(a) Cd(II)
(b) Ni(II)
(c) Pb(II)
for AS3 system

On the basis of Cd(II), Ni(II) and Pb(II) adsorption data the isotherms adsorption were calculated and they are presented in Figure 3 as the Kurbatov plots (log adsorption – log concentration). A linear fitting can be observed for these systems. The same relationship was observed for oxides AS1 and AS8.

The presence of metal ions leads to an increase in the number of negatively charged sites at the metal oxide surfaces. The most significant influence was observed for the highest metal concentration of (10^{-3}M, see Figures 4 (a), (b) and (c)).

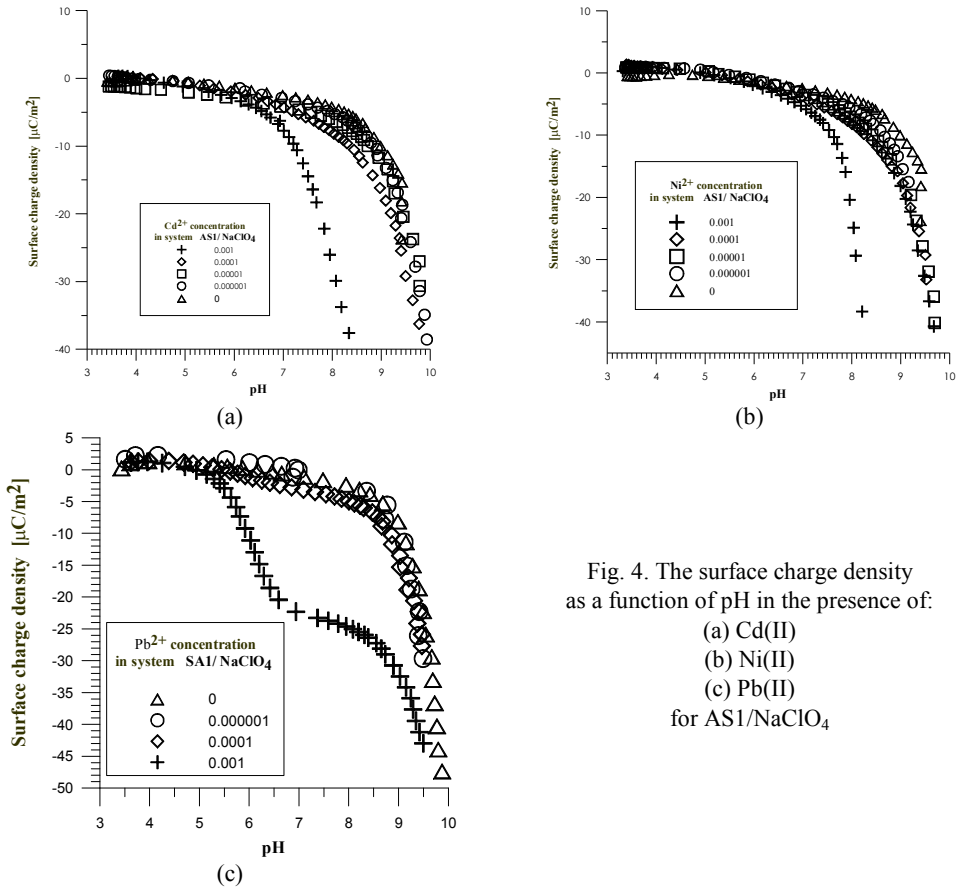

Fig. 4. The surface charge density as a function of pH in the presence of:
(a) Cd(II)
(b) Ni(II)
(c) Pb(II)
for AS1/$NaClO_4$

The presence of Cd(II), Ni(II) and Pb(II) cations causes changes of ζ potential in the studied systems. Such influence is shown in Figure 5. For the highest concentration of metal ions a charge reversal point was observed (CR2). This phenomenon is characteristic for the overcharging of the compact part of the edl as a result of specific ion adsorption. As it is seen this point (CR2) is at pH about 6.0 for Pb(II) ions and at pH about 8.0 for Cd(II) and Ni(II) ions. Dependence for cadmium and nickel was observed and it can be explained with a mentioned ability of these ions to hydrolysis, and therefore a small difference between their hydrolysis constant.

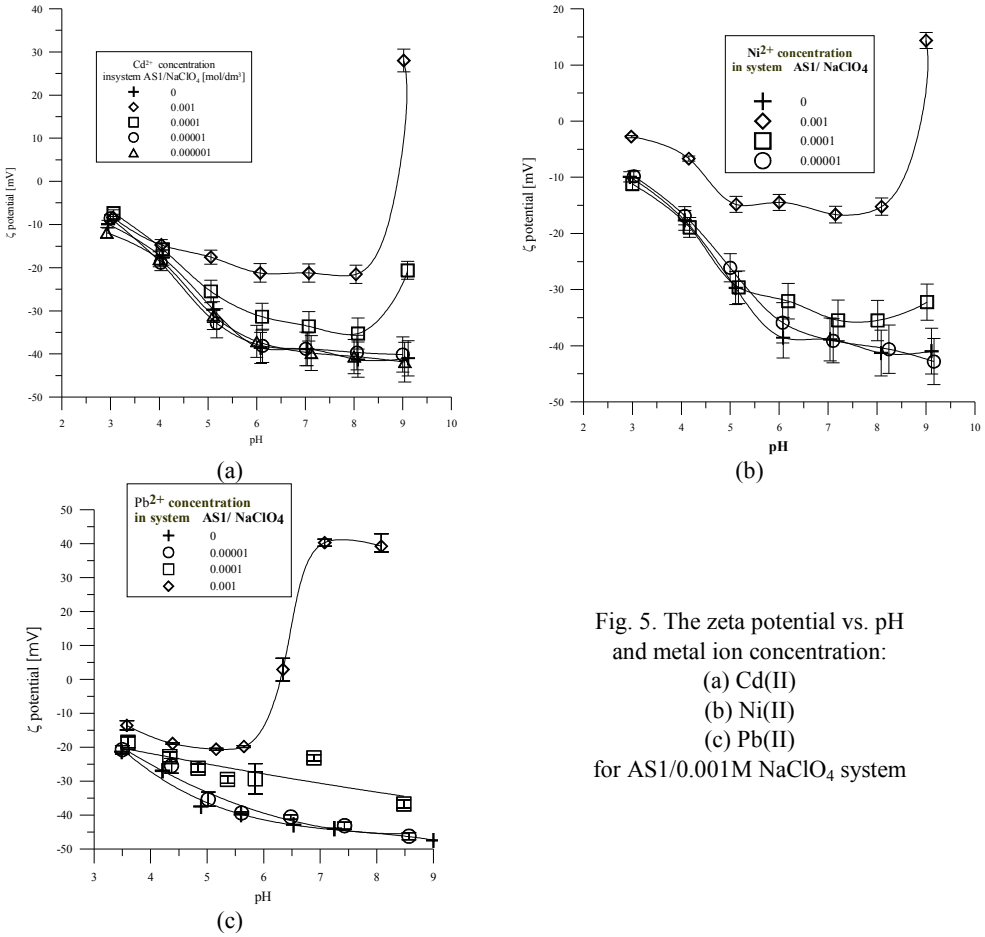

Fig. 5. The zeta potential vs. pH and metal ion concentration:
(a) Cd(II)
(b) Ni(II)
(c) Pb(II)
for AS1/0.001M $NaClO_4$ system

CONCLUSIONS

The samples of mixed alumina/silica oxides with a content of alumina ranging from 1 to 8% have the same pH_{pzc}. Adsorption of Cd(II), Ni(II) and Pb(II) ions can be described by the TLM model of electrical double layer. The shape of Cd(II), Ni(II) and Pb(II) ions adsorption as a function of pH on mixed alumina/silica oxides are similar to one on clean metal oxides. The adsorption process can be characterized by the adsorption edge, which can be described by two parameters: $pH_{50\%}$ and $\Delta pH_{10\text{-}90\%}$. The parameter characterizing the position of adsorption edge ($pH_{50\%}$) shifts towards higher pH values with the increase of the initial metal concentration for majority of samples. The adsorption isotherms of Cd(II), Ni(II) and Pb(II) ions as a function of log adsorption – log concentration are linear. For all mixed oxides the metal adsorption can be fitted by a Freudlich isotherm. The specific adsorption of bivalent cations

causes a shift of the pH_{iep} towards alkaline pH values and an increase of the ζ potential. The high concentration of adsorbing bivalent cations (Cd, Ni and Pb) causes the overcharging of the compact part of edl and appearance of CR2 point. The presence of bivalent cations causes an increase of the negative surface sites and shifts pH_{pzc} towards lower pH values.

REFERENCE

ALLOWAY B.J., Heavy Metals in soils, Blackie Acad. &Professional, London, (1995).

BAILEY S. E., OLIN T. J., BRICKA R. M. ADRIAN D.D., (1999) *A Review of Potentially Low-Cost Sorbents for Heavy Metal*s, Wat. Res. Vol. 33, No. 11, pp. 2469-2479.

GUN'KO V.M., ZARKO V.I., LEBODA R., MARCINIAK M., JANUSZ W., CHIBOWSKI S., (2000), *Highly dispersed X/SiO_2 and C/X/SiO_2 (X=Alumina, Titania, Alumina/Titania) in the Gas and Liquid media,* J. Colloid Interface Sci. 230, 396-409.

HAYES K.F., KATZ L.E, (1996) in: Physics and Chemistry of Mineral Surfaces, Ed. P.V. Brady, CRC Press, New York, pp 147-224.

JAMES R.O., PARKS G.A., (1982) *Characterization of Aqueous Colloids by Their Electrical Double-Layer and Intrinsic Surface Chemical Properties*, in: Surface and Colloid Sci., vol. 12, 229.Wiley-Interscience, New York.

JANUSZ W., SKWAREK E., ZARKO V.I., GUN'KO (2007) V.M. *Structure of electrical double layer at the Al_2O_3-SiO_2/electrolyte solution interfaces* Physicochemical Problems of Mineral Processing 41, 215-225.

KARVELAS M., KATSOYIANNIS A., SAMARA C., (2003) *Occurrence and fate of heavy metals in the wastewater treatment process* Chemosphere 53, 1201–1210.

ROBERTSON A.P., LECKIE J.O., (1997) *Cation binding predictions of surface complexation models: effects of pH, ionic strength, cation loading, surface complex and model Fit,* J. Colloid Interface Sci. 188 444.

SCHINDLER P.W., FÜRST B., DICK R., WOLF P.U., (1976) *Ligand properties of silanol groups* J. Colloid Interface Sci. 55-469.

SPOSITO G., The Surface Chemistry of Soils, Oxford University Press, New York, (1984).

WIESE G.R., JAMES R.O., YATES D.E., HEALY T.W., (1976), *Electrochemistry of the colloid – water interface,* in: Electrochemistry of Colloid – Water Interface, Int. Review Sci. Phys. Chem., Series 2, London, Butterworths, 6, 53-87.

E. Skwarek, M. Matysek–Nawrocka, W. Janusz, V.I. Zarko, V.M. Gun'ko, *Adsorpcja jonów metali ciężkich w podwójnej warstwie elektrycznej na granicy faz Al_2O_3-SiO_2/$NaClO_4$.* Physicochemical Problems of Mineral Processing, 42 (2008), 153-164 (w jęz. ang)

Kadm, ołów i nikiel są toksycznymi metalami ciężkim, który stanowią wciąż poważne zagrożenie dla organizmów żywych. W środowisku naturalnym oraz w wielu procesach technologicznych mamy do czynienia ze skomplikowanymi układami gdzie występują obok siebie tlenki typu Al_2O_3-SiO_2 oraz jony metali ciężkich. Przeprowadzono badania adsorpcji jonów niklu, kadmu i ołowiu dla różnych stężeń początkowych, w funkcji pH dla układów AS1, AS3, AS8/roztwór NaCl. Kształt krzywych adsorpcji w funkcji pH ma postać krawędzi adsorpcji. Wzrost stężenia początkowego jonów metali ciężkich, powoduje przesunięcie krawędzi w kierunku zasadowym skali pH. Wyznaczono charakterystyczne parametry krawędzi

adsorpcji tj. $pH_{50\%}$ i $\Delta pH_{10\text{-}90\%}$, w oparciu o zależność adsorpcji od pH stosując model TLM, obliczono również stałe reakcji adsorpcji jonów Ni(II), Cd(II), Pb(II) metodą optymalizacji numerycznej. Zależność gęstości ładunku powierzchniowego od pH w obecności jonów metali ciężkich, jest w dobrej korelacji z zależnością adsorpcji jonów Ni(II), Cd(II), Pb(II) od pH. Adsorpcja badanych jonów na powierzchni AS1, AS3, AS8 prowadzi do wzrostu stężenia grup ujemnie naładowanych.

słowa kluczowa: adsorpcja kationów, metale ciężkie, Cd(II), Ni(II), Pb(II), podwójna warstwa elektryczna, Al_2O_3-SiO_2, potencjał dżeta

Physicochemical Problems of Mineral Processing, 42 (2008), 165-176
Fizykochemiczne Problemy Mineralurgii, 42 (2008), 165-176

Suzan S. Ibrahim*, Ayman A. El-Midany*

EFFECT OF TRIBLOCK-COPOLYMERIC COMPATIBILIZING ADDIDTIVES ON IMPROVING THE MECHANICAL PROPERTIES OF SILICA FLOUR -FILLED POLYPROPYLENE COMPOSITES

Received May 15, 2008; reviewed; accepted July 31, 2008

Minerals are introduced during the compounding processes into the polymeric host matrix in most thermoplastics industries to accomplish a variety of modified physical characteristics to the new-born composites. The introduction of well-dispersed silica flour particulates; tailored with respect to grade and fineness; into the virgin polypropylene matrix has shown an extreme improvement in the performance characteristics of the end-product. This could be attributed to the relatively low thermal expansion coefficient of silica. In this study, purified silica flour was blended with polypropylene to produce the finished masterbatch formulation for plastics industry. The flour was added during compounding stage with different loading levels from 1.5% to 15% by volume. Results showed substantial improving in many physical properties, i.e., increase in Young's modulus, impact strength, and yield stress measures. Moreover, silica addition resulted drop in all strain measures of the end products with various loading levels. On the other-hand, the addition of styrene-ethylene/butylene-styrene block SEBS and its grafted maleic anhydride surface compatibilizers was extra added during the blend digestion process to enhance silica/ PP wettability. After the addition of SEBS compatible reagent, results did not show improving in both Young's modulus and yield strength measures. Yet, remarkable improvement in impact strength and strain characters was noticed.

key words: silica, polymers, properties, Young's modulus, impact strength, yield stress, polypropylene

INTRODUCTION

Minerals as fillers have wide applications in different industries. Their addition advantages are twofold either performance enhancing and/or cost reduction. In the

* Central Metallurgical R&D Institute (CMRDI), P. O. Box 87, Helwan, Cairo, Egypt

first case, the mineral is called the functional filler because the mineral addition is incorporated to achieve a specific performance attribute to the end-product. Among these properties are the particle shape, the particle size and size distribution, purity, chemical and thermal inertness, (Table 1), (O'Driscoll, M., 1994). Whilst in the second case where the reduction of total formulation cost is being the principle driving force, the mineral represents merely the bulk filler or the extender for the costly polymer base matrix (Trivedi, N.C., Hagemeyer, R.W., 1994; Lee S., 2000; Dearmitt, C., 2000).

Table 1. Different plastic requirement needed to certain filler characteristics (O'Driscoll, M., 1994)

Compounding/plastic requirements	Filler requirements
Optimum compounding	Mean particle size, good wettability, good dispersion, no static charge
Low viscosity during compounding	Particles round as possible, small specific surface, low absorpitivity
High compounding speed	Low specific heat, high thermal conductivity
Low shrinkage, low internal stresses, no cracks	Low specific heat, high thermal conductivity, low thermal expansion, uniform filler distribution, good adhesion between filler and plastic
No abrasion in processing machines	Low hardness, small round particles, good thermal stability of any surface treatment used
High tensile strength & elongation, flextural strength	superior strength to matrix, high aspect ratio, good fiber/matrix adhesion, good distribution,
High stiffness	high aspect ratio in fiber, high modulus of elasticity
Good impact strength	Long fibers, adhesion to polymer matrix should not be perfect

Table 2. Effect of different mineral fillers with certain loading % on the properties of standard news prints (Johnston, J. H., 1997)

Property of 48.4 g/m^2 standard newsprint	Filled with type I silica at 1.8 wt% addition level	Filled with calcined clay at 1.7wt% addition level
Brightness change (points)	+1.7	+1.4
Opacity change (points)	+1.7	+1.1
L* change (points)	+0.9	+0.8
Porosity	+15%	0%
Top side roughness	-10%	0%
Burst strength	-10%	-9%
Tensile strength	-6%	0%
Coefficient of friction	+41	Not measured
Print through reduction	30-36%	20%

Silica is one of the most extensively and cheapest mineral commodity used in filler applications. When silica flour is embedded in a polymer matrix, it is constrained by its siliceous surface properties and its high degree of hydrophilicity in polymeric matrices (Lofthouse, C.H., 1997). Silica application ranges from using as an extender to a functional filler, Table 2 (Johnston, J.H., 1997). In plastics, it is used to increase

abrasion, heat and scratch resistance in thermoset kitchen sinks. In electrical end-uses, it improves compressive, flexural strength, and dielectric properties. It is often used in corrosion protection systems, due to its superior resistance to corrosion, (Bryk, M.T., 1991; Scherbakoff, N., 1993; Payne, H. F., 1985; Zhang, Y.; Cameron, J., 1993;Shang, S. W.; Williams, J. W.; Soderholm, K-J. M., 1994; Leempoel, P., 1997; Sahnoune, F.; Karad, S.; Lopez Cuesta, J.-M. Crespy, A., 1997; Kauly, T.; Karen, B.; Siegmann, A., Narkis, M., 1997; Lyman, M.J., 1991; Krysztafkiewicz, A.; Maik, M.; Rager, B., 1992; Stricker, F., Friedrich, C., Mulhaupt, R., 1998).

EXPERIMENTAL

A representative white silica sand sample was supplied from high quality Edfo deposit. Microscopic evaluation as well as chemical investigation of the original sample was carried out. The sample was subjected to different steps of dry beneficiation process. At first, sieve classification was carried out to reject both +0.60mm and –0.10 mm fractions. The rejection of these two size fractions is mostly applied to remove most of the iron oxides inclusions especially in the coarser fraction as well as removing most of the ferroginatd clayey fines below 0.10 mm. The classified sand sample was directed to dry high intensity magnetic separation using Magnaroll separator to remove coloring impurities such as iron and titanium oxides. The clean sample was ground in a porcelain Fritsch ball mill to produce silica flour. Particle size distribution of the ground sample as well as the some physical measures were measured.

Fig. 1. ZK 25 T COLLIN Tischcompounder Extruder

Pure polypropylene powder of 0.91g/cm^3 in density, as the host matrix of the blend was prepared with different silica flour additions from 1.5% to 15% by volume. Sometimes, surface compatibilizers like styrene-ethylene/butylene-styrene block and

its grafted maleic anhydride form of 0.90 g/cm^3 in density. They were added in two additions 2.5% and 5% by volume. These loading percentages were chosen according to literature survey. The components of each batch were dried separately for 2 hours at 110°C. They were thoroughly mixed together for 15 min in a plastic tumbling mixer. The final weight of each batch was 600 gm. The blends were subjected to compounding process using "Collin Twin Screw" Extruder at 200°C (Figure 1). Different operations were illustrated in Figure 2 (O'Driscoll, M., 1994).

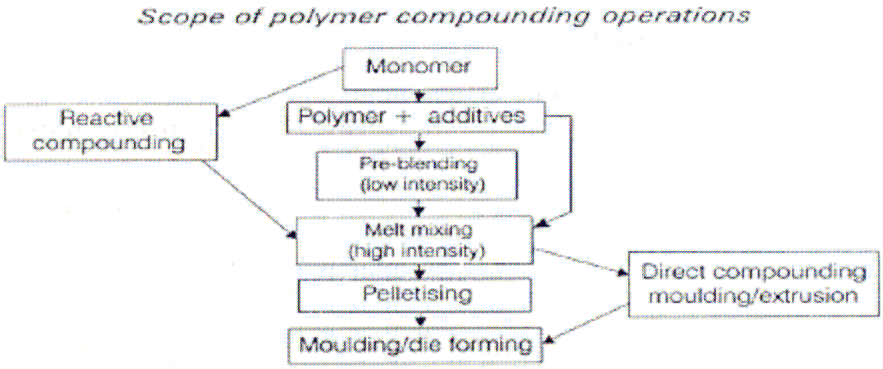

Fig. 2. Scope of Various Compounding Operations (O'Driscoll, M., 1994)

The materials were then fed by a horizontal metering screw hopper with 2 kg/hr feeding rate. The Chilled Rolls Take-off unit with a water bath was added to the system. A Collin Granulator (Figure 3). It was connected to cut the compounded film samples into short specimens of 1 cm length.

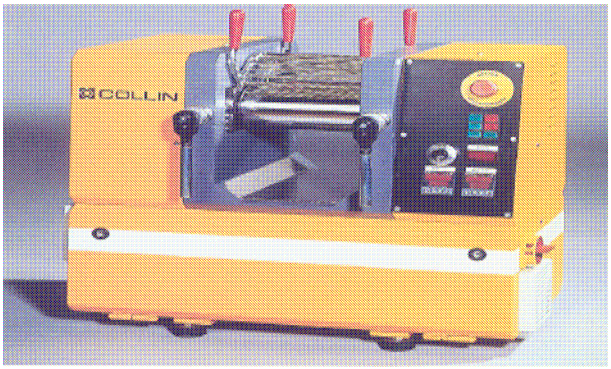

Fig. 3. W 100 T COLLIN Tischwalzwerk Granulator

The samples were subjected to a Milacron K-TEC 40 injection moulder to be prepared as 60mmx 10mmx 4mm rectangular bars for mechanical measures (Figure 4). Meanwhile, 10mm × 6mm × 2mm rectangular bars samples were shaped for impact

strength measures. At least six readings were taken for each test, where the average measure was reported. Tests were performed at ambient temperature around 25^{o}C and constant humidity around 55%. The measures were plotted versus silica content.

Fig. 4. FERROMATIK MILACORN Shaping Unit

RESULTS AND DISCUSSION

Microscopic examination of the original white sand sample showed the presence of some reddish brown inclusions contaminated coarse particles. Traces of colored particulates in finer sizes was detected (Table 3). Sieve classification followed by the rejection of both +0.6mm and -0.1mm fractions removed most of these undesirables. The magnaroll dry high intensity magnetic separator succeeded to reject trace particles of various magnetic nature. Chemical analysis of beneficiated sample was illustrated in Table 4.

Table 3. Chemical composition of original silica sample

Constituent, %	Wt.%
SiO_2	99.32
Al_2O_3	0.04
Fe_2O_3	0.02
TiO_2	0.003
Na_2O	<0.01
K_2O	<0.01
CaO	0.06
MgO	0.02
L.O.I.	0.30

Table 4. Chemical composition of ground refined silica sample

Constituent	Wt.%
SiO_2	99.85
Al_2O_3	0.020
Fe_2O_3	0.016
TiO_2	0.017
Na_2O	---
CaO	0.026
MgO	---

Table 4 shows the high a quality of the prepared sample under investigation, where as Table 5 shows the physical properties of the ground refined silica sample.

Table 5. Some physical properties of the ground refined silica sample

Property	Measure
Refractive Index	1.55
Specific Gravity	2.65
Hardness	7.0
Oil Absorption	35
Surface Area	4.75
Dry Brightness	88
D_{98} D_{50}	20 10

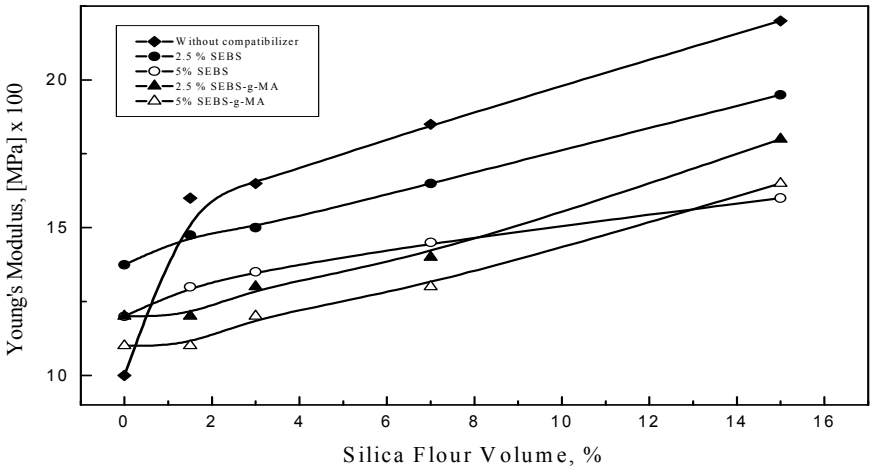

Fig. 5. Influence of silica content on the modulus of filled-PP blends

Figure 5 illustrates the effect of silica content on Young's modulus measures. It was noticed that the effect of silica content followed two stages. The first stage from 0% (without silica) up to 3% silica content and the second stage was above 3% to 15% silica content. In the first stage, the Young's modulus increased rapidly from 1000 to 1600 MPa by increasing the silica content. While in the second stage a gradual increase in the modulus, from 1600 to 2200 MPa, was noticed with increasing the silica content from 3 to 15%. The rate of change in the modulus with varaitation of silica content was 200 MPa per each 1% silica content in the first stage and 50MPa per each 1% silica content in the second stage. In other words, the rate of change in the modulus in the first stage is 4-fold the second stage. The addition of styrene-ethylene/butylene-styrene block and its grafted maleic anhydride as silica/PP surface compatibilizers was negatively affected the modulus character of end-product as

shown in Figure 5. This could be explained after the high dispersion of hydrophilic silica particulates in the polymeric system.

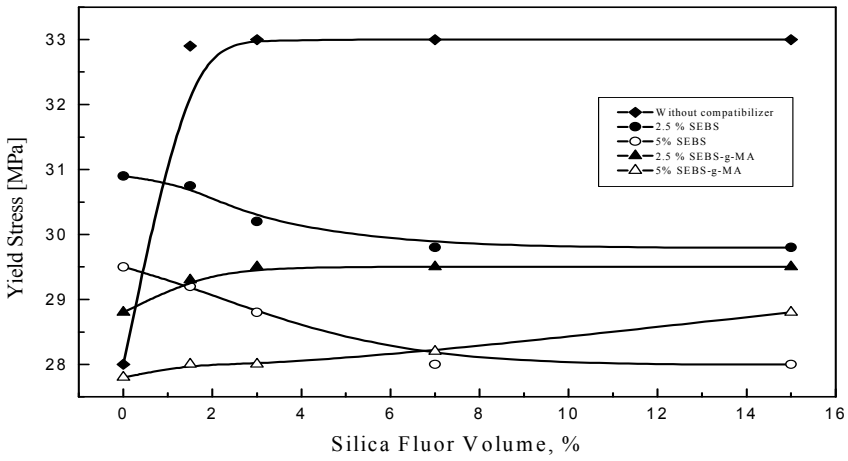

Fig. 6. Influence of silica content on the yield stress of filled-PP blends

Figure 6 illustrates the effect of silica loading level on yield strength measures. The same behaviour was noticed in case of yield strength. An increase reached 32.9 MPa in the 3 % silica content from 28 MPa in the pure sample with an achievement of 17.5%. The yield strength measure was then kept constant at higher silica levels, as shown in Figure 6. The addition of the both surface compatibilizers to the silica/PP system was inversely affected the yield strength. The yield strength was lower in case of additives. Additionally, for each compatibilizer, it was clear that no difference in yield strength measures with variation in silica content as shown in Figure 6.

Figure 7 depicts the Izod impact strength measures versus silica content in filled-PP. Gradual increase in impact measures from 1.6 kJ/m^2 in the neat system to 2.15 kJ/m^2 in the 15% silica filled system. An improvement reached 34.4% in the impact measures was remarked, as shown in Figure 7. It is well known that the presence of large particles and agglomerates >10-30 micron diameter, dramatically reduces impact strength measures of polypropylene masterbatch. These large particles acted as flaws where cracks can initiate. On the other hand, the inclusion of small well dispersed particles can have a very positive influence on the impact strength of PP systems (Valji, S.E., 1999). The incorporation of surface compatibilizers on fine products enhanced dispersion by reducing the interfacial strength (Hawley, G.C., 2000; Fellahi, S.; Boukobbal, F., 1993; Gaskell, P., 1997). This has been found to give a further improvement in impact performance This idea was confirmed to a great extent where the addition of both compatibilizers improved the impact strength measures of end-products as shown in Figure 7. At low silica content levels, 1.5% and 3%, addition of

2.5% SEBS-g-MA increased the impact strength from 1.8 kJ/m^2 to 2.6 kJ/m^2 with an improvement reached about 44%. At higher silica containing systems, 7% and 15% the addition of 5% SEBS-g-MA increased impact strength values from 2.10 kJ/m^2 to 2.70 kJ/m^2 with an improvement ratio of 28.6%.

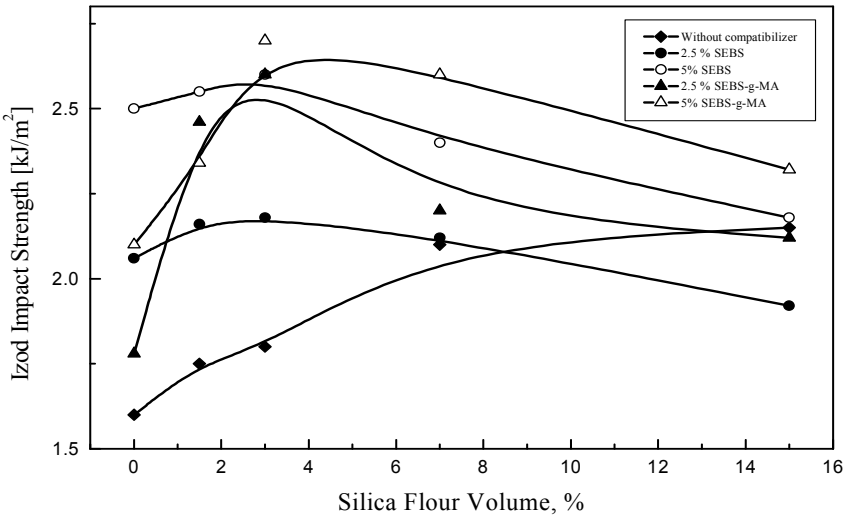

Fig. 7. Influence of silica content on izod impact strength of filled-PP blends

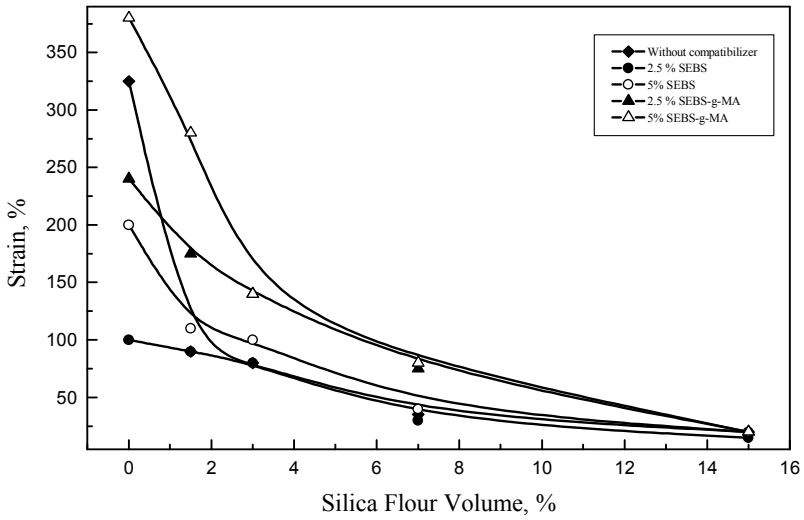

Fig. 8. Influence of silica content on the strain% of the filled-PP blends

The effect of silica addition on strain of filled/PP blends is shown in Figure 8. It was obvious that silica addition with any ratio negatively affected the strain%. In case of neat sample, strain measure reached 325%. After that, it showed dramatic decrease and reached 90% by adding 1.5% silica. It continued its decreasing to 20% at silica content of 15%. Yet some studies followed the influence of processing behavior of the mineral/polymer inside the extruder on the strain. This was carried out by controlling sample stretching during the process (Fourty, G., 1997). It was concluded that the increase in the orientation of the blend during melting i.e. the extrusion stage, could improve the strain. Morever, it was supposed that a better mineral filler orientation in injection molded parts could also improve not only the strain, but also the end-product impact strength (Fourty, G., 1997).

CONCLUSIONS

1. Minerals deposits are considered commercially viable for filler applications when the mineral could be applied without special treatment. However, dry beneficiation is preferable than wet operations to avoid extra operations like filtration and dryness of fine and ultrafine ranges.
2. High grade white sand sample was subjected to dry beneficiation including sieve classification and RE high gradient magnetic separation. The clean sample was ground to prepare pure silica flour.
3. Silica flour was applied in polypropylene masterbatch formulation with various additions. Results showed gradual improvement in Young's modulus as well as the impact strength with increasing silica content in the blend. An increase in the yield stress was taken place at silica content of 3%. All silica filled blends showed dramatic drop in the strain measures. Yet some studies concluded that sample orientation controlling during extrusion could improve strain property as well as impact strength.
4. The addition of some surface modifiers e.g. SEBS and SEBS-g-MA was shown to improve some physical properties of silica filled/PP blends due to the increase in the mineral/ polymer interfacial wettability

ACKNOWLEDGMENT

The authors would like to express their great gratitude to Prof. Friedrich, C. ; Dr. Nitz, H., and all the assistance staff of Freibrger Materialforschungzentrum, der Albert-Ludwigs-Universitat, Germany for supporting this work through the DFG programms.

REFERENCES

O'DRISCOLL, M., "Plastic Compounding, Where Mineral Meets Polymer", Industrial Minerals, pp 35-43, December 1994

TRIVEDI, N.C., HAGEMEYER, R.W., "Fillers and Coatings", Industrial Minerals and Rocks, 6 th Edition, Senior Editor Donald D. Carr, 1994

LEE, S.,"Thermal, Mechanical and Morphological Characterization of Highly Filled Polyethylene Film", International Conference of Alternative White Pigments and TiO_2 Extenders for Coatings, Paper and Plastics, Orlando, USA, 2000

DEARMITT, C., "Filled-PP Possibilities and Optimization", International Conference of Alternative White Pigments and TiO_2 Extenders for Coatings, Paper and Plastics, Orlando, USA, 2000

LOFTHOUSE, C.H., "Production of Mineral Fillers", International Conference of Filled Polymers and Fillers "Eurofillers 97" Manchester, UK, 1997

JOHNSTON, J. H., "High Performance Natural Amorphous Silicas and Silicates for the Paper Industry", Advancing Papermaking 97, Frankfurt, Germany, Oct. 1997

BRYK, M.T., "Degradation of Filled Polymers" Ellis Horwood, London, 1991

SCHERBAKOFF, N., "Rheological, Interfacial and Morphological Changes Produced By Fillers in Immiscible blends", Diss. Abstr. Int., Vol. 54, No. 4, pp.257, Oct. 1993

PAYNE, H. F., "Organic Coating Technology", John Willey and Sons Publications, New York, 1985

ZHANG, Y.; CAMERON, J., "Silica Particle/Glass Fibre-Reinforced Polyester Resin", Journal of Composite Materials,USA, Vol. 27, No. 11, pp. 1114-1127, 1993

SHANG, S. W.; WILLIAMS, J. W.; SODERHOLM, K-J. M., "How the Work of Adhesion Affects the Mechanical Properties of Silica-Filled Polymer Composites", Journal of Material Science, UK, Vol. 29, No. 9, pp. 2406-2416, May 1994

LEEMPOEL, P., "Filler/Polymer Interface and Performance of Silicon Elastomers", Filled Polymers and Fillers Conference, Manchester, UK, 1997

SAHNOUNE, F.; KARAD, S.; LOPEZ CUESTA, J.-M. CRESPY, A., "Effect of Fillers and Interfacial Agents on the Mechanical and Morphological Properties of HDPE/PS Blends", International Conference of Filled Polymers and Fillers, Manchester, UK, 1997

KAULY, T.; KAREN, B.; SIEGMANN, A., NARKIS, M., "Highly Filled Particulate Thermoplastic Composites", Journal of Material Science, Vol. 32, Iss 3, 1997

LYMAN, M.J., "Silica Improves Thermoset Properties", Plastic Compounding , USA, Vol. 14, No. 7, pp. 61-63, Nov.-Dec., 1991

KRYSZTAFKIEWICZ, A.; MAIK, M.; RAGER, B., "Comparison of Waste Silica Fillers Modified With Various Proadhesive Compounds", Journal of Material Science ,UK, Vol. 27, No. 13, pp. 3581-3588, July 1992

STRICKER, F., FRIEDRICH, C., MULHAUPT, R., "Influence of Morphology on Rheological and Mechanical Properties of SEBS-Toughened, Glass-Bead-Filled Isotactic Polypropene", Journal of Applied Polymer Science, Vol.69, pp 2499-2506, 1998

VALJI, S.E., "Processing Technology, Increasing Profits in Industrial Minerals", Industrial Mineral Journal, Sept., 1999

HAWLEY, G.C., "Opacifiers in Paint & Plastics - An Overview", International Conference of Alternative White Pigments and TiO2 Extenders for Coatings, Paper and Plastics, Orlando, USA, 2000

FELLAHI, S.; BOUKOBBAL, F., "Study of the Effect of Fumed Silica on Rigid PVC Properties", Journal of Vinyl Technology, USA, Vol. 15, No. 1, pp. 17-21, Mar., 1993

GASKELL, P., "Mineral Fillers For Polypropylene", International Conference of Filled Polymers and Fillers, 8-11 Sept. Manchester, UK, pp 281-284, 1997

FOURTY, G., "Talc in Polypropylene", International Conference of Filled Polymers and Fillers, Manchester, UK, 1997

Ibrahim S. S., El-Midany A. A.,*Wpływ trójblokowych polimerów na poprawę mechanicznych właściwości materiałów kompozytowych wykonanych z polipropylenu z dodatkiem mączki kwarcowej.* Physicochemical Problems of Mineral Processing, 42 (2008), 165-176 (w jęz. ang)

Proszki mineralne są dodawane w trakcie tworzenia polimerowych matryc w przemysle termoplastycznych tworzyw sztucznych, dla modyfikacji cech fizycznych nowopowstałych materiałów kompozytowych. Przykładowo, dodanie dobrze rozdrobnionej mączki kwarcowej do czystej matrycy polipropylenowej (PP) powoduje korzystne zmiany w cechach produktu finalnego. Można to tłumaczyć względnie niski przewodnictwem cieplnym kwarcu. W badaniach, czysta mączka kwarcowa była mieszana z polipropylenem w celu przygotowania odpowiedniej receptury dla przemysłu tworzyw sztucznych. Dodatek mączki kwarcowej był różny i wynosił: od 1,5 do 15 % objętościowych. Otrzymane wyniki wskazują na poprawę cech fizycznych produktu końcowego takich jak: moduł Younga, wytrzymałość plastyczna i mechaniczna. Co więcej, dodatek warcu powodował obniżenie odkształcenia produktu końcowego, który został otrzymany przy wprowadzeniu różnych ilości mączki kwarcowej. Odwrotnie, dodane blokowego polimeru SEBS (styren-etylen/butylen-styren) i jego szczepionej formy przy użyciu bezwodnika maleinowego, spowodowało podwyższenie zwilżalności powierzchni kompozytu kwarc/PP. Dodanie SEBS nie spowodowało poprawę modułu Younga ani wytrzymałości plastycznej. Jednakże, wyraźna poprawa nastąpiła w odporności na uderzenie i wytrzymałości mechanizcnej materiału.

słowa kluczowe: krzemionka, polimery, właściwości, moduł Younga, odporność na udar, polipropylen

Physicochemical Problems of Mineral Processing, 42 (2008), 177-184
Fizykochemiczne Problemy Mineralurgii, 42 (2008), 177-184

Beata Miazga*, Władysława Mulak**,

LEACHING OF NICKEL FROM SPENT CATALYSTS IN HYDROCHLORIC ACID SOLUTIONS

Received May 15, 2008; reviewed; accepted July 31, 2008

The results of hydrochloric acid leaching of nickel from spent catalysts used for methanation of small quantities of carbon oxide from hydrogen and ammonia synthesis gases (RANG-19), as well as for hydrogenation of benzene to cyclohexane (KUB-3) are reported. The effects of acid concentration, temperature, solid-to-liquid ratio and reaction time on nickel and aluminium leaching were examined. The leaching of nickel is more affected by temperature in the case of KUB-3 catalyst than RANG-19. After one hour leaching at 60^{o}C in 3.0M HCl solution the extraction of nickel from RANG-19 catalyst amounts to 74%, whereas for KUB-3 after 45 min of leaching extraction of nickel is 99%. The highest leaching efficiency of nickel from both the catalysts are found to be: 3.0M HCl solution, temperature 60^{o}C, solid to liquid ratio of 1/10, particle size 3-8 mm. In these conditions 99% of nickel is extracted from KUB-3 catalyst after 3 hours of leaching, and 98% of nickel from RANG-19 after 4 hours of leaching, respectively.

key words: spent catalyst, nickel, leaching, hydrochloric acid

INTRODUCTION

Increasing demand for nickel requires further intensive studies of its extraction methods from low-grade ores and secondary resources. Extraction of nickel can be effectively performed from spent catalysts. Recycling of spent catalysts has become an unavoidable task not only to lower their costs but also to reduce the catalysts waste in order to prevent the environmental pollution. Nickel is widely used as a catalyst in several technological processes: in hydrogenation, hydrodesulphurisation, hydrorefin-

* University of Wroclaw, Institute of Archeology, Koszarowa 3, 51-149 Wrocław, Poland
** Wrocław University of Technology, Chemical Department, Wybrzeże Wyspiańskiego 27, 50-370 Wrocław, Poland; wladyslawa.mulak@pwr.wroc.pl

ing including fat hardening process (Ni, Mo/Al_2O_3, NiO/Al_2O_3, Raney nickel alloy); in refinery hydrocracing (NiS, $WS_3/SiO_2Al_2O_3$); in methanation of carbon oxide from hydrogen and ammonia synthesis gases (NiO/Al_2O_3, $NiSiO_2$) (Thomas, 1970). Typically, nickel spent catalysts contain metallic nickel and nickel oxide, although nickel aluminate, spinel-like compounds and nickel sulphides may occasionally occur, as well as admixtures of coke, hydrocarbons or fat.

Recently, relatively great attention has been paid to the research connected with the recovery of nickel from secondary resources (Mulak et al., 2005).

Invascan and Roman (1975) reported on the recovery of nickel from a spent catalyst used in the ammonia plant by leaching in sulphide acid. The nickel was recovered as $NiSO_4$ with high 99% yield. Al-Mansi and Abdel Monem (2002) studied the sulphuric acid leaching process for the recovery of nickel as a sulphate from a spent catalyst in the steam reforming industry. It was also shown that the high recovery of 99% nickel as nickel sulphate was achieved.

Chaudhary et al.,(1993) reported on hydrochloric acid leaching process for the recovery of nickel as nickel oxide from a spent catalyst containing 17.7% Ni. They found that the maximum of nickel extraction (73%) could be achieved by carrying out the leaching process with 28.8% HCl at 80^{o}C. In an attempt to further improve the nickel extraction the application of chlorine gas was investigated, however no appreciable change has been observed. Kolosnitsyn et al.,(2006) studied the recovery of nickel from a spent catalyst used for the steam conversion of methane. They found that the leaching of nickel is limited by the bulk of the leaching solution. In turn, Sulek et al.,(2004) and Mulak et al.,(2005) investigated a sulphuric acid leaching of spent catalysts used for methanation as well as for hydrogenation of benzene. The authors reported that nickel extraction from spent methanation catalysts is limited by a surface reaction. In the case of benzene hydrogenation catalyst diffusion through the solid is the slowest step of the process. Several other methods have been also reported for the leaching of nickel from a spent refinery catalyst (Furimsky, 1996).

In this paper the effects of hydrogenation acid concentration, temperature, solid/liquid ratio and the stirring speed on the extraction of nickel and aluminium from two different industrial spent catalysts (KUB-3 and RANG-19) have been investigated.

The main reaction for nickel extraction from both the catalysts is as follows:

$$NiO + 2HCl = NiCl_2 + H_2O, \quad (1)$$

whereas the side reaction is:

$$\alpha\text{-}Al_2O_3 + 6HCl = 2AlCl_3 + 3H_2O. \quad (2)$$

The rate of the side reaction is very slow since α-Al_2O_3 is inert towards acids.

EXPERIMENTAL

MATERIALS

Two investigated in the paper spent catalysts (NiO/Al_2O_3) were obtained from Fertilizer Research Institute in Pulawy (Poland). Catalyst KUB-3 was used for hydrogenation of benzene to cyclohexane, whereas RANG-19 was applied for methanation of small quantities of carbon oxide from hydrogen and ammonia synthesis gases. Both spent catalysts were in form of granules with a diameter of 3.0-8.0 mm.

Table1. Chemical analysis of spent catalysts

Element, %	Ni	Al	Ca	Mg	C	H
KUB-3	30.1	18.2	2.55	0.05	2.45	1.17
RANG-19	13.5	40.2	0.33	0.05	1.08	0.31

LEACHING EXPERIMENTS

The leaching experiments were performed in a 500 cm^3 glass reaction vessel immersed in a controlled temperature bath during 60 min. At the start of the process, the spent catalyst sample as granules of size 3.0-8.0 mm (0.25g) was added to 200 cm^3 of hydrochloric acid solution (at desired concentration and temperature). The reaction mixture was agitated at a rate of 600 rev/min. After selected time intervals 1 cm^3 solution samples were taken for determination of nickel by AAS method. The aluminium concentration in the final solution was determined complexometrically.

RESULTS AND DISCUSSION

EFFECT OF STIRRING SPPED

The influence of the stirring speed on the nickel extraction from the spent catalysts (RANG-19 and KUB-3) was investigated in the solution containing 2.0 M HCl at 50^oC. The variation of the stirring speed within the range of 300-1200 rev/min had no effect on the reaction rate. This indicates that the reactant diffusion from the solution toward the surface of particles, as well as the reaction products away from the particles to the solution occurs quickly and hence does not control the leaching rate within the range of the stirring speed tested. All the subsequent experiments were carried out at a stirring speed of 300 min^{-1} to assure invariance of this parameter.

EFFECT OF HYDROCHLORIC ACID

The influence of HCl concentration on the leaching efficiency was determined by varying the initial concentration of the acid from 1.0 to 5.0 M.

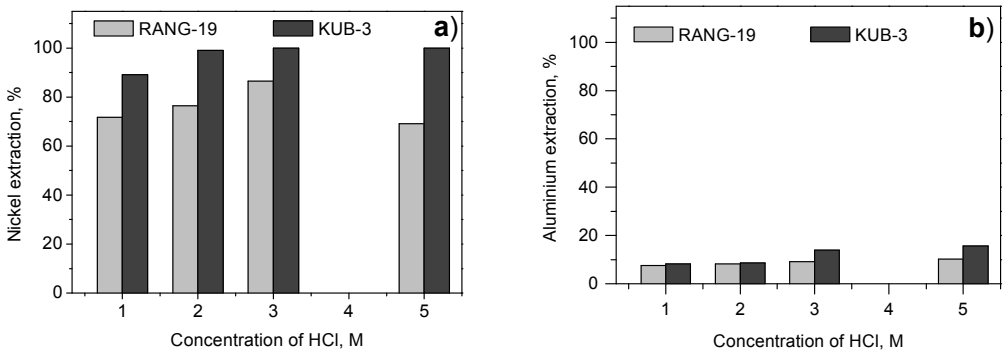

Fig. 1. Effect of hydrochloric acid concentration on nickel and aluminium extraction at 50°C after 1 hour leaching: a) nickel extraction, b) aluminium extraction

The extraction of nickel from KUB-3 catalyst was practically not affected by HCl concentration in the range from 2.0 to 5.0 M. In the case of RANG-19 catalyst, however, increasing the HCl concentration from 1.0 to 3.0 M, the nickel extraction was growing up from 71 to 86%, respectively, whereas for 5.0 M HCl a decrease of leaching efficiency was observed. The latter was probably caused by the fact that all the acid had been already reacted up to this moment. In turn, aluminium is feebly extracted (about 8% for RANG-19, and 15% for KUB-3 catalyst) for the above HCl concentrations.

EFFECT OF TEMPERATURE

The leaching was performed within temperature range 30-70°C with 2.0 M hydrochloric acid solution. The kinetic data for temperature influence on nickel extraction from both the catalysts are presented in Figure 2a and 2b, respectively.

The extraction of nickel is more affected by temperature in the case of KUB-3 catalyst than RANG-19. For instance, after one hour leaching at 50°C the extraction of nickel from RANG-19 catalyst achieved 74%, whereas for KUB-3 after 45 min of leaching the extraction of nickel raised up to 99%. During each one hour leaching the temperature change within the range 30-70°C causes a gradual increase in aluminium extraction from 8 to 14% for RANG-19, and from 2 to 10% for KUB-3. Figure 3 shows the difference in the leaching rate between both the catalysts versus leaching time at 50°C. In order to achieve 98% of nickel from RANG-19 catalyst one needs even up to 5 hours of leaching.

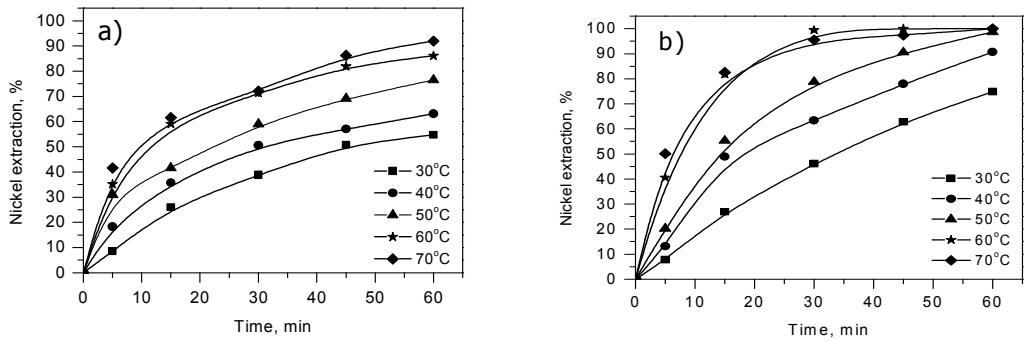

Fig. 2. Effect of temperature on nickel extraction in 2.0 M HCl: a) RANG-19 b) KUB-3.

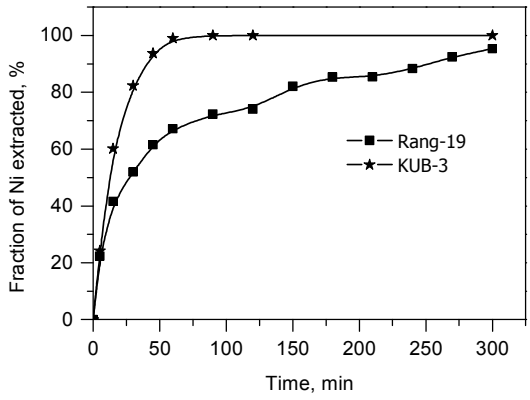

Fig. 3. Influence of leaching time on nickel extraction from the spent catalysts in 2.0 M HCl at 50°C.

EFFECT OF THE SOLID TO LIQUID RATIO

Figure 4 illustrates the influence of the pulp density on nickel extraction at 50°C in 2.0 M HCl after one hour leaching.

The solid to liquid ratio changed in the leaching tests from 1/40 to 1/5 [w/v]. Within this range the pulp density has practically no influence on the extraction of nickel from Rang-19 catalyst. However, for KUB-3 due to the overstoichiometric nickel content (Eq. 1) with respect to the hydrochloric acid in the pulps of high solid to liquid ratio (particularly for w/v =1/5), a decrease in nickel extraction is observed.

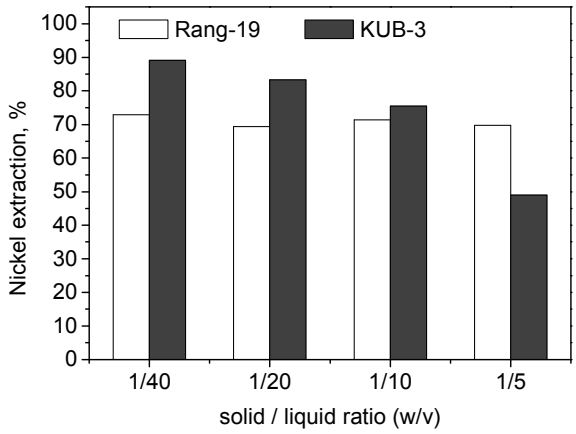

Fig. 4. Influence of the solid to liquid ratio on nickel extraction from the spent catalysts in 2.0 M HCl at 50°C after 1 hour leaching.

CONCLUSIONS

1. The leaching rate of nickel from the investigated spent catalysts is independent of the stirring speed. It indicates that the reaction is not controlled by diffusion in the liqiud phase.
2. The leaching rate of nickel depends more strongly on temperature for KUB-3 catalyst than for RANG-19.
3. For aluminium extraction the effect of temperature variation was also more distinguishable for KUB-3 catalyst than for RANG-19.
4. Based on the leaching experiments on a laboratory scale the highest leaching efficiency of nickel in hydrochloric acid for both the catalysts are found to be: 3.0M HCl solution, temperature 60°C, the solid to liquid ratio of 1/10. The particle size 3-8 mm - such particles were delivered from the technological process. In the above conditions 99% of nickel was extracted from KUB-3 spent catalyst after 3 hour leaching time, and respectively 98% from RANG-19 catalyst after 4 hours of leaching.

REFERENCES

AL-MANSI N.M., ABDEL MONEM N.M., 2002, *Recovery of nickel oxide from spent catalyst.* Waste Management 22, 85-90.

CHAUDHARY A.J., DONALDSON J.D., BODDINGTON S.C., GRIMES S.M., 1993, *Heavy metals in*

environment. Part II: a hydrochloric acid leaching process for the recovery of nickel value from a spent catalyst. Hydrometallurgy 34, 137-150.

FURIMSKY E., 1996, *Spent refinery catalysts: environment, safety and utilization*. Catalysis Today 30, 223-286.

IVASCAN S., ROMAN O., 1975. *Nickel recovery from spent catalyst*. Bul. Inst. Politeh. Iasi, Sect. 2, 21,47-51.

KOLOSNITSYN V.S., KOSTERNOVA S.P., YAPRYNTSEVA O.A., IVASHCHENKO A.A., ALEKSEEV S.V., 2006, *Recovery of nickel with sulfuric amid solutions from spent catalysts for steram conversion of methane*. Russian Journal of Applied Chemistry, 79, 539-543.

MULAK W., MIAZGA B., SZYMCZYCHA A., 2005, *Kinetics of nickel leaching from spent catalyst in sylphuric amid solution.* Int.J.Miner.Process., 77, 131-235.

MULAK W., MIAZGA B., SZYMCZYCHA A., 2005, *Hydrometalurgiczny odzysk niklu z materiałów odpadowych.* Rudy Met. Nieżelaz. 50, 114-119.

THOMAS C.L.; 1970, *Catalytic Process and Proven catalysts*. Academic Press, New York and London.

SUŁEK B., SZYMCZYCHA A., MULAK W., 2004, *Sulphuric acid leaching of nickel from a spent catalysts.* Proceedings of Global Symposium on Recycling, Waste Managment and Clean Technology, Madryt, 2081-2090.

Miazga B., Mulak W., *Ługowanie niklu z zużytych katalizatorów w roztworze kwasu solnego,* Physicochemical Problems of Mineral Processing, 42 (2008), 179-186 (w jęz. ang).

Przedstawiono wyniki ługowania niklu z dwóch zużytych katalizatorów: katalizatora metalizacji (RANG-19) oraz katalizatora uwodornienia benzenu (KUB-3), stosując roztwory kwasu solnego. Określono wpływ stężenia HCl, temperatury, stosunku fazy stałej do ciekłej oraz intensywności mieszania na wydajność ługowania niklu. Wykazano, że temperatura znacznie bardziej wpływa na szybkość ługowania niklu z katalizatora KUB-3 aniżeli z RANG-19. Po 1 godzinie ługowania w temperaturze 60^{o}C w 3.0M HCl ekstrakcja niklu z katalizatora RANG-19 wynosi 74%, podczas gdy z katalizatora KUB-3 po 45 min wyługowania niklu wynosi 99%. Najwyższą wydajność ługowania niklu z obu katalizatorów bez dodatkowego rozdrobnienia (granulki 3-8 mm) uzyskano w 3.0M roztworze HCl, w temperaturze 60^{o}C przy stosunku fazy stałej do ciekłej 1/10. W powyższych warunkach ekstrakcja niklu z katalizatora KUB-3 wynosi 99% po 3 godzinach ługowania, natomiast 98% niklu wyługowano z katalizatora RANG-19 po 4 godzinach ługowania.

słowa kluczowe: zużyty katalizator, nikiel, ługowanie, kwas solny

Physicochemical Problems of Mineral Processing, 42 (2008), 185-194
Fizykochemiczne Problemy Mineralurgii, 42 (2008), 185 -194

Mohamed Fahmy Raslan*

BENEFICIATION OF URANIUM-RICH FLUORITE FROM EL - MISSIKAT MINERALIZED GRANITE, CENTRAL EASTERN DESERT, EGYPT

Received June 5, 2008; reviewed; accepted July 31, 2008

In a previous study, the occurrence and mineralogy of unique highly radioactive fluorite-rich granites from El-Missikat uranium occurrence was discussed. The uranium content of the bulk composite sample collected from the studied fluorite - bearing granites equal 1950 ppm. The presence of uranium element in the core of fluorite is quite evident. The fluorite crystals are mainly responsible for the radioactivity in the granitic samples. Microscopic examination for the accessory heavy minerals revealed that radioactive fluorite represents about 20% by weight of the original rock sample. Also, radioactive fluorite represents about 90% of the total accessory heavy minerals in addition to iron oxides and mica (fluoro-phlogopite). Physical upgrading of radioactive fluorite was carried out using gravitative and magnetic separation techniques. Under optimum conditions it was possible to attain a good concentrate with an acceptable recovery. Accordingly, the final concentrate contains up to 1.0274% U with a final recovery of 79.29% in a weight of 15.05% out of the original sample assays 0.1950% U.

key words: uranium, radioactive fluorite, heavy minerals, granite, upgrading

INTRODUCTION

El-Missikat granite pluton is located in the central part of the Eastern Desert at about 85 km midway between Safaga on the Red Sea Coast and Qena in the Nile Vally (Fig. 1). Uranium mineralization (mainly uranophane) is associated with jasperoid veins which occur within shear zones (Bakhit 1978; Abu Dief 1985; Hussein et al.,1986 and Abu Dief et al.,1997). However, unlike all the mineralized silicious veins in El-Missikat, visible deep blue to violet fluorite crystals occur as disseminations in

* Nuclear Materials Authority, Cairo, Egypt

the highly sheared granite of El-Missikat granite pluton with very strong radioactivity but without visible secondary uranium mineralization (Fig. 2a). The presence of uranium element in the core of fluorite is quite evident. Electron Microprobe analyses for El-Missikat radioactive fluorite revealed that the uranium content ranges from 0.10 to 0.22 % with an average of 0.06 % and thorium ranges from 0.25 to 0.75 % with an average of 0.25 %, Raslan (In preparation). Microscopic examination for the accessory heavy minerals revealed that radioactive fluorite represents about 20% by weight of the original rock sample.

The aim of this study is to investigate the potentiality of physical upgrading of the radioactive fluorite-rich granite using mainly gravitative and magnetic separation techniques.

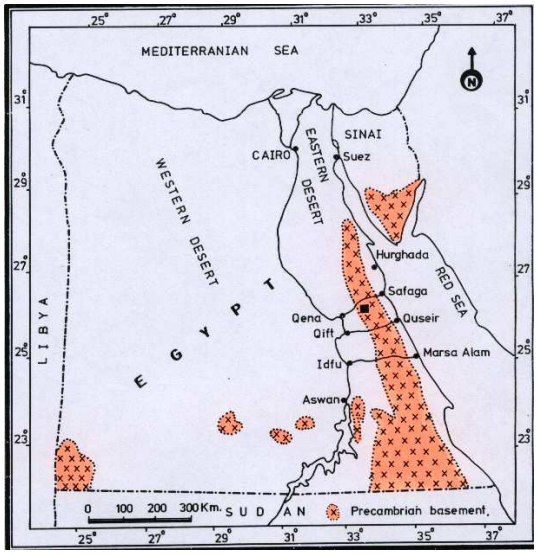

Fig. 1. Location map of El-Missikat uranium occurrence

a b

Fig. 2. a- Close-up photograph showing El-Missikat radioactive fluorite- bearing granite. b- Separated blue to violet radioactive fluorite crystals. Binocular microscope

EXPERIMENTAL METHODS

For the purpose of the present study a technological bulk composite sample weighing ~15 kg representing El-Missikat radioactive fluorite-bearing granite was used. The latter was subjected to the conventional mineral separation procedures namley; disintegration, sizing and heavy liquid separation by bromoform (2.85 gm/cm^3) to estimate the heavy mineral content of each size fraction. The magnetic proparties of the studied heavy mineral fractions was investigated using Frantz Isodynamic separator.

The physical benficiation applied in the present study mainly consists of comminution and concentration processes. The latter were carried out using the laboratory wet Wilfely shaking table (No.13) and the Carpco high intensity lift-type magnetic separator Model MLH (13) III-5 for gravity and magnetic separation respectively. Uranium content of the various size fractions and their concentrates was determined using gamma spectrometric analysis.

PRELIMINARY INVESTIGATION

A preliminary crushing test was carried out to reduce the size of the head sample to pass 1.00 mm screen for the liberation investigation. The deslimed fraction was dried and fractionated using a set of screens starting from 1.00 mm down to 0.045. Microscopic examination were carried out for the various size fractions.

It was found that the size fraction (- 0.800 +0.045) mm can be considered as the best grain size for good liberation for the radioactive fluorite and also suitable for the used mineral separation techniques. Heavy minerals mineralogy revealed that the content of the accessory minerals in the studied granitic sample amount to about 20%. Radioactive blue to violet fluorite (Fig. 2b) represents about 90% of the obtained heavy fractions and the rest are minor amounts of magnetite, hematite and mica.

A representative quantity of the total bulk heavy mineral fraction was obtained and subjected to magnetic separation using hand magnet in order to remove the magnetite. A proper magnetite free - feed was then prepared and subjected to magnetic separation using the Frantz Isodynamic separator (L-I). The purpose was to determine the behaviour of each heavy mineral during various magnetic field intensities. The setting of the separator during this study was (20°) forward slope and (5°) side slope. The obtained results shown in Table 1 revealed that the majority of fluorite crystals (92.75%) are concentrated as non-magnetic fraction at 1.5 ampers. About 7.25% of the total fluorite were attracted at magnetic fractions mainly due to the presence of iron oxide inclusions in these crystals.

It is quite clear that the difference in the magnetic susceptibilities between fluorite and other heavy minerals (magnetite, hematite and mica) would constitute the basis for their final magnetic separation. On the other hand, differences in the specific

gravities between the studied heavy minerals and the associated gangue minerals would render the gravitative concentration by shaking table as an efficient tool for their primary separation.

Table 1. Cummulative percent of individual minerals separated as magnetic fractions at different current intensities. Frantz Isodynamic Separator at setting of 20° forward slope and 5° side slope

Current (A) / Mineral	0.2	0.5	0.7	1.0	1.2	1.5	Non-mag. 1.5
Fluorite	0.30	0.70	1.20	1.35	4.00	7.25	100.00
Hematite	3.50	96.40	100.00	-	-	-	-
Mica	100.00	-	-	-	-	-	-

SAMPLE PREPARATION

Preparation of a suitable feed for the separation is very useful for attaining the maximum efficiency of the used equipment. The size of the separated particles is the most important factor affecting separation.This matter has been discused by several authors (Taggart 1944; Jones 1959; Pryor 1974 and Gaudin 1980). According to Wills (1979), the correct degree of liberation is the key to the success in mineral processing. Controlled comminution operation (crushing and grinding) was carried out on representative bulk sample collected from El-Missikat shear zone (assaying 0.1950% U) in order to reduce the size of the head sample to pass 5.0mm screen. This has been achieved by applying a combination of jaw crushers and a roll mill crusher. The oversized (+5 mm) fraction was recycled to the secondary jaw crusher. The under- size (-5 mm) fraction was fed to a roll mill crusher followed by screening at 0.8 mm. The +0.800 mm fraction was recycled to the roll mill while the under size (-0.800 mm) was deslimed using a desliming cone. The deslimed size fraction (-0.800 mm) was dried and screened using a set of screens represented by (0.800, 0.600, 0.400, 0.200, 0.045 mm) screens. The latter was chosen in the light of liberation investigation and to save the majority of fluorite crystals in the liberation size fraction. The size fractions were collected, weighed and representative portions from each fraction was subjected to uranium determination using gamma spectrometric analysis. The sequence of processes followed in the crushing and liberation of the studied samples is presented in the flowsheet (Fig. 4). The obtained results of size analysis and the distribution of uranium in different size fractions are given in Table 2.

Both the -0.045 mm and slimes fractions contained 13.52% of the total uranium in the original sample. The obtained results reveal that about 86.48% from the original uranium present in the original sample was saved within 90.20% by weight. Also, these results indicate that the crushing operation was successful for saving the majority of radioactive fluorite within the deslimed size fracion (-0.800 +0.045).

Table 2. Granulometric analyses and uranium distribution among the various size fractions of El-Missikat radioactive fluorite-bearing granite

Size (mm)	Wt %	Assay eU%	Distribution eU%
-0.800 +0.600	20.92	0.1680	18.02
-0.600 +0.400	22.95	0.1790	21.07
-0.400 +0.200	30.35	0.1950	30.35
-0.200 +0.045	15.98	0.2080	17.04
Deslimed -0.600 +0.045	90.20	0.1870	86.48
-0.045 +Slimes	9.80	0.2690	13.52
Original	100.00	0.1950	100.00

GRAVITATIVE SEPARATION

In order to reduce the bulk light gangue minerals from the deslimed size fractions and attain clean concentrate for each size fraction, the deslimed size fractions (-0.800 + 0.600 mm), (-0.600 + 0.400 mm) and (-0.200 + 0.045 mm) were separately fed to the Wilfely shaking table to obtain a primary concentration.

Table 3. Assay and material balance of the various products of gravitative separation

Size (mm)	Products	Wt%	Assay eU%	Distribution eU%
- 0.800 +0.600	Concentrate	3.66	0.8550	15.95
	Tails	17.26	0.0233	2.07
	Feed	20.92	0.1680	18.02
- 0.600 +0.400	Concentrate	4.15	0.8920	18.98
	Tails	18.80	0.0217	2.09
	Feed	22.95	0.1790	21.07
- 0.400 +0.200	Concentrate	5.61	0.9900	28.48
	Tails	24.74	0.0148	1.87
	Feed	30.35	0.1950	30.35
- 0.200 +0.045	Concentrate	3.06	1.0250	16.08
	Tails	12.92	0.0145	0.96
	Feed	15.98	0.2080	17.04

This operation was optimized by using less feed, less water, less tilt as much as possible, shorter length of stroke beside a low speed of the deck. The obtained cleaner concentrates were mainly composed of fluorite, iron oxides and mica. The efficiency of tabling was found to increase by decreasing the size range of the feed.

The results of the tabling operations shown in Table 3 and Table 5 reveal that the final concentrates of tabling operations containing 0.9418% U with a recovery of 91.92% in 18.27% by weight out of the deslimed size fraction (-0.800 +0.045) feed having 0.1870% U.

MAGNETIC SEPARATION

The tabling concentrate of each size fraction was then subjected to the laboratory Carpco high intensity lift-type magnetic separator Model MLH (13) III-5 in order to obtain pure concentrates of radioactive fluorite. In this type of dry separator, the magnetic materials are lifted magnetically up aginest gravity in comparison to other separators that have gravity operating in the same general direction as magnetic force. This separator utilizes a vibratory feeder to transport the feed horizontaly through an adjustable magnetic field zone where the magnetic force acting on the particles is perpendicular upwards. The advantage of this principle is a production of high purity magnetic products and also separation of more than one magnetic materials. The principles and gap adjustment of the used separator is shown in Figure 3.

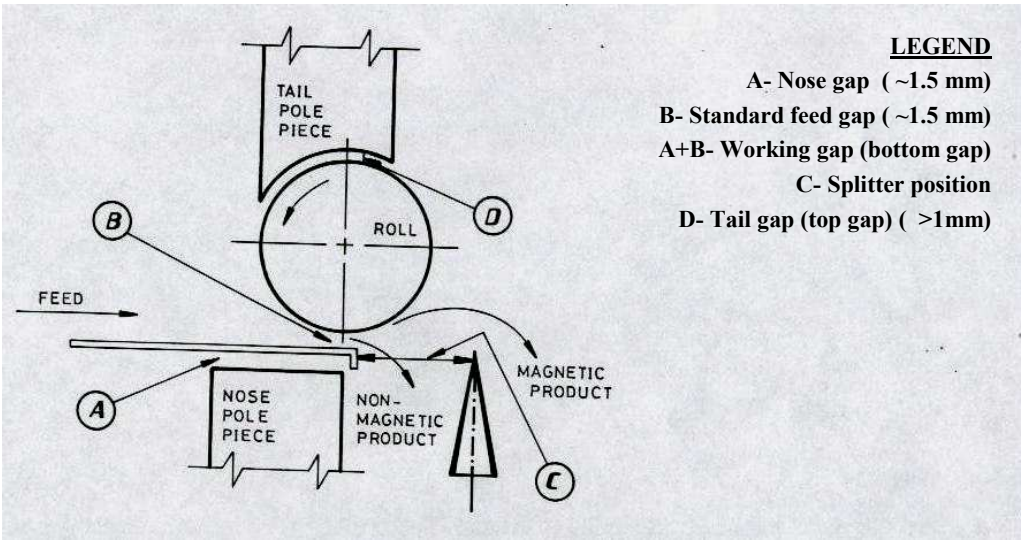

Fig. 3. Gap adjustment diagram for the high intensity
lift-type magnetic separator (Carpco), Model MLH (13) 111-5

Magnetic separation was achieved at a magnetic field current of 1.0 amp. The speed of the roll and the feed rate were adjusted at 50 rpm and 200g/min respectively. The air gap between the induced roll and the feed plate was 1.5 cm. The dividing splitter was controlled visually. The obtained results in Table 4 indicated that the final non-magnetic concentrate of radioactive fluorite assays up to 1.0274% U with a recovery of 99.75% in 91.32% by weight out of feed having 0.9418% U.

Table 4. Assay and material balance of the different products of magnetic separation for the concentrates of tabling.

Size (mm)	Products	Wt%	Assay, U%	Distribution, U%
-0.800 +0.600	Magnetic fr.	0.37	0.0310	0.06
	Non mag. fr.	3.29	0.9420	15.89
	Concentrate of tabling	3.66	0.8550	15.95
-0.600 +0.400	Magnetic fr.	0.38	0.0280	0.05
	Non mag. fr.	3.77	0.9800	18.93
	Concentrate of tabling	4.15	0.8920	18.98
-0.400 +0.200	Magnetic fr.	0.45	0.0230	0.05
	Non mag. fr.	5.16	1.0750	28.43
	Concentrate of tabling	5.61	0.9900	28.48
-0.200 +0.045	Magnetic fr.	0.23	0.0230	0.04
	Non mag. fr.	2.83	1.1050	16.04
	Concentrate of tabling	3.06	1.0250	16.08

Table 5. Material balance of the proposed flowsheet for upgrading El-Missikat radioactive fluorite

Products	Wt%	Assay, U%	Distribution, U%
1) Desliming and sizing:			
-0.800 +0.045 mm	90.20	0.1870	86.48
Slimes and -0.045 mm	9.80	0.2690	13.52
Original (Head Sample)	100.00	0.1950	100.00
2) Gravitative separation:			
Final Concentrates of Tabling	16.48	0.9418	79.49
Final Tails of Tabling	73.72	0.0185	6.99
-0.800 +0.045 mm	90.20	0.1870	86.48
3) Magnetic separation:			
Final fluorite Concentrates (non-magnetic)	15.05	1.0274	79.29
Final magnetic fraction	1.43	0.0265	0.20
Final concentrates of Tabling	16.48	0.9418	79.49

A material balance for the different processes is shown in Table 5. The final non-magnetic fluorite concentrate contains up to 1.0274% U with a final recovery of 79.29% in a weight of 15.05% out of the original sample assays 0.1950% U. A schematic sequence of the processes followed in the upgrading operations is presented in the form of a proposed flowsheet in Figure 4.

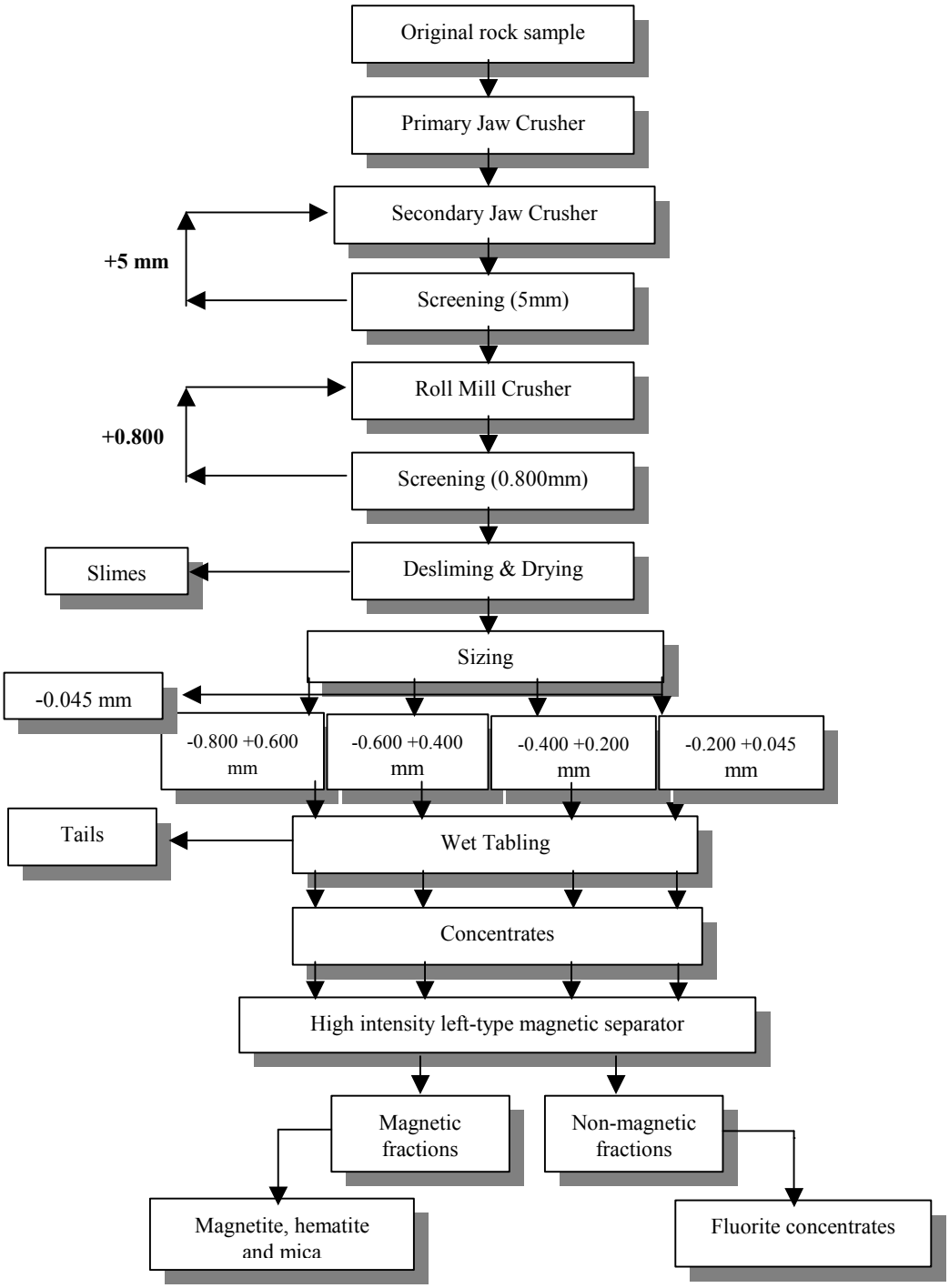

Fig. 4. A proposed flowsheet for upgrading radioactive fluorite from El-Missikat fluorite-bearing granite

CONCLUSIONS

Mineralogy of the studied radioactive fluorite-bearing granite from El-Missikat area revealed that radioactive fluorite represent about 20% by the weight of the original rock sample. Radioactive blue to violet fluorite represent about 90% of the total accessory heavy minerals. Gravitative and magnetic separation were used respectively to upgrading the radioactive fluorite. The final non-magnetic fluorite concentrate contains up to 1.0274% U with a final recovery of 79.29% in a weight of 15.05% out of the original sample assays 0.1950% U.

REFERENCES

ABU DEIF, A., (1985): Geology of uranium mineralization in EL Missikat area, Qena-Safaga road, Eastern Desert, Egypt. M.Sc. Thesis, Al Azhar University, 109pp.

ABU DEIF, A., AMMAR, S. E. MOHAMED, N. A. (1997): Geological and geochemical studies of black silica at El-Missikat pluton, Central Eastern Desert, Egypt. Proc.Egypt. Acad. Sci. 47: 335-346.

BAKHIT, F. S., (1978): Geology and radioactive mineralization of Gabal EL-Missikat area, Eastern Desert, Egypt. Ph.D. Thesis, Faculty of Science, Ain Shams Univ., Cairo. 289 p.

GAUDIN, A. M. (1980): Principles of mineral dressing, TATA McGraw Hill publishing Co. Ltd, New Delhi.

HUSSEIN, H. A., HASSAN, M. A., EL-TAHIR, M. A., ABU DEIF, A. (1986): Uranium bearing siliceous veins in younger granites, Eastern Desert, Egypt. IAEA, TECDOC 361, 143-157.

JONES, M. P. (1959): Mineral dressing tests on the extraction of columbite and other heavy minerals from the Olegi younger granite, Rec. Geol. Surv. Nigeria (published in 1960).

PRYOR, E. J. (1974): Mineral processing. Applied Science publishers Limited. Third Edition, London.

RASLAN, M. F. (In preparation): Mineralogical and geochemical characteristices of uranium-rich fluorite in El-Missikat mineralized granite, Central Eastern Desert, Egypt.

TAGGART, A. F. (1944): Hand book of mineral dressing and industrial minerals. John Wiley and Sons, Inc. New York, London, Sedney.

WILLS, B. A. (1979): Mineral processing technology, Pergamon Press, Oxford, New York, Toronto, Sydney, Paris, Frankfurt.

Raslan M.F., *Wzbogacanie fluorytu bagatego w uran ze złoża El-Missikat o mineralizacji granitowej z pustyni w centralo-wschodniej części Egiptu.* Physicochemical Problems of Mineral Processing, 42 (2008), 185-194 (w jęz. ang)

Występowanie i właściwości mineralogiczne fluorytu o wysokim stopniu radiacji, ze złoża w El-Missikat, były dyskutowane we wcześniejszych pracach. Zawartość uranu w próbce pobranej do badań nad fluorytem wynosiła 1950 ppm. Obecność uranu w strukturze fluorytu była ewidentna. Kryształy fluorytu wykazywały znaczą radioaktywność. Badania mikroskopowe, prowadzone pod kątem akcesoryjnych minerałów ciężkich, potwierdziły, że radioaktywny fluoryt reprezentuje około 20 % wagowych pobranej próbki skalnej. Również, radioaktywny fluoryt stanowił około 90% całości akcesoryjnych minerałów ciężkich obok tlenków żelaza i miki. Fizyczne wzbogacanie radioaktywnego fluorytu zostało przeprowadzone stosując techniki grawitacyjne i separacji magnetycznej. Przy zastosowaniu optymalnych

warunków, jest możliwość wzbogacenie uranu do poziomu 1.0274% z końcowym uzyskiem 79.29 % (wag). Wychód masowy wynosi 15.05%, zaś zawartość uranu w nadawie wynosiła 0.1950%.

słowa kluczowe: uran, radioaktywny fluoryt, minerały ciężkie, granit, wzbogacanie

Physicochemical Problems of Mineral Processing, 42 (2008), 195-210
Fizykochemiczne Problemy Mineralurgii, 42 (2008), 195-210

Piotr Wodziński*

CERTAIN PROPERTIES OF HUMID GRANULAR MATERIALS

Received May 15, 2008; reviewed; accepted July 31, 2008

This study deals with the properties of humid granular materials. The processes involving these materials are very frequently encountered under industrial conditions because in fact the processing of completely dry materials does not exist. Water vapour is present in the air under any conditions which means a certain amount of moisture in the granular bed. A general friction coefficient of granular materials has been proposed as contributing to a moisture influence on processing. The friction coefficient constitutes a basic independent variable encompassing an impact of moisture on the behaviour of a humid granular material in the mechanical process. Furthermore, the function of outflow has been proposed as an important analytical-empirical parameter to describe the processing of solids.

key words: screening, friction in granular material, granular material, humidity, water capacity

INTRODUCTION

It must be mentioned that dry granular materials do not exist. A certain portion of a granular material even after its removal from a drier constitutes a two-phase solid-liquid system because it is exposed to water vapour present in the air. Hence, analysing a mechanical (dry) process with a granular material, e.g. screening, we deal with such a small amount of moisture that the granular material behaves as if it were dry though actually it contains some moisture. It is an appropriate increase in a moisture content in the granular material that influences its behaviour in the mechanical process.

Thus it is crucial to consider a moisture content in a granular material, in particular in the case of such mechanical processes as screening or proportioning. This study

* Technical University of Lodz, Faculty of Process and Environmental Engineering, Department of Process Equipment, Institute of Material Classification, wodzinsk@wipos.p.lodz.pl

describes certain notions whereby one may take into consideration an impact of humidity on the behaviour of grain layers in industrial and laboratory technological processes.

CHARACTERISTICS OF HUMID GRANULAR MATERIALS

The basic characteristic of a humid granular material is its moisture content, i.e. humidity:

$$W = \frac{g_w}{g_s} 100\% \tag{1}$$

where: g_w – mass of water in the material portion examined, kg
g_s – mass of a dry material portion, kg

In the real granular materials one distinguishes two types of moisture:

W_{pr} – passing moisture, defined by an amount of water which is removed during air drying, reaching an equilibrium state with the atmospheric humidity

W_h – air-dry material moisture comprising water remaining in the material after air drying, evaporated after drying at the temperature 105 - 110◦C.

We may consider the total humidity W_c which is the total of two previously mentioned types of moisture. The extent of a humid process is illustrated in the form of a numerical – humid curve in Fig.1. In Figure 1 three critical humidity coefficients are presented (a moisture content):

W_p – transient coefficient
W_d – dynamic humidity coefficient
W_s – static humidity coefficient

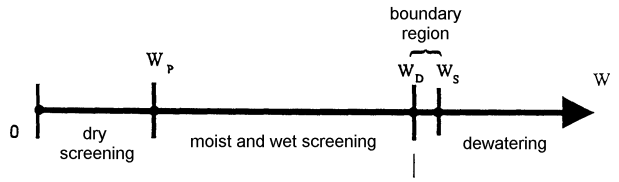

Fig. 1. Humidity axis

The transient coefficient W_p is defined in the following way: it is such humidity of granular material that causes the elongation of the time of a process. To exemplify, in the case of screening the time indispensable to screen the same mass of a humid material is elongated. It is not possible to establish one universal value of the transient humidity for all the materials screened. For one type of materials the moisture content 1–2% brings about a double elongation of the screening time. For other types the screening time is established on the level of 10–12%.

A granular bed at the lag time may be defined using the static humidity coefficient W_s. This is an amount of moisture (water) which may be contained in a granular bed (a granular layer) in the lag time. Nevertheless, when a granular bed is placed onto a vibrating screen, one may observe a quick removal of a certain amount of water from this bed and, thus, obtain the so-called dynamic humidity coefficient W_d. The dynamic humidity coefficient is always smaller that the static one. That is why the dynamic humidity coefficient of a granular bed may be defined as a moisture content in a material in spite of its exposure to the action of the inertial forces (the driving forces of the process).

Above the boundary $W_d - W_s$, defined by the dynamic and static humidity coefficient, one may notice the dehydration and washing zone of granular materials. In the case of certain granular materials one may observe such a considerable influence of moisture that a humid screening zone is not present. The separation of the upper and bottom class is possible under the exposure of excess water and it occurs in the dehydration or washing zone.

The subsequent essential parameter determining the mechanical processes, the process of humid screening in particular, is a shape of grains which constitute a granular bed. It is until recently that in the calculations concerning granular materials processing as well as in other processes one has applied a surface factor of a grain shape. The factor is defined as a quotient of the surface area of a grain to the surface area of a sphere, being of the same volume as the grain. Due to the fact that in the mechanical processes, including the process of screening, the application of this factor is seemingly unjustified, a spherical factor of a grain shape has been proposed. In a mineral grain we may distinguish the so-called main dimensions of a grain (Fig. 2) including the length, width and thickness of a grain (a, b, c respectively). Furthermore, having a > b > c, the spherical factor of a grain is given by the formula:

$$\varepsilon_K = \frac{b \cdot c}{a^2} \qquad 0 < \varepsilon_K \leq 1 \tag{2}$$

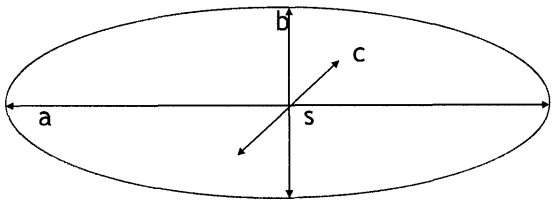

Fig. 2. Spherical factor of a grain shape

It is worth mentioning that for a cube and a sphere the factor reaches value 1. The more isometric a grain is, the more the value of ε_k approaches 1. The more anisometric

the grain is (e.g. the predominance of one dimension – a needle shape), the more ε_k approaches 0 but it never reaches this value.

The author of this paper proposes a different, simple method taking into account the grains of the materials which are subjected to different processing operations. Three basic shapes of grains are distinguished (Fig. 3):

- spherical grains (Fig. 3a)
- sharp-edge grains (Fig. 3b)
- irregular grains (Fig. 3c)

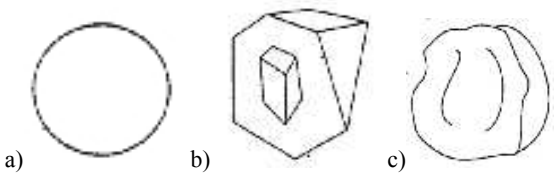

Fig. 3. Models of grain shape

The previous papers concerning the topic proposed 9 different grain shapes. Nonetheless, the results of the research of, for instance, the screening of one of the separated mixtures were similar and, thus, applying the method of the subsequent reductions of particular groups, the three aforementioned shapes have been proposed. It has been demonstrated that a great number of real grain materials, being screened and processed in different branches of the national economy, may bear a strong resemblance to one of the aforementioned groups. This way of describing a grain shape is based on attributing a concrete material to one model mixture and, next, on using the appropriate project correlations required for a given model mixture. The whole research carried out by the author of this study is done independently for three model materials which are as follows: spherical grains – agalite (ceramic material, siliceous, being, for example, waste in various chemical processes); sharp-edge grains – aggregate of rock materials; irregular grains – natural mining sands. The method which takes into consideration the shape of a grain is a very primitive one but for many materials it gives good practical results.

The last parameters extremely important in the processes of the granular material processing are an internal and external friction coefficient of those materials. Determination of those coefficients is done using the method of direct shearing, which is known in the literature as the Jenike method. To carry out such examination spherical boxes and a special research stand are used. In the investigation of direct shearing the idea of inducing such deformation of a sample (Fig. 4) is applied in order to have make it occur along the plane required. Next, a horizontal slip of one box with regard to another one – immovable – is forced with a simultaneous measurement of the shearing force. However, to determine the external friction coefficient of a given

grain medium on a given surface (a sieve, for instance) – one measures the force being needed to move the spherical box on this surface.

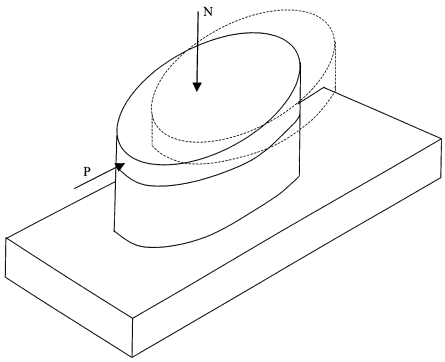

Fig. 4. Shearing boxes of linear motion (Jenike, 1964)

Another shearing box known apart from the Jenike box is a shearing box invented by Schulze (1996). The method is based on the rotating shearing motion of the box as in contrast with the previously analysed method of linear motion (Fig. 5). It must be underlined that applying the methods positive results may be gained which will characterise a humid grain material. Nevertheless, it is the Jenike method which has become more widespread nowadays. The shearing boxes of the device in a cross-section are demonstrated in Figure 6.

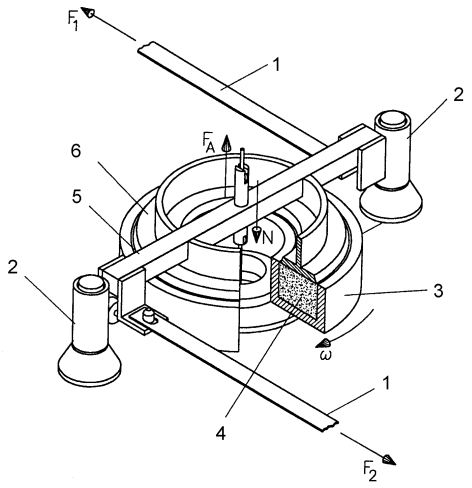

Fig. 5. Rotating shearing box (Schulze, 1996) 1 – pulling slat; 2 – guide roll; 3 – shearing box; 4 – granular material; 5 – support beam; 6 – cover

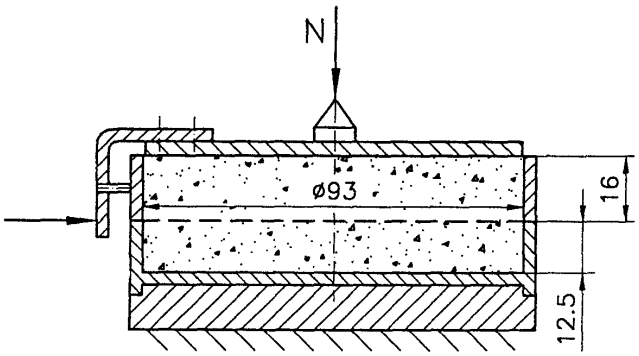

Fig. 6. Box of linear motion used for direct shearing of granular materials (Jenike, 1964)

To characterise the fluidity of a granular material one may use the factor ff_c [5]. It is a quotient of the tension of a material σ_1 to its resistance σ_c:

$$ff_C = \frac{\sigma_1}{\sigma_C} \tag{3}$$

According to Jenike [1964], the following ranges of the parameter may be distinguished:

ff_c <1 a non-flowing material

1 < ff_c < 2 a very cohesive material

2 < ff_c < 4 a cohesive material

4 < ff_c < 10 a slowly flowing material

10 < ff_c solely flowing

The dependencies (the extents of flowing) have been graphically demonstrated in Figure 7.

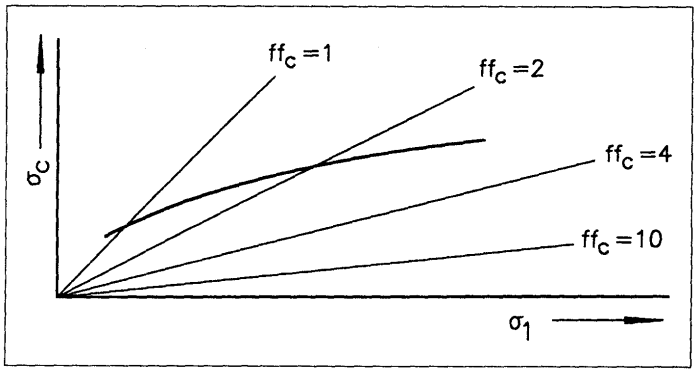

Fig. 7. Flowing zones of granular materials

RESULTS OF EXAMINATION OF GRANULAR MATERIALS MODEL PROPERTIES

MATERIALS AND METHODS

An important quality of a granular material, which is subjected to mechanical processing is a coefficient of internal friction. In Poland the research is in compliance with the standard requirements PN-88/B-04481. To carry out the examinations properly it is important to select an appropriate normal thrust which is reflected in the dependence of a shearing force upon the way of shearing. The curves obtained as a result of the test are of a shape demonstrated in Figure 8. The normal thrust is to be obtained by the method of the force N alteration in the shearing boxes (Fig. 6). The curve illustrates the state of the material consolidation surplus which may occur in the case of humid materials. Then, it is essential to decrease the load N. When we deal with the curve in the form 8b, then it means that the material is too loose and it becomes necessary to increase the load N (Fig. 9). On the examination of the shearing coefficient, which is to be applied to the characteristics of a granular material during screening, the normal thrust of a minimum value must be considered. Nonetheless, this minimum value of the normal thrust should enable to reach the curve demonstrated in Fig. 8c.

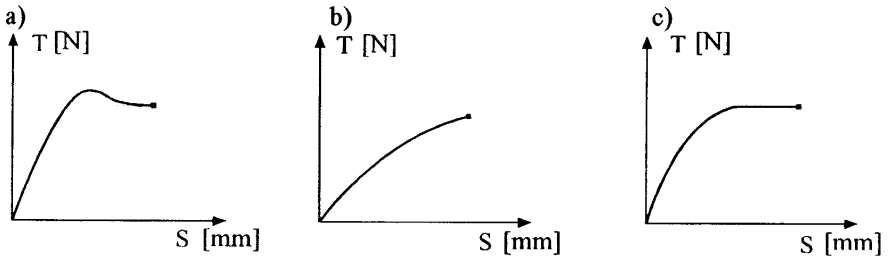

Fig. 8. Curves of shearing

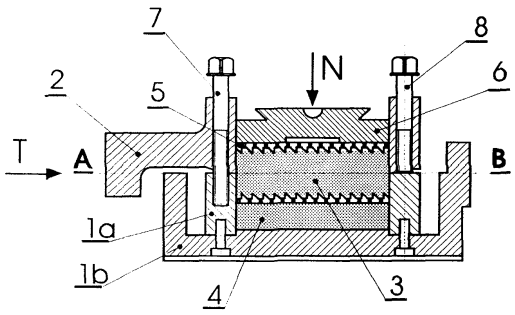

Fig. 9. Shearing box

Another very important feature of the granular materials screening process, including loose media, is a function of outflow [Schmidt, 1984; Schulze, 1996]. The function of outflow is the relation of the length of a sieve or the screening time to the height (thickness) of a layer on a sieve or the mass of a material remaining in the screening layer on the sieve. It may be noted that this is a kinetics curve of screening, the physical reflection of which is the line of an upper layer on a sieve during screening (Figure 10). A dumping curve starts at the point A and up to the point B we have gravitational dumping. Then we can observe screening up to the end point which is the length of the sieve L_{opt} or the time of screening t_{opt}. The curve constitutes an outline of the upper layer surface. According to the ease or difficulty of screening (this depends on the material humidity), the function of outflow, being an exponential function of a base e, acquires different forms (Fig.10). At the end of screening, in the end cross-section of the layer we have a thick grain bed (an over-screen product) of the thickness H_{KG} and a fine grain bed (an under-screen product) of the thickness H_{KD}. The whole thickness of the layer comprises two thicknesses. The effectiveness of screening is determined by a share of H_{KD} in the whole H_K. In Figure 10 one may also observe a dumping layer of the thickness H_W. It may be defined as such a close-to-a sieve layer of the thickness H_W from which, during one cycle of the work of a screening machine, the whole bottom class, contained in the layer, outflows. Hence, one of the aims of this study is the empirical determination of the function of outflow for the aforementioned model materials. To perform the experiment, the laboratory shakers of a vertical sieve motion and the dynamic coefficient K=3:6 were used.

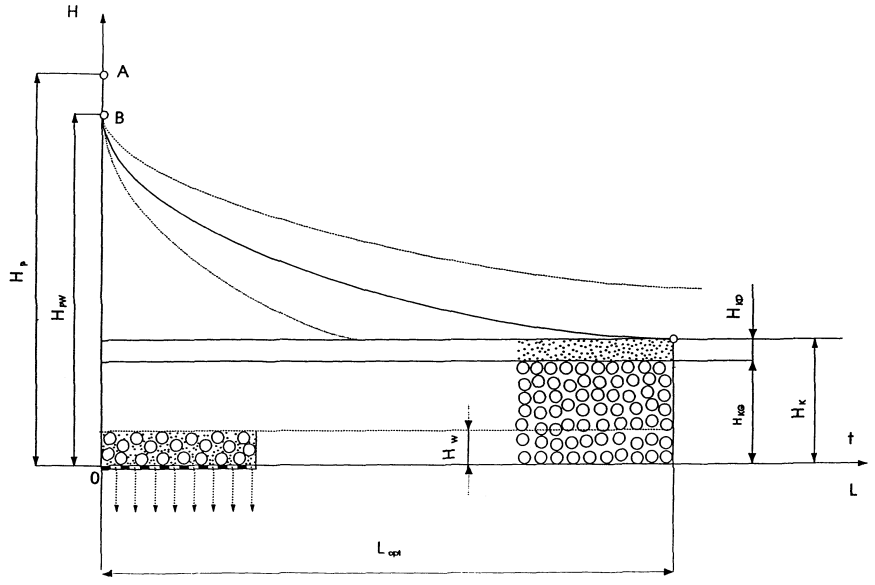

Fig. 10. Function of outflow

RESULTS OF MODEL GRANULAR MATERIALS' SHEARING INVESTIGATION

As a consequence of the model granular materials' shearing examination the tangent of the friction angle (the internal friction coefficient) of those materials was calculated. The value of the normal thrust N=347.92N was taken in accordance with the previously analysed conditions. The parameter μ_0 (the internal friction coefficient) replaces the humidity of the material and other parameters being characteristic of a granular bed. It must be underlined that the parameter μ_0 defines more accurately the ability of the granular material to move and behave in various mechanical processes.

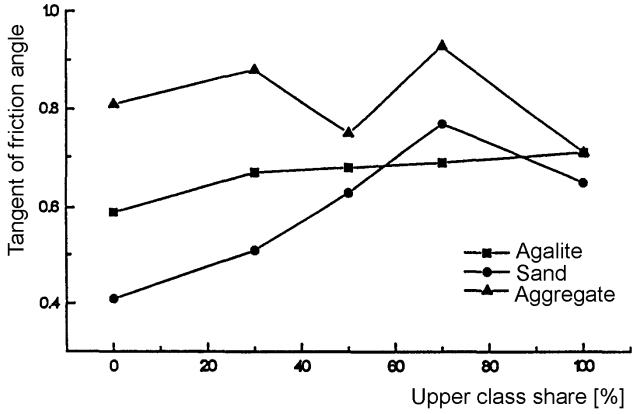

Fig. 11. Dependence of the upper class upon the tangent of friction angle (W=0%)

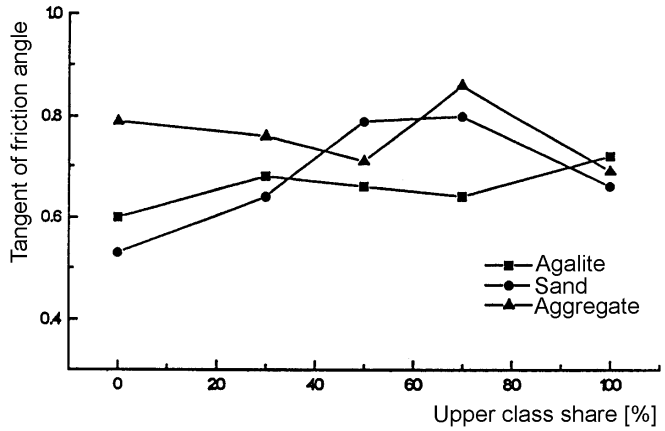

Fig. 12. Dependence of the upper class upon the tangent of friction angle (W=4%)

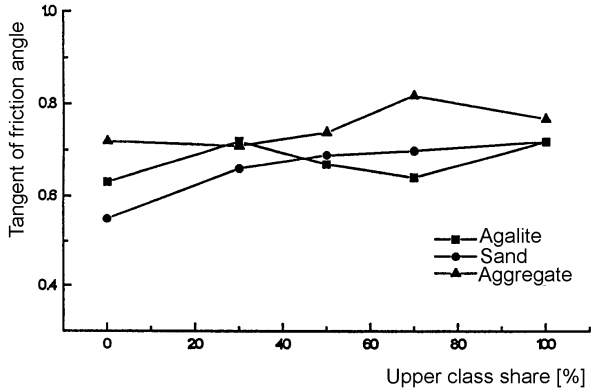

Fig. 13. Dependence of the upper class upon the tangent of friction angle (W=8%)

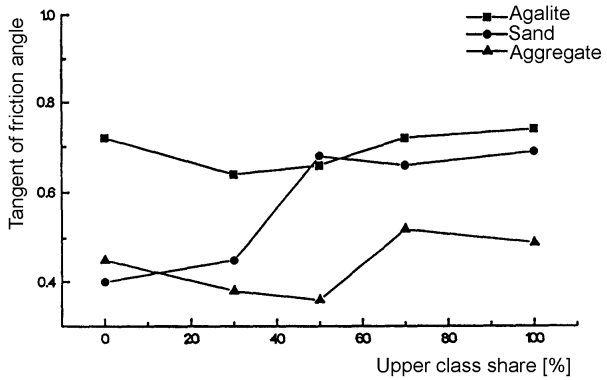

Fig. 14. Dependence of the upper class upon the tangent of friction angle (W=12%)

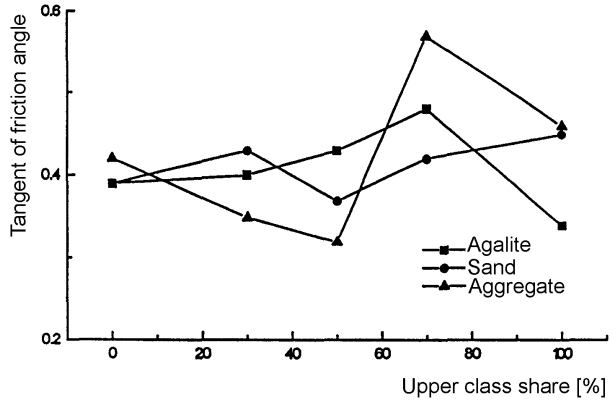

Fig. 15. Dependence of the upper class upon the tangent of friction angle ($W=W_S$)

In Fig. 11 – 15 the dependence of the upper class in a screening bed upon the friction coefficient (the tangent of the friction angle), for the three model granular materials is demonstrated. Each diagram is applicable to a different level of moisture in the material. The values of the humidity are as follows: W=0%, 4%, 8%, 12% and W_s (the static humidity on the humidity axis).

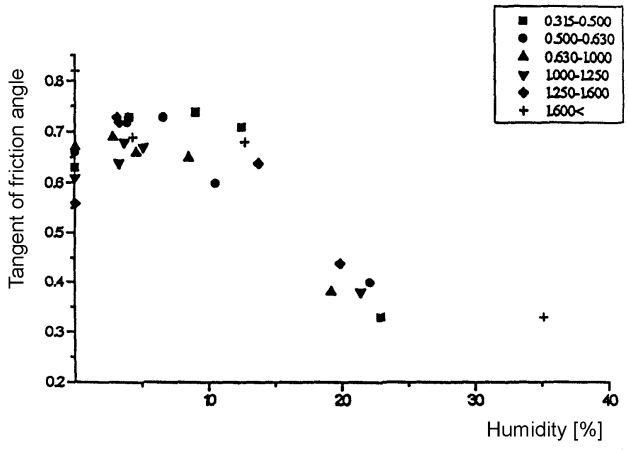

Fig. 16. Dependence $\mu=\mu(W)$ for agalite

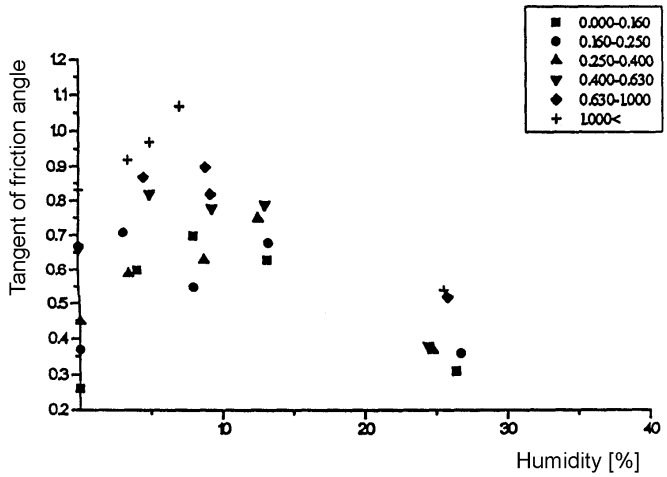

Fig. 17. Dependence $\mu=\mu(W)$ for sand

In Fig. 16 – 18 the dependence of the model material humidity on the tangent of the friction angle for particular grain classes is demonstrated (the size ranges of the classes are provided in mm). The diagrams present agalite, sand and aggregate.

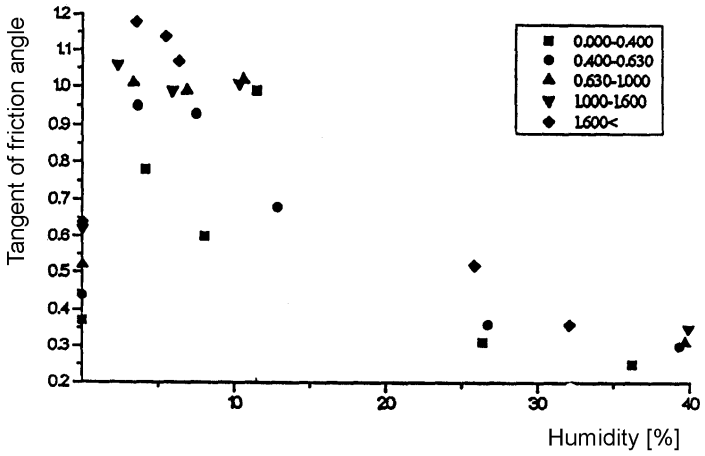

Fig. 18. Dependence $\mu=\mu(W)$ for marble aggregate

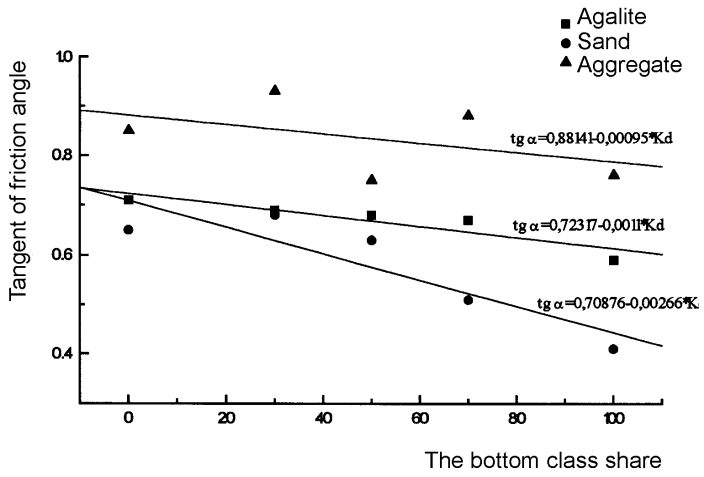

Fig. 19. Coefficient of internal friction for dry materials (W=0%).

In Fig. 19 the coefficient of internal friction (the tangent of the friction angle) for the model materials (agalite, sand, marble aggregate), being dry W=0% and depending on the bottom class in %, is presented. The dependence was correlated in the form of the linear function as follows:

$$\mu_0 = \mathrm{f}(K_d) = A+BK_d \tag{4}$$

The results of the examination allow to estimate the coefficient of internal friction for granular materials. The coefficient encompasses the physical properties of a given

material, the humidity and its influence on various mechanical processes, including screening. The parameter plays a role of an independent variable.

RESULTS OF THE EXAMINATION OF MODEL GRANULAR MATERIALS WATER CAPACITY

Two coefficients of water capacity of the model granular materials (static and dynamic) were determined. The results of the examination are presented in Figs 20-22. Considering the process of graining of the model materials, the boundaries between the upper and bottom classes are as follows:

- for agalite -1 = 1.0 mm
- for sand -1 = 0.4 mm
- for aggregate -1 = 1.0 mm.

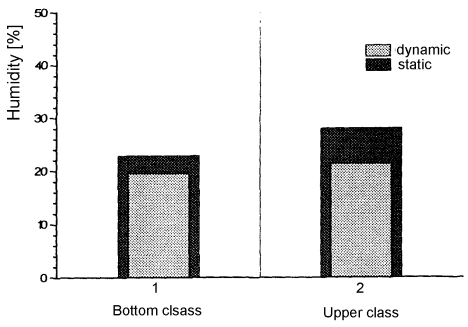

Fig. 20. Bar chart showing static and dynamic humidity for agalite

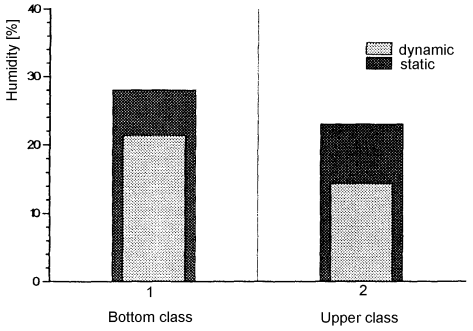

Fig. 21. Bar chart showing static and dynamic humidity for sand

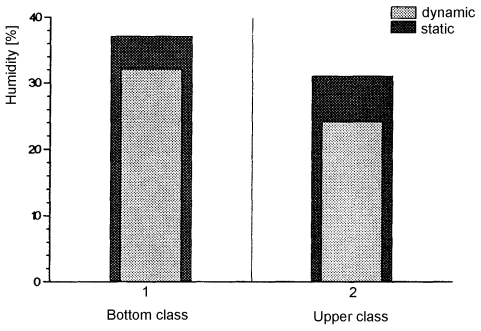

Fig. 22. Bar chart showing static and dynamic humidity for aggregate

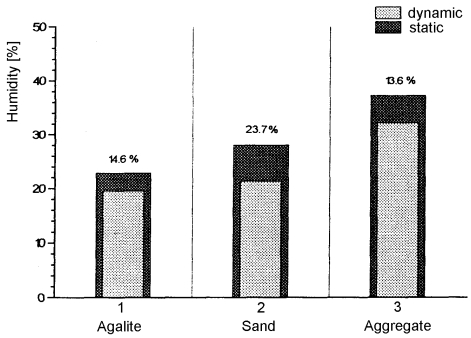

Fig. 23. Collective bar graph showing the bottom class static and dynamic humidity

In Figs 23 and 24 the moisture content in the bottom and upper classes is demonstrated. Furthermore, for each of the material the percentage decrease of the dynamic water capacity relative to the static one was calculated. A decrease in the dynamic water capacity regardless of the grain composition of the material may be noticed.

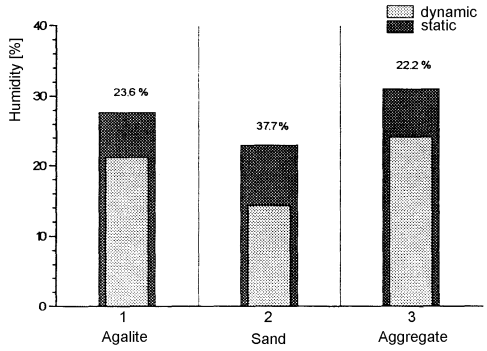

Fig. 24. Collective bar graph showing the upper class static and dynamic humidity

CONCLUSIONS

In this paper a relative humidity axis of the granular material has been introduced. The axis defines the influence of the humidity on the behaviour of the granular material during screening or another mechanical process. As a result of the research the boundary zone on the axis was determined, depicting the processes of dehydration and screening. It contributed to the determination of the static and dynamic water capacities of the granular material.

The subsequent element of this paper is an introduction of the spherical factor of a grain shape as a new characteristic defining a shape of grains in a loose material. The factor describes an external form of a grain. To the second way of determining a grain shape one may account the application of the three grain materials: spherical, irregular and sharp-edge grains. The whole research and correlations obtained were carried out for the three aforementioned model media.

The following stage of the study was the application of the general friction coefficient of a grain material which defines the aptitude of the material to screen. The coefficient may be successfully applied to other mechanical processes involving grain materials. It is advocated to replace the coefficient in the research concerning humid materials, taking into consideration the fact that various materials respond differently to their moisture content. The standardized methods of the coefficient determination exist and, thus, the possibility of easy and simple determination of the parameter has appeared.

In the mining industry the process of dehydration on sieves is applied, being one of the unit operations with humid (two-phase) granular materials. To accomplish this aim, it is the most convenient to use a wave sieve (Fig. 25) which is more efficient than a screening table.

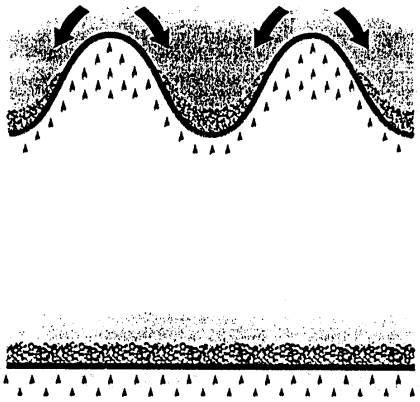

Fig. 25. Wave sieve and screening table

ACKNOWLEDGMENTS

The study undertaken within the frameworks of the Ministry of Science and Higher Education developmental grant research project no. R 1401403

REFERENCES

JANIKE A. W., Storage and Flour of Solids; Bull. No. 123, Engng. Exp. Station, Uniw. Utah, 1964
SCHMIDT P., Das Siebklassieren, Chem. Ing. Tech. 56 (12), 897-907, 1984
SCHULZE D., Vergleich das Fliessverhateno leicht fliestender Schuttguter, Schuttgut 2. Nr 3, 347-356, 1996
WODZIŃSKI P., Screening and Screens, Łódź Technical University Publishers, Łódź, 1997 (in Polish).
WODZIŃSKI P., Screening of Fine Granular Material Coal Prep. 23 (4), 185-213, 2003

LIST OF SYMBOLS

K – dynamic indicator of a screen [-]
α - inclination angle of a screen [1^o]
n – frequency of a screen [Hz], [min^{-1}]
B – width of a screen [m]

L – length of a screen [m]
H – length (thickness) of a layer on a screen [m]
t – time [s]
W – humidity [-], [%]
ε_K – spherical factor of a grain shape [-]
μ - friction coefficient
σ_I – operating shear [Pa]
σ_C – shearing resistance of a granular material (bed) [Pa]

P. Wodziński, *O pewnych właściwościach wilgotnych materiałów ziarnistych,* Physicochemical Problems of Mineral Processing, 42 (2008), 195-210 (w jęz. ang)

Niniejsza praca dotyczy właściwości wilgotnych materiałów ziarnistych. Procesy z udziałem tych materiałów występują bardzo często w warunkach przemysłowych, bo tak naprawdę przeróbka całkowicie suchych materiałów nie istnieje. W każdych warunkach mamy do czynienia z parą wodną w powietrzu, a to oznacza zawsze pewną ilość wilgoci w medium ziarnistym. Jako miernik wpływu wilgoci na przebieg procesów przeróbczych zaproponowano nie zawartość wilgoci w materiale (jak dotychczas), ale uogólniony współczynnik tarcia materiału ziarnistego. Stanowi on podstawową zmienną niezależną, uwzględniającą wpływ wilgoci na zachowanie się wilgotnego materiału ziarnistego w procesie mechanicznym. Podano ponadto funkcję wypływu będącą ważnym, parametrem analityczno-empirycznym dla opisu różnych procesów przeróbczych ciał stałych

słowa kluczowe: przesiewanie, tarcie ziarnistego materiału, ziarnisty materiał, wilgotność, przepuszczalność wodna

Physicochemical Problems of Mineral Processing, 42 (2008), 211-222
Fizykochemiczne Problemy Mineralurgii, 42 (2008), 211-222

Adriana Zaleska*

CHARACTERISTICS OF DOPED-TIO_2 PHOTOCATALYSTS

Received June 24, 2008; reviewed; accepted July 31, 2008

Titanium dioxide represents an effective photocatalyst for water and air purification and for self-cleaning surfaces. TiO_2 shows relatively high reactivity and chemical stability under ultraviolet light (λ<387nm), whose energy exceeds the band gap of 3.3 eV in the anatase crystalline phase. The development of photocatalysts exhibiting high reactivity under visible light (λ>380nm) should allow the main part of the solar spectrum, even under poor illumination of interior lighting, to be used. In this work the influence of TiO_2 structure on visible light photoactivity and novel photocatalysts doped with sulfur, nitrogen, boron and carbon are presented. The photocatalytic activity of obtained powders was referred to dopant chemical form, crystalline structure, crystallite size, surface area and preparation method.

key words: doped-TiO_2, heterogeneous photocatalysis, visible light-driven photocatalysis

INTRODUCTION

Titanium dioxide has semi-conducting properties which make it an attractive material to be used as a photoactive catalyst. TiO_2 is widely used for air purification, deodorization, sterilization, anti-fouling, and mist removal (Fujishima and Zhang, 2006). Activity of TiO_2 depends on its surface area, porosity and acid-basic properties. It was also found that the photoactivity depends on the crystallite size and relative abundance of the crystallite phases (anatase/rutile). Both the crystallite size and crystalline phases modify the TiO_2 band gap. The pristine TiO_2 is only active upon ultraviolet light ($\lambda < 387$ nm) because of its band gap (3.2 eV in the anatase TiO_2 crystalline phase). To improve the photocatalytic reactivity of TiO_2 and to extend its light ab-

* Department of Chemical Technology, Gdansk University of Technology, ul. G. Narutowicza 11/12, 80-952 Gdansk, Poland, azal@chem.pg.gda.pl

sorption into the visible region, several attempts have been made: one is to dope transition metal into TiO_2 (Anpo, 2000), and another is to form reduced TiO_x photocatalysts (Takeuchi et al., 2000).

Table 1. Synthesis methods and characteristics of non-metal moped TiO_2

Doping moiety	Preparation method	Chemical composition	Photoactivity	Ref.
N	Atmospheric-pressure plasma-enhanced nanoparticles synthesis (electric discharge in mixture of N_2, TIP and H_2O, followed by calcination at 500ºC)	Presence of nitrogen was confirmed by XPS technique (peaks N 1s at around 402 eV i 400 eV)	$TiO_{2-x}N_x$ was more effective in removing of isopropanol under both UV and visible light than the un-doped TiO_2	(Chen et al., 2007)
	Hydrolysis of TIP or $TiCl_4$ with an aqueous ammonia solution, followed by calcination at 300ºC, 330ºC, 400ºC and 500ºC	$TiO_{1,71}N_{0,036}$ (350ºC) $TiO_{1,85}N_{0,017}$ (500ºC)	UV: there is no significant difference between pure and doped samples. Vis: N-TiO_2 was active for CO photooxidation; the activity increases with increasing calcinations temperature up to 400°C and then decreases with further increase in temperature of calcination	(Sato et al., 2005)
S	Heating the TiS_2 powder in air (sample A: at 500°C for 90 min. and sample B: at 600°C for 24h)	Sulfur presence was confirmed by XPS technique as a Ti-S bonds (signal around 160 eV)	Activity (decomposition of methylene blue) of sample A and B was comparable to that of the undoped anatase during UV irradiation. Sample A induced the photocatalytic decomposition of MB under Vis light.	(Umebayashi et al., 2003)
	Hydrolysis of TIP in ethanol in the presence of thiourea. Separation of precipitate and calcinations at temperatures form 400 to 700°C	S^{4+} was substituted for some of the lattice titanium atoms. The atomic content of S on surface was 1.6%	S-TiO_2 calcinated at 400°C for 3h showed the highest activity under visible light (λ>500 nm)	(Ohno et al., 2004)
C	Modified sol-gel process using different alkoxide precurors: $Ti(OEt)_4$; Ti(O-*n*Pr)$_4$; Ti(O-*i*Pr)$_4$; Ti(O-*n*Bu)$_4$; Ti(O-*i*Bu)$_4$; Ti(O-*t*Bu); Calcination at 65ºC (3 h) and 250ºC(3 h)	C content [wt.%]: 0.06 $Ti(OEt)_4$; 0.31 Ti(O-*n*Pr)$_4$ 0.13 Ti(O-*i*Pr)$_4$ 0.6 Ti(O-*n*Bu)$_4$ 0.3 Ti(O-*i*Bu)$_4$ 0.4 Ti(O-*t*Bu)$_4$	4-chlorophenol conversion after 100min of irradiation by visible light: 25% for TiO_2 obtained from $Ti(OEt)_4$; 40% for TiO_2 obtained from Ti(O-*n*Pr)$_4$ 30% for TiO_2 obtained from Ti(O-*i*Pr)$_4$ 43% for TiO_2 obtained from Ti(O-*n*Bu)$_4$ 52% for TiO_2 obtained from Ti(O-*i*Bu)$_4$ 35% for TiO_2 obtained from Ti(O-*t*Bu)$_4$	(Lettmann et al., 2001)
B	Hydrolysis of $Ti(OC_2H_5)_4$ in presence of $(C_2H_5O)_3B$ and 2,4-pentanedione as a organic ligand under Ar atmosphere. Calcination at 400÷900°C, followed by Pt impregnation	Presence of B_2O_3 was confirmed by XRD technique in sample calcinated at 400°C	Platinized B/Ti powder exhibited higher reactivity for the photocatalytic decomposition of water under UV than pure TiO_2 loaded wit Pt	(Moon et al., 2000)

* TIP - titanium tetra-isopropoxide

Both approaches introduce impurity/defect states in the band gap of TiO_2, which lead TiO_2 to absorb visible-light. However, transition metal doping, where quite local-

ized *d* states appear deep in the band gap of the host semiconductor, often results in the increase of the carrier recombination. Therefore, the lifetime of the mobile carriers may become shorter, giving lower photocatalytic activity. Reducing TiO_2 introduces localized oxygen vacancy states located at 0.75-1.18 eV below the conduction band (CBM) of TiO_2, which may promote photoreduction activity because a redox potential of the hydrogen evolution (H_2/H_2O) locates just below the CBM of TiO_2. In 2001, Asahi et al., presented a new type of visible light sensitive photocatalyst - nitrogen-doped TiO_2. Since Asahi paper, other non-metal doped TiO_2 photocatalysts were reported. TiO_2 doped with F (Yu et al, 2002), I (Hong et al., 2005) and P (Yu et al., 2003) showed higher photocatalytic activity under UV light and TiO_2 doped with N (Irie et al., 2003a; Asahi et al., 2007), C (Sakthivel and Kisch, 2003), S (Ohno et al., 2003) and codoped with Ni and B (Zhao et al., 2004) showed high photocatalytic activity under visible light. Sato et al.,(2005) have shown efficient photooxidation of CO under visible irradiation by a nitrogen-doped TiO_2. C-doped TiO_2 was obtained by acid-catalyzed sol-gel process (Lettmann et al., 2001) or by the oxidative annealing of TiC (Irie et al.,2003b). Examples of doping methods and selected properties of non-metal doped-TiO_2 are given in Table 1.

Non-metal doping opens up a new possibility for the development of solar- or daylight-induced photocatalytic materials. In the present work, several own nonmetal-doped photocatalysts are presented: C-doped, B,C codoped and S,N,C- tridoped TiO_2. The selected properties of the obtained photocatalysts were correlated with their photoactivity under visible light. Their intrinsic characteristics were investigated using X-ray diffraction (XRD), X-ray photoelectron spectroscopy (XPS) and UV-Vis spectroscopy. The photocatalytic activity of doped TiO_2 was evaluated by the degradation rate of phenol.

METHODS

PREPARATION OF NONMETAL-DOPED TiO_2 PHOTOCATALYSTS

C-doped TiO_2 was prepared by titanium(IV) isopropoxide (TIP, 97%, Sigma-Aldrich Co.) hydrolysis, followed by precipitate separation, drying at 80°C for 24 h and calcinations at 350°C for 1 h. Low calcination temperature favors to keep residual carbon in photocatalyst structure. Carbon comes from alkoxide TiO_2 precursor. B, C-codoped TiO_2 was obtained by sol-gel method (H-labeled) and by grinding anatase with boron precursors (G-labeled). Boric acid thriethyl ester (99%) and boric acid (99%) from Sigma-Aldrich Co) were used as a boron source in both procedures. In sol-gel method, TIP was hydrolyzed in the presence of appropriate dopant, followed by precipitate separation, drying at 80°C for 24 h and calcinations at 450°C for 1 h. Titanium dioxide ST-01 from Ishihara-Sangyo, Japan, was used in the second proce-

dure. ST-01 has 320 m^2/g specific surface area and consists only of crystalline anatase phase with 7 nm particle size. Boron-modified TiO_2 powders were prepared by grinding ST-01 in agate mortar with H_3BO_3 or $(C_2H_5O)_3B$, respectively. The obtained powders were dried for 24h at temperature 80°C and calcinated at 450ºC.

S, N, C-tridoped photocatalysts were obtained by sol-gel method. Thioacetamide (99%) from POCH S.A. and thiourea (99%) from Sigma-Aldrich Co. were used as sulfur and nitrogen source in catalyst preparation procedures. TIP was hydrolyzed in the presence of appropriate dopant, followed by precipitate separation, drying at 80°C for 24 h and calcinations at 450°C for 1 h. The detailed experimental procedure can be found in previous studies (Zaleska et al., 2007; Zaleska et al., 2008; Górska et al., 2008).

CHARACTERIZATION

ESCALAB-210 spectrometer (VG Scientific) was used for X-ray photoelectron spectroscopy (XPS) measurements with the Al Kα X-ray source operated at 300W (15kV, 20mA). The spectrometer chamber pressure was about 5×10^{-9}mbar. The survey spectra were recorded for all the samples in the energy range from 0 to 1350 eV with 0.4 eV step. High resolution spectra were recorded with 0.1 eV step, 100 ms dwell time and 20 eV pass energy. 90° take-off angle was used in all measurements. AVANTAGE data system software served for curve fitting. The background was fit using nonlinear Shirley model. Scofield sensivity factors and measured transmission function were used for quantification. Carbon contamination C1s peak at 284.60 eV was used as reference of binding energy. The catalyst powder crystal structure was determined from XRD pattern measured in the range of $2\theta=20\div80^{o}$ using X-ray diffractometer (Xpert PRO-MPD, Philips) with Cu target Kα-ray (λ=1.5404 Å). The diffuse absorption spectra DRS were characterized using UV-VIS spectrometer (Jasco, V-530) equipped with an integrating sphere accessory for diffuse reflectance.

ASAP 2405 instrument (Micromeritics) was used for measurements of BET surface area and pore size of the catalysts by physical adsorption and desorption of nitrogen. The S_{BET} values were calculated according to the BET method using adsorption data at relative pressures p/p_o between 0.05 and 0.25, where p and p_o denote the equilibrium pressure. Mesopore-size distribution was calculated with the Barrett-Joyner-Halenda method of isotherm.

MEASUREMENT OF PHOTOCATALYTIC ACTIVITY

The photocatalytic activity of doped-TiO_2 powders in visible light ($\lambda > 400$ nm) was estimated by measuring the decomposition rate of phenol (0.21 $mmol/dm^3$) in an aqueous solution. Photocatalytic degradation runs were proceeded with blind tests in the absence of catalyst or illumination.

25 cm^3 of catalyst suspension (125 mg) was stirred using magnetic stirrer and aerated (5 dm^3/h) prior and during the photocatalytic process. Aliquots of 1.0 cm^3 of the aqueous suspension were collected at regular time periods during irradiation and filtered through syringe filters (Ø=0.2 μm) to remove catalyst particles. Phenol concentration was estimated by colorimetric method using UV-VIS spectrophotometer (DU-7, Beckman). The suspension was irradiated using 1000 W Xenon lamp (Oriel), which emits both UV and Vis light. To limit the irradiation wavelength, the light beam was passed through GG400 to cut-off wavelengths shorter than 400 nm.

RESULTS AND DISCUSSION

The selected properties of nonmetal-doped photocatalysts and pure TiO_2 as a reference sample are given in Table 2. Phenol degradation rate was calculated as an average phenol amount removal after 60 min. visible light illumination. It was observed, that C-doped TiO_2 (sample T_350 obtained by TIP hydrolysis without any dopant and calcination at 350°C) revealed similar photoactivity to S,N,C-tridoped TiO_2 (sample TH_5 obtained by modification with thiourea). Phenol degradation rate under visible light was 2.93 and 2.82 $\mu mol \cdot dm^{-3} \cdot min^{-1}$ for TH_5 and T_350, respectively. For pure TiO_2 the observed phenol degradation ranged from 0.6 (TiO_2 prepared by sol-gel method) to 0.9 $\mu mol \cdot dm^{-3} \cdot min^{-1}$ (commercially available TiO_2 ST01).

The obtained results suggested that visible-light-activated TiO_2 could be prepared by carbon, sulfur, nitrogen or boron doping or co-doping of those moieties. For TiO_2 modified with thioacetamide, thiourea or boric acid triethyl ester, phenol degradation rate exceeded 2 $\mu mol \cdot dm^{-3} \cdot min^{-1}$.

XRD was used to investigate the phase structure of nonmetal-doped TiO_2 powders (see data on crystalline phase in Table 2). For all highly-active C-doped and S,N,C-tridoped photocatalysts a homogenous crystalline phase of anatase appeared in the XRD pattern. B,C-codoped TiO_2 obtained by the sol-gel method, except the sample BA-H(0.5), appeared as amorphous TiO_2, while pure TiO_2 obtained by the same method without any dopant was in the anatase form. Addition of $(C_2H_5O)_3B$ or H_3BO_3 inhibited crystallite growth and/or transformation from amorphous to anatase structure. Only addition of the smallest amount of H_3BO_3 (0.5 wt.%), resulted in anatase structure (Table 2).

All samples obtained by grinding of ST-01 with boron compounds still contained the anatase phase. The XRD pattern of samples BA-G(10) and BE-G(10) shows diffraction lines attributed to the diboron trioxide phase besides the peak due to anatase. Chen et al.,(2006) found that appearance of separate boron phase is related not only to the calcination temperature but also the molar ratio of B to Ti. For samples with molar ratio Ti : B =10 the diboron trioxide crystal appeared during calcination over 600°C. When Ti : B was 20, the B_2O_2 phase emerged at 500°C. In our study, B_2O_3 structure

was observed for samples prepared by grinding with 10 wt.% of boron in two different precursors. Apparently 0.5 wt.% was not enough to form clearly evident B_2O_3.

Table 2. Visible-light activity of nonmetal-doped TiO_2 photocatalysts

Doping moiety	Sample name*	Dopant precursor**	Dopant amount [wt. %]	Calcination temperature [°C]	Phase composition	Band gap energy [eV]	Phenol decomposition reaction rate [μmol·dm^{-3}·min^{-1}]
S, N, C	TA0.5	thioacetamide	0.5	450	anatase	3.37	1.8
	TA1	thioacetamide	1.0	450	anatase	3.36	2.1
	TA2	thioacetamide	2.0	450	anatase	3.36	2.3
	TA5	thioacetamide	5.0	450	anatase	3.36	2.4
	TH0.5	thiourea	0.5	450	anatase	3.34	1.3
	TH1	thiourea	1.0	450	anatase	3.33	1.2
	TH2	thiourea de	2.0	450	anatase	3.37	2.5
	TH5	thiourea	5.0	450	anatase	3.37	2.9
B, C	BE-H(0.5)	BATE	0.5	450	amorphous	3.28	0.5
	BE-H1	BATE	1.0	450	amorphous	3.37	0.7
	BE-H(5)	BATE	5.0	450	amorphous	3.41	0.5
	BE-H(10)	BATE	10.0	450	amorphous	3.36	0.8
	BE-G(0.5)	BATE	0.5	450	anatase	3.36	2.1
	BE-G(10)	BATE	10.0	450	anatase + B_2O_3	3.37	1.4
	BA-H(0.5)	boric acid	0.5	450	anatase	3.34	0.6
	BA-H(10)	boric acid	10.0	450	amorphous	3.40	0.9
	BA-G(0.5)	boric acid	0.5	450	anatase	3.30	0.6
	BA-G(10)	boric acid	10.0	450	anatase + B_2O_3	3.33	0.7
C	T_350	no dopant	-	350	anatase	3.41	2.8
-	T_450	no dopant	-	450	anatase	3.33	0.6
	TiO_2 ST-01	no dopant	-	450	anatase	3.30	0.9

* TA, TH, BE-H and BA-H series – prepared by TIP hydrolysis in the presence of an appropriate dopant; BE-G and BA-G series – prepared by grinding of ST01 with an appropriate dopant

** BATE - boric acid triethyl ester

The band gap for doped-TiO_2 fluctuated from 3.28 to 3.41 eV. The highest *Eg* was observed for highly active C-doped TiO_2 (sample T_350 obtained by TIP hydrolysis followed by calcination at 350°) and inactive B,C-codoped TiO_2 (sample BE-H(5) prepared by sol-gel method using 5 wt.% of boric acid triethyl ester), see Table 2. Band gap narrowing has not been observed in case of any nonmetal-doped TiO_2, which is in good agreement with theoretical calculation made by Xu et al.,(2006), but contrary to Asahi et al.,(2001) hypothesis. Asahi et al.,(2001) postulated band gap narrowing as the main modification mechanism of TiO_2 doped with nonmetals.

Usually, nonmetal doping affects light absorption characteristics of TiO_2. Figure 1 shows the UV-vis diffuse reflectance spectra of pure TiO_2, S,N,C-tridoped TiO_2 (Fig. 1A) and B,C-codoped TiO_2 (Fig. 1B). All nonmetal-doped TiO_2 powders better absorbed visible light, however, the red shift is negligible. Photoabsorption in the visible region was stronger for TiO_2 doped with S, N, B or C atoms than for pure TiO_2 (Fig. 1). Only for S,N,C-tridoped TiO_2 clear correlation between absorption spectra and photoactivity was observed, i.e. for increased photoactivity absorption in visible region also increased (reflectance decreased).

To investigate the chemical states of nonmetals atoms incorporated into TiO_2 binding energies were measured by X-ray photoemission spectroscopy. Table 3 shows chemical content, as well as phenol degradation efficiency under visible light, for selected – the most active photocatalysts. Photocatalysts are listed from higher to lower photoactivity. In all doped-TiO_2 samples the peak attributed to C 1s at around 289-284 eV was observed. In most cases, the C 1s region consists of three peaks: the first peak (~288.9 eV) related to COOH groups bonds, the second peak (~286 eV) to C-OH bonds and the third peak (~284.6 eV) related to C-C aromatic bonds. Thus, carbon content is presented as a total C content, C-C structure (both C-C_{alif} and C-C_{arom}) and as carbon in form of C-C_{arom}. All visible-light-activated photocatalysts contain carbon including carbon in the form of C-C_{arom}.

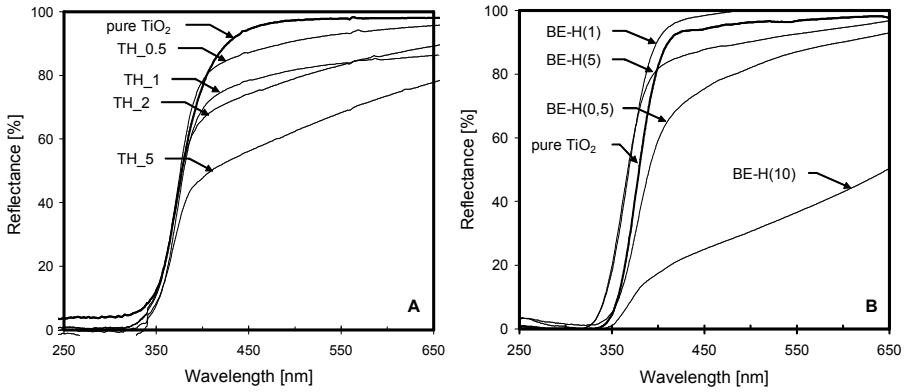

Fig. 1. Diffuse reflectance spectra of pure and doped-TiO_2: (A) S,N,C-tridoped TiO_2 prepared by hydrolysis of TIP in the presence of thiourea, (B) B,C-codoped TiO_2 prepared by hydrolysis of TIP in the presence of $(C_2H_5O)_3B$

Among all obtained powders, the highest visible-light activity was observed for the S,N,C-tridoped TiO_2 - prepared with 5 wt.% of thiourea. The rate constant for phenol and 4-chlorophenol decomposition was 0.054 and 0.041 min^{-1}, respectively. The most effective catalyst contained 1.3 at.% of nitrogen, 7.21 at.% of carbon and 0.33 at. % of sulfur, as indicated by XPS analysis. TH5 sample is one of the richest in sulfur (Table 3), mainly in S^{6+} species. On the other hand, TH5 carbon content remained in medium range.

Table 3. Chemical characterization of most visible light activated TiO_2 photocatalysts

Sample No	XPS-determined content, [at.%]						Phenol degradation efficiency after 60 min. irradiation
	ΣC	C-C	C-C_{arom}	S	N	B	
TH_5	7.21	3.69	1.71	0.33	1.3	-	97
T_350	15.2	10.1	10.1	-	-	-	82
TH_2	14.89	9.86	9.86	0.33	1.15	-	82
TA_5	6.37	4.95	2.76	0.16	1.24	-	81
TA_2	2.52	1.5	0.83	-	1.21	-	72
BE-G(0.5)	18.54	12.77	12.77	-	-	3.21	61
BE-G(10)	18.43	9.55	9.55	-	-	12.33	45

High visible-light activity was also observed for C-doped TiO_2, containing residual carbon from organic titanium dioxide precursor. Since surface area and pore size distribution are important factors for heterogeneous photocatalysis, the sample T_350 had high BET surface area (205.8 m^2/g) and small crystallite size (8.4 nm) and average pore diameter (8.3 nm). Enhanced visible light-activity probably results from the presence of carbon (15.2 at.%), mainly in the form of C-C species, as well as from high surface area. Although, there is no red shift observed for sample T_350, it exhibited better light absorption in Vis – moreover, the absorption tail was extended to 750 nm.

According to Sakthivel and Kisch (2001) hypothesis, there is an optimal amount of dopant responsible for enhanced visible light activity. Besides the dopant amount, the chemical character of incorporated element is also important. Literature data and obtained results suggested that carbon in the form of carbonate and boron as boron trioxide suppress visible-light activity. Lettmann et al.,(2001), as well as Umebayashi et al.,(2003) stated that carbon species works as sensitizer and single oxygen is formed without TiO_2 excitation. Yu and co-workers (2005) provided an alternative explanation that sulfur doping can indeed create intra-band gap states close to the conduction band edges, and thus induces visible-light absorption at the sub-band energy. It was also found, that constitution of the TiO_2 (doped and undoped TiO_2) also plays an important role in its high photoactivity (Yu et al., 2006). Usually, the composite of two kinds of semiconductor or two phases of the same semiconductor is beneficial in reducing the recombination of photo-generated electrons and holes, and thus enhances photocatalytic activity. The interface between the two phases may act as a rapid separation site for the photo-generated electrons and holes due to the difference in the energy level of their conduction bands and valence bands. Therefore, Yu et al.,(2006) suggested that N,S-codoped TiO_2 powders prepared by hydrolysis method exhibit significant photoactivity under daylight illumination due to the fact that the as-prepared TiO_2 powders consist of two phases of undoped TiO_2 and N,S-codoped TiO_2.

CONCLUSION

1. Using several new dopants, a series of TiO_2 catalyst samples was selected for investigation aimed at correlation of their structure and photoactivity. Particularly S,N,C-tridoped (obtained by TIP hydrolysis in the presence of thioacetamide and thermal treating at 450°C) and C-doped (obtained by TIP hydrolysis in the absence of any dopant and thermal treating at 350°C) photocatalysts were active under visible light at wavelengths greater than 400 nm.
2. B^{3+}, S^{+} and carbon in the form of C-$C_{arom.}$ species showed beneficial influence on photodegradation efficiency in visible light.
3. For S,N,C-tridoped photocatalysts, the experimental data clearly indicate the presence of correlation between absorption and photoactivity of the obtained powders - for increased photoactivity absorption in visible region also increased.
4. The experimental data confirm earlier observations, that a lack of band gap narrowing with simultaneous increase of the absorption intensity can still lead to effective degradation of the organic compounds, which is mainly controlled by presence of sensitizers (residual carbon).

ACKNOWLEDGMENTS

This research was supported by Polish Ministry of Science and Higher Education (contract No.: N205 077 31/3729). Dr. Beata Tryba from Department of Water Technology and Environmental Engineering, Szczecin University of Technology is gratefully acknowledged for assistance in UV-Vis spectroscopy.

REFERENCES

ANPO M., (2000) Use of visible light. Second-generation titanium dioxide photocatalysts prepared by the application of an advanced metal ion-implantation method. Pure Appl. Chem. 72, 1787-1792.

ASAHI, R., MORIKAWA, T., (2007) Nitrogen complex species ant its chemical nature in TiO2 for visible-light sensitized photocatalysis. Chem. Phys. 339, 57-63.

ASAHI, R., MORIKAWA, T., OHWAKI, T., AOKI, K., TAGA, Y., (2001) Visible-Light Photocatalysis in Nitrogen-Doped Titanium. Science 293, 269-271.

CHEN, C., BAI, H., CHANG, S., CHANG, C., DEN, W., (2007) Preparation of N-doped TiO2 photocatalyst by atmospheric pressure plasma process for VOCs decomposition under UV and visible light sources. J. Nanoparticle Res. 9, 365-375.

CHEN, D., YANG, D., WANG, Q., JIANG, Z., (2006) Effects of boron doping on photocatalytic activity and microstructure of titanium dioxide nanoparticles. Ind. Eng. Chem. Res. 45 , 4110 -4116.

FUJISHIMA, A., ZHANG, X., (2006) Titanium dioxide photocatalysis: present situation and future approaches. C.R. Chemie 9, 750-760.

GÓRSKA, P., ZALESKA, A., KLIMCZUK, T., SOBCZAK, J.W., SKWAREK, E., HUPKA, J., (2008) The influence of calcinations temperature on TiO2 structure, surface properties and photoactivity under UV and visible light. Appl. Catal. doi: 10.1016/j.apcatb.2008.04.028.

HONG, X.T., WANG, Z.P., CAI, W.M., LU, F., ZHANG, J., YANG, Y.Z., MA, N., LIU, Y.J., (2005) Visible-Light-Activated Nanoparticle Photocatalyst of Iodine-Doped Titanium Dioxide. Chem. Matter. 17, 1548-1552.

IRIE, H., WATANABE, Y., HASHIMOTO, K., (2003) Carbon-doped anatase TiO2 powders as a visible-light sensitive photocatalyst. Chem. Lett. 32, 772-773.

IRIE, H., WATANABE, Y., HASHIMOTO, K., (2003) Nitrogen-concentration dependence on photocatalytic activity of TiO2-xNx powders. J Phys Chem B 107, 5483-5486.

LETTMANN, C., HILDEBRAND, K., KISCH, H., MACYK, W., MAIER, W.F., (2001) Visible light photodegradation of 4-chlorophenol with a coke-containing titanium dioxide photocatalyst. Appl. Catal. B 32, 215-227.

MOON, S.C., MAMETSUKA, H., TABATA, S., SUZUKI, E., (2007) Photocatalytic production of hydrogen from water usung TiO2 and B/TiO. Catal. Today 58, 125-132.

OHNO, T., AKIYOSHI, M., UMEBAYASHI, T., ASAI, K., MITSUI, T., MATSUMURA, M., (2004) Preparation of S-doped TiO2 photocatalysts and their photocatalytic activities under visible light. Appl. Catal. A 265, 115-121.

OHNO, T., MITSUI, T., MATSUMURA, M., (2003) Photocatalytic activity of S-doped TiO2 photocatalyst under visible light. Chem. Lett. 32, 364-365.

SAKTHIVEL, S., KISCH, H., (2003) Daylight photocatalysts by carbon-modified titanium dioxide. Angew Chem Int Ed 42, 4908-4911.

SATO, S., NAKAMURA, R., ABE, S., (2005) Visible Light sensitization of TiO2 photocatalysts by wet-method N doping. Appl. Catal. A 284, 131-137.

TAKEUCHI, K., NAKAMURA, I., MATSUMOTO, O., SUGIHARA, S., ANDO, M., IHARA, T., (2000) Preparation of visible-light-responsive titanium oxide photocatalysts by plasma treatment. Chem. Lett. 29, 1354-1355.

UMEBAYASHI, T., YAMAKI, T., TANAKA, S., ASAI, K., (2003) Visible Light-Induced Degradation of Methylene Blue on S-doped TiO2. Chem. Lett. 32, 330-331.

XU, T., SONG, C., LIU, Y., HAN, G., (2006) Band structures of TiO2 doped with N, C and B. Zhejijang Univ Science B 7, 299-303.

YU, J., ZHOU, M., CHENG, B., ZHAO, X., (2006) Preparation, characterization and photocatalytic activity of in siti N,S-codoped TiO2 powders. J. Molec. Catal. A 246, 176-184.

YU, J.C., HO, W., YO, J., YIP, H., WONG, P.K., ZHAO, J., (2005) Efficient visible-light-induced photocatalytic disinfection on sulfur-doped nanocrystalline titania. Environ. Sci. Technol. 39, 1175-1179.

YU, J.C., YU, J., HO, W., JIANG, Z., ZHANG, L., (2002) Effects of F- Doping on the Photocatalytic Activity and Microstructures of Nanocrystalline TiO2 Powders. Chem. Matter. 14, 3808-3816.

YU, J.C., ZHANG, L., ZHENG, Z., ZHAO, J., (2003) Synthesis and Characterization of Phosphated Mesoporous Titanium Dioxide with High Photocatalytic Activity. Chem. Matter. 15, 2280-2286.

ZALESKA, A., GÓRSKA, P., SOBCZAK, J.W., HUPKA, J., (2007) Thioacetamide and thiourea impact on visible light activity of TiO2. Appl. Catal. B 76, 1-8.

ZALESKA, A., SOBCZAK, J.W., GRABOWSKA, E., HUPKA, J., (2008) Preparation and photocatalytic activity of boron-modified TiO2 under UV and visible light. Appl. Catal. B 78, 92-100.

ZHAO, W., MA, W., CHEN, C., ZHAO, J., SHUAI, Z., (2004) Efficient degradation of toxic pollutants with Ni2O3/TiO2-xBx under visible irradiation. A. Am. Chem. Soc. 126, 4782-4783.

Zaleska A., *Characteristics of doped-TiO_2 photocatalysts*, Physicochemical Problems of Mineral Processing, 42 (2008), 213-224 (w jęz. ang)

Fotokatalityczne właściwości TiO_2 wykorzystywane są między innymi do eliminacji substancji organicznych z fazy gazowej i ciekłej oraz w samooczyszczaniu powierzchni. Tlenek tytanu (IV) absorbuje prawie wyłącznie promieniowanie UV, dlatego podczas fotokatalizy wykorzystać można zaledwie od 3 do 5 % promieniowania słonecznego. Zatem otrzymanie półprzewodnika tytanowego nowej generacji aktywnego w zakresie promieniowania widzialnego (λ>400 nm), znacząco rozszerzyłoby możliwości aplikacyjne fotokatalizy heterogenicznej w ochronie środowiska, przez wykorzystanie głównej części spektrum światła słonecznego lub zastosowanie źródła światła o mniejszym natężeniu promieniowania. W niniejszej pracy omówiono nowe fotokatalizatory aktywne pod wpływem światła widzialnego, otrzymane poprzez modyfikację TiO_2 związkami siarki, azotu, boru oraz węgla. Fotoaktywność otrzymanych fotokatalizatorów została odniesiona do charakteru chemicznego wprowadzonej domieszki, struktury krystalicznej, wielkości krystalitów, powierzchni właściwej fotokatalizatora oraz metody otrzymywania.

słowa kluczowe: półprzewodnik-TiO_2, fotokataliza heterogeniczna, fotokatalizatory aktywne pod wpływem światła widzialnego

Physicochemical Problems of Mineral Processing, 42 (2008), 223-236
Fizykochemiczne Problemy Mineralurgii, 42 (2008), 223-236

Justyna Łuczak*, Monika Joskowska*, Jan Hupka*

IMIDAZOLIUM IONIC LIQUIDS IN MINERAL PROCESSING

Received June 18, 2008; reviewed; accepted July 31, 2008

Imidazolium ionic liquids (ILs) represent promising potential for industrial and technological applications - considering ILs as a new class of compounds. Usability of ILs in the mineral processing area described in the literature is up to now limited. Their application was indicated for minerals leaching, solvent extraction as well as electrochemical processes showing that these compounds may play an important role in the recovery and purification of high-value metals from water as well as ores. Imidazolium derivatives may be used as either efficient solvents or active compounds promoting separation. Environmental impact and recycling possibilities were also described. Nevertheless, their potential industrial applications in mineral processing require further detailed examination.

key words: imidazolium ionic liquids, minerals leaching, extraction, micelle formation

INTRODUCTION

Majority of chemical processes are carried out mainly in water as generally available solvent. Application of alcohols, halogen derivatives and condensed gases (SO_2, NH_3) has also found application to carry out chemical reactions. Volatile organic solvents (VOC), liquid ammonia are still in common use in the laboratory scale as well as in the chemical industry. There is tendency to eliminate organic solvents by projecting new, environmentally friendly technologies. One of the groups of compounds, which could replace traditional solvents, are ionic liquids (ILs) - organic salts with melting point lower than 100^{o}C. As distinct from organic solvents, ionic liquids are entirely composed of ions. Moreover, conventional salts such as sodium chloride consist of small, close packed cation and anion which form a solid with high melting

* Department of Chemical Technology, Chemical Faculty, Gdańsk University of Technology, 80-952 Gdansk, Poland, juha@chem.pg.gda.pl

point, that limit their application as a reaction media. On the contrary, ILs are composed of bulky organic cation and small/large anion (Fig. 1). More difficult packing and weaker attractions between ions result in a liquid state of matter (Deetlefs et al.,2006; Blesic et al.,2007).

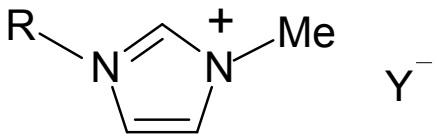

Fig. 1. Chemical structure of 1-alkyl-3-methylimidazolium ionic liquid

Their properties (selectivity, negligible volatility, inflammability, thermal stability ect.) cause that ILs may play promising role as alternative media in a number of industrial applications like catalytical (Welton, 2004; Sheldon, 2001), separation (Visser et al., 2002; Huddleston et al., 1998), electrochemical processes as well in combined reaction-separation processes. ILs are often called designer solvents or task-specific ionic liquids (TSILs) because of possibility to being tailored to fulfil technological demands of the variety applications. IL properties can be significantly adjusted e.g. hydrophobic vs. hydrophilic by interchange of the anion type, or a slight modification of the number or length of alkyl chains in the cation (Visser and Rogers, 2003). Selection of anion may significantly change the miscibility of ILs with water, whereas manipulation in alkyl chain length may have only a slight effect. Moreover, solubility in water might be increased by addition of e.g. short chain alcohols or chaotropes (Welton, 2004; Alfassi et al., 2003; Huddleston et al., 2001).

In this paper we reviewed the literature on ILs application in mineral processing, since ILs may offer potential for development of efficient, environmentally friendly metal recovery technologies from ores and wastes. Some own data on ILs surface properties are also included.

MINERALS LEACHING

The most important step of metallurgical processing is efficient separation of metals from ores followed by metals recovery from concentrate. Depletion of resources leads to using more lean ores and favours the hydrometallurgical approach.

ILs were examined as solvents (either as a neat liquid or as aqueous mixtures) for the leaching of gold, silver, copper and base metals from sulphidic ores (Whitehead et al., 2004; Whitehead et al., 2007). At present, mainly cyanides are used for the commercial hydrometallurgical leaching of gold and silver from ores and concentrates. However, due to the highly toxic nature of cyanide and environmental consequences, the process is very controversial and provokes examination of new leaching species.

C_4MIM HSO_4 (1-butyl-3-methyl-imidazolium hydrogen sulphate) and similar compounds in the presence of thiourea (or other S-containing compounds) and iron(III) as oxidant were used to separate gold and silver from ores.

The extraction of gold was achieved to be >85% from synthetic oxidic ore as well as natural sulphidic ore at 20-50°C using ionic liquid as a solvent. Gold extraction was close to results achieved for aqueous system H_2SO_4/tiourea/$Fe_2(SO_4)_3$, whereas recovery of silver from the natural sulphidic ore was significantly higher (≥60%) for the neat IL compared with an aqueous acid solution (<10%) as presented in Fig. 2. Moreover, high selectivity for the extraction of gold and silver was reported, with minimal selectivity of other metals (Cu, Zn, Pb and Fe).

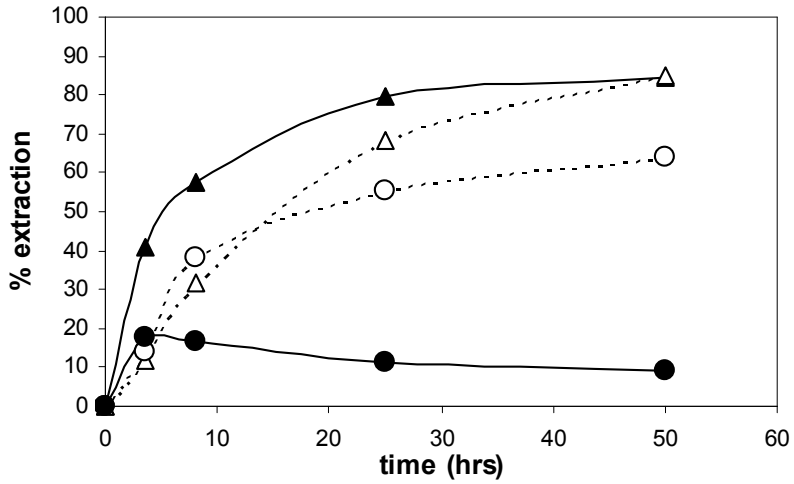

Fig. 2. Comparative leaching of gold and silver from ore using aqueous H_2SO_4 or C_4MIM HSO_4 in presence of $Fe_2(SO_4)_3$ and tiourea

Extension of n-alkyl chain length in imidazolium cation resulted in decreasing extraction efficiency of gold and silver, that might resulted from the increasing viscosity of ILs. The analysis of leaching results obtained for ILs with varied chain length and different types of anions showed that C_4MIM HSO_4 was the most effective medium that is important taking into account relatively low price of this compound.

Table 1. Effect of C_4MIM HSO_4 concentration on copper extraction from chalcopyrite at 70°C (Whitehead et al., 2007)

C_4MIM HSO_4 [%w/w]	Cu extracted [%]
10	55.7
20	58.1
50	82.2
100	86.6
1 M H_2SO_4	23.2

Copper extraction from chalcopyrite showed selective extraction of copper towards iron in the ionic liquid medium at 70 °C. Application of neat IL was more efficient (efficiency 87% of copper) than its solution (55% for 10%w/w) as shown in Table 1. Moreover, the recycling ability of $C_4MIM\ HSO_4$ by separation of gold and silver on activated charcoal was proposed without decomposition or significant change in the structure of IL (Whitehead et al., 2004; Whitehead et al., 2007).

MINERALS BENEFICIATION

One of the most important beneficiation processes is froth flotation of minerals, which requires hydrophobicity of the mineral particle. Only a few minerals naturally posses hydrophobic surface, hence, variety of reagents (collectors) providing hydrophobicity of the surface are used (Drzymała, 2001; Fuerstenau et al., 1985). The difficulty in the recovery of oxide-containing minerals causes that search of the new collectors is of utmost importance. So far some research involved application of pyridinuim salts (which are also describes as ionic liquids) in potash ores, phosphate rock, sulphide, oxide, silicate ores and coal (Madaan et al., 2008). Similarities in the composition of pyridinium and imidazolium salts allow assuming that imidazolium ILs may also behave like cationic collectors being suitable for oxide ores. ILs may form films at the surface of negatively charged particles by ion-ion interaction or interact by free electron pair of the nitrogen atom in cation with the ore surface that might increase hydrophobicity of ore particles. However, there is lack of research including application of the imidazolium ILs in flotation.

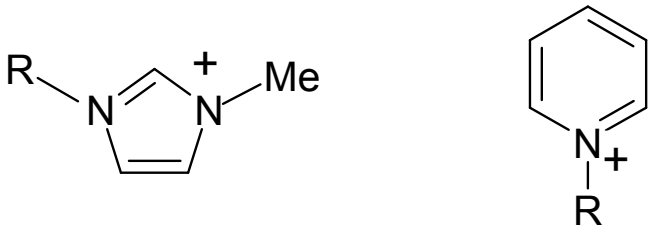

Fig. 3. Comparison of the structures of 1-alkyl-3-methylimidazolium and alkylpyridinium cation

SOLVENT EXTRACTION OF METAL IONS FROM AQUEOUS SOLUTION

Another consideration is given to application of ionic liquids in separations in order to replace organic solvents used in traditional liquid-liquid extraction of metal

ions from aqueous solutions. Some properties which make ILs attractive as alternative media in extraction processes are tunability, negligible vapour pressure, good thermal stability, and a wide liquid range. Since the partitioning of metal ions from aqueous solutions into ionic liquids is inefficient as a result of the tendency of the metal cations to remain hydrated in the aqueous phase, additional extractants, type of crown ethers (Dai et al., 1999; Chun et al., 2001), calixarenes (Luo et al., 2004), ditizone ditizone (Wei et al., 2003) and others (Visser and Rogers, 2003) were used. These species significantly enhance the partitioning of metal ions by forming complexes. The variety of tests were curried out in regard to extract heavy metals (Dai et al., 1999; Wei et al., 2003), alkali metals (Chun et al., 2001), actinides (Visser and Rogers, 2003) and lanthanoid ions (Kozonoi et al., 2007).

Modification of commonly used ILs by including a metal ion-ligating functional group in structure of one of the ions provides TSILs which play dual role of both hydrophobic solvents and extractants. Visser presented new thiourea, urea and thioether derivative of ILs designed to extract heavy metal ions (e.g. Hg^{2+} and Cd^{2+}) (Visser et al., 2001; Visser et al., 2002). According to the literature, preliminary research indicates that the application of ILs as an alternative solvent to replace traditional organic solvents in liquid - liquid extraction of metal ions is very promising.

ILs may also offer potential for the development of efficient processing of nuclear materials. The method for treating or reprocessing spent nuclear fuel using ionic liquids, and in particular to recover uranium and plutonium, was patented (Thied et al., 1999).

OTHER APPLICATIONS

We have also indicated several applications of ILs which not necessarily refer to mineral processing, however, are important in neighbouring technological areas such as metal electrowinning and waste material recycling. ILs may have potential to reduce energy consumption due to their low melting point.

Preliminary research on ILs in the electrorefining and electrowinning technologies pertains mainly aluminium processing (Nogrady, 2006; Kamavaram et al., 2003). The possibilities of aluminium refining is limited due to a strong affinity to oxygen, and cannot be electrolyzed in an aqueous solution due to its negative reduction potential (Zhang et al., 2003). Aluminium production through electrodeposition needs dissolvation of alumina in molten cryolite (Na_3AlF_6) bath. To keep cryolite liquid the temperature of 1000°C is needed consuming large amounts of energy. Application of ILs instead of cryolite might diminish energy demand in a significant way. Electrorefining of aluminium alloy in acidic C_4MIM $AlCl_4$ (1-butyl-3-methylimidazolium tertachloroaluminate) was curried out, resulting in obtaining high purity aluminum (99.89%). Energy consumption was estimated to be about 3 kWh/kg-Al in comparison to 17-18 kWh/kg-Al for the existing industrial refining process (Kamavaram et al., 2003).

Moreover, aluminium was also recovered from waste aluminium metal matrix composite by electrolysis in C_4MIM $AlCl_4$ at 103°C. A high purity product (>98%Al) was obtained (Kamavaram et al., 2005). What is characteristic for electrolysis in ILs is high purity of metal deposits obtained, high current densities possible as well as low energy consumption.

The possibility of application of ILs in processing of copper sulfide ores and base metal sulfides supported by preliminary findings in the use of ionic liquids in the electrorefining of chalcopyrite ($CuFeS_2$) was also indicated (McCluscey et al., 2001).

The possibility of electrolytic purification and electrowinning is a results of the immiscibility of selected ionic liquids with water and some organic solvents and theirs electrical conductivity. Especially wide electrochemical windows make ILs predominant towards conventional aqueous and organic electrochemistry in the electrodeposition of certain metals (Nogrady, 2006).

POSSIBILITY OF RECYCLING

Despite a number of advantages successful commercialization of ILs will depend on price and possibilities of recycling. Due to chemical stability and negligible volatility, ionic liquids are amenable to multiply recycling which allows decreasing the cost of a process. Solubility contributes most likely to the transport in environment and resulting spreading of contaminates. However, the loss of ILs into aqueous solution during e.g. solvent extraction will be important factor in process cost estimation (Alfassi et al., 2003). It was shown, that supercritical as well as relatively low-pressure gaseous CO_2 can be used to separate ILs from organic mixtures and water (Scurto et al., 2003; Blanchard and Brennecke, 2001). Additionally, the ionic liquid can be recycled following separation of metals e.g. gold or silver on activated carbon (Whitehead et al., 2004).

Presently ILs are very expensive, however, when production on a mass scale will start the price of ILs is expected to drop significantly.

ENVIRONMENTAL IMPACT

The wide range of possible industrial applications requires an evaluation of ionic liquids with respect to their (eco)toxicity. The impact should be assessed before they enter the environment as a part of sustainable development of chemical production.

Toxicity of the common class of imidazolium ionic liquids was measured using the variety of bioassay tests including bacteria, algae, mammalian cell lines (Ranke et al., 2005; Zhao et al., 2007) as well as their biodegrability using activated sludge (Garcia et al., 2005; Gathergood et al., 2006). Imidazolium derivatives were found to be more toxic than selected organic solvents (acetone, acetonitrile, metha-

nol), poorly biodegradable and relatively resistant to photodegradation (Stepnowski and Zalewska, 2004). Increasing toxicity with elongation of alkyl chain length was also observed. The high level of biodegrability was achieved by the incorporation of an ester in the side chain of the imidazolium cation and combination with octylsulfate anion (Gathergood et al., 2006). As an effective disposal method for difficult biodegradable ionic liquid cations - the electrochemical wastewater treatment was proposed. The electrolysis results in complete destruction of 1-butyl-3-methylimidazolium cation to easily biodegradable products (Stolte et al., 2008).

SURFACE ACTIVITY

Imidazolizum ionic liquids with long chain are generally seen to behave as amphiphilic compounds, displaying interface interaction. Likewise surfactants, ionic liquids also depend on chain length regarding the interface ordering phenomena (Blesic et al., 2007; Miskolczy et al., 2004; Vanyur et al., 2007; Jungnickel et al., 2008). Amphiphilic ILs possess significant promise in miscellaneous industrial applications, where high surface areas, modification of the interfacial activity or stability of colloidal systems are required. However, the state of knowledge of ILs structure and behaviour in an aqueous solution is so far limited. The phenomena of ILs self-organization in aqueous solutions are currently under investigation by our group as well as other authors (Vanyur et al., 2007; Inoue et al., 2007; Łuczak et al., 2007). The length of the alkyl chain substituents, the degree of substitution, type of counterion as well as temperature were found to have vital effect on the CMC values of ILs. There is lack of studies concerning more composed systems including e.g. electrolytes or cosurfactants.

In our previous research we have determined CMC of 1-alkyl-3-methylimidazolium ionic liquids with alkyl chain lengths 4 -18 and chloride anion (CnMIM Cl) by surface tension and electrical conductivity measurements. The results of the surface tension measurements for the aqueous solutions as a function of the ILs concentration are presented in Fig. 4.

Discontinuities are observed only for compounds possessing the alkyl chain equal or longer than 8 carbon atoms, suggesting that only these imidazolium derivatives may be able to form micelles at 298K. The CMCs for $[C_4MIM]$ Cl and $[C_6MIM]$ Cl were not observed, even though the surface tension measurements of high concentrated solutions were conducted. The micelle formation in these ILs cannot be positively confirmed in the current conditions of measurements (298 K) that might result from theirs composition - too short alkyl chain in cation or high Krafft point of these compounds. The experimental results of the break points indicating CMCs are presented in Table 2.

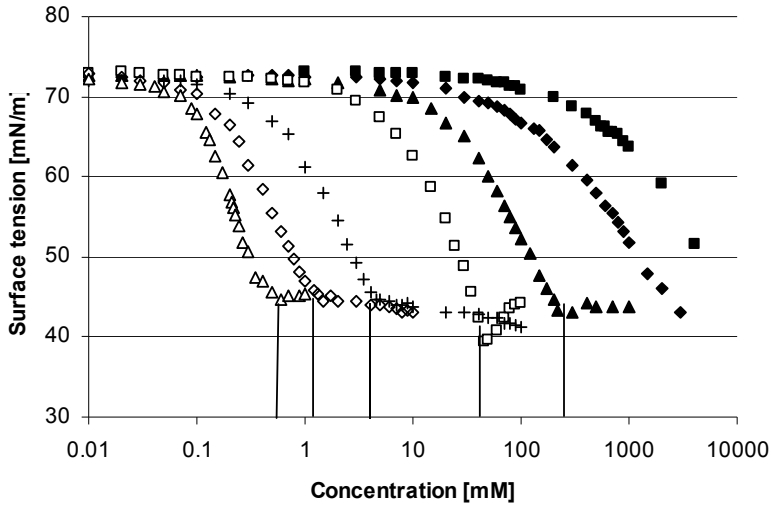

Fig. 4. Surface tension data versus IL concentration isotherms measured at 298 K for aqueous solutions of [C_4MIM] Cl (■), [C_6MIM] Cl (◆), [C_8MIM] Cl (▲), [C_{10}MIM] Cl (□), [C_{14}MIM] Cl (+), [C_{16}MIM] Cl (◇) and C_{18}MIM Cl (Δ)

Table 2. Comparison of CMC results of CnMIM Cl and literature data of CnMIM Br, cationic surfactants of the alkyltrimethylammonium chlorides and bromides and sodium alkylsulphates in 298K

Nr of C atoms	CnMIM Cl	CnMIM Br	C_nTAC	C_nTAB	SAS*
8	220[1] 234[1]	150[2]		225[3]	140[4] 139[5]
10	59.9[1] 53.8[1]	41[7]	94.7[6] 96[9]	62[3] 62.7[11] 60.2[11]	33[4] 33[5]
12		9.8[7] 9.5[8]	22.2[6] 22[9]	14.3[3] 14.8[12]** 15.7[12]**	8.6[4] 8.59[5]
14	3.38[1] 3.15[1]	2.5[7] 2.6[8]	5.63[6] 5.5[9]	4.08[12]** 3.94[12]**	2.2[4] 2.12[5]
16	1.26[1] 1.14[1]	0.61[7] 0.65[8]	1.3[10]**	0.93[12]** 0.92[12]**	0.58[4] 0.58[5]
18	0.40[1] 0.45[1]				0.23[4] 0.16[5]

[1]our previous work (Jungnickel et al.,2008)
[2] (Goodchild et al., 2007)
[3] (D'errico et al., 2001)
[4] (Shaw, 1992)
[5] (Huibers et al., 1997)
[6] (Perger and Bester – Rogac, 2007)
[7] (Vanyur et al., 2007)
[8] (Inoue et al., 2007)
[9] (Hayami et al., 1998)
[10] (Blesic et al., 2007)
[11] (Chakraborty and Moulik, 2007)
[12] (Basu Ray et al., 2005)
*313 K, **296 K

Described results show that elongation of the carbon chain decreases the CMC meaning that increasing the hydrophobic part of the IL cations favours micelle formation - as has been shown in the literature (Hunter, 1989). For homologous series of 1-alkyl-methylimidazolium chlorides, linear relationship between the logarithm of CMC and the number of carbon atoms in the alkyl chain of the cation has been found to be:

$$y = 4.5 - 0.28x \quad (\log CMC = A - Bx)$$

where *A*, *B* are constants for a particular homologous series and temperature, and *x* is number of carbon atoms in the hydrocarbon chain. Constant *A* varies with the nature and number of hydrophilic groups while *B* is a constant which reflects the effect of each additional methylene group on the CMC. This equation is in good agreement with the relationship calculated for values published by Belsic (y = 4.7 – 0.29x) (Blesic et al., 2007).

Comparison of CMC data of imidazolium derivatives with the common surfactants let to conclude that we can observe similar CMC vs. number of carbon atoms in chain relationships between ILs and surfactants. The CMC values of $[C_nMIM][Cl]$ ionic liquids were found to locate between those of C_nTAC and SAS possessing alkyl moiety with the analogical number of carbon atoms. An analogical relationship was also found for $[C_nMIM][Br]$, C_nTABr and SAS, as shown in Fig. 5. The lower CMC values of ILs in comparison to the alkyltrimethylammonium salts might be attributed to the structure of the imidazolium head group which has weaker affinity to the hydrogen bond formation with water. On the other hand, IL as salt possessing some ionic strength may have tendency to stronger salting-out effect. Moreover, it may be also the result of interactions between anion and aromatic ring in imidazolium derivatives which did not occur in the case of typical surfactants. The lower values for compound with Br^- than Cl^- anions can be explained by the influence of the anion size. The larger ion is, the weaker hydration occurs. The weaker hydrated anions are easily adsorbed on the surface of the micelles which decreases electrostatic repulsion and in this way facilitates aggregation (Hunter, 1989).

A linear relationship between the CMC values and carbon atoms number for mentioned ILs as well as surfactants is presented in Fig. 5.

As mentioned before, the CMC determination may strongly depend on the solubility of surfactant. For ionic surfactants, there is a temperature called the Kraft temperature (K_T), below which the solubility decreases dramatically. It is necessary to measure the CMC of surfactants above the Krafft temperature since there is no micelle formation below the K_T. With rising the temperature the solubility slowly increases until at the Krafft temperature CMC is reached. The Krafft temperature and CMC of the surfactants provide information about the conditions at which the compound acts as an amphiphile (Hunter, 1989; Holmberg, 2002).

Fig. 6 presents an exemplary result of Krafft temperature determination by the conductivity method. During temperature transition the electrical conductivity increases with the increasing temperature, due to larger dissolution of the IL until the K_T

is reached. After K_T the conductance increases slowly due to the increase in ionic mobility.

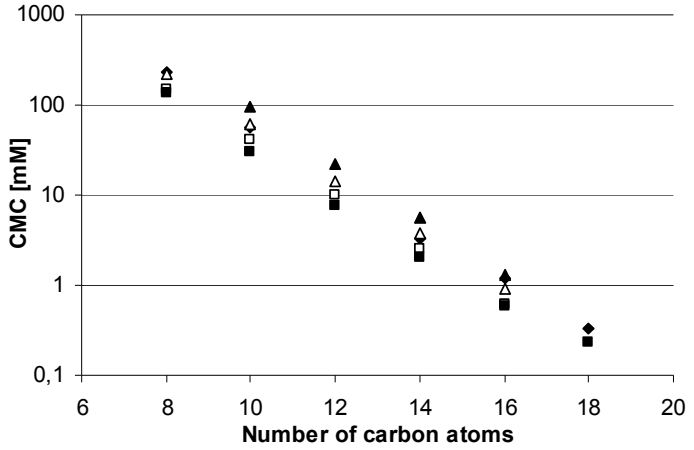

Fig. 5. CMC dependence on alkyl chain length in 298 K:
C_nMIM Cl (◆), C_nMIM Br (□), C_nTAC (▲), C_nTAB (Δ) and SAS (■)

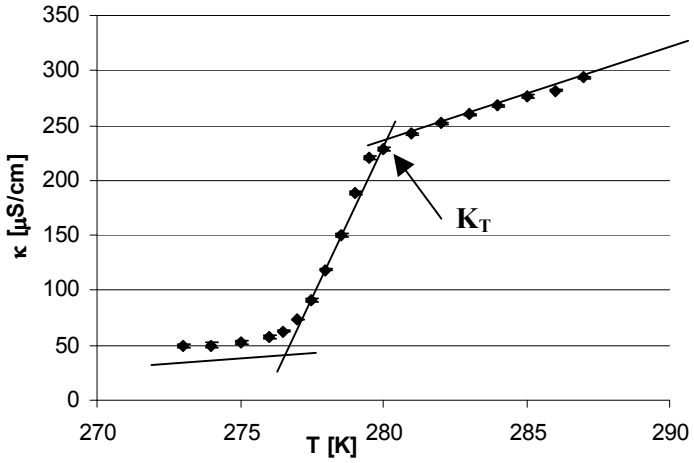

Fig. 6. The Krafft temperature determination of [C_{16}MIM]Cl

The Krafft temperatures listed in Table 5 show that determination of K_T by this method was only possible for ILs possessing more than 16 carbon atoms in chain length. The K_T for the rest of the compounds could not be determined as there was no visible turbidity even at a few degrees below 0°C. In Table 3 we report the Krafft temperatures for 1-alkyl-3-methylimidazolium chlorides, alkyltrimethylammonium bromide as well as sodium alkyl sulphates compounds. Results show that the Krafft

temperatures of ILs are lower than those of the C_nTAB and much lower than SAS homologues, presenting behaviour opposite to CMC dependence, meaning that imidazolium derivatives behave like surfactants at lower temperatures.

Table 3. The Krafft temperatures of imidazolium ILs and alkyltrimethylammonium bromides compounds

Number of Carbon atoms	8	10	12	14	16	18
C_nMIM Cl	< 273	< 273	< 273	< 273	279.5	297
C_nTAB	< 273[1]	< 273[1]	< 273[1]	~273[1]	297[2]	308-309[1]
SAS		281[3]	289[3]	303[3]	318[3]	329[3]

[1] (Davey et al., 1989)
[2] (Adam and Pankhurst, 1946)
[3] (Shaw, 1992)

CONCLUSIONS

The application of imidazolium ionic liquids as media for separation (e.g. leaching) is growing promptly mainly because of the adjustable nature of both cation and anion. The separation possibilities are very wide including recovery of valuable metals from waste waters, ores as well as organic molecules and gases. Moreover, they offer potential to projecting and developing processes with reduced energy consumption as a result of their low melting point.

Ionic liquids are considered as promising compounds mainly thanks to their negligible vapour pressure, hence, there is no loss of ILs through evaporation. However, most of ILs described nowadays in literature for catalysis, electrochemical and separation processes consist of halogen containing anions which might be toxic and corrosive. Therefore, it is important to find methods to take advantage of the nonvolatile nature of ionic liquids that is untypical for wide used liquid media.

For the sake of many advantageous properties and successful initial experiments considering potential applications projecting of inherently non-toxic, hydrolysis stable and biodegradable compounds is crucial.

ACKNOWLEDGEMENTS

Financial support was provided by the Polish Ministry of Science and Higher Education in the years 2007-2010 grant No.: N205 041 32/2340 and Gdańsk University of Technology contract No.: BW 014694/039.

REFERENCES

ADAM H.K., PANKHURST K.G.A., 1946. *The solubility of some paraffin-chain salts,* Trans. Faraday Soc., 42, 523.

ALFASSI Z.B., HUIE R.E., MILMAN B.L., NETA P., 2003. *Electrospray ionization mass spectrometry of ionic liquids and determination of their solubility in water,* Anal. Bioanal. Chem., 377, 159-164.

BASU RAY G., CHAKRABORTY I., GHOSH S., MOULIK S.P., PALEPU R., 2005. *Self Aggregation of Alkyltrimethylammonium Bromides (C10-, C12-, C14-, and C16TAB) and Their Binary Mixtures in Aqueous Medium: A Critical and Comprehensive Assessment of Interfacial Behavior and Bulk Properties with Reference to Two Types of Micelle Formation,* Langmuir, 21, 10958-10967.

BLANCHARD L.A., BRENNECKE J.F., 2001. *Recovery of Organic Products from Ionic Liquids Using Supercritical Carbon Dioxide,* Ind. Eng. Chem. Res., 40, 287-292.

BLESIC M., MARQUES M.H., PLECHKOVA N.V., SEDDON K.R., REBELO L.P.N., LOPES A., 2007. *Self-aggregation of ionic liquids: micelle formation in aqueous solution,* Green Chem., 9, 481–490.

CASSOL C.C., UMPIERE A.P., EBELING G., FERRERA B., CHIARO S.S.X., DUPONT J., 2007. *On the Extraction of Aromatic Compounds from Hydrocarbons by Imidazolium Ionic Liquids,*
Int. J. Mol. Sci., 8, 593-605.

CHAKRABORTY I., MOULIK S.P., 2007. *Self-Aggregation of Ionic C10 Surfactants Having Different Headgroups with Special Reference to the Behavior of Decyltrimethylammonium Bromie in Different Salt Environments: A Calorimetric Study with Energetic Analysis,* J. Phys. Chem. B, 111, 3658-3664.

CHUN S., DZYUBA S.V., BARTSCH R.A., 2001. *Influence of Structural Variation in Room-Temperature Ionic Liquids on the Selectivity and Efficiency of Competitive Alkali Metal Salt Extraction by a Crown Ether,* Anal. Chem., 73, 3737-3741.

DAI S., JU Y.H., BBARNES C. E., 1999. *Solvent extraction of strontium nitrate by a crown ether using room-temperature ionic liquids,* J. Chem. Soc., Dalton Trans., 1201-1202.

DAVEY T.W., DUCKER W.A., HAYMAN A.R., SIMPSON J., 1998. *Krafft Temperature Depression in Quaternary Ammonium Bromide Surfactants,* Langmuir, 14, 3210-3213.

DEETLEFS M., SEDDON K.R., SHARA M., 2006. *Predicting physical properties of ionic liquids,* Phys. Chem. Chem. Phys., 8, 1-8.

D'ERRICO G., ORTONA O., PADUANO L., VITAGLIANO V., 2001. *Transport Properties of Aqueous Solutions of Alkyltrimethylammonium Bromide Surfactants at 25°C,* J. Colloid Interface Sci., 239, 264-271.

DONG B., LI N., ZHENG L., YU L., INOUE T., 2007. *Surface Adsorption and Micelle Formation*
Of Surface Active Ionic Liquids in Aqueous Solution, Langmuir, 23, 4178-4182.

DRZYMAŁA J., 2001. Podstawy mineralurgii, Oficyna Wydawnicza Politechniki Wrocławskiej, Wrocław, Polska.

FUERSTENAU M.C., MILLER J.D., KUHN M.C., 1985. Chemistry of flotation, Society of Mining Engineers of the American Institute of MIning, Metallurgical and Petroleum Engineers, Inc, New York.

GARCIA T.M., GATHERGOOD N., SCAMMELS P., 2005. *Biodegradable ionic liquids. Part II. Effect of the anion and toxicology,* Green Chem., 7, 9-14.

GATHERGOOD N., SCAMELLS P.J., GARCIA M.T., 2006. *Biodegradable ionic liquids. Part III. The first readily biodegradable ionic liquids,* Green Chem., 8, 156-160.

GOODCHILD I., COLLIER L., MILLAR S.L., PROKEŠ I., LORD J.C.D., BUTTS C.P.B., BOWERS J., WEBSTER J.R.P., HEENAN R.K., 2007. *Structural studies of the phase, aggregation and surface behaviour of 1-alkyl-3-methylimidazolium halide + water mixtures,* J. Colloid Interface Sci., 307, 445-468.

HAYAMI Y., ICHIKAWA H., SOMEYA A., ARATONO M., MOTOMURA K., 1998. *Thermodynamic study on the adsorption and micelle formation of long chain alkyltrimethylammonium chlorides,* Colloid Polym. Sci., 276: 595-600.

HOLMBERG, K., 2002. Handbook of Applied Surface and Colloid Chemistry, Vol. 1-2, John Wiley & Sons, U.K.

HUDDLESTON J.G.,. WILLAUER H.D, SWATLOWSKI R.P., VISSER A., ROBERTS D.W., 1998. *Room temperature ionic liquids as novel media for 'clean' liquid–liquid extraction,* Chem. Commun., 1765-1766.

HUDDLESTON J.G., VISSER A.E., REICHERT W.M., MATTHEW W., WILLAUER H.D., BROKER G.A., ROGERS R.D., 2001. *Characterization and comparison of hydrophilic and hydrophobic room temperature ionic liquids incorporating the imidazolium cation,* Green Chem., 3, 156-164.

HUIBERS P.D.T., LOBANOV V.S., KATRITZKY A.R., SHAH D.O., KARELSON M., 1997. *Prediction of Critical Micelle Concentration Using a Quantitative Structure-Property Relationship Approach: 2. Anionic Surfactants,,* J. Colloid Interface Sci., 187, 113-120.

HUNTER R.J., 1989. Foundations of Colloid Science. Vol. 1, Oxford University Press, New York, USA.

INOUE T., EBINA H., DONG B., ZHENG L., 2007. *Electrical conductivity study on micelle formation of long-chain imidazolium ionic liquids in aqueous solution,* J. Colloid and Interface Sci., 314, 236-241.

JUNGNICKEL C., ŁUCZAK J., RANKE J., FERNANDEZ J.F., MÜLLER A., THÖMING J., 2008. *Micelle Formation of Imidazolium Ionic Liquids in Aqueous Solution,* Colloids and Surfaces A: Physicochem. Eng. Aspects, 316, 278-284.

KAMAVARAM V., MANTHA D., REDDY R.G., 2003. *Electrorefining of aluminium alloy in ionic liquids at low temperatures,* J. Min. Met., 39, 43 - 58.

KAMAVARAM V., MANTHA D., REDDY R.G., 2005. *Recycling of aluminum metal matrix composite using ionic liquids: Effect of process variables on current efficiency and deposit characteristics,* 50, 3286-3295.

KOZONOI N., IKEDA Y., 2007. *Extraction Mechanism of Metal Ion from Aqueous Solution to the Hydrophobic Ionic Liquid, 1-Butyl-3-methylimidazolium Nonafluorobutanesulfonate,* Monatsh. Chem., 138, 1145-1151.

LUO H., DAI S., BONNESEN P.V., BUCHANAN A. C., HOLBREY J. D., BRIDGES N., ROGERS R. D., 2004. *Extraction of Cesium Ions from Aqueous Solutions Using Calix[4]arene-bis(tert-octylbenzo-crown-6) in Ionic Liquids,* Anal. Chem., 76, 3078-3083.

ŁUCZAK, J., HUPKA, J., THOEMING, J., JUNGNICKEL, C., 2007. *Thermodynamics of aggregate formation of 1methyl-3-tetradecylimidazolium chloride in aqueous solution*, In Proceedings of the International Scientific Conference, Surfactants and Dispersed Systems in Theory and Practice, PALMA Press, Wrocław, 149-153.

MADAAN P., TYAGI V.K., 2008. *Quaternary pyridinuim salts: a review,* J. Oleo Sci. 57, 197-215.

McCLUSCEY A., LAWRANCE G. A., OWEN M., HAMILTON I.C., 2001. *Ionic Liquids: From Green Chemistry to Ore Refining*. Procidings of the Green (or Greener) Industrial Applications of Ionic Liquids, 221st American Chemical Society National Meeting, San Diego, USA.

MISKOLCZY Z., SEBOK-NAGY K., BICZOK L., GOKTURK S., 2004. *Aggregation and micelle formation of ionic liquids in aqueous solution,,* Chem. Phys. Lett., 400, 296-300.

NOGRADY B., 2006. *Cutting aluminium energy bills: Designer solvents,* Process, 6: 6-7.

RANKE J., STOCK F., STORMANN R., MOLTER K., HOFFMANN J., ONDRUSCHKA B., JASTORFF B., 2005. *Preliminary (Eco-)Toxicological Risk Profiles of Ionic Liquids in Multiphase Homogeneous Catalysis*, ed. B. Cornils Editors, Weinheim: Wiley-VCH. 588-600.

SCURTO A.M., AKI S.N.V.K., BRENNECKE J. F., 2003. *Carbon dioxide induced separation of ionic liquids and water,* Chem. Commun. 572-573.

SHAW D.J., 1992,. Colloid & Surface Chemistry, Butterworth Heinemann, Oxford, U.K.,

SHELDON, R., 2001. *Catalytic reactions in ionic liquids,* Chem. Commun., 23, 2399-2407.

STEPNOWSKI P., ZALESKA A., 2004. *Comparison of different advanced oxidation processes for the degradation of room temperature ionic liquids,* J. Photochem. Photobiol. A, 170, 45-50.

STOLTE S., ABDULKARIM S., ARNING J., BLOMEYER-NIENSTEDT A.K., BOTTIN-WEBER U., MATZKE M., RANKE J., JASTORFF B., THOMING J., 2008. *Primary biodegradation of ionic liquid cations, identification of degradation products of 1-methyl-3-octylimidazolium chloride and electrochemical wastewater treatment of poorly biodegradable compounds,* Green Chem., 10, 214–224.

THIED R.C., SEDDON K.R., PITNER W.R., ROONEY D.W., 1999. *Nuclear fuel reprocessing*, Patent Nr WO 99/41752.

VANYUR, R., BICZOK, L., MISKOLCZY, Z., 2007. *Micelle formation of 1-alkyl-3-methylimidazolium bromide ionic liquids in aqueous solution,* Colloids and Surfaces A: Physicochem. Eng. Aspects, 299, 256-261.

VISSER, A., SWATLOWSKI, R.P., REICHERT, R.M., MAYTON, R., SHEFF, S., WIERZBICKI, A., DAVIS, J.H., ROGERS, R. D., 2001. *Task-specific ionic liquids for the extraction of metal ions from aqueous solutions,* Chem. Commun., 135-136.

VISSER, A., SWATLOWSKI, R.P., REICHERT, R.M., MAYTON, R., SHEFF, S., WIERZBICKI, A., DAVIS, J.H., ROGERS, R. D., 2002. *Task-Specific Ionic Liquids Incorporating Novel Cations for the Coordination and Extraction of* Hg^{2+} *and* Cd^{2+}*: Synthesis, Characterization, and Extraction Studies,* Environ. Sci. Technol., 36, 2523-2529.

VISSER, A.E., ROGERS, R.D., 2003. *Room-temperature ionic liquids: new solvents for f-element separations and associated solution chemistry,* J. Solid State Chem., 171, 109-113.

WEI G.T., YANG Z., CHEN C.J., 2003. *Room temperature ionic liquid as a novel medium for liquid/liquid extraction of metal ions,* Anal. Chim. Acta, 488, 183-192.

WELTON, T., 2004. *Ionic liquids in catalysis,* Coord. Chem. Rev., 248, 2459-2477.

WHITEHEAD J.A., LAWRANCE G.A., McCLUSKEY A., 2004. *'Green' leaching: recyclable and selective leaching of gold-bearing ore in an ionic liquid,* Green Chem., 6, 313-315.

WHITEHEAD J.A., ZHANG J., PEREIRA N., McCLUSKEY A., LAWRANCE G.A., 2007. *Application of 1-alkyl-3-methyl-imidazolium ionic liquids in the oxidative leaching of sulphidic copper, gold and silver ores,* Hydrometallurgy, 88, 109-120.

ZHANG M., KAMAVARAM V., REDDY R.G., 2003. *New electrolytes for aluminum production: Ionic liquids,* JOM, 55, 54-57.

ZHAO D., LIAO Y., ZHANG Z., 2007. *Toxicity of Ionic Liquids,* Clean, 35, 42 - 48.

Łuczak, J., Joskowska, M., Hupka J., *Imidazoliowe ciecze jonowe w mineralurgii*, Physicochemical Problems of Mineral Processing, 42 (2008), 223-236 (w jęz. ang)

Imidazoliowe ciecze jonowe (ILs) stanowią nową klasę związków o szerokich możliwościach przemysłowego zastosowania. Z przeglądu dostępnej literatury wynika, że ILs mogłyby zostać wykorzystane do odzysku i oczyszczania metali ze środowiska wodnego oraz rud w procesach ługowania, ekstrakcji rozpuszczalnikowej oraz w procesach elektrochemicznych. Pochodne imidazoliowe mogą być wykorzystywane zarówno jako rozpuszczalniki jak i aktywne czynniki separujące. W pracy uwzględniono także wpływ na środowisko oraz możliwości odzysku ILs. Wykazano, że potencjalne zastosowanie w mineralurgii wymaga dalszych systematycznych badań.

słowa kluczowe: imidazoliowe ciecze jonowe, ługowanie mineralne, ekstrakcja, formowanie miceli

Physicochemical Problems of Mineral Processing, 42 (2008), 237-250
Fizykochemiczne Problemy Mineralurgii, 42 (2008), 237-250

Janina Grodzka*, Jan Drzymała**, Andrzej Pomianowski***

INTERFACIAL MATERIAL CONSTANTS FOR SYSTEM OF FINE SIZES

Received May 15, 2008; reviewed; accepted July 31, 2008

The properties of bulk and interfacial regions was presented in the paper taking onto account suspensions, colloids, micellar solutions, microemulsions and the so-called soft matter, which understanding is as important as the inorganic matter. A special attention was paid to the role and diversity of material constants necessary for delineation of the state and properties of the considered systems.

key words: material constants, suspension, colloid, micellar solution, microemulsion, soft matter

INTRODUCTION

The ratio between surface area and volume of any system changes substantially with the decreasing size. The same is valid for energy and other properties. As a result the interfacial regions are always different from the bulk regions.

Interfacial effects, resulting from the existence of surface, can frequently be neglected for large bulky systems while in finally divided systems their properties depend practically only on the interfacial regions properties. The interface accumulates the excess free energy of the system. The excess free energy is the source of the interfacial tension, the principal material constant of the interfacial regions as well as the reason of changing properties with the size of one and multi component substances. When we consider properties of individual atoms or molecules, knowing their atomic or molecular constants, we know that they do not allow directly describe the bulk properties build from the mentioned elements. Each bulk phase has however characteristic material constants, only when the bond lengths between atoms and molecules are very small in comparison with their location from the interface. The

* HCP Medical Center, Poznan, Poland, janina.grodzka@wp.pl
** Wroclaw University of Technology, 50-370 Wroclaw, Poland, jan.drzymala@pwr.wroc.pl
*** PAN Krakow, prof. em., Poland, izabela.pomianowska@neostrada.pl

are very small in comparison with their location from the interface. The interfacial material constant (imc) become essential when this condition is not fulfilled. In this article nanometrically dispersed systems will be discussed. In finally divided systems practically all system properties are depended on the imc values.

HIERARCHY OF MATERIAL CONSTANTS

The material constants characterize the whole materialist world and differ in their generalization degree. The first category material constants occupying the top of a generalization pyramid are universal constants, including the speed of light in vacuum c, the Planck h, Boltzmann constants k as well as gravity constant g. They have always the same value and occur in equations dealing with properties of materials.

The second category of material constants is made of partial derivatives of different degree with respect to different parameters of chemical potentials of any type of material. The requirement is the thermodynamic equilibrium of the system with its surroundings. These constants are important parameters and are present in numerous textbooks and handbooks. The most important role, in his category of imc, is the excess molar free energy of interfacial regions ω^s.

The third category, still greater group of constants, characterizes matter in the course of transformation. We select from this group a category of processes running with a constant, limited velocity. They are called the steady state or stationary processes. They are very important for delineation of processes taking place in living organisms. These process are investigated by biochemists and biophysicists and the system in which they occur belong to the colloidal systems category. To realized the complexity of the issue it must be recalled how numerous and diversified are metabolic reactions in living organisms. For their description we need precise information on such systems as for example breathing and blood circulation. We need both qualitative and quantitative characteristics of colloids which form particular types of tissues and body fluids.

The fourth category, the lowest in the hierarchy, is formed by material constants which are normative and relative in their character.

PRINCIPLES OF MATERIAL CONSTANT CLASSIFICATION

Stating type and value of any material constant requires an additional and precise information on what material it represents. Therefore, formally, also the material constant name, being a kind of nickname, signaling its definition, is also a material constant. It represent the lowest level of the hierarchy of material constants because is defined relatively, and does not have any established value. For example the term gold means not only all gold isotopes of Au but also frequently its alloys of different

caratages. More precisely, the properties of gold ingots are different from those of gold used in jewelry as leaves and whiskers of colloidal dimensions. Therefore, besides name, we have to state precisely, parameters which allow to univocally define the considered material constant.

From the presented above example of gold results that besides common parameters of state such as pressure p, volume V, temperature T, and time t**,** also important is information on the size and shape of the considered piece of matter. The issue of shape and size is essential for understanding and description of the nature of matter.

Material, which is essential for development of living organism and technology is water. Most of the material constants of our interest is somehow connected with water and its solutions. It is a natural trend in science to qualitatively and theoretically delineate, starting from the foundations, the results of scientific observations. At the present level of development of science, the most general tool is the quantum mechanics and statistical thermodynamics, while modeling of real systems usually is based on the molecular dynamics. Systems, on which we are focused the most, are stable hydrophilic colloids at high concentrations. The principal type of bond, which determines the structure of colloid is the hydrogen bond. Until today, despite a dozen of models of water molecule, there is a lack of a uniform model describing the water structure and its solutions, due to lack of quantum approach to the hydrogen bond. Only properly modified existing principles of the quantum mechanics can fulfill this gap.

Let us discuss this issue further. We know that matter is energy which permanently changes its forms. In addition to that, it is certain that its principal elements are electrical charges of opposite signs, while the principal element of structure is represented by the hydrogen atom. Mills (2002) proposed a change in the mathematical formalism presently used by the quantum mechanics. Even Newton noticed that we either measure or compare only forces acting in systems, while the existence of mass is only postulated. A statistical picture of the potential energy is given by the Coulomb law, which determines how a change of a distance between the charges, either of the same or opposite signs, increases, or decrease, the energy of the system. Mills (2002) defined the term of two-dimensional orbitsphere, which takes into account the mass of electron m_e, defined by a well experimentally determined de Broglie relation between electron linear momentum $m_e v_n$ through its materialistic wave of appropriate length λ_n:$\lambda_n = h/m_e v_n$. He also assumed that if an electron, having linear momentum $m_e v_n$, is present in the hydrogen atom on orbitspheres of Bohr radius r_n, then the energy is not emitted. The energy is either emitted or adsorbed only when the electron is transferred between orbitspheres of different n values. To define other quantum numbers he used the Maxwell equation for delineation of the electron on an orbitsphere and for connecting the motion of charges and magnetic field, getting as, a consequence, an expression for spin functions. The author claims that after taking into account the universal gravity constant g, his modified quantum mechanics provide quantitative description of matter staring from the hydrogen atom property, up to the average tem-

perature, and the expansion and shrinking period of the Universe as well as materialistic character of the black holes. Maybe this type of small modification of the principles of quantum mechanics will help to explain the nature of the hydrogen bond.

A point does not have any dimension. However, the point model of a neutral hydrogen atom has a mass, which is a sum of the mass of the electron and proton, and thus, the energy given by the Einstein formula. Having a collection of points in an infinite space we can, using the law of physics and mathematics build a model of a materialistic Universe. We need for it two types of parameters, material constants as well as the size and shape. We can build a sphere having the radius of Bohr's hydrogen atom up to complicated structures of nebulas and black holes. In other words, the shape is replaced with known rules of symmetry delineating systems of any size.

We can classified the systems into:

1) divided molecularly (angstrom scale)
2) divided nonometrically (nanometer scale)
3) divided colloidally (micrometer scale)
4) suspensions (macro scale).

Regardless of system size, there are states of matter:

- gaseous
- condensed, including liquid, crystalline, hard, and soft matter.

A system can be considered as:

- equilibrium state
- steady state
- non-steady state.

It depends on our choice how high in the hierarchy the material constant which characterizes the considered system is located.

At a constant temperature the surface tension is the excess specific change of the thermodynamic potential of a substance. In one-phase systems, regardless of their state of matter, the surface tension is defined as a half of maximum cohesion work needed for formation of a unit of free surface and is related only to the interface of a chemically pure substance at equilibrium with its saturated vapors. In practice the measurements are conducted in the presence of the so-called neutral gases, and their difficult-to-predict influence on the results, frequently significantly alters the properties of the interfacial regions.

A precise definition requires an additional decision whether or not the surface formation process is considered under constant volume, constant pressure, or constant potential of open systems ($\Omega = -pV$). Not always the excess free surface energy has one, well determined value, because in condensed phases it frequently becomes a tensor.

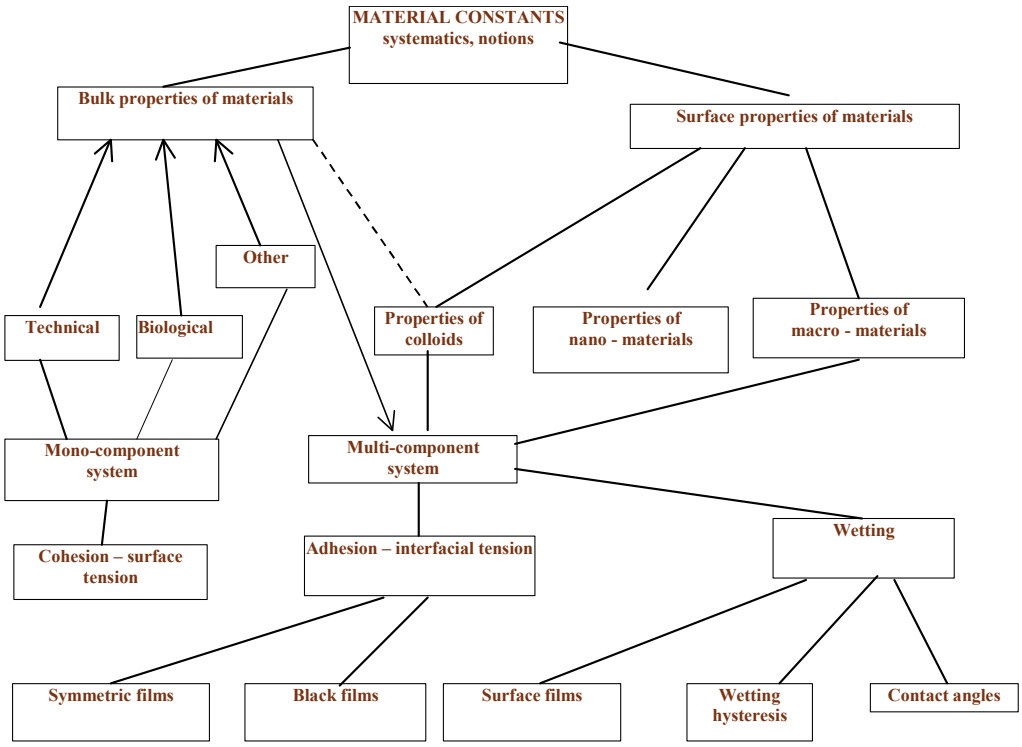

Another important material constant of a one-phase one-component material is connected with the density. It is viscosity, also called the internal friction, and lies at the border of equilibrium and stationary states. The detection and measurements of viscosity requires initiation in the liquid phase observable flow (motion). Due to permanent, at equilibrium, thermal motion of the molecules inside the liquids, the values of the viscosity are needed for delineation of their material constant called self-diffusion. The principal element needed for delineation of the stationary states is the thermodynamic driving force, that is a parameter which initiates the flow between reservoirs in which the system is kept at equilibrium. The other parameter is the intensity of the flux. For initiation of a flow of heat, a temperature gradient is needed. For electrical charge flow the driving force is the electrical potential gradient. Any flux, or generally an movement is accompanied by phenomena resulting from the specificity of the medium resistance in which the movement takes palace. The nature of flux is based on interconnection of fluxes resulting from the nature of the medium. It is worthwhile to notice different characters of the force fields which cause formation, in the media, concrete gradients. A great variation of stationary material constants is connected with the character of the force fields determining the nature of the appropriate gradient, and is also connected with the character of resistance encountered by

the fluxes. The flow of charge causes, in a conducting medium, appearance of precisely determined magnetic field linked to the electrical field.

We know very well that equilibrium systems are not static. Its characteristic feature is a tremendous dynamics of matter movement but only on the atomic (molecular) scale. We know that the movement does not stop even at zero kelvin. They are characterized by the values of vibration energy at the so-called states also known as standard states. Great scientist Clausius offered a hypothesis of the so-called thermal death of the Universe. He based his hypothesis on the fact of increasing entropy of systems which dissipate their energy in non-reversible processes through transfer of the energy to the surrounding as heat. In contrary to the internal energy, portions of entropy are transport either as work or heat and they are not functions of state. Physically, their quantities are not total derivatives, and their values depend on the way the change occurs.

Introduction of time and defining the source of entropy density in thermodynamics allowed to consider the resistance, which dissipates energy, and provide a quantitative measure of the dissipation. It provided conditions for definition of the material constants for stationary systems as partial derivatives of volumetric source of entropy, while the stationary interfacial material constants are obtained as derivatives of quantities of original excess functions.

For thermodynamics of stationary states, the equivalent of Maxwell relation for the thermodynamics of equilibrium systems is the Onsager rule. Both deal with the so-called crossed effects between partial derivatives of total differentials.

The gradients of intensive parameters of state of a system are thermodynamic driving forces which cause flows of system's elements. Dissipative resistance of the medium which decides about the values of the phenomenological coefficients of flows are an essential source of entropy of irreversible processes taking place in the investigated systems. The most important two processes, defined in such a way irreversibility, and thus dissipation of energy, are diffusive fluxes of components of system, caused by gradient of their chemical potentials and fluxes of energy as heat under influence of temperature.

The smallest elements of macroscopic systems structure are atoms and individual molecules. If at least one of the dimension of the elemental component of the system: macromolecules, stable aggregation or association of molecules, particles, droplets of the dispersed condensed phase lies below 1 μm, the system is called colloid.

COLLOIDAL SYSTEMS

Non-dissipative, Newtonian character of movement in isolated ideal gases allowed to define the principal parameter of all materialistic systems, the absolute temperature T as a parameter describing energy state of gases resulting from elastic collisions of atoms, treated as materialistic points having certain momentum. When in the volume

V there is one such atom or molecule, then $T=pV/k$, because the number of atoms N_A is equal to the Avogadro number $T=pV/R$. In colloidal systems, tending to form coagula and precipitates, the process, leading to formation of still greater aggregates, is diffusion of molecules. Due to investigations of the Brownian motion, as a results of chaotic self-diffusive thermal movement of either molecules or particles, the rules regarding the particles diffusion were adopted from the terminology and laws established for diffusion of atoms. The change from the description of the movement of materialistic points to the properties and processes in real systems requires to give concrete sizes and shapes of the components and their interactions. Modeling colloidal systems, due to the ease of calculations, the simplest assumption is sphericity of the particles. Additional difficulty is, however, the polydispersity. A sample of a particular polyelectrolyte consists of a mixture of molecules differing in polymerization degree, thus in molecular mass. The molecular mass M_i, by definition, is the mass of N_A=6.023·10^{23} molecules of i type. A composition of the whole sample is determined by mole fractions x_i of all component i. Two methods are used to get average values. Number average $\tilde{M}_n = m/n = (\Sigma_i n_i M_i)/(\Sigma_i n_i)$ or as weight average molecular mass $\tilde{M}_m=\Sigma_i (m_i/m M_i$, where m_i denotes the mass of a fraction having molecular mass M_i, while m is the mass of the whole sample $m = \Sigma_i m_i$).

In 1905/6, considering the nature of the Brownian motion, independent by Einstein and Smoluchowski found a relationship between diffusion coefficient D and the average value of the square of the shift $\overline{l^2} = 2Dt$ for a colloidal particle in a certain direction at the same time intervals. Assuming sphericity of the colloidal particles Einstein derived a relation between particles radius and internal friction coefficient that is viscosity of the medium in which they are dispersed. The diffusive flux of the particles is caused by a gradient of their chemical potential in the investigated system. The stationary state of the flux stabilizes when caused by the existing gradient of chemical potential μ, the force acting on the particle is balanced by the force of medium resistance dependent on the values of its viscosity η, radius of the particle r and stationary velocity of its movement v, meaning a stationary flow, that is the movement of the particles of c_i concentration with a constant velocity v, hence $dc_i/dz = - v c_i (6\pi\eta r)/kT$, if $x_i = c_i$. The diffusion stream of colloidal particles is described by the first Fick law $j_i = - D\, dc_i/dz$, and therefore $(D = kT/6\pi\eta r)$. The diffusion coefficient D is a phenomenological coefficient λ, while the concentration gradient is a stimulus of flow of the Onsager theory. The thermodynamic forces are gradients of intensive parameters of the state, and, when they appear in the system, they cause irreversible flows which act to restore the equilibrium. The intensity of the flux of any component j_i depends on the value of certain gradient $\boldsymbol{w}_m$, and phenomenological coefficient λ_{im}, which characterizes the resistance of the medium $j_i = \Sigma_i \lambda_{im} \boldsymbol{w}_m$. The fluxes are linear functions of gradients and the Onsager rule says that the source of entropy is the sum of products of combined fluxes (j_r) and thermodynamic gradients ($\boldsymbol{w}_r$) $(\partial s/\partial t)_T = 1/T \Sigma_r j_r \boldsymbol{w}_r$. The Onsager relations describe the phenomenon of symmetry existing between selected irreversible processes. The principle of the

irreversible processes. The principle of the description of these relations is the relation $(\partial j_r / \partial \boldsymbol{w}_m) = (\partial j_m / \partial \boldsymbol{w}_r)$ where $\boldsymbol{j}_r$ is the flux of the component, $\boldsymbol{j}_m$ is the flux of thermal energy, $\partial \boldsymbol{w}_m$ denotes the chemical potential gradient of a component, and $\partial \boldsymbol{w}_r$ is the temperature gradient.

HYDROPHILIC COLLOIDS AND MICELLIZATION

Typical hydrophilic colloids are formed during preparation of solution of substances which are called surfactants. Surfactant molecule posses in its structure an organic hydrophobic group while the other part is polar with certain affinity towards water. In a wide range of temperatures, above the Kraft temperature, and also above the critical temperature, when the solution is enough concentrated, there is a spontaneous process leading to the formation of thermodynamically stable colloidal solution. The process is called micellization. Initially micelles are spherical in which the hydrocarbon chains occupy the interior of micelle while the polar groups form the outer sphere and are directed towards the surrounding medium. As a result of compensation of entropic and enthalpic components of the free energy, a state of its minimum value is established. A further addition of the surfactant causes neither further change in the solution nor noticeable changes of the surface tension nor monomer concentration. There is an increase of spherical micelles concentration. There is no saturation of the solution with the micelles. At certain, appropriate for a given system, surfactant concentration, micelles change their shape. The concentration of the spherical micelles decreases while the population of the cylindrical micelles increases. The cylindrical micelles, with increasing concentration, change into flat structures. In each micellar system there are many such shape transformations. An average spherical micelle contains from a dozen to hundreds of surfactant molecules. An appearance of other than spherical shapes makes that more and more regions of the system are ordered. The micellization equilibrium constant is the result of the minimization of the free energy of the whole system. The entropy decreases due to increased ordering of system elements while enthalpy changes as a result of replacement of contacts of the groups as a result of replacement of contacts of hydrophobic groups of individual surfactant molecules with water for the interactions of hydrocarbon groups between themselves in the interior of each micelle.

Rehbinder at the conference in Berlin (1966) showed that the presence of fragments of different hydrophobicities in the molecules structure alone is not enough to form micellar solutions. Using German terminology he proposed to reserve the term real or true tensides only for substances able to form micelles. Presently they are called surfactants. He noticed that surface activity in the sense of different molecular compositions of the interfaces and bulk is a universal phenomenon regarding all systems. Micellization is formation of a new phase characteristic only for systems fulfilling special conditions. Among material constants characterizing micellar systems, the

main role is player by the already mentioned Kraft temperature, below which surfactant has, as any substance, a limited solubility in water and does not form micelles. The phase transition is possible above the Kraft temperature. Rehbinder (1966), analyzing the complexity of the affinity of different fragments of complex structure towards water, noticed a low value of the enthalpy component as a characteristic feature of micellization process. The higher temperature, the greater probability of free energy minimalization due to the formation of new phases. Different temperature relations of entropic components and enthalpic local ordered states lead to the formation of structures beneficial for attaining minimum. The system gather the whole reserve of energy in their significantly developed interfacial regions.

INVERSED MICELLES

Discussing micellization we paid attention to aqueous surfactant solutions and characteristic structures of surface active substances, which greatly decrease the surface tension of water. They, due to the presence of hydrophobic groups in their structure, manifest also certain solubility in typical organic solvents. The molecules of surface active substances are gathered in these solutions at the interfaces and are oriented with the hydrophobic groups towards medium of lower polarity. This property is utilized for formation of colloidal systems called reversed micelles. In a hydrophobic medium, as the concentration increases, the aggregation is not taking place as fast as in water. Small amount of water may help the aggregation. The formed inversed micelles have, as a rule, greater diameter than the micelles in the aqueous medium. The reason is solubilization, relying on incorporation of a number of water molecules inside of each micelle. Their number depends on the nature of the polar groups in the surface active molecule directed towards the center of each reversed micelle. The knowledge of material constant values characterizing the equilibrium of solubilization has a great importance in technology.

In a formal thermodynamic approach micelle can be treated as a neutral particle because the stability of the system requires that eventual electrical charge its ionized polar groups was, in the interfacial region of the micelle, completely neutralized by ions of the opposite sign. Thus, the ions neutralize their charges within the micelle structure. The discussed neutral system is stable in the states determined by the material constant which is here the equilibrium constant of the dynamic micellization reaction.

A numerous group of hydrophilic colloids is formed by proteins. The principal elements of the proteins structure are amino acids. Sometimes large protein macromolecule containing hundreds or thousands of amino acid units can be prepared by suitable methods in crystalline form, as a chemical of well established composition. The material constant of proteins are type, number, and structure of amino acids. A biochemical activity is possessed only by native proteins which have secondary, terti-

ary and ternary structures which require, besides peptide bonds, also formation of hydrogen and disulfide bridges. Improper temperature, electrolytes concentration, the presence of additional substances or solution pH cause either partial or total lost of protein activity, that is temporary or irreversible denaturation. Biochemical monographs accumulate more and more material constants for proteins.

Historically important issue is proteins coagulation. Noticed many years ago salting out of protein, leading to the turbidity of the chicken egg white solutions in the presence of electrolytes. Such observations lead to classification of ions according to their salting out effect. The strongest are ions with great heat of hydration. At high, about molar, concentrations the ions compete for water, while the water-protein structures provide stability of the hydrophilic colloids. Most anions are much more hydrated than cations, hence popularity of the Hofmeister series in which anions are ordered according to their coagulation ability (citric > tartaric > SO_4^{2-} > acetate > Cl^- > NO_3^- > Br^- > I^- > SCN^-).

A change of type and concentration of electrolyte makes the weakly mutually interacting neutral particles of hydrophilic colloids to modify their distribution of potentials in the surrounding electrical double layer. Within a wide region of changes of system parameters it does not cause thermodynamic destabilization. The hydrophilic colloids can form thermodynamically stable systems, while hydrophobic ones always undergo destabilization.

MICROEMULSIONS

In contrast to emulsions, microemulsions are thermodynamically stable. Similarly to emulsions, microemulsions are formed by mixing water, or other polar liquid, with a non-polar liquid, also called oil. It can be a hydrocarbon such as octane, a long chain fatty acid, or aromatic hydrocarbon with a low affinity for polar liquid. There are two types of emulsions: oil in water and water in oil. In unstable emulsions, the interfacial tension between droplets of the dispersed phase and the dispersing medium is much above zero. A spontaneous coalescence causes a decrease of the interfacial area and the fee energy of the system significantly decreases. To stabilize the emulsion system, we add a third component which strongly reduces the interfacial tension. This component, having the ability to be present in both phases can cause solubilization. An increase of the sorption in the interfacial regions decreases the interfacial tension while formed in the system new colloidal phases decrease further their free energy. When only one component aggregates, the surface tension of the colloidal solution does not drop below a dozen of mN/m, while in a multicomponent microemulsion system it decreases to one tenth of a mN/m and sometimes to one thousandth of a mN/m. To measure such low values of surface tension, a special device was constructed able to record changes of the shape of small droplets rotating with a precisely regulated velocity. Presently, a direct computer recording and graphical representation of equilib-

ria in the form of classic isothermal Gibbs triangle and a plot taking into account evolution of phase composition with temperature is possible.

A typical example (Miller and Neogi, 1985) of a multicomponent microemulsion system is the water/anionic surfactant/short chain alcohol/oil/sodium chloride system. Depending on the composition and temperature the system can, due to gravity, split into two or three, differing in densities, phases. When, in the presence of salt, the system containing equal amounts of oil and 1% aqueous alcohol solution (containing an anionic surfactant) is shaken, we observe initially two-phase system, and a third phase appears and next disappears. Traditionally it is called the middle phase.

The oily upper phase is transparent while the aqueous salt solution forms the lower phase. Practically the whole surfactant is gathered in the middle phase having not yet established structure.

An increase of the salinity leads to the transition of the microemulsion from the aqueous to oily continuous phase. At optimal salinity, a formation of a bicontinuous phase is postulated. It means that within the whole volume of the system it is possible, from a point selected in any of two phases, to go very near to any other point of that system. An any point of such a system the interfacial region has the saddle curvature shape which main radius of curvature is constant. Due to practical importance of the microemulsion for removal of remaining crude oil from the exploited deposits, the discussed systems are intensively investigated by physical chemists specializing in oil and mineral processing.

HYDROPHOBIC COLLOIDS AND THEIR INSTABILITY

A colloidal hydrophobic particle is stabilized, in a given dispersing medium, by the surface electrical charge. The greater is the charge, the more difficult, for accidental thermal motion, to cause the collision of the particles. The electrical field, regulated by the Coulomb law, causes an increasing, with the approaching particles, repulsion. The changes of the repulsion depend on the dielectric constant of the medium and the ions concentration. A direct collision is possible when the kinetic energy caused by thermal movement of a concrete pair of particles is greater than the potential energy of repulsion. Only a direct contact of both objects, especially when they have significant adhesion energy, make attractive forces come into play promoting onset of coagulation.

From the earliest period of colloidal systems investigation, they were conducted by means of two approaches. As a result, rules were created which describe the influence of electrolytes on the stability of system and the theory of the coagulation has been developing. Simple rules for the behavior of colloids were formulated by Hardy and Schulze. They established that ions can cause coagulation when their electrical charge was of opposite sing in relation to the electrokinetic potential of the colloid. The ions concentration initiating coagulation was found to change proportionally do

the 6th power of reciprocal of their valence. Organic ions with large sizes do not follow the rule. The Hardy and Schulze was confirmed theoretically (Hsu and Kuo, 1995).

The theoretical foundation of electrolytic coagulation (the so-called theory of fast coagulation) were provided independently by Einstein and Smoluchowski. Simple calculations of Smoluchowski, assuming that for a reaction which does not need activation after time t of sedimentation the concentration c_k of the aggregates containing k particles of a monomer is $c_k = c_0 \ (t/\tau)^{k-1}/(1+t/\tau)^{k+1}$, where τ denotes the time after which half of the initial number of colloidal particles aggregated. Thus, the total colloid concentration is $c = \Sigma c_k$ (sum for k from 1 do ∞) is $c = c_o/(1+ t/\tau)$.

The experiments of Zsigmondy and others confirmed rapid coagulation of colloids for which the absolute values of the electrokinetic potential is below a critical value of ζ_{kr}. However, not each collision of individual particles results in aggregation.

Coagulation requiring activation energy and when is sterically hindered by unsuitable orientation of the non-spherical particles at the moment of their touching is called slow coagulation. Then, the equation describing such coagulation require suitable modification.

SOFT MATTER

The definition of the soft matter assumes that its lowest size is that of molecules, and includes, as especially interesting group of substances, polymers and polyelectrolytes as well as mezoscopic porous objects. All such systems are characterized, in contrast to the condensed crystalline phases, not only lack of macroscopic ordering at great distances, but also the presence of more or less ordered domains. In addition, a small change of the composition, pressure and/or temperature frequently leads to a phase transition having a great number of diverse structures. It confirms a great role of defining characteristic interfacial constants which would allow univocally determine the nature and properties of the discussed materials. A summary of the present state of art and literature data is available in the Internet at the web site of Robert Hołyst (2008). The most important features of matter, which cannot be classified as liquid or solid, he considers partial ordering of orientation or translation and topologic complexity or geometric structure. As a result of broken translation and/or rotational symmetry, the visco-elasticity and elastic deformation appear. The Young modulus of the liquid crystals is four orders smaller than that of the solids. Water, as a main component of soft matter, determines the temperature range of its existence. Although the structural effects appear in proper solutions only in the region of free surfaces, or interfacial regions, they are of decisive importance for the delineation of the soft matter of living organisms.

Ordering decreases entropy, therefore it is not usually spontaneous. Minimization of thermodynamic potential is based on the sum of the enthalpic and entropic compo-

nents. For states of matter covered by the definition of soft matter, the domain structure dominates. Frequently, when the parameters of the system change, in the volume of homogenous structure there is a spontaneous phase transition and two or more domain regions having different structure can appear. Ordering of some of them can visible increase. Locally, there is a drop of entropy, which is compensated by an appropriate enthalpy change. For the whole system, the rule of minimum fee energy is preserved.

Richness of phases of different structures is characteristic for soft matter and results from a tremendous role played in such systems by structural interactions of short range, especially those which are called hydrophobic forces. It emphasizes an urgent necessity of development of the hydrogen bonding theory. Depending on the affinity towards water present in the system, the molecule (or surface), breaks locally, depending on the domain structure, certain number out of four hydrogen bonds, which are at disposal of each water molecule in the uninterrupted net of these bonds. The local strength of the hydrogen bonds is therefore the principal material constant, which characterizes a concrete type of the soft matter.

Unfortunately, a lack of a proper description of the quantum mechanics prevents us from creation of a full and quantitative definition of the soft matter. Literature on bio-chemical and bio-physical issues shows that this is a key point of development of these disciplines. This situation can be easily justified by comparing, in kT units, the energy of principal interactions deciding about the structure of matter. The energy of hydrogen bond is a dozen-fold greater than the energy of thermal movement of particles and by one order greater than that resulting from the DLVO theory for particles approaching the separation of a bond length. So, the hydrophobic interactions, which do not have much importance in comparison with long-range interactions, however they determine the domain structure of the soft matter.

In the system of nanometric size, the surface curvature of the domains, according to the thermodynamic condition determined by the Kelvin equation, leads to local pressure tensors approaching even 0.1 gigapascals. Under such conditions, valid is only the description based on the third Gibbs chemical potential $\Omega = -pV$. At the same time, gases present in systems with nano-bubbles being at equilibrium, must have local densities characteristic for critical states, similar to the liquid water, and can exists solely at the border with highly hydrophobic surfaces.

Making summary, let us compare our state of knowledge on material constants of the hard matter resulting, according to crystallography, from the 32 symmetry classes of crystalline matter, with the present description of the soft matter. Periodical arrangement, providing ordering of long range of atoms and molecules, is possible only within the frame of the mentioned classes. The domain structure of soft matter, not having ordered structure of long range, breaks the condition of the symmetry. A classification of such systems was initiated with research of the so-called glassy phases and liquid crystals. The structure of phases, characteristic for these systems, is called

mezomorphic or partially ordered, and such phases as smectic, nematic and cholesterolic are distinguished.

The base for delineation of the pieces of soft master ordering was provided, half a centaury ago, by Landau (Kleman et al., 2003), as a function of density distribution ρ. Mutual orientation of molecules in each, determined by vector $\boldsymbol{r}$, point of the phase, is given by the value of three Euler angles ω and $\rho(\boldsymbol{r}, \omega) = \langle \Sigma\, \delta(\boldsymbol{r} - r_i)\, \delta(\omega - \omega_i)$. Averaging summation regards all positions of the molecules from i = 1 to i = M, within the domain of each phase.

From the given above relations, taking into account the size and structure of a given molecule forming the soft matter and, according to the statistical mechanics rules, a great number of symmetry classes was established as the characteristic material constants. Rules were presented which decide about the possibility of transformation between the phases belonging to different classes.

ACKNOWLEDGEMENTS

Financial support from the Ministry of Science and Higher Education (zlec. 350-464) is gratefully acknowledged.

REFERENCES

Hołyst R., 2008, http://www.ichf.edu.pl/Softmatter/miekka-materia.pdf

Hsu J.-P., Kuo Y.-C., 1995. An extension of the Schulze–Hardy rule to asymmetric electrolytes, J. Colloid Interface Sci., 171, 254–255

Kleman M., Lavrentovich O.D., Friedel J., 2003, Soft matter physics, Springer

Miller C.A., Neogi P., 1985. Interfacial Phenomena, Marcel Dekker4 Inc., N.Y. &Basel

Mills R.L., 2002, The grand unified theory of classical quantum mechanics, International Journal of Hydrogen Energy, 27 (5), 565-590

Rehbinder P.A., 1966. Grenzflächen- und Volumeneigenschaften von Tensidlősungen, III. Internationale Vortragstagung űber Grenzflächenaktive Stoffe, Abhhandlungen der Deutschen Akademie der Wissenschaften zu Berlin, Klasse fűr Chemie, Geologie u. Biologie, Jahr., Nr. 6b, S. 521 – 530.

Grodzka J., Drzymała J., Pomianowski A. *Powierzchniowe stałe materiałowe w układach silnie rozdrobnionych* Physicochemical Problems of Mineral Processing, 42 (2008), 237-250 (w jęz. ang)

W pracy szeroko scharakteryzowano właściwości materii i obszarów granicznych pomiędzy elementami materii o różnym rozdrobnieniu biorąc pod uwagę zawiesiny, koloidy, roztwory micelarne, mikroemulsje oraz tzw. materię miękką, której znajomość jest tak samo ważna jak materii nieożywionej. Szczególną uwagę zwrócono na rolę i różnorodność stałych materiałowych niezbędnych do opis stanu i właściwości rozpatrywanych przykładów.

słowa kluczowe: stałe materiałowe, zawiesina, kolloid, rozwtór micelarny, mikroemulsja, materia miękka

Physicochemical Problems of Mineral Processing, 42 (2008), 251-262
Fizykochemiczne Problemy Mineralurgii, 42 (2008), 251-262

Daria Hołownia*, Irmina Kwiatkowska*, Jan Hupka*

AN INVESTIGATION ON WETTING OF POROUS MATERIALS

Received June 27, 2008; reviewed; accepted July 31, 2008

Indirect methods of evaluation of wetting properties of fine particles or porous materials require selection of a reference liquid, for which the contact angle is equal to zero. In our investigation, the capillary rise method and film flotation were used for: glass microglobules - water and glass microglobules – decane systems. The data for the reference liquid and the examined one are introduced into the modified Washburn equation and the contact angle is calculated.

key words: capillary rise, film flotation, porous materials,wetting, contact angle

INTRODUCTION

There are several simple and fast methods to determine contact angle on a flat surface, e.g. sessile drop (captive bubble), inclined plate, and Wilhelmy's plate methods. However, determination of the contact angle on porous materials is more challenging. Intermediate methods are required to evaluate wetting properties of porous or loose materials. The methods include: the capillary rise, “wick”, compressed disc, film flotation and recently the atomic force microscopy (Xu and Masliyah, 2002). In our paper the capillary rise method was combined with the film flotation method. Such approach to finding the reference liquid is proposed for the first time.

CAPILLARY RISE METHOD

The capillary rise method is based on measurements of capillary pressure difference or velocity of liquid penetration through a porous material. Bartell et al. (1932, 1934) were first to employ this method in research. The quantity they measured was

* Department of Chemical Technology, Chemical Faculty, Gdansk University of Technology, G. Narutowicza Str. 11/12, 80-952 Gdansk, Poland, e-mail adress: dariam@chem.pg.gda.pl

the value of pressure applied to the system, while the quantity determined was the pressure required to stop the liquid from penetrating further into the bed. When the velocity of penetration is equal to zero the system is in equilibrium described by the formula:

$$\Delta P = \frac{2\gamma \cdot \cos\theta}{r} \tag{1}$$

where r is the average diameter of capillaries in the porous material.

The apparatus for measuring capillary pressure is shown on Fig. 1.

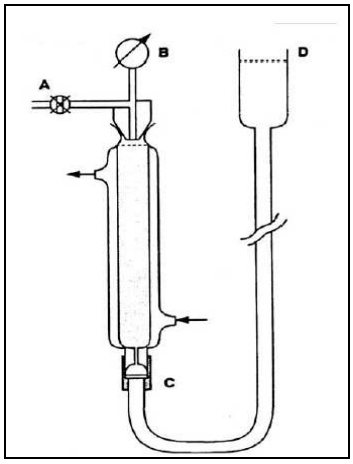

Fig. 1. Capillary pressure measuring apparatus: A - control valve, B - pressure converter, C -capillary pipe, D - liquid container (Diggins et al., 1990).

The velocity of penetration is measured in a column with a filler. The method is based on the assumption introduced by Washburn (1921) that the porous system comprises of n-cylindrical capillary pipes.

Levine et al., (1980) and Xue (2006) assumed that porous materials behave like a bundle of capillaries and a modified Lucas-Washburn (Hamraoui and Nylander, 2002; Xue et al., 2006) equation is used:

$$h^2 = \frac{(c\bar{r})\gamma_{LV} \cdot \cos\theta \cdot t}{2\eta} \tag{2}$$

where c is a constant.

After reforming previous equation we obtain:

$$r = \frac{6\eta\gamma_{LV}\cos\theta \cdot h^2}{-2\rho g\eta h^3 + 3\gamma_{LV}^2\cos^2\theta \cdot t}. \tag{3}$$

In the last equation θ is the only unknown parameter.

The capillary rise method is based on the Washburn equation that has been derived from Poiseuille equation:

$$dV = \frac{r^4 \cdot \Delta P \cdot \pi}{8\eta \cdot h} dt. \tag{4}$$

Thus, the Washburn equation is (Washburn 1921):

$$h^2 = \frac{r \cdot \gamma \cdot \cos\theta}{2\eta} t. \tag{5}$$

Additionally, the following simplifications are employed in the capillary rise method:

a) the flow is laminar and stationary
b) there is no slip, i.e. no flow on the solid body - liquid interface
c) no internal pressure.

It is more convenient to use the modified Washburn equation which represents the dependence of change in liquid mass on time (Siebold, 1997, Diggins, 1990)

$$m^2 = \frac{C \cdot \rho \cdot \gamma \cdot \cos\theta}{\eta} \cdot t \tag{6}$$

where constant C is:

$$C = \frac{r\left(\pi R_k^2\right)^2 \varepsilon^2}{2} \tag{7}$$

and where:

h – height of penetration
r – average capillary pipe diameter
γ –penetrating liquid surface tension
η – penetrating liquid viscosity
θ – contact angle
ε –bed porosity
ρ – penetrating liquid density
t – time of penetration
m – penetrating liquid mass increase
R_k – glass tube inner diameter.

One way to determinate contact angle are investigations involving two liquids – the reference and examined (Studebaker, 1955) ones. For the reference liquid:

$$h^2 = \frac{r\gamma_0}{2\eta_0} t_0. \tag{8}$$

For identical beds r is constant, therefore, for the liquid being examined we have:

$$h^2 = \frac{r\gamma_1 \cos\theta}{2\eta_1} t_1 . \tag{9}$$

Dividing equations (8) and (9) we obtain

$$\cos\theta = K \frac{t_0}{t_1} \tag{10}$$

where

$$K = \frac{\gamma_0 \cdot \eta_1}{\gamma_1 \cdot \eta_0} \tag{11}$$

and where

t_0, γ_0, η_0 → time of penetration, surface tension and viscosity of reference liquid
t_1, γ_1, η_1 → time of penetration, surface tension and viscosity of liquid investigated.

Another way to determine contact angle is to calculate the mean capillary radius (assuming that the glass microglobules behave like a bundle of capillaries) using Eq. (3) and then calculating the contact angle using the Washburn equation (Eq. 15).

FILM FLOTATION METHOD

The method of film flotation is used to determine the contact angle of fine particles. The behavior of a small particle in contact with surface of a liquid depends mainly on surface tension of the given liquid. The following states of the particle are distinguished: State I occurs when the particle is dropped toward the surface of the liquid but is still in the gas phase. State II occurs when the particle contacts the surface of the liquid. Next, depending on the contact angle of the substance either State III (the formation of a three-phase wetting line) or State IV (the particle stays just below the surface of the liquid - it is fully immersed) is obtained or the particle sinks (Fig. 2) (Bartell and Walton, 1932; Churaev, 2005; Feurstenau et al., 1991).

The total sum of energy (transition from State I to State IV) is the sum of kinetic, potential and interfacial energies:

$$\Delta G_r = \Delta G_K + \Delta G_P + \Delta G_I \tag{12}$$

The change in interfacial energy is, in turn, the sum of changes in adhesion, spill and immersion energies:

$$\Delta G_I = \Delta G_a + \Delta G_i + \Delta G_s \tag{13}$$

$$\Delta G_a = -\gamma_{SV} + \gamma_{SL} - \gamma_{LV} \qquad \text{adhesion work} \tag{14}$$

$$\Delta G_i = - \gamma_{SV} + \gamma_{SL} \qquad \text{immersion work} \tag{15}$$

$$\Delta G_s = - \gamma_{SV} + \gamma_{SL} + \gamma_{LV} \qquad \text{spill work} \tag{16}$$

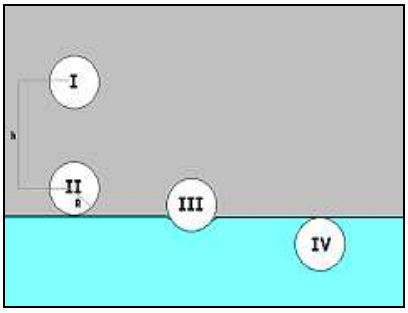

Fig. 2. Behavior of particles on a liquid surface

Employing the Young equation:

$$\gamma_{SV} - \gamma_{SL} = \gamma_{LV} \cos \theta \tag{17}$$

one obtaines:

$$\Delta G_a = -\gamma_{LV} (\cos \theta + 1) \tag{18}$$

$$\Delta G_i = -\gamma_{LV} \cos \theta \tag{19}$$

$$\Delta G_s = \gamma_{LV} (\cos \theta - 1). \tag{20}$$

When $\theta < 180^o$ the adhesional wetting will be spontaneous, when $\theta<90^o$ immersion wetting will be spontaneous and when $\theta = 0^o$ spill wetting will be spontaneous.

EXPERIMENTAL PART

Glass microglobules of real density 2410 kg/m^3 (apparent density 1773 kg/m^3) and diameter 150 – 250 μm (see Fig. 3) were used. The oxide composition is as follows:

SiO_2	70 – 73%
Na_2O	13 – 15%
CaO	7 – 11%
Fe_2O_3	max 0,1%.

Before the experiment, microglobules were thoroughly cleaned and degreased, first by immersion in a mixture of solvents comprising of methanol : acetone : chloroform (1:1:1 by volume) and subsequently, washed with chloroform, methanol, acetone and water. Finally, they were dried at 130˚C for a constant weight. Glass capillaries

were filled with predetermined amount of beads and placed in a shaker in order to provide uniform packing of glass spheres in the bed.

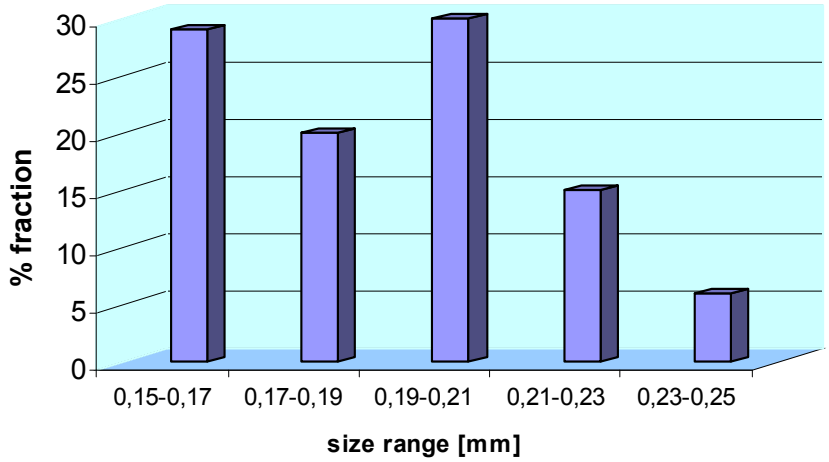

Fig. 3. Glass microglobules size distribution

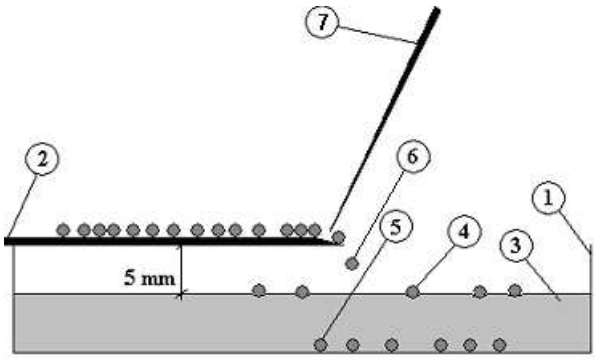

Fig. 4. Film flotation arrangement used in our investigation, 1 – glass vessel, 2 – horizontal plate, 3 – liquid being examined, 4 – floating particles, 5 – sinking particles, 6 – falling particle, 7 - needle

The reference liquid used for calculation of contact angle was determined using the film flotation method. It was assumed that the reference liquid - possessing ideal wetting ability (contact angle equal to zero) is that liquid for which 1% of microglobules remains at the surface.

The test was carried out by placing a single glass microglobule on liquid surface and the percent of floating particles out of 100 was determined. For each liquid three runs were practiced. The laboratory setup used for the experiments is shown in Fig. 4 and Fig. 5.

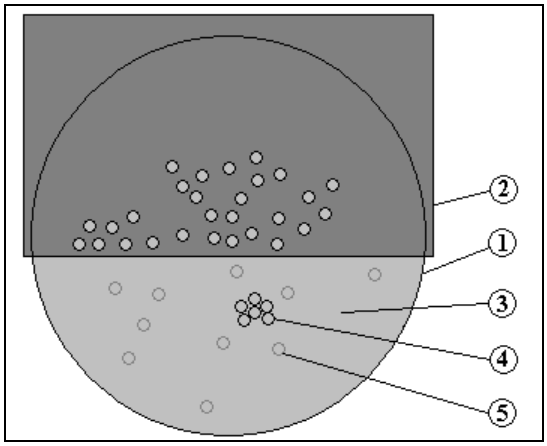

Fig. 5. Film flotation experiment arrangement - top view. 1 – glass vessel, 2 – horizontal plate, 3 – liquid being examined, 4 – floating particles, 5 – sinking particles, 6.

The experimental data for all investigated liquids are shown in Table 1. The capillary rise was determined using apparatus shown in Fig 6.

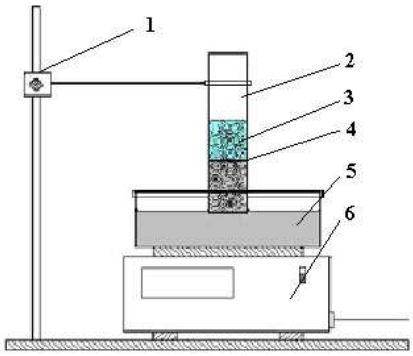

Fig. 6. Experimental setup for determining capillary rise: 1 - support, 2 - capillary, 3 – packing of glass microspheres, 4 - head of liquid, 5 - vessel with liquid, 6 – balance linked to computer (Trong and Hupka, 2005)

A computer program was used to register balance readings and the results were saved to a file. After the measurement, a plot was made for each liquid showing relation between squared mass increase v.s. time of penetration. The results obtained for the investigated and reference liquids are shown in Figs 7, 8, and 9. Based on the graphs, the time of penetration was found (39 s for methylene chloride, 49 s for water and 131 s for decane) and the contact angle for water and decane was calculated. Using Eq. (10) we obtain 44.5˚ for water and 41.4˚ for decane, and using mean radius of capillary (Eq. (3) and the Washburn equation we obtain 43.5˚ for water and 40.2˚ for decane.

Table 1. Liquids examined by film flotation method

Liquid	Surface tension, [mJ/m^2]	Viscosity [mPa·s]	Density [kg/m^3]	% flotating microglobules
Pentane	16.00	0.25	630	0
Isooctane	18.80	18.80	690	0
Heptane	19.30	0.42	710	0
Octane	21.80	0.55	700	0
Ethanol	22.00	1.20	0,81	0
Methanol	22.10	0.54	790	0
Acetone	22.68	0.30	790	0
Decane	23.90	0.93	726	0
n-butyl acetate	25.10	0.74	880	0
CCl_4	26.95	0.90	1590	0
Toluene	27.80	0.55	870	0
Xylene	28.30	0.65	860	0
Cycloheksanone	34.00	2.20	950	0
Nitric acid	41.20	0.75	1526	0
2-propanol	18.30	2.07	780	1
Dichloromethane	27.20	0.42	1320	1
Ethylene bromide	38.40		2180	2
Nitromethane	36.20	0.61	1140	3
Pyridine	38.00	0.95	980	4
Water	72.30	1.00	998	13
Sulfur acid	55.10	24.54	1840	23
Hydrazine	91.50	0.91	1000	30
o-Toluidine	40.00		990	40
Aniline	42.90	4.40	1020	45
Oleic acid	32.50	39.00	890	81
Benzyl alcohol	39.00	5.04	1042	90
Hexanol	24.08	4.59	820	95
Ethylene glycol	47.00	21.00	1110	100
Glycerol	62.50	945.00	1260	100

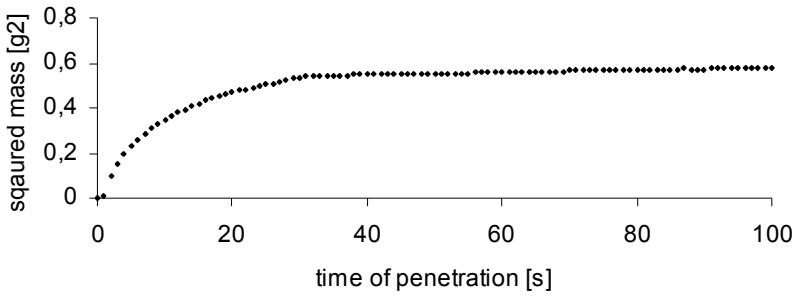

Fig. 7. The relationship between squared mass of methylene chloride (reference liquid) vs. time of penetration.

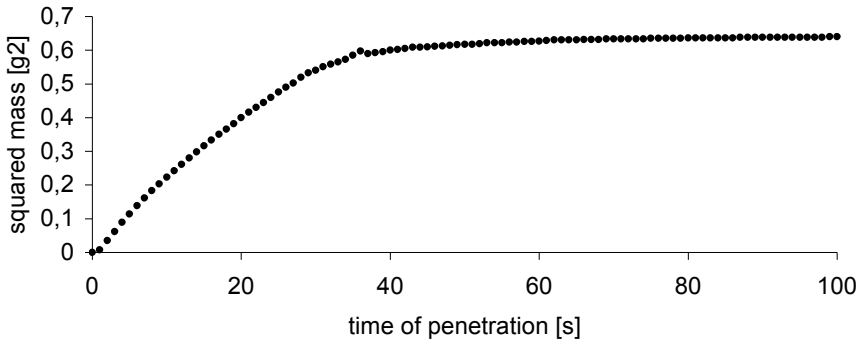

Fig. 8. The relationship between squared mass of water vs. time of penetration

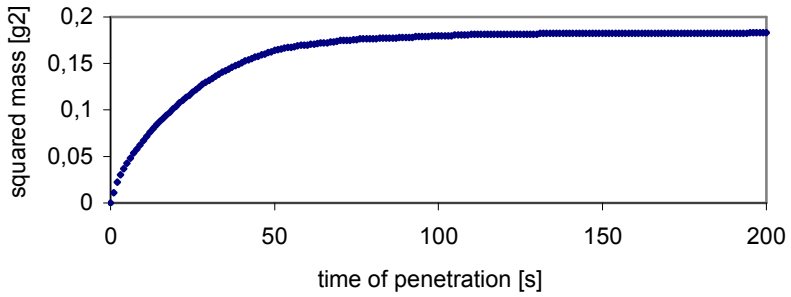

Fig. 9. The relationship between squared mass of decane vs. time of penetration

FINAL COMMENTS

The capillary rise method employed for the investigation possesses many advantages, it is convenient and fast to use, does not require expensive and complex apparatus, measurement errors are minimized while changing the working conditions (ambient temperature), the results obtained possess error resulting only from non-linear changes of substance properties. The big disadvantage, however, is the necessity to choose a reference liquid - the one ideally wetting the material examined.

If another reference liquid, chosen depending on another criterion, had been used, the result would have been different. Moreover, if another liquids were examined they could prove to better wet loose material and the final result would also be different.

ACKNOWLEDGEMENTS

Financial support from Gdansk University of Technology, contracts No.: DS 014668/003 and BW 014694/039, is acknowledged.

REFERENCES

BARTELL F. E., WALTON C. W. Jr., Alteration of the surface properties of stibnite as revealed by adhesion tension studies, J. Phys. Chem., 1934, 38, 503–511.

BARTELL F. E., WHITNEY C. E., Adhesion tension. III, J. Phys. Chem., 1932, 36, 3115-3126.

CHURAEV N.V., Aqueous wetting films in contact with a solid phase, Preface, *Advances in Colloid and Internface Science*, 2005, 114-115, 3-7.

DIGGINS D., FOKKINK L. G. S., RALSTON J., The wetting of angular quartz particle: capillary pressure and contact angles, Colloid Surf. A, 1990, 44, 299–313.

FEURSTENAU D. W., DIAO J., WILLIAMS M.C., Characterization of the wettability of solid particles by film flotation. 1. Experimental investigation, *Colloid and Surfaces*, 1991, 60, 127-144.

HAMRAOUI A., NYLANDER T., Analytical approach for the Lucas-Washburn equation,J. Colloid Interface Sci., 250 (2002) 415–421.

LEVINE S., LOWNDES J., WATSON E.J., NEALE G., A theory of capillary rise of a liquid in a vertical cylindrical tube and in a parallel-plate channel Washburn equation modified to account for the meniscus with slippage at the contact line J. Colloid Interface Sci. 1980, 73, 136.

SIEBOLD A., NARDIN M., SCHULTZ J., WALLISER A., OPPLIGER M., Effect of dynamic contact angles on capillary rise phenomena, Colloid Surf. A, 2000, 161, 81–87.

STUDEBAKER M. L., SNOW C. W., The influence of ultimate composition upon the wettability of carbon blacks, Wettability of Carbon Blacks, 59 (1955) 973–976.

TRONG. D. V., Charakterystyka układu porowatego metodą wzniesienia kapilarnego za pomoca równania Washburn'a, praca doktorska, Gdańsk 2005.

TRONG D.-V., HUPKA J., Characterization of porous materials by capillary rise method, Physicochemical Problems of Mineral Processing, 2005, 39, 47-65

WASHBURN E. W., The dynamics of capillary flow, Phys. Rev., 1921, 17, 273–283.

XU Z., MASLIYAH J. H., Contact angle measurement on oxide and related surfaces, in: Encyclopedia of Surface and Colloid Science, Hubbard A. (ed.), Marcel Dekker, New York 2002, 1228–1241.

XUE H.T., FANG Z.N., YANG Y., HUANG J.P., ZHOU L.W., Contact angle determined by spontaneous dynamic capillary rise with hydrostatic effects: Experiment and theory, Chemical Physics Letters, 2006, 432, 326-330.

Hołownia D., Kwiatkowska I., Hupka J., *An investigation on wetting of porous materials*, Physicochemical Problems of Mineral Processing, 42 (2008), 251-260 (w jęz. ang)

Pośrednie metody oceny zdolności zwilżania drobnych cząstek lub materiałów porowatych wymagają wyboru cieczy odniesienia, dla której kąt zwilżania jest równy zeru. W badaniach własnych zastosowano metodę wzniesienia kapilarnego oraz metodę flotacji filmowej dla układów mikrokulki szklane-woda i mikrokulki szklane-dekan. Uzyskane dane dla cieczy odniesienia i dla cieczy badanej wprowadzano do zmodyfikowanego równania Washburn'a i wyznaczano wartość kąta zwilżania.

Słowa kluczowe: wzniesienie kapilarne, flotacja filmowa, materiały porowate, zwilżalność, kąt zwilżania

Physicochemical Problems of Mineral Processing, 42 (2008), 261-269
Fizykochemiczne Problemy Mineralurgii, 42 (2008), 261-269

Anna Bastrzyk*, Izabela Polowczyk*, Ewa Szeląg*, Zygmunt Sadowski*

THE EFFECT OF PROTEIN-SURFACTANT INTERACTION ON MAGNESITE ROCK FLOTATION

Received June 18, 2008; reviewed; accepted July 31, 2008

For many years, interaction of proteins with surfactants in solution has been a subject of extensive studies. The addition of surfactants and proteins to solution leads to the formation of protein-surfactant complex. The structure of these objects depends on many factors, e.g. the reagent concentrations, the type of chemical compounds used, the order of protein and surfactant addition. The aim of this work was to examine the way of adsorption of protein (chicken egg albumin) and surfactant (sodium dodecyl sulphate) on the mineral surface (magnesite rock) affects the properties of magnesite suspensions. The effect of these interactions on the flotation of magnesite has been investigated. Effeciency of flotation (yield and separation of magnesite from quartz) was higher when both SDS and albumin were adsorbed at the particle surface.

key words: protein-surfactant interaction, adsorption, SDS, flotation

INTRODUCTION

Interactions of surfactants with proteins are very important in a wide variety of industrial, biological, pharmaceutical, and cosmetic applications. They may lead to the formation of protein-surfactant complexes which can be soluble or insoluble in aqueous medium (Miller, 2000; Moren, 1999). Due to the existence of nonpolar and ionic amino acid side-chains in protein molecule, the formation of these complexes is driven by electrostatic interactions between the charged headgroups of the surfactant and the oppositely charged units of the protein and also by hydrophobic interactions (Gonzales-Perez, 2003; Aida, 2003). The structure of the protein-surfactant complex can be described by following models: rigid rod, flexible helix or necklace model

* Wroclaw University of Technology, Faculty of Chemistry, Wybrzeze Wyspianskiego 27, 50-370 Wroclaw, POLAND, e-mail: Zygmunt.Sadowski@pwr.wroc.pl

(Valstar, 2000). The structure of the polymer-surfactant system can affect the stability of mineral suspension and can be an essential factor in many industrial processes, involving sedimentation or flotation, such as water treatment, mineral processing and sludge dewatering (Sadowski, 2001).

Adsorption of polymer/surfactant mixture at the mineral-solution interface depends on many factors, like the nature of surfactant and polymer, type of solvent, surface properties of solid and order of addition of polymer and surfactant (Sadowski, 2001; Malmsten, 2003). Both modifiers present in the suspension can either compete with each other for adsorption or favour the adsorption of one species (Treiner, 2002). Adsorbed protein can be removed from the solid-liquid interface by surfactants, according to one of two mechanisms: 1- surfactant binds to the protein and solubilises it, 2- protein is removed by surfactant replacing it at the surface (Malmsten, 2003).

The structure of adsorbed layers of mixture of proteins and surfactants has been discussed by Mackie (2004).The results showed that if the surfactant itself is a good stabilizing agent, then stability can be maintained even when the protein is displaced.

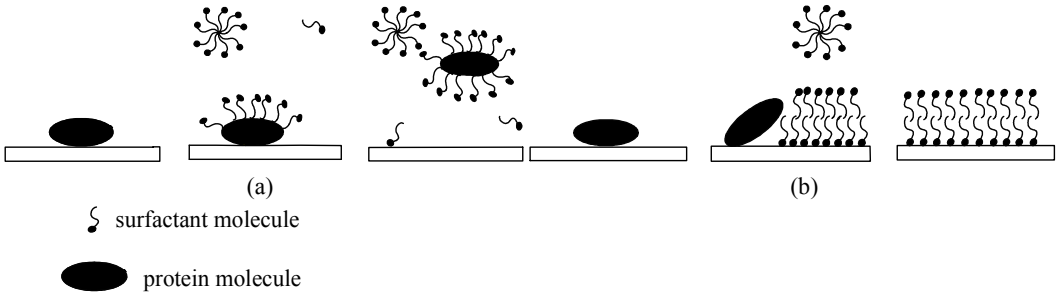

Fig. 1. The solubilization (a) and displacement (b) mechanism of protein removal (MALMSTEN, 2003).

One of a most practical application of surfactant-protein complex adsorption onto solid surfaces can be separation of fine particles from suspension using floc-flotation process. The presence of these species in suspension may change the properties of particle surfaces from hydrophilic to hydrophobic, which enables gas bubbles, introduced in the system, to stick to the particles. Than they are able to move to the air-water interface and can be separated from the aqueous medium.

Magnesite (magnesium carbonate) is an important raw material in the refractory industry as the main source of magnesium oxide. Magnesite rarely occurs in any significant deposit pure enough to be used directly. Its ores contain a variety of gangue minerals, mostly other carbonates, silicates and oxides. Among the methods used in the beneficiation of magnesite ores, flotation is an outstanding one. The silicates are floated away, and the depressed fraction becomes the magnesite concentrate (Gence, 1995; Santana, 2001).

Ovalbumin is a major component of egg white protein. It has molecular weight of 45,000 and belongs to the globular proteins, possessing one or more polypeptide

chains unfolded compactly and uniquely together to form a three-dimensional structure with a roughly spherical shape and a complicated surface topology. It contains single chain of 385 amino acid residues, with a total of 105 titrable ones, as well as a single disulphide bond and glycosylation site. Ovalbumin is an important food supply (GONZALEZ-PEREZ, 2004; DICKINSON, 1993).

In this paper, the effects of protein-surfactant interaction on the magnesite-solution interface are tested because there are no fundamental data on protein-SDS adsorption on magnesite and the resulting floatability of magnesite.

MATERIALS AND METHODS

The investigations have been carried out using magnesite rock from magnesite mine "Sobótka Wiry" (Lower Silesia, Poland). The product was ground to the size below 45 μm. The particle size analysis, by means of Malvern Mastersizer 2000, indicated the mean diameter was ca. 1.4μm. Chemical analysis showed that magnesite solid waste contained about 45.7% of $MgCO_3$. The BET surface area of the powder was measured using the Flow Sorb II 2300 apparatus and it was found to be 10.3m^2/g. The density of this mineral was 2.60g/cm^3. The anionic surfactant sodium dodecyl sulphate (SDS) and albumin from chicken egg (ovalbumin) were purchased from J.T. Baker Chemical Co. and POCh, respectively.

ADSORPTION ISOTHERMS DETERMINATION

Sodium dodecyl sulphate ($C_{12}H_{25}SO_4Na$) and protein adsorption isotherms have been determined by mixing 1g of mineral powder with total 100cm^3 of surfactant and protein solutions. The suspensions were shaken for 1 day and then centrifuged. The adsorption experiments were carried out at the pH values between 8.5 and 9.5. The protein concentration was determined using the Lowry method.

FLOTATION EXPERIMENTS

The flotation experiments have been conducted in the glass flotation column (height of 43 cm, diameter of 3.8 cm). The total volume of column was about 500 cm^3. The air and suspension were provided at the lower part of flotation cell through a peristaltic pomp. The mineral suspension was transferred to the flotation cell and the air was introduced. Floated aggregates were collected after 3, 5, 7, 10, 15 and 20 minutes, dried and weighted. In each experiment 5g of minerals was used.

First, either SDS or protein solution was added to beaker which contained known amount of powder, then the prepared mixture was left for 24 hours. After this time,

the second compound was added to suspension and left for 24 hours, then the flotation process was carried out.

RESULTS AND DISCUSSION

Figures 2 and 3 present the isotherms of sodium dodecyl sulphate (SDS) and ovalbumin adsorption on the magnesite rock surface.

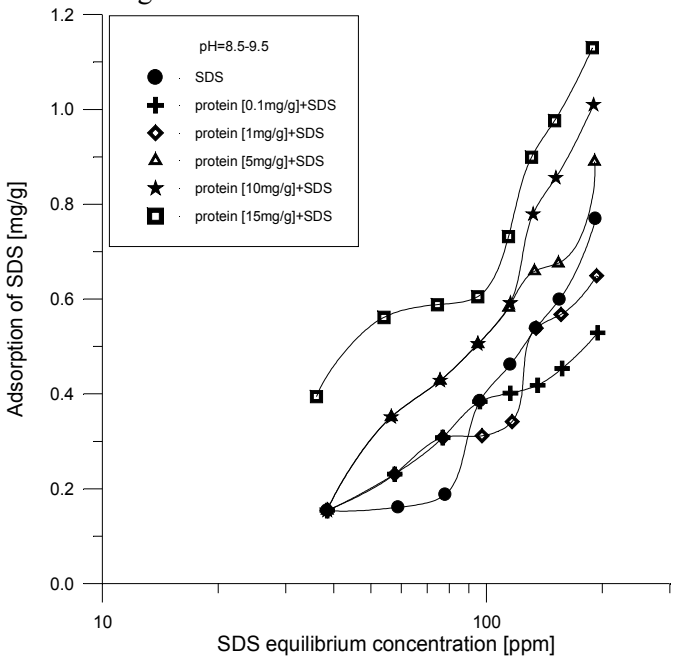

Fig. 2. Adsorption isotherms of SDS at the mineral particles' surface after protein adsorption

Figure 2 depicts the adsorption isotherms of SDS following protein adsorption. One can see that in the presence of polymer the shape of the surfactant isotherms is almost the same. However, the addition of protein strongly affected surfactant adsorption. The formation of contacts between protein and solid surface may cause deformation of the protein molecules, with the loss of the secondary structure, which is called the unfolding or denaturation process (Su, 1998; Sun, 2004). These changes might enable the interactions of surfactant molecules with the protein. SDS binding to several water-soluble proteins reduces disulfide bonds (Imamura, 2002). Su and coworkers (1998) used neutron reflectometry to observe mechanism of SDS interaction with protein (BSA). Initially, SDS was adsorbed at the protein layer, then, when the surfactant concentration in solution was sufficiently high, mixed layer of protein and SDS was removed from the surface. Choi and Foster (2003) obtained very similar result for the interaction of cetyl trimethylammonium bromide CTAB and SDS with human se-

rum albumin HSA adsorbed on the SAM (self-assembled monolayers). However, the contact with surfactant solution removed the adsorbed HSA from the solid surface. Thus, this removal of protein from solid surface caused by bonded surfactant creates gaps in the layer. Surfactant molecules from the bulk can adsorb then at the particle solid (Fig. 1). Besides of this, it has been observed that SDS binds more readily to proteins such as BSA and β-lactoglobulin at pH values higher than pI (Madgassi, 1996).

The pH value maintained in the current work was 8.5-9.5, while pI of egg albumin is 4.6. The removal of protein depends not only on the surfactant but also on the nature of protein layer. In these experiments, the amount of surfactant added to the suspension and the quantity of protein adsorbed onto solid surface were different in each sample, which means that the structure of the layer at the surface was not the same in all cases. At low concentration of ovalbumin at the solid surface the adsorption of SDS was slightly lower than in an absence of protein, particularly at high SDS concentration. Probably, the protein layer did not cover the surface completely, and there was a higher possibility for the protein to adapt to the surface by changing its conformation leading to lower eluatability (Malmsten, 2003). However, when the amount of protein increased, the adsorption of surfactant molecules was higher. Xu and coworkers (Xu, 2003) observed that at the high protein concentration, bovine serum albumin BSA molecules tend to aggregate into clusters and then adsorb onto solid surface, resulting in better eluatability by SDS. Morever, the gap between the adsorbed single protein molecules is smaller than the one between the adsorbed clusters, which might affect the amount of surfactant adsorbed at the particles surface.

The adsorption of ovalbumin, both in the presence and absence of anionic surfactant (SDS) added, is shown in the Fig. 3. According to the literature, the experimental results are described by the Langmuir isotherm (Seki, 2003). The presence of surfactant layer affected the adsorption of protein molecules at the mineral surface. Better adsorption was observed in the presence of SDS but the plateau value for the amount of polymer absorbed decreased with an increase of SDS concentration. The presence of surfactant at the particles surface might lead to higher affinity of protein to this surface, as this was observed at low concentration of SDS (0.1 mg/g_{solid}). On the other hand, it can be noted that at high amount of SDS (up to $5mg/g_{solid}$) the adsorption of protein on the solid surface was almost the same as without surfactant. Increasing amount of surfactant at the particle surface increased its hydrophobicity and the interaction between protein and SDS was most probably of hydrophobic character.

Figure 4 shows the effect of SDS concentration on the floatability of magnesite rock at the natural pH range (8.5-9.5). The maximum flotation yield (67.12%) corresponds with the maximum of SDS concentration ($30mg/g_{solid}$). This behaviour can be explained by chemisorption of SDS.

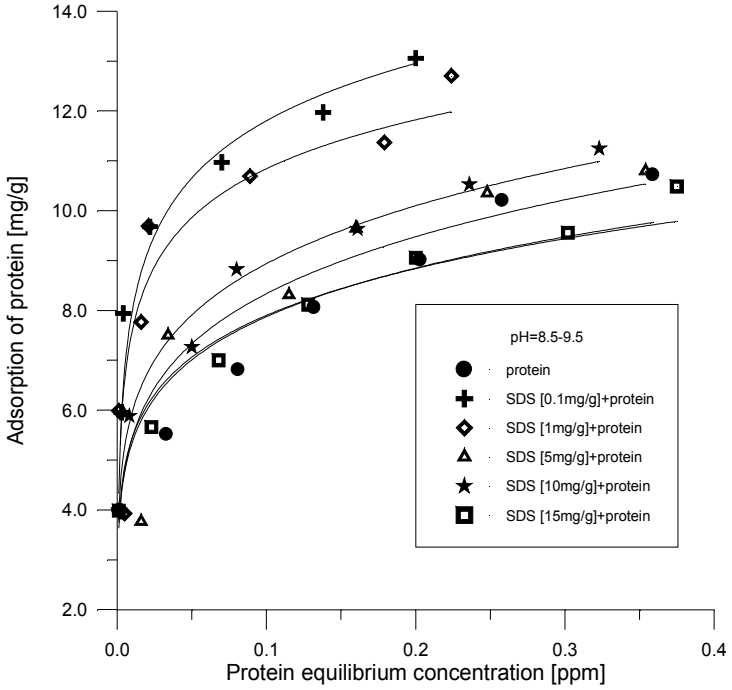

Fig. 3. Adsorption isotherms of protein onto mineral surface after SDS adsorption

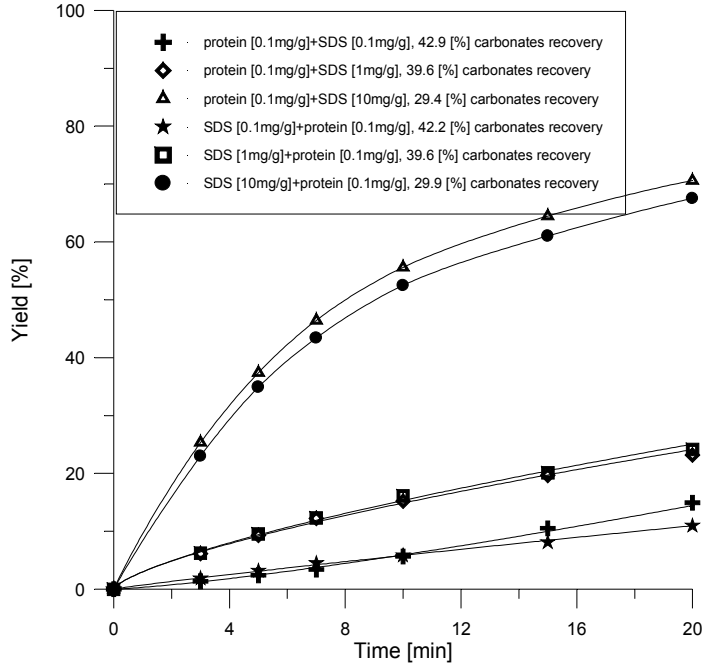

Fig. 4. Flotation of magnesite rock in the presence of SDS

The surface became more hydrophobic resulting in enhance of floatability (GENCE, 1995; BREMMELL, 1999). However, the grade of carbonates in the flotation concentrate was smaller than in the feed and it decreased with the increase of the flotation output. It means that the main component of flotation concentrate was silica. An anionic surfactant can interact with silica surface activated by Mg^{2+} ions which were present on the surface. This caused that the surface of silica is able to adsorb anionic collector and silica particles were attached to the air bubbles and floated.

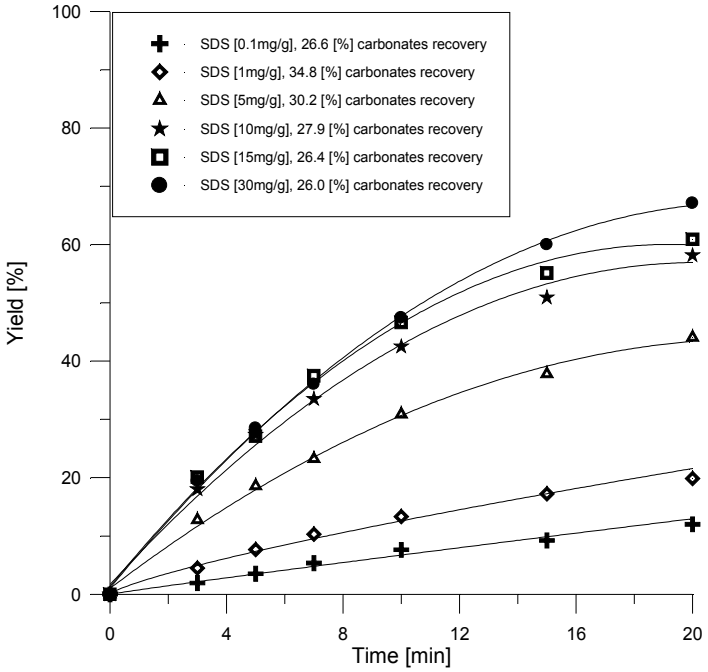

Fig. 5. Flotation of magnesite rock in the presence SDS and protein

The adsorption of SDS increases with the protein concentration (Fig. 2). Also the protein adsorption increases when the SDS addition his increased (Fig. 3). These trends have been tested in flotation experiments. Figure 5 shows the flotation data obtained using a different order of reagents addition. As can bee seen, the order of reagents addition has no effect on both flotation yield and carbonate recovery. It should be noted that flotation concentrate recovery increased but the percentage of carbonates yield decreased.

Although the exact co-adsorption mechanism of protein and surfactant is difficult to identify at this stage, it seems that the presence of a mixed layer on the particles surface caused the inhibition of carbonate flotation.

CONCLUSIONS

The magnesite rock used in these studies has been examined for identification of separation conditions of magnesite and silica. From initial considerations, the following conclusion can be derived:

1. The anionic surfactant (SDS) and ovalbumin can be used as modifying reagents for the magnesite surface.
2. The experimental data show that the addition of SDS and albumin had a strong effect on the flotation recovery of magnesite rock.
3. The yield of carbonate in flotation concentrate decreased with increasing of surfactant concentration at the low amount of protein (0.1 mg/g $_{solid}$). It should be a prospective way of investigation.
4. The order of both reagents addition has no affected the flotation results.

REFERENCES

BASTRZYK A., POLOWCZYK I., SADOWSKI Z., 2005, *The effect of surfactants adsorption on the hindered settling of magnesite solid waste*, Physicochemical Problems of Mineral Processing, 39, 211-218.

BREMMELL K. E., JAMESON G. J., BIGGS S., 1999, *Adsorption of ionic surfactans in particulate systems: flotation, stability and interaction forces*, Colloids Surfaces A: Physicochemical and Engineering Aspects 146, 75-87.

DICKINSON E., 1993, *Interaction of surfactant with polymers and proteins Chapter 7: Proteins in solution and at interfaces*, CRC Press. Inc. 295-427.

GENCE N., ÖZDAĞ H., 1995, *Surface properties of magnesite and surfactant adsorption mechanism*, Inter. J. Mineral Processing, 43, 37-47.

GONZÁLEZ-PÈREZ A., RUSO J. M., PRIETO G., SARMIENTO F.,2004, *Physicochemical study of ovalbumin in the presence of sodium dodecyl sulphate in aqueous media*, Colloid Polym. Sci. 282, 351-356.

IMAMURA T.2002, *Surfactant-protein interactions, Encyclopedia of Surface and Colloid Science*, 2002, 5230-5243.

MACKIE R.A., 2004, *Structure of adsorbed layer of mixtures of proteins and surfactants,* Current Opinion Colloid Inter. Sci., 9, 357-361.

MADGASSI S., VINETSKY Y., RELKIN P.,1996, *Formation and structural heat-stability of β-lactoglobulin/surfactant complex*, Colloids Surfaces B: Biointerfaces 6, 353-362.

MALMSTEN M., 2003, *Biopolymers at interfaces*, Marcel Dekker, Inc., 2003.

MILLER R., FAINERMAN V. B., MAKIEVSKI A. V., KRÄGEL J., GRIGORIEV D. O., KAZAKOV O. V., SINYACHENKO O. V., 2000, *Dynamics of protein and mixed protein/surfactant adsorption layers at the water/fluid interface*, Advances in Colloid Interface Sci., 43, 39-82.

MORÉN K. A., KHAN A.,1999, *Phase Behaviour and phase structure of protein-surfactant-water system*, Journal Colloid Interface Sci., 218, 397-403.

MURPHY J. D., 1995, *The role of micellar structures in the flocculation. Part 1: Flocculation of quartz with acrylamine surfactants*, Colloids Surfaces 96, 143-154.

PALACIOS C. A., ANTONELLI L. M., LA MESA C., 2004, *Interactions between bovine serum albumin and sodium taurodeoxycholate: thermodynamic properties*, Thermodynamica Acta, 418, 69-77.

POLOWCZYK I., JAŻDŻYK E., SADOWSKI Z., MALISZEWSKA I., SZUBERT A., 2004, *Protein-surfactant interactions in the polymineral water suspension,* Theoretical and experimental studies of interfacial phenomena and their technological applications. VIII Ukrainian-Polish symposium, 254-257.

SADOWSKI Z., POLOWCZYK I., 2001, *Effect of polymer-surfactant adsorption on the hindered settling of a mineral suspension*, Adsorption Science Technology, 19, 245-254.

SANTANA A.N., PERES A.E., C., 2001, *Technical note reverse magnesite flotation*, Minerals Engineering, Vol. 14, (1) 107-111.

SEKI H., SUZUKI A.; 2003, *Flocculation of diatomite by methylated egg albumin*, Journal Colloid Inter. Scie. 263, 42-46.

SHIMABAYASHI S., UNO T., NAKAGAKI M., 1997, *Formation of a surface complex between polymer and surfactant and its effect on the dispersion of solid particles*, Colloids Surfaces A: Physicochemical and Engineering Aspects 123-124, 283-295.

SU T. J., LU J. R., 1998, *The conformational structure of Bovine Serum Albumin layers adsorbed at the silica-water interface*, J. Phys. Chem. B, 102, 8100-8108.

SUN C., YANG J., WU X., LIU S., SU B., 2004, *Study on the fluorescent enhancement effect in terbium-gadolinium-protein-sodium dodecyl benzene sulfonate system and its application on sensitive detection of protein at nanogram level*, Biochemie, 86, 569-578.

TREINER C., 2002, *Surfactant adsorption and adsorption induced by surfactant at solid-water interfaces*, Encyclopedia of Surface and Colloid Science, 5154-5168.

VALSTAR A., 2000, *Protein-Surfactant Interactions*, Comprehensive Summaries of Uppsala Dissertations from the Faculty of Science and Technology, 563, 7-48.

Xu T., Fu R., Yan L., 2003, *A new insight into the adsorption of bovine serum albumin onto porous polyethylene membrane by zeta potential measurements, FTIR analyses and AFM observation*, Journal of Colloid and Interface Science 262, 342-350.

Bastrzyk A., Polowczyk I., Szeląg E., Sadowski Z., *Wpływ oddziaływań białko-surfaktant na flotację skały magnezytowej.* Physicochemical Problems of Mineral Processing, 42 (2008), 261-269(w jęz. ang)

Od wielu lat prowadzone są badania nad wzajemnym oddziaływaniem cząstek białka i surfaktantu. Efektem tego oddziaływania jest powstanie kompleksu białko-surfaktant. Celem pracy było sprawdzenie, w jaki sposób kompleks białko-surfaktant, powstały na powierzchni ciał stałego, wpływa na właściwości powierzchniowe ciał stałych. W badaniach użyto, jako białka albuminy a jako surfaktantu SDS. Badania były prowadzone na skale magnezytowej z kopalni Wiry. Badano adsorpcję odczynników na powierzchni ciała stałego i flotację. Otrzymane wyniki częściowo wyjaśniają problem oraz stanowią asumpt do dalszych badań nad separacją magnezytu od krzemionki.

słowa kluczowe: oddziaływanie białko-surfaktant, adsorpcja, SDS, flotacja

Our books are available in *Tech* bookstore
plac Grunwaldzki 13
50-377 Wrocław, D-1 PWr., tel. (071) 320 32 52
Orders can also be sent by post

ISSN 1643-1049
Physicochemical Problems of Mineral Processing, 42 (2008)